ISSN 1881-7815 Online ISSN 1881-7823

BST BioScience Trends

Volume 17, Number 1
February, 2023

IRCA BSSA

IACMHR

www.biosciencetrends.com

BST
BioScience Trends

ISSN: 1881-7815
Online ISSN: 1881-7823
CODEN: BTIRCZ
Issues/Year: 6
Language: English
Publisher: IACMHR Co., Ltd.

BioScience Trends is one of a series of peer-reviewed journals of the International Research and Cooperation Association for Bio & Socio-Sciences Advancement (IRCA-BSSA) Group. It is published bimonthly by the International Advancement Center for Medicine & Health Research Co., Ltd. (IACMHR Co., Ltd.) and supported by the IRCA-BSSA.

BioScience Trends devotes to publishing the latest and most exciting advances in scientific research. Articles cover fields of life science such as biochemistry, molecular biology, clinical research, public health, medical care system, and social science in order to encourage cooperation and exchange among scientists and clinical researchers.

BioScience Trends publishes Original Articles, Brief Reports, Reviews, Policy Forum articles, Communications, Editorials, News, and Letters on all aspects of the field of life science. All contributions should seek to promote international collaboration.

Editorial Board

Editorial and Head Office

Pearl City Koishikawa 603,
2-4-5 Kasuga, Bunkyo-ku, Tokyo 112-0003, Japan
E-mail: office@biosciencetrends.com

BioScience Trends

Editorial and Head Office

Pearl City Koishikawa 603, 2-4-5 Kasuga, Bunkyo-ku,
Tokyo 112-0003, Japan

E-mail: office@biosciencetrends.com
URL: www.biosciencetrends.com

Editorial Board Members

CONTENTS

Volume 17, Number 1, 2023

Review

Original Article

Correspondence

Comment

Letter to the Editor

Review

DOI: 10.5582/bst.2023.01013

The initiation, exploration, and development of hospital-based health technology assessment in China: 2005 – 2022

Mi Tang[1,§], Xueyan Zhang[2,§], Ziping Ye[3], Lvfan Feng[1], Yan Yang[1], Zhiying Hou[1], Fei Bai[4], Xia Lin[4], Xinyu Liu[5], Hai Yang[6], Shanlian Hu[7], Peipei Song[8,*], Jiangjiang He[1,*]

[1] Shanghai Health Development Research Center, Shanghai, China;
[2] Shanghai Municipal Center for Health Promotion, Shanghai, China;
[3] School of Public Administration, Hainan University, Hainan, China;
[4] National Center for Medical Service Administration, National Health Commission of the People's Republic of China, Beijing, China;
[5] Shenzhen Municipal Health Commission, Shenzhen, China;
[6] Shanghai Sixth People's Hospital affiliated to Shanghai Jiao Tong University School of Medicine, Shanghai, China;
[7] School of Public Health, Fudan University, Shanghai, China;
[8] Center for Clinical Sciences, National Center for Global Health and Medicine of Japan, Tokyo, Japan.

SUMMARY A hospital-based health technology assessment (HB-HTA) can provide the evidence needed to inform clinical decisions at the administrative level. With the implementation of a new round of medical and health care system reforms in China, such as the abolition of medical mark-ups, adoption of modern hospital management systems, reform of diagnosis related groups (DRGs) payment, and performance evaluations for public hospitals, medical institutions increasingly need HB-HTA. The development of HB-HTA in China can be divided into three phases: An initiation phase (2005–2014), a preliminary exploratory phase (2015–2017), and a rapid development phase (2018–present). HB-HTA has been used to manage medical consumables, medical devices, and medicines, but there are still problems and challenges in terms of concept recognition, the mode of development, and limited professionals and data. To promote and use HB-HTA in developing countries, we have identifies the development paths and recommendations for implementation based on a case study in China, which can be summarized as follows: enhancing the top-level design of HB-HTA, formulating HB-HTA guidelines, further promoting the main ideas of HB-HTA, concentrating on the training of evaluation personnel, establishing an HB-HTA network and paying attention to the flexibility of HB-HTA in the application process, and multi- stakeholder participation.

Keywords hospital-based health technology assessment, health technology assessment, lean management, value-based healthcare, methods of payment, modern hospital management system

1. Introduction

Health technology refers to a specific product, commodity, treatment plan, or knowledge system used in the health care system. This includes drugs, medical devices, surgery, program plans, hospital management systems, and support systems. There are two sides to the development and use of health technology. On the one hand, its development has helped to improve diagnostic capabilities and the ability to prevent and treat disease and to improve the quality of life of patients. On the other hand, it has also had many negative impacts, such as the side effects of health technology, the unreasonable and rapid growth of medical costs, and ethical and moral issues (*1*). Health technology assessment (HTA) emerged in this context. HTA is a systematic and multidisciplinary evaluation of the characteristics of health technologies and interventions, including their direct and indirect consequences, that aims to determine the value of a health technology and to provide guidance on how these technologies can be used in health care systems. HTA is an important part of the international, national, and regional health care decision-making process. However, there are still some high-value innovative technologies that cannot be implemented in clinical practice in time. At the same time, there are some health technologies that have low value that are used in clinical practice. Hospitals are the main entryway for health technologies, but related knowledge and tools to evaluate these new technologies are insufficient in hospitals. Thus, hospitals have difficulty selecting and using these new technologies scientifically. In an era of relatively fixed

and diminishing hospital budgets, hospital administrators need to provide the best care at the lowest cost, which means they must maximize the value of hospital inputs (*2*). Hence, the use of HTA at the hospital level is becoming more widespread in the selection of, admission to, and use of new technologies (*3,4*). Hospitals increasingly want to use HTA to optimize their resources through systematic multidisciplinary evidence-based management of health technologies (*5*).

Since the introduction of the concept of HTA in the 1980s, a wealth of research has been conducted in China. However, most of the current HTA guidelines are formulated at the national or regional level. Hospitals of different levels, types, and scales have different information needs for HTA, the methods and tools for obtaining and utilizing technical information differ, and they follow different guidelines and make different decisions. A survey found that hospital administrators and clinicians generally believe that HTA reports from national or regional research institutes are not sufficiently relevant to hospitals' daily clinical management (*6*). Hospital administrators usually need faster access to HTA information to support decision-making, while HTA reports from national or regional research institutes often take a long time, so the hospitals' decision-making needs cannot be met in a timely manner (*7*).

Based on the hospital setting specifically, hospital-based HTA (HB-HTA) aims to help hospitals make decisions on various health technologies *via* HTA. It can provide hospital managers with evidence to assess whether the hospital needs to adopt a new technology, so that the hospital can avoid introducing inappropriate technology or reduce its unnecessary use, optimize purchasing decisions, improve the efficiency with which healthcare resources are allocated (*8*). With the continued progress of China's new round of medical and health care system reforms, compensation mechanism for public hospitals requires the control of the growth of unreasonable medical costs at medical institutions (*9*), and the creation of a hierarchical medical system requires the establishment of a framework for value-based care (*10*). In particular, "Healthy China 2030" proposes to create a modern system of public hospital management (*e.g.*, comprehensive budget management) (*11*). At the same time, the method of paying health insurance has changed from a post-payment system to a pre-payment system (such as a total prepayment system or individual payment) or a bundled payment system (such as payment by disease type or payment by diagnosis related groups (DRGs)) (*12*). Many profit centers in the former economic operation of hospitals have transformed into cost sources, requiring hospital managers to allocate resources based on evaluation of the value of a health technology in the hospital environment in order to effectively control costs and improve quality. At the same time, in the context of reforms to "streamline administration, delegate power, strengthen regulations, and improve care", hospitals have greater autonomy to make various decisions. In 2015, the former National Health and Family Planning Commission revoked approval for admission to clinical use of class-three medical technology, clearly indicating that "medical institutions have the main responsibility for the clinical use and management of their own medical technologies" (*13*). In this context, HB-HTA needs to be adopted to create an evidence-based management system for hospitals and to improve the scientific level of hospital decision-making. However, the implementation of HB-HTA in China is still in its development stage, and there are still many problems and challenges. This paper aims to systematically review the development process, current status, and challenges of HB-HTA in China and to summarize the development paths and suggestions for implementation of HB-HTA in order to serve as reference for the development of HB-HTA in developing countries.

2. Literature search strategies and methods

2.1. Data sources and search strategy

The databases searched included: PubMed, Web of Science, EMBASE, CNKI, CQVIP, WanFang, as well as the websites of government agencies such as the National Health Commission and the National Healthcare Security Administration, HTA institutions and medical institutions. The search strategy for each database was devised by combining subject terms and free words. The search strategy for PubMed was as follows: ((health technology assessment) OR (HTA) OR (the ambassador model) OR (the internal committee) OR (the mini-HTA) OR (the HTA unit) OR (HTA)) AND ((decision making) OR (decision support techniques) OR (decision aid) OR (health system)) AND ((hospital) OR (health facility) OR (medical institution)) AND China. The most recent search was conducted on October 31, 2022. Since we only searched literature in English and simplified Chinese, HB-HTA studies in Taiwan, Hongkong and Macao are less likely to be included apart from those published in English. Moreover, all references in relevant studies were reviewed in the event that eligible studies were not identified.

2.2. Inclusion and exclusion criteria

Inclusion criteria: *i*) From the research perspective of hospital management in China; *ii*) The research includes the HB-HTA evaluation of a specific health technology; *iii*) Evidence-based hospital decision-making research; Research about how to conduct a hospital health technology assessment or evidence-based in-hospital decision-making research (process, quality assessment and control, report of results, decision application, *etc*.); and *iv*) HB-HTA related policy research.

Exclusion criteria: *i*) HTA research not including hospital management; *ii*) The abstract or full text could not be obtained by contacting the authors; and *iii*) A source with duplicate content or duplicate publication.

2.3. Literature screening process

Titles and abstracts were evaluated by 2 authors independently. Potentially relevant studies were reviewed in a full paper by 2 scholars, with any disagreement resolved by consensus by a third author. The flow chart for literature screening is shown in Figure 1.

3. History of the development of HB-HTA in China

Based on the year of publication, content of the literature, and website materials, the development of HB-HTA in China can be divided into three phases: An initiation phase (2005–2014), a preliminary exploratory phase (2015–2017), and a rapid development phase (2018–present).

3.1. Initiation phase (2005–2014)

HTA was first introduced in China in the 1980s and evidence-based medicine in the 1990s (*14*), Xia *et al*. published "Health Technology Assessment and Hospital Management" in 2005, the first Chinese source related to HB-HTA (*15*), which analyzed the relationship between HTA and management of medical technology management, drug and medical devices in the hospital settings. Although the concept of HB-HTA was not mentioned in the paper, as a pioneer in exploring the application of health technology assessment in hospitals in China, it is of great significance for the beginning of HB-HTA in China (*16*). In August of the same year, Zhao *et al*. emphasized in their article that clinical management decisions in hospitals should be based on high-quality research evidence (*17*). Evidence-based ideas began to sprout in hospitals. Since 2006, the Consumables Management Department of the Sixth People's Hospital affiliated to Shanghai Jiao Tong University School of Medicine has started to implement an evidence-based management system for the entire procurement and supply chain management system of medical consumables (*18,19*). With the development of HB-HTA in the world, the mini-HTA tools are emerging and gradually becoming an important tool for healthcare decision-making at the global hospital level. In 2014, Huang *et al*. presented in detail the evaluation elements and application scenarios of mini-HTA tool in detail in a Chinese journal (*20*), which can be used as a tool for HB-HTA in China. At this phase, the concept of HB-HTA has not yet been officially proposed in China, but the idea of evidence-based decision-making, which is related to HB-HTA, has already gained acceptance in hospitals.

3.2. Preliminary Exploratory Phase (2015–2017)

From 2015 to 2017, the former National Health and Family Planning Commission of China issued a series of policies to guide and strengthen the implementation of HTA in China, and also began to include HTA in process of formulating specific policy. The Ministry of Human Resources and Social Security of the People's Republic of China also included HTA evidence as one of the criteria to determine whether a drug should be included in the national drug reimbursement list. The demand for HTA-related decisions in China increased (*21*). As the reform of the payment method of health insurance and the reimbursement mechanism of public hospitals progressed, China's health administration department

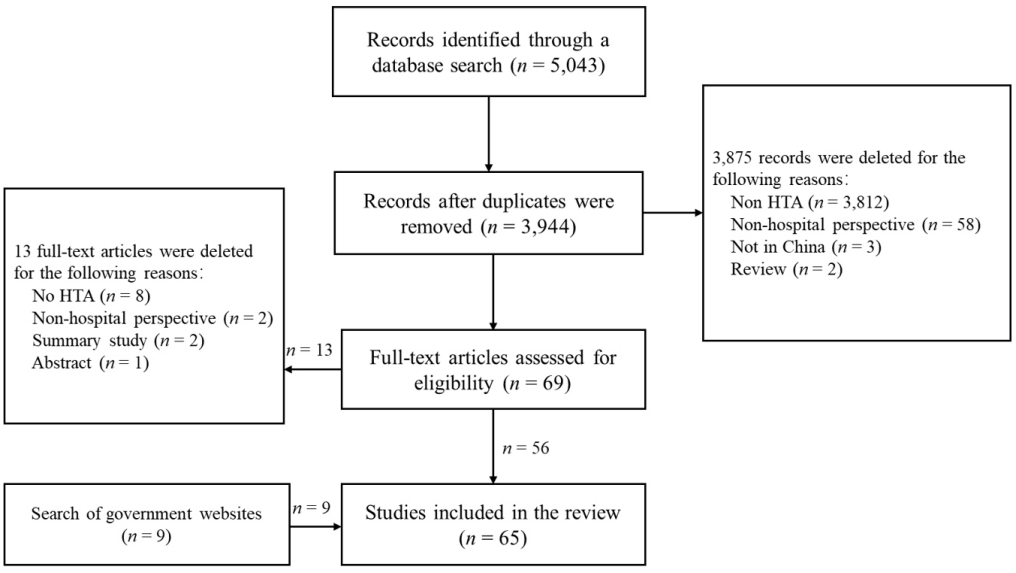

Figure 1. Flow chart for literature screening.

cancelled the approval for admission to the third type of medical technology for clinical use, and medical institutions took primary responsibility for managing the clinical use of their own medical technology. Medical institutions began to explore the use of HB-HTA to assist management and improve the level of scientific decision-making. HB-HTA in China has begun to enter the preliminary exploratory phase.

The literature during this period mainly focused on the study of relevant international experiences, and cases from hospital practices were rare. In 2015, Zhang *et al*. first introduced the international concept of HB-HTA in China and the basic methods of HB-HTA, laying a theoretical foundation for HB-HTA in China (*22*). In 2016, Lv *et al*. discussed the path for introducing HTA into management of medical technology in China by referring to the process and methods of HTA used to manage medical technology in the UK (*23*). In September 2017, the Shanghai Health Development Research Center compiled the Hospital Health Technology Assessment Manual and Toolkit, a research and development result of the European Union HB-HTA Project (AdHopHTA), which provided information and tools for the establishment and implementation of HB-HTA in hospitals and conducted extensive academic exchanges(*24*). At this stage, most scholars are disseminating concepts related to HB-HTA and reviewing the methods and tools of HB-HTA. HB-HTA has not yet been promoted, used, or transformed into policies in Chinese hospitals.

3.3. Rapid Development Phase (2018–present)

With the rapid development of HTA in China, China issued a series of policy documents (*25-28*) from 2018 to 2019 (Table 1) that have created a good policy foundation for the development of HB-HTA, and HB-HTA has entered a phase of rapid development.

At the national level, from 2018 to 2019, National Center for Medical Service Administration of the National Health Commission (hereinafter referred to as the National Medical Management Center) consecutively conducted two sets of HB-HTA pilot projects in 12 public tertiary hospitals in China (*29,30*), significantly improving the pilot hospitals' knowledge of and emphasis on HB-HTA. In April 2019, the National Health Commission's department of drug policy and essential medicine began to promote nationwide monitoring of drug use and comprehensive clinical evaluation, and it proposed that medical institutions should make full use of the HTA methods and routine drug monitoring tools to assist them in drug procurement and use according to their actual needs. In July 2021, the National Center for Medicine and Health Technology Assessment published a management guideline (*31*) and three technical guidelines (*32*) for comprehensive clinical evaluation of drugs. To date, comprehensive clinical evaluation of medicines has been widely conducted as an application of HB-HTA to the clinical use of medicines in Chinese hospitals.

At the local level, China's developed areas such as Shanghai and Shenzhen have taken appropriate action regarding HB-HTA. In September 2018, the Shanghai Hospital Association and Shanghai Medical Device Industry Association presented an expert consensus on the development of HB-HTA in Shanghai to specify the direction for the development of HB-HTA in Shanghai (*33*). Implementation of the "Shenzhen Model" of HB-HTA was proposed by the Zhongxing Telecom Equipment (ZTE) Foundation HTA Center. In August 2020, the Shenzhen Municipal Health Commission appointed 7 hospitals as pilot hospitals, and the ZTE Foundation HTA Center collected the drug evaluation requirements at the pilot hospitals. After a drug evaluation report was

Table 1. HB-HTA-related policies in China from 2018 to 2019

Date of Publication	Issuing agency	Name of Publication	Related Content
July 2018	The State Council of the P.R.C.	Regulations on the Prevention and Handling of Medical Disputes.	Medical institutions adopting new medical technologies shall conduct a technical evaluation and ethical review.
August 2018	The State Council of the P.R.C.	Guidelines of the General Office of the State Council of the P.R.C. on Reforming and Improving the Comprehensive Supervision System of the medical and health industry.	A health technology assessment should be conducted to support decisions regarding clinical admission, standardized application, and discontinuation and elimination of medical technologies, drugs, and medical devices.
June 2019	National Health Commission	Administrative Measures for Medical Consumables in Medical Institutions.	Management of medical consumables should be patient-centered and based on medicine, and the entire process of purchasing, storing, using, tracking, monitoring, evaluating, and supervising medical consumables should be effectively organized, implemented, and managed.
December 2019	The Standing Committee of the N.P.C.	Law of the P.R.C. on the Promotion of Basic Medical Care and Health.	To organize the assessment of the quality of care and the use of medical technology, drugs, and medical devices in medical and health care institutions.

P.R.C. : People's Republic of China; N.P.C. : National People's Congress.

prepared, the pilot hospitals used it as a reference for the admission of new drugs to hospitals (*34*). This provides evidence for the admission of new drugs by other hospitals that have not yet implemented HB-HTA, and it greatly improves the efficiency of decision-making for HB-HTA research.

Since 2018, with policy support, the path of HB-HTA has been explored at the national and local levels, focusing on the implementation and application of HB-HTA. Many hospitals in China have reported the use of HB-HTA (*35-40*). In the process of practical application, some new theoretical methods, such as multiple-criteria decision analysis (MCDA), have been gradually integrated into HB-HTA (*41*), and HB-HTA has been gradually improved in the process of practical application.

The characteristics of HB-HTA in all three phases of development in China are summarized in Figure 2.

4. Current status of HB-HTA development in China

The current status of hospitals that have conducted HB-HTA in China from 2005 to 2022 is as follows:

4.1. Institutions conducting HB-HTA

Based on the status of the HB-HTA pilot hospitals selected by the National Medical Management Center and the literature, the current HB-HTA institutions in China are shown in Supplemental Table S1 (*https://www.biosciencetrends.com/supplementaldata/135*) (*29,36,38-54*). The medical institutions are located in 16 provinces/municipalities/autonomous regions, with the largest number being located in Guangdong Province, Beijing, Shanghai, and Jiangsu Province. Currently, the medical institution conducting HB-HTA are mainly concentrated in the developed regions of China (Figure 3), which are mainly public tertiary general hospitals.

4.2. Organizational management of HB-HTA

In 2008, the HTA international (HTAi) Hospital Based Health Technology Assessment Sub-Interest Group divided HB-HTA into four modes, *i.e.*, an internal committee mode, an ambassador mode, a mini-HTA mode, and an HB-HTA unit mode, depending on the organizational complexity and focus of action (*55*). Most of China's HB-HTA activities were still based on expert opinions or committee decisions, and no HB-HTA units were internationally recognized (*56*). Lin *et al*. surveyed 30 public hospitals in China in 2018 and found that all of the surveyed hospitals had established health technology assessment systems in forms, mainly with the internal committee mode and mini-HTA mode, and that about 1/3 of admission to hospital devices was determined *via* a model similar to mini-HTA (*57*). In general, the Expert Committee is chaired by the director or deputy director of a hospital, and the members include experts in clinical medicine, clinical pharmacy, biomedical engineering, evidence-based medicine, health economics, health care management, ethics, library and information science, and other relevant fields (Figure 4). In some hospitals, the committee to manage medical technology assumes the role of an HB-HTA committee. For example, Shanghai Sixth People's Hospital affiliated to Shanghai Jiao Tong University School of Medicine explored and adopted a method of voting by committee based on a simple assessment, which is similar to an internal HB-HTA committee. Later, an HB-HTA interest group was established, involving biomedical engineering, health economics, health policy, hospital management, *etc.* (*56*).

China has not yet developed a uniform HB-HTA assessment procedure. Different hospitals have different procedures for different evaluation contents, but generally there are key steps such as application, evaluation, and voting. Taking the mini-HTA of medical devices at the Aviation General Hospital of China Medical

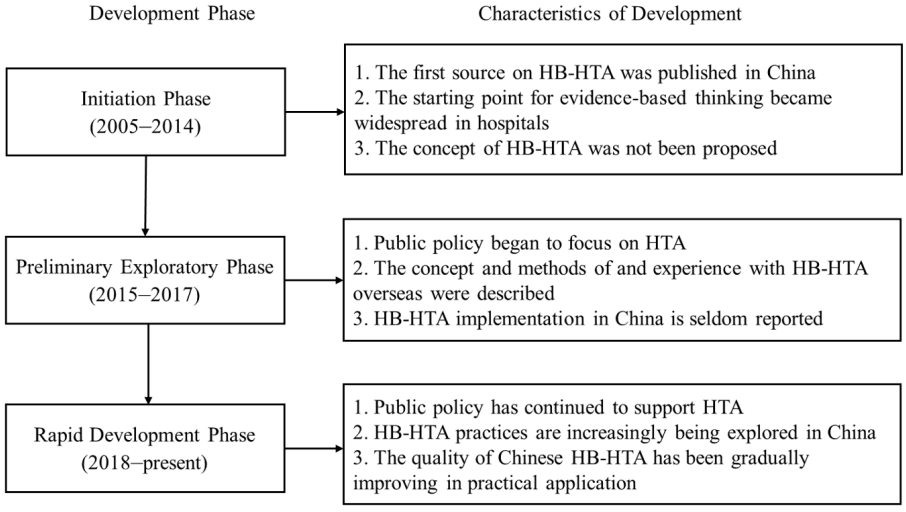

Figure 2. History of HB-HTA development in China.

University as an example, first, a clinical department makes an application, a medical department conducts the evaluation, and then the Medical Devices Committee makes the final decision by voting. Subsequently, the Medical Department and the Purchasing Center take action together (Figure 5) (*44*). HB-HTA usually uses intermediate indices as measurement standards, and the evaluation cycle is about 1-6 months. For example, the mini-HTA of an intermittent pneumatic compression device at a tertiary hospital in Shanghai took 2.5 months (*47*) and the mini-HTA of a special anti-magnetic anesthesia machine in West China Hospital of Sichuan University took only 1 month (*58*). A mini-HTA report is usually submitted in addition to the full assessment report and the rapid assessment report.

4.3. Scope of application of HB-HTA

HB-HTA in China is most often conducted for medical devices (*59*), followed by drugs. However, it can be applied to diagnosis and treatment technology (*60*), medical or surgical disposal, support systems,

Figure 3. Distribution of HB-HTA institutions in China.

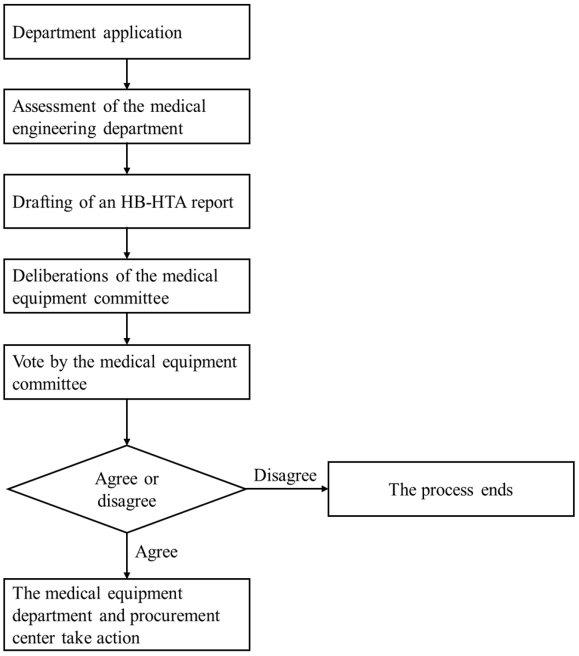

Figure 5. Mini-HTA flow for medical devices at the Aviation General Hospital, China Medical University.

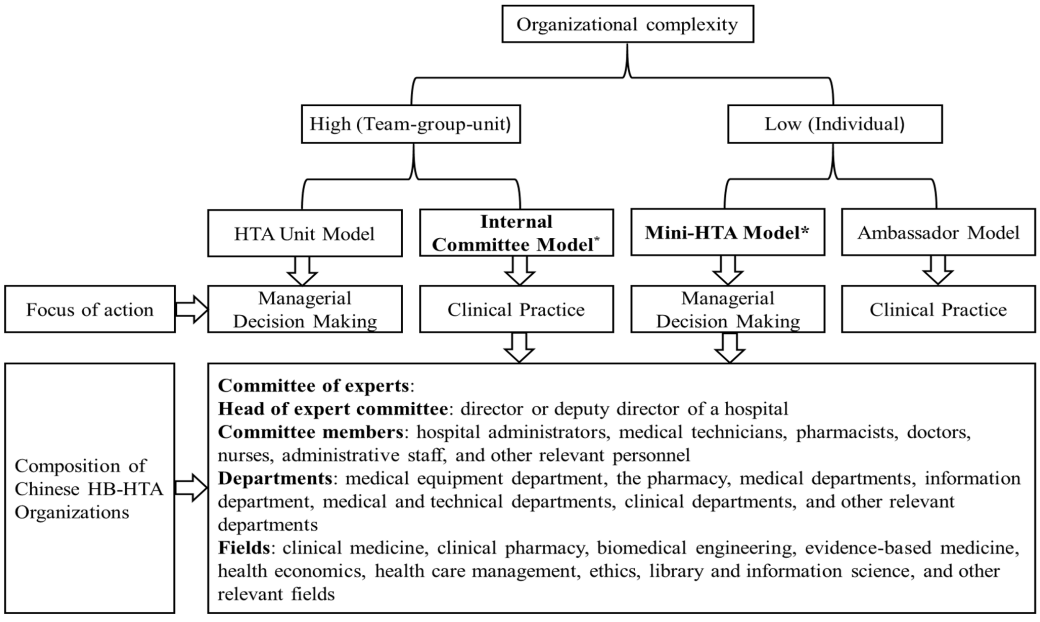

Figure 4. Organizational management of HB-HTA departments in China.

organizational management systems, and other aspects, though the scope of application is still relatively limited (*49*). In the area of medical devices, diagnostic equipment (such as Computed Tomography (CT) and Magnetic Resonance Imaging (MRI) machines and doppler ultrasound diagnostic apparatus), treatment equipment (such as intra-aortic balloon counterpulsation pumps, temperature-maintaining devices during the perioperative period, intermittent pneumatic compression devices, and high-frequency thermotherapy ablation machines), auxiliary devices (such as robots for intravenous drugs allocation) and medical consumables (such as dressings and materials for the repair of peripheral nerve defects) have been evaluated. Some hospitals use the mini-HTA assessment list to conduct HB-HTA, and some develop their own HB-HTA tools depending to their situation. They have evaluated the technical level, patient level, hospital level and economic level. The HB-HTA activities of most hospitals mainly play a decision support role in the admission management of medical devices, and a small number of hospitals also conduct HB-HTA to support decision-making in the use of medical devices (Table 2, Online Table, *https://www.biosciencetrends.com/supplementaldata/135*) (*36-39,42,44,47,48,51-53,58,61-66*). This improves the scientificity and refined management level of medical devices admission and use, and helps hospitals control costs sensibly and reduces the burden on patients. HB-HTA of pharmaceuticals focuses mainly on drugs of antineoplastic and immunomodulating agents, cardiovascular system, alimentary tract and metabolism, musculo-skeletal system, anti-infectives for systemic use, nervous system and blood and blood forming organs. Most hospitals use self-made evaluation tools. One hospital uses an evidence and value: impact on decision-making (EVIDEM) framework to evaluate. They have evaluated drug safety, effectiveness, economics, innovation, suitability, and other aspects. The HB-HTA activities in hospitals play a decision-supporting role in the admission management and use management of drugs (Table 3) (*34,40,41,43,54,67-70*), and improves the scientificity of hospital selection of drugs and the level of clinical safety and rational drug use (Figure 6).

Table 3. Typical examples of HB-HTA application to pharmaceuticals in China

Lead author (year)	Site	Scenario for application	What is assessed	Assessment tool	Assessment dimensions
Yun B (*41*) (2020)	Gansu Province	AM	Drugs (alimentary tract and metabolism drugs)	The MCDA method and the EVIDEM framework.	Clinical need, clinical comparative results, type of clinical benefit, economics, intervention background, normative criteria, feasibility criteria, opportunity cost
ZTE Public Welfare HTA Center (*34,43*) (2020-present)	City of Shenzhen	AM	Drugs (antineoplastic and immunomodulating agents drugs, cardiovascular system drugs, alimentary tract and metabolism drugs, musculo-skeletal system drugs, anti-infectives for systemic use drugs, nervous system drugs, blood and blood forming organs drugs, *etc.*)	The "Operating Code for Dynamic Adjustment of Hospital Drug Lists Based on HTA" was developed by the ZTE Public Welfare HTA Center, including 10 sets of assessment forms.	Relative safety, relative effectiveness, innovative value and suitability of drugs, economic value of drugs
Wang Q (*54*) (2021)	City of Chongqing	AM, UM	Drugs (alimentary tract and metabolism drugs)	Rapid scoring system established by the hospital	Necessity of clinical use, effectiveness, safety, economics, attributes of national essential medicines, attributes of medical insurance, quality level, packaging attributes, nature of pharmaceutical companies, market attributes, *etc.*
Qiu B (*40,67,68*) (2021)	Hebei Province	AM, UM	Drugs (anti-infectives for systemic use drugs, alimentary tract and metabolism drugs)	Based on "Guidelines for the Assessment and Management of Drug List Selection in Public Medical Institutions in Hebei Province"	Safety, effectiveness, economics, innovation, suitability, accessibility
Duan BJ (*69*), Ren BN (*70*), (2020-2021)	Hebei Province	AM, UM	Drugs (nervous system drugs, antineoplastic and immunomodulating agents drugs)	The Mini HTA Scale developed by the hospital	Pharmaceutical properties, effectiveness, safety, economics, attributes of national insured drugs, attributes of national essential drugs, storage attributes, market attributes, attributes of companies

AM, Admission management; UM, Usage management.

5. Challenges in the development of HB-HTA in China

Although HB-HTA in China has made some progress, it is still in its early developmental stage compared to other developed countries and regions. There are still some challenges in terms of concept recognition, the model of development, limited professionals, and data source on HB-HTA in China.

5.1. Lack of recognition of HB-HTA

Although China has introduced a series of policies to

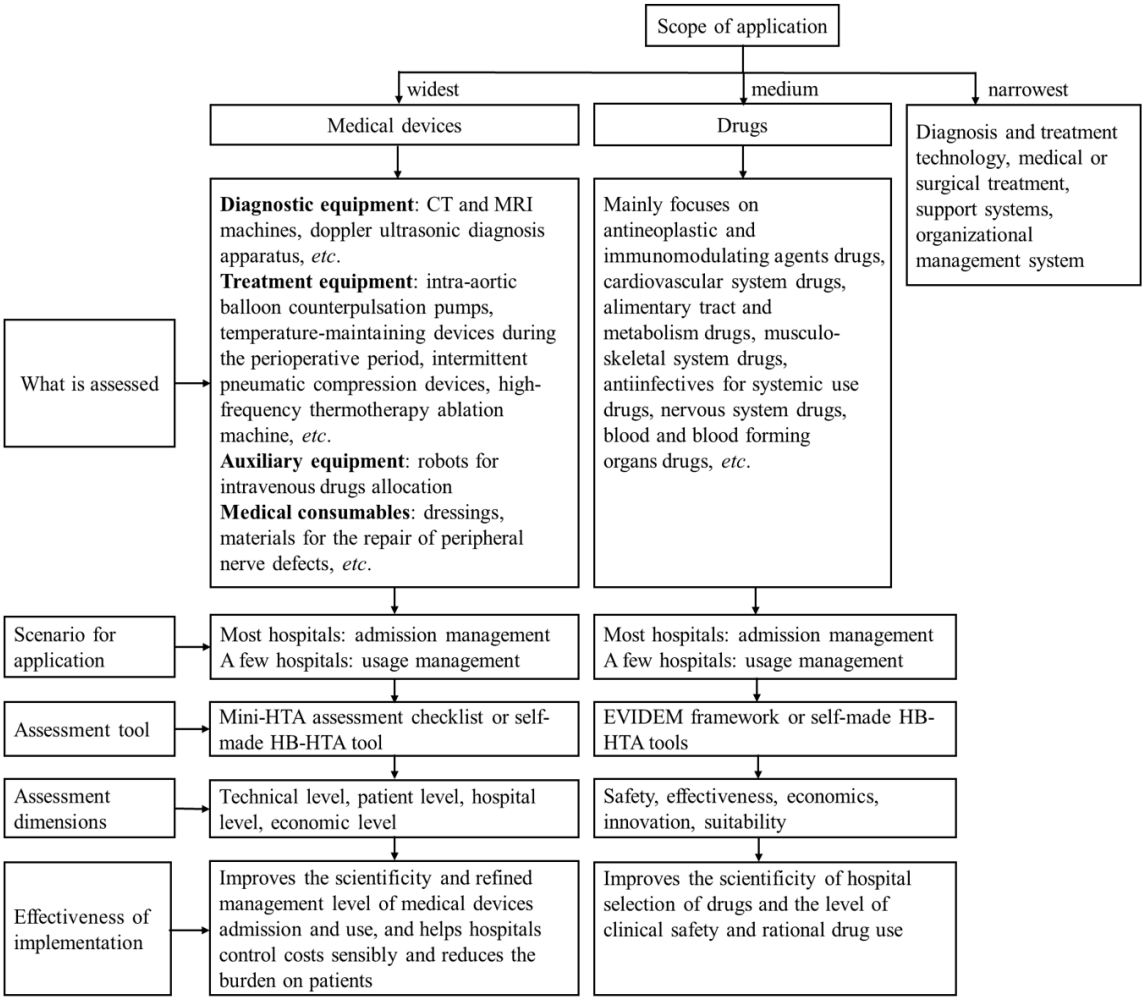

Figure 6. Application of HB-HTA in China.

support the development of HB-HTA in recent years, the policy documents are mainly guidelines, and HB-HTA has not been deemed a requirement. Therefore, the attitude of hospital decision-makers towards HB-HTA will influence the development of HB-HTA. However, hospital decision-makers currently have an insufficient understanding of the value of using HB-HTA and its importance in guiding clinical decision-making (*29,49*), so they rarely consider the results of HB-HTA as an important basis for their decisions. At present, most clinical decisions still depend largely on expert opinions and experience rather than HB-HTA evidence. Patients, companies, and other stakeholders are less likely to be involved.

5.2. The model of HB-HTA development is not standardized

China has not yet established a national HTA organization to formulate and implement standards for HB-HTA and to coordinate and supervise the implementation of HB-HTA. Although the National Medical Management Center has conducted two sets of HB-HTA pilot projects, the use of HB-HTA in China is still mainly considered independently by a few hospitals, and it has not been implemented on a large scale (*29*). There are no official HB-HTA operating guidelines (*57*). As a result, the process of evaluating HB-HTA is relatively arbitrary and the relevant knowledge of evaluators is also insufficient. Reports are of low quality.

5.3. Lack of professionals and unbalanced development among medical institutions

At present, Chinese medical institutions have no mandatory policy documents requiring them to conduct HB-HTA and there is no special financial support for HB-HTA. Therefore, medical institutions do not have sufficient motivation to conduct HB-HTA. In most cases, there is no full-time HB-HTA staff. Most hospital staff participating in HB-HTA belong to the medical equipment department, a medical department, a performance management department, or other specialized departments such as medicine, management, engineering, or library and information science. Researchers with professional HTA backgrounds are

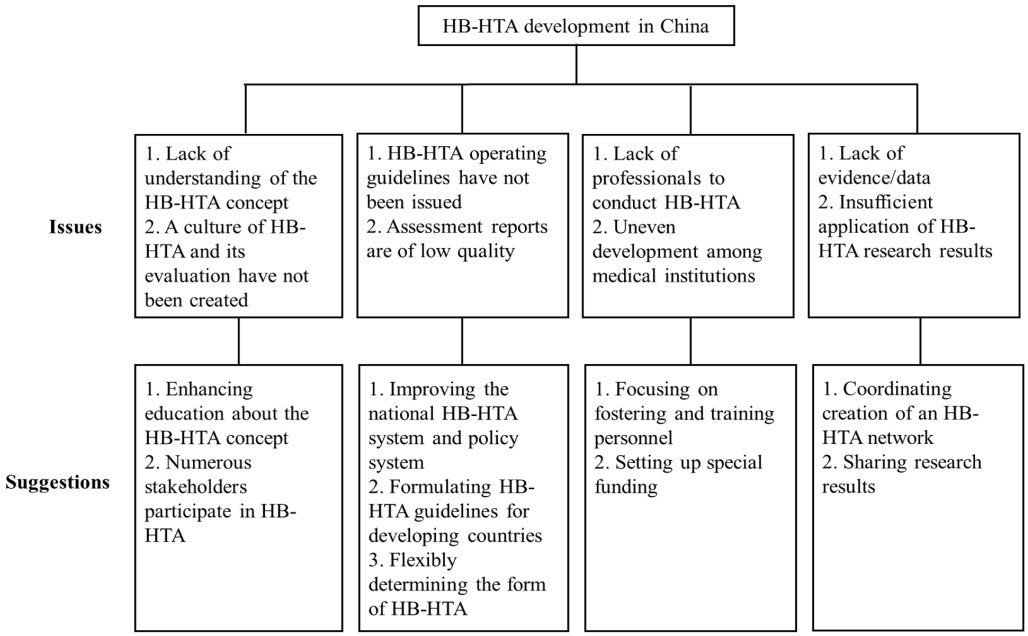

Figure 7. Problems with the development of HB-HTA in China and corresponding solutions.

very rare. Lin *et al*. also found that the shortage of HTA personnel was a relatively common problem among surveyed hospitals (*29,57*). Medical institutions that frequently conduct HB-HTA in China are mainly concentrated in top medical institutions in economically developed regions such as Guangdong, Beijing, Shanghai, and Jiangsu. This is due to the differences in medical resources, human resources, and management skills among medical institutions in different regions. There is still a big gap in the development and use of HB-HTA in primary medical institutions or economically underdeveloped areas (*16*). Some tertiary hospitals in China conduct assessments based on their own specialties and have continued to develop a sophisticated assessment system (*49*), but most hospitals do not have HB-HTA standards and a complete process.

5.4. Lack of evidence/data and insufficient application of results

When implementing HB-HTA, the lack of evidence/data is also one of the main difficulties (*56*). Taking medical devices as an example, evidence of their effectiveness is quite limited. Moreover, there are few comparisons of similar products. The quality of research reports is generally not high (*71*). Decision-making in hospitals is usually very timely. In practice, reports from HB-HTA are often too time-consuming to keep up with the demands of decision-makers (*29*), or the lack of communication with the evaluators leads to an asymmetry between the content of the evaluation reports and the information needs of the decision-makers. At the same time, the wording of research reports is too technical, making them difficult for decision-makers to read and understand the results of the HB-HTA research. This leads to insufficient application of findings from HB-HTA research.

6. Suggestions for the development of HB-HTA

HB-HTA concepts and methods are effective means of supporting hospital management. Based on China's experience with problems promoting and developing HB-HTA, we have tentatively proposed a development path and suggestions for implementation of HB-HTA in line with those in developing countries (Figure 7).

6.1. Enhancing the top-level design of HB-HTA and issuing national HB-HTA guidelines

Several studies have pointed out that the main reasons for the limited use of HTA in low-income and middle-income countries are: lack of official HTA institutions, political factors, and lack of resources (*72*). A national HB-HTA system, including specialized HB-HTA agencies and organizations, needs to be established and budgetary resources need to be allocated in accordance with national goals for development of HB-HTA (*73*). We strongly recommend that special HB-HTA departments be established in hospitals. An internal committee and mini-HTA are preferred for the time being (*74*). However, the current HB-HTA guidelines, manuals, and toolkits are all from developed countries and may not be fully transferable to developing countries (*75*). The experiences of HB-HTA pilot projects need to be summarized and combined with internationally recognized or verified HB-HTA manuals, toolkits, or experiences from other countries. Further development

of HB-HTA requires established HB-HTA procedures and methods at the national level, as well as HB-HTA guidelines and tools that reflect current medical realities in developing countries.

6.2. Raising awareness of HB-HTA and encouraging a wide range of stakeholders to participate in HB-HTA efforts

The basic ideas of HB-HTA need to be promoted at medical institutions and empirical cases needed to be given to decision-makers and heads of relevant departments in order to enhance the concept of evidence-based management and to promote the awareness of evidence-based decision-making (*76*). Decisions about health technologies in hospitals involve many stakeholders with different interests, including the hospital, the pharmaceutical industry, the public, and patients. Early and broad stakeholder participation is particularly important for the implementation of HB-HTA. However, most hospitals make their own decisions about access to new technologies and other stakeholders are rarely involved. The process of technology assessment should not ignore the values of patients and other stakeholders (*73,77*).

6.3. Enhancing the fostering of evaluation personnel

Studies have indicated that lack of expertise and related training are barriers to the development of HB-HTA (*78*). The implementation of HB-HTA requires the joint participation of multidisciplinary teams from medicine, economics, management, sociology, law, and other disciplines. A system for training HTA personnel should be created and development strategies should be formulated (*23*). More attention should be paid to the training of evaluation personnel in hospitals, and especially in health economics (*57*). To alleviate the shortage of professionals, evaluation personnel in medicine at all levels, at research institutes, at colleges and universities, and in associations should be involved in the short term.

6.4. Establishing an HB-HTA network to share research results

HB-HTA is an important part of an HTA network. The most common difficulty in evidence-based work is the lack of high-quality evidence and timely research results (*71,79*). Global HTA institutions are exploring the use of real-world data to complement and enrich evidence related to health technologies (*74*). Establishing a common database will allow the development of a three-tier HTA network – the nation, region, and hospital – to be coordinated (*80,81*). Health agencies and national and regional HTA institutions should support the establishment and development of HB-HTA departments (*73*). Through the HB-HTA network, the latest results from HB-HTA research should be shared in a timely manner and theoretical knowledge should be disseminated. Mutual acceptance of assessment results among medical institutions should be promoted based on a transparent assessment process, scientific methods of assessment, and credible assessment results. Hospitals should increase the dissemination and sharing of assessment results and assessment reports through the HB-HTA network to avoid duplication. Evidence/data on HB-HTA should be continuously updated through the network for the future.

6.5. Flexibly determining the form of HB-HTA

There is no model that is universally applicable to hospitals (*82-84*). The type of HB-HTA to be undertaken depends on the external policy environment, the specific hospital culture, the stage and sophistication of health technology development, the type of technology, the use of resources, the quantity and quality of evidence, the requirements for quality and completeness of reports, the demand for timeliness, and other factors (*85*). For example, the evaluation of consumables and devices is easier to quantify and the evaluation process is more repeatable and versatile, whereas the quantitative assessment of new clinical technologies in diagnostics and surgery is more difficult (*29*). If the quality of the available evidence is low or even missing, the HB-HTA report is presented in the form of a checklist. In practice, the form of HB-HTA can be flexible, depending on the technical assessment requirements and the resources available to decision-makers.

7. Conclusion

Improving the rational allocation of medical resources is an urgent need under the status quo of the irrational and rapid growth of medical expenses, meanwhile, it is also a higher realistic requirement for hospitals in terms of expense control, quality improvement, and scientific management under the background of new healthcare system reform. As a tool to effectively control medical costs and improve quality, HB-HTA can help medical institutions achieve scientific management and decision-making, improve the allocation efficiency of health care resources, and ensure medical quality and safety. In the context of comprehensively promoting the construction of a healthy China and deepening the reform of the medical and health care system, it has become an appropriate strategy for Chinese medical institutions to carry out HB-HTA activities. From 2005 to 2022, the development of HB-HTA in China has gone through the initiation phase and the preliminary exploratory phase, and now it has entered a period of rapid development. China basically has the foundation for the development of HB-HTA, and has accumulated some application

cases. In order to further promote the application of HB-HTA in developing countries, it is necessary to solve the core problems in terms of concept recognition, the mode of development, and limited professionals and data based on a case study in China, formulate a integrated development strategy in line with national conditions, establish the application mechanism and the implementation roadmap of HB-HTA, and promote the sustainable development of HB-HTA.

Funding: This work was supported by a grant from the Natural Science Foundation Program of China (no. 71904126).

Conflict of Interest: The authors have no conflicts of interest to disclose.

References

1. Mohr PE, Mueller C, Neumann P, *et al.* The impact of medical technology on future health care cost, Final report. The Project Hope Center for Health Affairs, Chicago: University of Chicago, 2011; pp.1-28.
2. Umscheid CA, Williams K, Brennan PJ. Hospital-based comparative effectiveness centers: Translating research into practice to improve the quality, safety and value of patient care. J Genl Intern Med. 2010; 25:1352-1355.
3. Laura Sampietro-Colom. Final Report Summary - ADHOPHTA (Adopting Hospital Based Health Technology Assessment in EU). *http://cordis.europa.eu/result/rcn/184859_en.html* (accessed June 20, 2022).
4. AdHopHTA project. AdHopHTA: An European project on hospital based health technology assessment. *http://www.adhophta.eu/adhophta-european-project-hospital-based-health-technology-assessment* (accessed June 20, 2022).
5. Lholm, AM, Kidholm K, Birk-Olsen M, Christensen JB. Hospital managers' need for information on health technology investments. Int J Tech Assess in Health Care. 2015; 31:414-425.
6. McGregor M. What decision-makers want and what they have been getting. Value in Health. 2006; 9:181-185.
7. Sampietro-Colom L, Morilla-Bachs I, Gutierrez-Moreno S, *et al*. Development and test of a decision support tool for hospital health technology assessment. Int J Tech Assess in Health Care. 2012; 28:460-465.
8. AdHopHTA project. Introduction to HB-HTA and the AdHopHTA products. *http://www.adhophta.eu/tags/materials* (accessed June 20, 2022).
9. National Health and Family Planning Commission (former name). Notice on printing and distribution of opinions on controlling unreasonable growth of medical expenses at public hospitals. *http://www.nhc.gov.cn/tigs/s3577/201511/0038da2bf8fe43d69511fb675e205d37.shtml* (accessed June 20, 2022). (in Chinese)
10. General Office of the State Council. Guidelines of promoting the creation of a hierarchical medical system. *http://www.gov.cn/zhengce/content/2015-09/11/content_10158.htm* (accessed June 26, 2022). (in Chinese)
11. CPC Central Committee, The State Council. Outline of "Healthy China 2030". *http://www.gov.cn/zhengce/2016-10/25/content_5124174.htm* (accessed June 26, 2022). (in Chinese)
12. General Office of the State Council. Guidelines of further reforming methods of paying for basic medical insurance. *http://www.gov.cn/zhengce/content/2017-06/28/content_5206315.htm* (accessed June 20, 2022). (in Chinese)
13. National Health and Family Planning Commission (former name). Notice of the National Health and Family Planning Commission on revocation of approval for clinical use of class-three medical technology. *http://www.nhc.gov.cn/yzygj/s3585/201507/c529dd6bb8084e09883ae417256b3c49.shtml* (accessed June 20, 2022). (in Chinese)
14. Chen Y, Banta D, Tang, Z. Development of health technology assessment in China. Int J Technol Assess Health Care. 2009; 25:202-209. (accessed June 26, 2022). (in Chinese)
15. Xia L, Dong J, Xu YY. Health technology assessment and hospital management. J Military Med College. 2005; 23-24. (in Chinese)
16. Xu SM, Dai ZQ, Wu X, Li MM, Liao X. A general review of health technology assessment in hospitals at home and abroad. Chinese J Trad Chinese Med. 2022; 47:3136-3143. (in Chinese)
17. Zhao NZ, Guo AY, Chen F. Application of evidence-based medicine to hospital management. North China Natl Defense Med. 2005; 17:3. (in Chinese)
18. Yang H. Evidence-based management of medical consumables. Chinese J Med Devices. 2009; 33:134-136. (in Chinese)
19. Yang H. The role of evidence-based evaluation and economic evaluation in the pricing of medical consumables. Chinese J Med Devices. 2010; 34:221-223. (in Chinese)
20. Huang J, Zhang YG, Liu YQ, Liao G, Du L. Introduction to mini health technology assessment. Chinese J Evidence-based Medicine. 2014; 14:901-904. (in Chinese)
21. Chen YY, He Y, Chi XYZ, Wei Y, Shi LZ. Development of health technology assessment in China: New challenges. BioSci Trends. 2018; 12:102-108.
22. Zhang XT, Liu SL. Overview of health technology assessment of hospital medical devices. Proceedings of the 15th National Annual Conference of the Chinese Medical Engineering Society. 2015; 339-343. (in Chinese)
23. Lv LT, Fu RH. Discussion on the way to introduce medical technology assessment in medical technology management. Chinese Hosp Mgmt. 2016; 36:17-20. (in Chinese)
24. European Union AdHopHTA Project Team. Hospital health technology assessment: Handbook and toolkit. Shanghai Jiao Tong University Press. Shanghai, 2017. (in Chinese)
25. Central People's Government of the People's Republic of China. Regulations on the prevention and handling of medical disputes. *http://www.gov.cn/zhengce/content/2018-08/31/content_5318057.htm* (accessed June 28, 2022). (in Chinese)
26. Central People's Government of the People's Republic of China. Guidelines of the General Office of the State Council on reforming and improving the system for comprehensive supervision of the medical and health care industry. *http://www.gov.cn/zhengce/content/2018-08/03/content_5311548.htm* (accessed June 28, 2022). (in Chinese)
27. Central People's Government of the People's Republic of China. Administrative measures for medical consumables at medical Institutions. *http://www.gov.cn/gongbao/*

content/2019/content_5442286.htm (accessed June 28, 2022). (in Chinese)
28. The National People's Congress. Law of the People's Republic of China to Promote Basic Medical Care and Health. *http://www.npc.gov.cn/npc/c30834/201912/15b7b1cfda374666a2d4c43d1e15457c.shtml* (accessed June 28, 2022). (in Chinese)
29. Lin X, Bai F, Lv LT, Wang HY, He JJ, Jin CL. Experimental results of and strategies to promote hospital technology assessment in China. Chinese J Evidence-based Med. 2020; 20:94-97. (in Chinese)
30. Bai F, Lin X. Carefully administered pilot projects at 7 hospitals. China Health. 2019; 71-73. (in Chinese)
31. Department of Drug Policy and Essential Medicine System, National Health Commission. Notice of the National Health Committee General Office on the comprehensive clinical evaluation of drugs. *http://www.nhc.gov.cn/yaozs/s2908/202107/532e20800a47415d84adf3797b0f4869.shtml* (accessed June 21, 2022). (in Chinese)
32. Health Development Research Center, National Health Commission. Notice of the National Center for Comprehensive Evaluation of Drugs and Health Technology on the issuance of technical guidelines for comprehensive clinical evaluation of cardiovascular, antitumor, and pediatric drugs. *https://mp.weixin.qq.com/s/kfelcNNn6RaqBUmWgkLMhQ* (accessed June 21, 2022). (in Chinese)
33. Zeyu Salon. Expert consensus on implementing hospital health technology assessment to manage medical equipment. *https://mp.weixin.qq.com/s/Wp2tFWVwF6qrsoNII4zaWQ* (accessed June 21, 2022). (in Chinese)
34. ZTE Public Welfare HTA Center. HTA Report. *http://www.ztehta.com/reporttype/hta-reports/* (accessed June 15, 2022). (in Chinese)
35. Bao JL, Zhu ZY. Framework for microhygiene technology assessment of medical devices. China Med Equip. 2020; 35:6-10. (in Chinese)
36. Hua T, Zheng K, Li BP, Shi J, Cheng XQ, Shen XL. Exploration of a health technology evaluation scale to manage access to high value consumables in medical institutions. China Med Equip. 2022; 37:1-4,19. (in Chinese)
37. Yang H, Tang M, Li B, Tao MF, Yin SK. Exploration of the management of medical consumables based on a hospital technology assessment. Health Resources in China. 2018; 21:101-105. (in Chinese)
38. Fei M. Exploration of the process of accepting new medical consumables based on a health technology assessment. China Med Equip. 2020; 35:24-28. (in Chinese)
39. Zhao ZZ, Fan R, Cheng XH. Application of health technology assessment to management of medical equipment allocation at this hospital. China Med Equip. 2018; 33:170-172,177. (in Chinese)
40. Qiu B, Wang XC, Li CX, Dong ZJ. Application of hospital health technology assessment to the selection and evaluation of oral hepatoprotective drugs. Med Rev. 2021; 40:1443-1449. (in Chinese)
41. Bao Y, Gao B, Meng M, Ge B, Yang Y, Ding C, Shi B, Tian L. Impact on decision making framework for medicine purchasing in Chinese public hospital decision-making: determining the value of five dipeptidyl peptidase 4 (DPP-4) inhibitors. BMC Health Serv Res. 2021; 21:807.
42. Xiang Q, Yang HB, Guo Y, Wu WX, Wu RH, Liu XH, Wei Q. Application and exploration of hospital health technology assessment in a medical equipment procurement decision. Res on Health Econ. 2021; 38:54-57. (in Chinese)
43. ZTE Public Welfare HTA Center. The 5th Guangming Pharmaceutical Forum successfully held: The "Shenzhen Model of Health Technology Assessment". *http://u3v.cn/6l1plv* (accessed July 15, 2022). (in Chinese)
44. Gu YT, Feng R, Xi Q, Application of hospital health technology assessment to purchasing an intravenous drug dispensing robot. J Practical Clin Med. 2020; 24:8-11. (in Chinese)
45. Nie HX. Improvement and practice of managing access to medical consumables at this hospital. Chinese Med Equip. 2017; 32:157-159. (in Chinese)
46. Wang Q, Zhang R. Status of application status and development concepts of hospital health technology assessment in drug management. China Pharmacy. 2020; 31:773-777. (in Chinese)
47. Wan YZ, Ji CD, Zhu LY, Xu C, Ma Y, Chen X, Fu QQ. Introduction of mini health technology assessment through assessment cases. Chinese J Med Res Mgmt. 2016; 29:335-337. (in Chinese)
48. Yang K, Wu XF, Shao L. Evaluation and application of a health technology assessment based on a log analysis of large equipment. Surg Res and New Tech.2019; 8:205-207,215. (in Chinese)
49. Lv LT, Fu JL, Lin X, Bai F. Difficulties with and solutions to health technology assessment in Chinese hospitals. Chinese Hosp Mgmt. 2019; 39:7-10. (in Chinese)
50. Zhou L. Management and practice of accepting medical consumables. Med and Health Care Equip. 2019; 40:83-85. (in Chinese)
51. Shu YY. Refined management of medical consumables based on hospital health technology assessment and disease diagnosis-related grouping. Med Equip. 2021; 34:76-77. (in Chinese)
52. Jiang YB. Comprehensive evaluation and discussion of the benefit of using valuable medical equipment in hospitals. China Med Equip. 2020; 35:150-154. (in Chinese)
53. Yang C, Wang Y, Hu X, Chen Y, Qian L, Li F, Gu W, Liu Q, Wang D, Chai X. Improving hospital based medical procurement decisions with health technology assessment and multi-criteria decision analysis. Inquiry. 2021; 58:1-14.
54. Wang Q, Liu D, Wang Q, Zhang R. Application of hospital health technology assessment to the selection and evaluation of three SGLT2 inhibitors. J Pharmacoepidem. 2021; 30:579-585. (in Chinese)
55. Gagnon MP. Hospital-based health technology assessment:Developments to date. Pharmacoecon. 2014; 32:819-824.
56. Yang H. Application of hospital health technology assessment to the management of medical consumables. China Med Equip. 2017; 32:123-126. (in Chinese)
57. Lin X, Lv LT, Jin D, Teng YJ, Li N, Bai F. Feasibility analysis of broadening hospital health technology assessment in China. Chinese Hosp Mgmt. 2019; 39:11-13. (in Chinese)
58. Qiu XH, Yang C, Liu J, Huang J. Application of mini-health technology assessment to management of the allocation of special nonmagnetic anesthesia machines. West China Med Sci. 2019; 34:665-668. (in Chinese)
59. Bai F, Li MX, Liu XF, Lin X, Li YF, Xing X, Li R, Li

XX, Yang KH. Bibliometric analysis of hospital health technology assessment. Chinese J Evidence-based Med. 2022; 22:948-954. (in Chinese)
60. Fu QQ, Ji CD, Xu C, Yao CX, Ma Y, Ai HJ. Mini-health technology assessment based on the needs of healthcare facilities. Chinese J Hosp Mgmt. 2018; 25:131-134. (in Chinese)
61. Tang M, Yang H. Discussion of the procurement process and inclusion criteria for newly added medical consumables at this hospital. China Med Equip. 2018; 33:162-165. (in Chinese)
62. Luo L, Tang M, Yang H, Bai F, Lin X. Application of hospital health technology assessment to management of medical consumables: A case study of a material to repair peripheral nerve defects. Chinese Hosp Mgmt. 2019; 39:47-49. (in Chinese)
63. Zhang H, Xia HL, Gao GX. Design and implementation of a model to assess access to medical equipment. Chinese Health Qual Mgmt. 2021; 28:1-5,8. (in Chinese)
64. Zhu DD, Gao GX, Wang XJ, Xia HL, Li YF, Zhang XY, Bian LJ. Creation and use of a model to assess access for clinical trials of medical devices. Chinese Health Qual Mgmt. 2021; 28:6-9. (in Chinese)
65. Yan HF, Li ZG, Wang Y, Zhao J. Study on a system for assessment of the allocation of hospital CT equipment based on a health technology assessment. China Med Equip. 2022; 19:132-137. (in Chinese)
66. Cao XM, Gao S, Zhu X, Wang M, Zhang HZ, Cheng XH. Mini-health technology assessment of a combined thermal and cold ablation system for tumor treatment. Chinese Pharmacoecon. 2022; 17:51-55. (in Chinese)
67. Qiu B, Yang HT, Song HJ, Du RX, Dong ZJ. Application of hospital health technology assessment to the selection and evaluation of macrolide antibiotics. Chinese Modern Applied Pharmacy. 2021; 38:1228-1236. (in Chinese)
68. Qiu B, Li X, Yang HT, Du RX, Dong ZJ. Application of hospital health technology assessment to the selection and evaluation of sulfonylurea drugs. Chinese J Pharm Sci. 2021; 56:153-161. (in Chinese)
69. Duan BJ, Fang LZ, Li XM, Cao GX, Dong ZJ. Mini health technology assessment of fluoxetine and Paxil. Med Rev. 2021; 40:1361-1367. (in Chinese)
70. Ren BN, Xue CJ, Li X, Zhao Y, Dong ZJ. Mini health technology assessment of four antiangiogenic drugs for the treatment of non-small cell lung cancer. Chinese J New Drugs. 2021; 30:2009-2016. (in Chinese)
71. Wang CY. Analysis of the difficulties of and solutions to technical assessment of medical devices in hospitals. China Health Industry. 2018; 15:156-157. (in Chinese)
72. Attieh R, Gagnon MP. Implementation of local/hospital-based health technology assessment initiatives in low- and middle-income countries. Int J Technol Assess Health Care. 2012; 28:445-451.
73. He JJ, Geng JS, He D, Ren XX, Yang H, Wang HY, Chen MX, Jin CL, Hu SL. Revelations for China from the European Hospital Technology Assessment Project. Chinese Health Resources. 2018; 21:94-100. (in Chinese)
74. Lv LT, Shi WK. Function of and implementation strategies for hospital health technology assessment in the context of DRG reform. Chinese Health Policy Res. 2020; 13:26-32. (in Chinese)
75. Lin X, Bai F, Qin XX, Fu C, Jin CL, Wang HY, He JJ, Tao HB. Considering developing hospital health technology assessment in China. Chinese J Evidence-based Med. 2018; 18:1376-1379. (in Chinese)
76. Nicolas, Martelli, Cyril, *et al*. Hospital-based health technology assessment in France: A focus on medical devices. Therapies. 2017; 72:115-123.
77. Tal O, Booch M, Bar-Yehuda S. Hospital staff perspectives towards health technology assessment: Data from a multidisciplinary survey. Health Res Policy Sys. 2019; 17:72.
78. Pereira C, Rabello R, Elias F. Hospital-based health technology assessment in Brazil: An overview of the initial experiences. Int J Tech Assess in Health Care. 2017; 33:227-231.
79. Halmesmäki E, Pasternack I, Roine R. Hospital-based health technology assessment (HTA) in Finland: A case study on collaboration between hospitals and the national HTA unit. Health Res Policy and Systems. 2016; 14:25.
80. Lv LT, Shi WK, Lin X, Bai F. Research on the path for implementation of a hospital health technology assessment based on international experience. Chinese Hospital Mgmt. 2019; 39:17-20. (in Chinese)
81. Peng XL. Exploring the application of hospital health technology assessment to management of medical consumables. Mgmt Observation. 2019; 191-192. (in Chinese)
82. Wang HY, Chen MX, He JJ, He D, Jin CL. The value of application and development strategies of hospital technology assessment in China. Chinese Health Resources. 2018; 21:83-85. (in Chinese)
83. Cicchetti A, Iacopino V, Coretti S, Fiore A, Marchetti M, Sampietro-Colom L, Kidholm K, Wasserfallen JB, Kahveci R, Halmesmäki E, Rosenmöller M, Wild C, Kivet RA. Toward a contingency model for hospital-based health technology assessment: Evidence from ADHOPHTA project. Int J Tech Assess in Health Care.2018; 1-7.
84. Więckowska B, Raulinajtys-Grzybek M, Byszek K. Using the dynamic SWOT analysis to assess options for implementing the HB-HTA model. Int J Environ Res Public Health. 2022; 19:7281.
85. Geng JS, Cao Y, He JJ, He D, Wang HY, Jin CL, Hu SL. Discussion of the operating principles of hospital technology assessment. Health Resources in China. 2018; 21:86-89, 110. (in Chinese)

Received November 3, 2022; Revised January 21, 2023; Accepted February 9, 2023.

[§]These authors contributed equally to this work.
**Address correspondence to:*
Jiangjiang He, Shanghai Health Development Research Center, Room 802, NO.1477 Beijing Road (West), Jing 'an District, Shanghai 200040, China.
E-mail: hejiangjiang@shdrc.org

Peipei Song, Center for Clinical Sciences, National Center for Global Health and Medicine, 1-21-1 Toyama, Shinjuku, Tokyo 162-8655, Japan.
E-mail: psong@it.ncgm.go.jp

Released online in J-STAGE as advance publication February 12, 2023.

Mini-Review

DOI: 10.5582/bst.2022.01534

Herbal medicines exhibit a high affinity for ACE2 in treating COVID-19

Bo Zhang[1], Fanghua Qi[2,*]

[1] Department of Traditional Chinese Medicine Orthopedics, Neck-Shoulder and Lumbocrural Pain Hospital affiliated to Shandong First Medical University, Ji'nan, China;
[2] Traditional Chinese Medicine, Shandong Provincial Hospital affiliated to Shandong First Medical University, Ji'nan, China.

SUMMARY Coronavirus Disease 2019 (COVID-19) has been an unprecedented disaster for people around the world. A point particularly worth noting is that herbal medicines have made great contributions to the prevention and treatment of COVID-19 in China. Angiotensin converting enzyme 2 (ACE2) has been identified as the critical functional receptor for SARS-CoV-2. It can bind to the receptor-binding domain (RBD) of the spike protein (S protein), which is responsible for the entry of the coronavirus into host cells. Therefore, ACE2 can be regarded as an important intervention target for COVID-19. Recently, many herbal medicines have exhibited a high affinity for ACE2 in treating COVID-19. The current work summarized these herbal medicines including formulas (such as Lianhua Qingwen capsules, Xuebijing injection, Qingfei Paidu Decoction, Huashi Baidu formula, Shufeng Jiedu capsules, and Maxing Shigan decoction), single herbs including *Ephedra sinica Stapf* (Mahuang), *Scutellariae radix* (Huangqin), *Lonicera japonica* (Jinyinhua), and *Houttuynia cordata* (Yuxingcao), and active ingredients (such as ursodeoxycholic acid, glycyrrhizic acid, glycyrrhizin, salvianolic acid, quercetin, and andrographidine C), which have exhibited a high affinity for ACE2 in treating COVID-19. We hope this work may provide meaningful and useful information on further research to investigate the mechanisms of herbal medicines against SARS-CoV-2 and follow-up drug discovery.

Keywords COVID-19, SARS-CoV-2, herbal medicines, ACE2, S protein

1. Introduction

Coronavirus Disease 2019 (COVID-19) has been an unprecedented disaster for people around the world. A point particularly worth noting is that herbal medicines have made great contributions to the prevention and treatment of COVID-19, and they have been used in over 90% of treatments across China. Many herbal medicines are reported to have antiviral, anti-inflammatory, and immunoregulatory action and to protect target organs during the treatment of COVID-19 by multiple components acting on multiple targets in multiple pathways (*1*).

Angiotensin converting enzyme 2 (ACE2) has been identified as the critical functional receptor for SARS-CoV-2. It can bind to the receptor-binding domain (RBD) of the spike protein (S protein), which is responsible for the entry of the coronavirus into host cells (*2*). After entry, the SARS-CoV-2 RNA genome is released into the cytosol, where it highjacks host replication machinery for viral replication, assemblage, as well as the release of new viral particles. Therefore, ACE2 should be a target to screen drugs inhibiting the replication and proliferation of SARS-COV-2.

Recently, many herbal medicines have exhibited a high affinity for ACE2 in treating COVID-19 (*3*). These herbal medicines can target ACE2 to prevent SARS-CoV-2 from entering into host cells. The current work has summarized these herbal medicines including formulas, single herbs, and active ingredients, which have exhibited a high affinity for ACE2 in treating COVID-19 (Figure 1). This work may provide meaningful and useful information on further research to investigate the mechanisms of herbal medicines against SARS-CoV-2.

2. Herbal formulas

COVID-19 is categorized as a pestilence according to traditional Chinese medicine (TCM) theory. Herbal medicines have been used to treat and prevent viral infections for thousands of years, and herbalists have

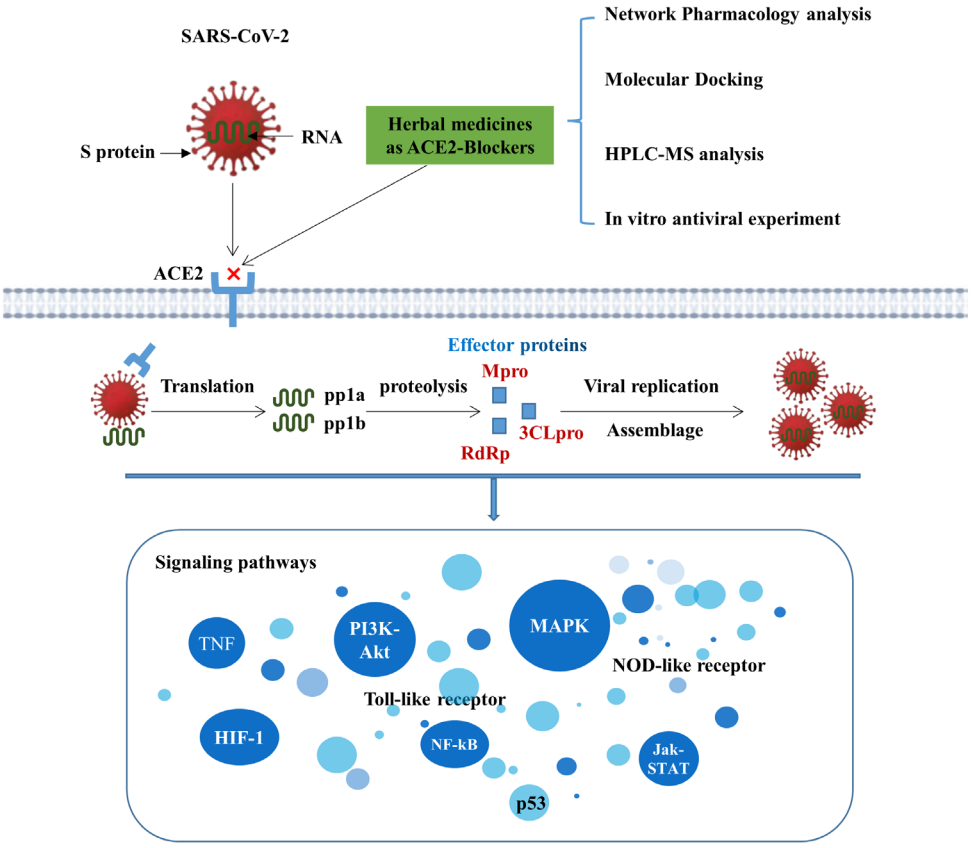

Figure 1. Overview of the probable anti-COVID-19 activities of herbal medicines. Herbal medicines might be ACE2-blockers against COVID-19.

accumulated a large amount of clinical experience and they have developed effective prescriptions (*4*). In guidelines on fighting COVID-19, the National Health Commission (NHC) of China has recommended some herbal formulas, and particularly "three Chinese patent medicines and three TCM prescriptions", which have proven to be efficacious in treating COVID-19 (*5*). Recently, numerous studies have indicated that the potential mechanisms of these herbal formulas in the treatment of COVID-19 might involve down-regulating ACE2 (Table 1).

Lianhua Qingwen capsules/granules have been officially repurposed by the China Food and Drug Administration (CFDA) for patients with mild COVID-19 since April 2020. Several components of Lianhua Qingwen capsules (rhein, forsythoside A, forsythoside I, neochlorogenic acid, and its isomers) not only showed a high affinity for ACE2 but also inhibited SARS-CoV-2 by affecting binding between ACE2 and the S protein (*6*). Xuebijing injection is the only Chinese patent medicine approved in China for the treatment of sepsis with efficacy in severe and critical COVID-19 cases. Based on a bioinformatic analysis, Xuebijing injection alleviated COVID-19-induced cardiac dysfunction by inhibiting oxidative stress, preventing atherosclerotic plaque formation, and limiting inflammation and apoptosis by targeting ACE2 and 7 hub genes (CCL2, CXCL8, FOS, IFNB1, IL-1A, IL-1B, and SERPINE1) (*7*). In addition, molecular docking results revealed that most of the active compounds in Xuebijing injection had a good binding activity with ACE2, 3CLpro, and the S protein; the three compounds with the highest affinity were anhydrosafflor yellow B, salvianolic acid B, and rutin (*8*).

Qingfei Paidu Decoction is recommended for all stages of COVID-19 according to the “Diagnosis and Treatment Program for COVID-19” issued by the NHC of China. Supported by network pharmacology, Qingfei Paidu Decoction and its major herbs including *Ephedra sinica*, Bupleurum chinense, Pogostemon cablin, Cinnamomum cassia, and Scutellariae Radix displayed anti-oxidative, immuno-modulatory, and antiviral action by preventing a cytokine storm and regulating ACE2 receptor binding (*9*). Three active components (oroxylin A, hesperetin and scutellarin) of Qingfei Paidu Decoction significantly inhibited the release of IL-6, IL-1β, and CXCL-10 from THP-1 macrophages challenged with the SARS-CoV-2 S protein, which suggested that the anti-inflammatory effects of Qingfei Paidu Decoction might be attributed to the effects of these active components (*10*). Oroxylin A inhibits the entry of SARS-CoV-2 pseudovirus into target cells and prevents SARS-CoV-2 S protein-mediated cell-cell fusion by binding with the ACE2 receptor.

Table 1. Some herbal formulas exhibiting a high affinity for ACE2 in treating COVID-19

Herbal formulas	Composition	Screened ingredients	Effects	Experimental method	*Ref.*
Lianhua Qingwen capsules	13 herbs: Lianqiao, Jinyinhua, Mahuang, Kuxingren, Shigao, Banlangen, Guanzhong, Yuxingcao, Huoxiang, Dahuang, Hongjingtian, Bohe, and Gancao	Rhein, forsythoside A, forsythoside I, neochlorogenic acid, and its isomers	(*i*) Exhibit a high affinity for ACE2, (*ii*) Inhibit SARS-CoV-2 by affecting the binding between ACE2 and S protein.	Biochromatography screening, molecular docking bioinformatics, and molecular docking technology	*6*
Xuebijing injection	5 herbs: Honghua, Chishao, Chuanxiong, Danshen, and Danggui	Quercetin	Target ACE2 and 7 hub genes (CCL2, CXCL8, FOS, IFNB1, IL-1A, IL-1B, SERPINE1).	Network pharmacology and RNA-sequencing	*7*
		Anhydrosafflor yellow B, salvianolic acid B and rutin	Bind with ACE2, 3CLpro, and S protein.	Network pharmacology and molecular docking	*8*
Qingfei Paidu Decoction	21 herbs: Mahuang, Gancao, Kuxingren, Shigao, Guizhi, Zexie, Zhuling, Baizhu, Fuling, Chaihu, Huangqin, Banxia, Shengjiang, Ziyuan, Kuandonghua, Shegan, Xixin, Shanyao, Zhishi, Chenpi, and Huoxiang	Oroxylin A, hesperetin and scutellarin	Inhibit the IL-6, IL-1β and CXCL-10 release and bind with ACE2.	Bioinformatics methods, network pharmacology, and molecular docking	*10*
Huashi Baidu formula	14 herbs: Mahuang, Huoxiang, Shigao, Kuxingren, Banxia, Houpu, Cangzhu, Caoguo, Fuling, Huangqi, Chisao, Tinglizi, Dahuang, and Gancao	Baicalein and quercetin	Bind with ACE2.	Network pharmacology and molecular docking	*11*
		Isotrifoliol and ellagic acid	Bind with ACE2, ADAM17, and 3CLpro.	Network pharmacology and molecular docking	*12*
Shufeng Jiedu capsule	8 herbs: Huzhang, Lianqiao, Banlangen, Chaihu, Baijiangcao, Mabiancao, Lugen, and Gancao	Kaempferol, Wogonin, and Baicalein	Exhibit a strong potential affinity for ACE2 and Mpro.	Network pharmacology and molecular docking	*13*
		β-sitosterol, luteolin, kaempferol, quercetin, and stigmasterol	Bind well with three typical target proteins including ACE2, 2OFZ, and 1SSK.	Network pharmacology and molecular docking	*14*
Maxing Shigan decoction	4 herbs: Mahuan, Kuxingren, Shigao, and Gancao	Amygdalin, euchrenone, glycyrrhizin, and glycyrol	Exhibit a strong potential affinity for ACE2, Mpro and RdRp.	Network pharmacology, molecular docking, and *in vitro* experimental verification	*15*

As one of the "three Chinese patent medicines and three TCM prescriptions", Huashi Baidu formula is usually recommended as an auxiliary medicine for the treatment of patients with severe COVID-19. A network analysis indicated that Huashi Baidu formula affected SARS-CoV-2 mainly by regulating multiple signaling pathways (TNF, PI3K-Akt, NOD-like receptor, MAPK, and HIF-1) through ACE2 (*11*). Baicalein and quercetin, the two leading compounds in Huashi Baidu formula, have a high affinity for ACE2, which indicated that they might play an important role in the treatment of COVID-19. Another network analysis indicated that the active ingredients in Huashi Baidu formula, such as isotrifoliol and ellagic acid, had an excellent binding ability with crucial proteins directly related to COVID-19, including ACE2, ADAM17, and 3CLpro, and that they were directly efficacious (*12*).

Shufeng Jiedu capsules are a Chinese patent medicine that is recommended as a basic prescription and used widely in the clinical treatment of COVID-19. According to a network analysis, the active components in Shufeng Jiedu capsules (such as kaempferol, wogonin, and baicalein) had good binding activity with both SARS-CoV-2-Mpro and ACE2 and acted on multiple signaling pathways (such as PI3K-Akt, TNF, HIF-1, p53, and Toll-like receptor), thus affecting novel coronaviruses (*13*). Another network analysis identified 5 key compounds (β-sitosterol, luteolin, kaempferol, quercetin, and stigmasterol) in Shufeng Jiedu capsules and 10 hub target genes (TP53, AKT1, NCOA1, EGFR, PRKCA, ANXA1, CTNNB1, NCOA2, RELA, and FOS) (*14*). The hub target genes were mainly enriched in pathways including the MAPK, PI3K-Akt, and cAMP signaling pathways, which could be the underlying pharmacological mechanisms of Shufeng Jiedu capsules for treating COVID-19. Moreover, the above key compounds had a high binding activity with three typical target proteins including ACE2, 2OFZ, and 1SSK.

Maxing Shigan decoction is a classic herbal formula that was first recorded in the famous book "Shanghan Zabing Lu" written by Zhang Zhongjing during the Eastern Han Dynasty (25-220 A.D.). The "three Chinese patent medicines and three TCM prescriptions", excluding the Xuebijing injection, contain Maxing Shigan Decoction. Maxing Shigan Decoction might play an antiviral, anti-inflammatory, and immunoregulatory role through the JAK-STAT and PI3K/AKT signaling pathways mainly *via Glycyrrhiza uralensis* (Gancao) and *Semen armeniacae amarum* (Kuxingren) (*15*). Moreover, the components with a strong potential affinity (the top 10) for ACE2, Mpro, and RdRp are mainly from Gancao and Kuxingren. Amygdalin was selected as the optimal candidate component to bind to all three key targets, and euchrenone, glycyrrhizin, and glycyrol also exhibited superior affinity for ACE2, Mpro, and RdRp, respectively.

3. Single herbs

Some single herbs have been widely used in Asia to treat lung diseases, such as a cold, cough, and asthma for thousands of years and they are the major constituent herbs of some famous formulas to treat COVID-19. These single herbs such as *Ephedra sinica* Stapf (Mahuang), *Scutellariae radix* (Huangqin), *Lonicera japonica* (Jinyinhua), and *Houttuynia cordata* (Yuxingcao) have displayed efficacy against pneumonia caused by SARS-CoV-2, and the potential mechanism might be related to ACE2 (Table 2).

Mahuang, as one of the major constituent herbs of a multi-component herbal formula, has been widely used to treat COVID-19 in China. Lv et al. found that three compounds (ephedrine, pseudoephedrine, and methylephedrine) screened out from Mahuang with ACE2-binding features acted as blockers, inhibiting the SARS-CoV-2 spike pseudovirus from entering ACE2h (HEK293T cells over-expressing ACE2) (*16*). Another similar study indicated that quinoline-2-carboxylic acids identified as novel active constituents of Mahuang could be considered as potential therapeutic agents for COVID-19 (*17*). They inhibited both the binding of SARS-CoV-2 RBD to ACE2 and the infectivity of SARS-CoV-2 S protein pseudoviruses in 293T-ACE2 and Calu-3 cells. The herb pair Mahuang-Kuxingren was used to prevent and treat COVID-19 by directly inhibiting the virus, regulating immune responses, and promoting body repair. Some key components of Mahuang-Kuxingren, such as β-sitosterol, estrone, and stigmasterol, had a high binding activity to 3CLpro and ACE2 according to a molecular docking simulation (*18*). In addition, the active compounds, and especially licorice glycoside E and xambioona, from the herb pair Mahuang-Gancao, bound well to COVID-19 related targets, including 3CLpro, the S protein, and ACE2 (*19*).

Huangqin is considered to be an "herbal antibiotic" that can fight against COVID-19. Based on a network analysis, Huangqin primarily regulated the MAPK and NF-κB signaling pathways *via* active components such as baicalein and scutellarin and blocked SARS-CoV-2 spike binding to human ACE2 receptors (*20*). In addition, *in vitro* bioassays showed that Baicalein inhibited SARS-CoV-2 from entering into Vero E6 cells. It was the most effective component in Huangqin, with both anti-inflammatory and antiviral action.

Based on its effect on heat-clearing and detoxification, Jinyinhua has been used as a dietary supplement, tea, or beverage for millennia. A Jinyinhua water extract demonstrated an interrupting effect on SARS-CoV-2-S protein/ACE2 binding, and chlorogenic acids were found to dominate the anti-inflammatory effects of Jinyinhua by inhibiting oxidative stress (*21*). Yuxingcao is a time-honored herb widely used in Asian countries to treat pneumonia, and it potentially exhibits antiviral activity against enveloped viruses. Some key

Table 2. Some single herbs and herb pairs exhibiting a high affinity for ACE2 in treating COVID-19

Chinese name	Scientific name	Screened ingredients	Effects	Experimental method	*Ref.*
Mahuang	*Ephedra sinica* Stapf	Ephedrine, pseudoephedrine, and methylephedrine	(*i*) Three active ingredients with ACE2-binding activity; (*ii*) Bind to SARS-CoV-2 RBD and prevent SARS-CoV-2 from entering $ACE2^h$ cells.	ACE2/CMC-HPLC-IT-TOF-MS approach, molecular docking, SPR assays, and *in vitro* antiviral experiment	*16*
	Ephedra sinica Stapf	Quinoline-2-carboxylic acids	Disrupt the interaction between ACE2 and SARS-CoV-2 RBD.	Competition inhibition assays, SPR assays, molecular docking, and *in vitro* antiviral experiment	*17*
Mahuang-Kuxingren	*Ephedra sinica* Stapf and *Semen armeniacae amarum*	β-sitosterol, estrone, and stigmasterol	Have a high binding activity for 3CLpro and ACE2.	Network pharmacology and molecular docking	*18*
Mahuang-Gancao	*Ephedra sinica* Stapf and *Glycyrrhiza uralensis*	Licorice glycoside E and xambioona	Bind well to COVID-19 related targets, including 3CLpro, S protein, and ACE2	Network pharmacology, molecular docking, and molecular dynamics	*19*
Huangqin	*Scutellariae radix*	Baicalein and scutellarin	Regulates the MAPK and NF-κB signaling pathways and blocks SARS-CoV-2 spike binding to ACE2.	Network pharmacology, HPLC-MS based plant metabolomics, and *in vitro* bioassays	*20*
Jinyinhua	*Lonicera japonica*	Chlorogenic acid, neochlorogenic acid, cryptochlorogenic acid and cynaroside	Inhibits SARS-CoV-2-S protein/ACE2 binding.	*In vitro* bioassays, bioassay-coupled HPLC approach, and MRM-MS/MS approach	*21*
Yuxingcao	*Houttuynia cordata*	Afzelin, apigenin, kaempferol, and quercetin	Binds with ACE2 and 3CLpro.	Network pharmacology and molecular docking	*22*

Note: Abbreviations: cell membrane chromatography (CMC); surface plasmon resonance (SPR); ACE2 over-expressed HEK293T cells ($ACE2^h$ cells); surface plasmon resonance (SPR); high-performance liquid chromatography (HPLC); multiple reaction monitoring tandem mass spectrometry (MRM-MS/MS).

components of Yuxingcao, such as afzelin, apigenin, kaempferol, and quercetin, have been reported to bind with ACE2 and 3CLpro of SARS-CoV-2 in four signaling pathways, including PI3K-Akt, Jak-STAT, MAPK, and NF-kB (*22*).

4. Active ingredients

Herbal medicine has a wide array of active ingredients with potential health benefits, including antiviral activity, that may be explored as an alternative treatment for COVID-19. Interestingly, some of these active ingredients might prevent SARS-CoV-2 from infecting human cells by blocking the ACE-2 protein (Table 3).

Ursodeoxycholic acid is a major active ingredient of the Chinese herb bear gall powder. A recent study indicated that ursodeoxycholic acid down-regulated ACE2 expression and reduced the susceptibility to SARS-CoV-2 infection *in vitro*, *in vivo*, and in human lungs and livers perfused *ex situ* (*23*). Moreover, ursodeoxycholic acid reduced ACE2 expression in the nasal epithelium in humans. Glycyrrhizic acid derived from the Chinese herb Gancao has been found to be a broad-spectrum anti-coronavirus candidate with low toxicity. Its antiviral mechanism might be due to disrupting viral uptake into host cells and impairing interaction between the RBD of SARS-COV2 and ACE2 (*24*). Glycyrrhizin, a main active ingredient of Gancao, prevents SARS-CoV-2 from entering cells and replicating by reducing the expression of ACE2 and inhibiting interaction between the S protein RBD and ACE2 (*25*).

Salvianolic acids (salvianolic acid A, salvianolic acid B, and salvianolic acid C), as major active ingredients of the Chinese herb *Salvia miltiorrhiza* (Danshen), inhibit the entry of the SARS-CoV-2 spike pseudovirus into HEK293T cells highly expressing ACE2 by binding to both the RBD of the SARS-CoV-2 S protein and receptor ACE2 (*26*). Salvianolic acid B displayed the greatest binding affinity and anti-SARS-CoV-2 pseudoviral action among these three compounds. Quercetin as a naturally abundant flavonoid that is widely found in various herbal medicines, such as *Forsythia suspensa* (Lianqiao) and *Lonicera japonica* (Jinyinhua). It might be a potential treatment for COVID-19-induced acute kidney injury (*27*). It might serve as a SARS-CoV-2 inhibitor by binding with the active sites of SARS-CoV-2 main protease 3CLpro and ACE2, therefore suppressing the functions of the proteins and interrupting the viral life cycle. In addition, andrographidine C, a major active ingredient of the Chinese herb *Andrographis paniculata* (Chuanxinlian), formed a stable complex with the key target ACE2, so it can be considered as a potential drug to treat COVID-19 (*28*).

5. Conclusion

The combination of the SARS-CoV-2 S protein with

Table 3. Some active ingredients exhibiting a high affinity for ACE2 in treating COVID-19

Ingredients	Chemical class	Source	Effects	Screening method	*Ref.*
Ursodeoxycholic acid	Steroids	Bear gall powder	(*i*) Downregulates ACE2 expression and reduces SARS-CoV-2 infection; (*ii*) Reduces ACE2 levels in the nasal epithelium of healthy individuals.	*In vitro*, *in vivo*, and *ex vivo* antiviral experiment	*23*
Glycyrrhizic acid	Terpenoids	Glycyrrhiza uralensis	Disrupts viral uptake into the host cells and impairs the interaction between RBD of SARS-COV2 and ACE2.	Computer-aided drug design and biological verification	*24*
Glycyrrhizin	Terpenoids	Glycyrrhiza uralensis	Reduces the expression of ACE2 and inhibits the interaction between the S protein RBD and ACE2.	Molecular docking and *in vitro* antiviral experiment	*25*
Salvianolic acid A, B and C	Phenols	Salvia miltiorrhiza	Binds to both RBD of SARS-CoV-2 S protein and receptor ACE2.	Molecular docking and *in vitro* antiviral experiment	*26*
Quercetin	Flavonoids	Various herbal medicines, such as Forsythia suspensa and Lonicera japonica	Binds with the active sites of SARS-CoV-2 main protease 3CL and ACE2.	Network pharmacology and molecular docking study	*27*
Andrographidine C	Flavonoids	Andrographis paniculata	Forms a stable complex with the key target ACE2	Network pharmacology, molecular docking, and molecular dynamics	*28*

Note: Abbreviations: angiotensin-converting enzyme 2 (ACE2); receptor-binding domain (RBD); spike protein (S protein).

ACE2 of the host cell to promote membrane fusion is an initial critical step for SARS-CoV-2 infection. Therefore, screening herbal medicines that inhibit the binding of the SARS-CoV-2 S protein and ACE2 might provide a feasible strategy for the treatment of COVID-19. This work has summarized some herbal medicines including formulas, single herbs, and active ingredients, that have exhibited a high affinity for ACE2 in treating COVID-19. We hope this work may provide meaningful and useful information on further research to investigate the mechanisms of herbal medicines against SARS-CoV-2 and follow-up drug discovery. However, most of the current research is based on network pharmacology, molecular docking, and *in vitro* bioassays, there is still a lot of work to be done in the real sense of drug design and development.

Funding: None.

Conflict of Interest: The authors have no conflicts of interest to disclose.

References

1. An X, Zhang Y, Duan L, Jin D, Zhao S, Zhou R, Duan Y, Lian F, Tong X. The direct evidence and mechanism of traditional Chinese medicine treatment of COVID-19. Biomed Pharmacother. 2021; 137:111267.
2. Scialo F, Daniele A, Amato F, Pastore L, Matera MG, Cazzola M, Castaldo G, Bianco A. ACE2: The major cell entry receptor for SARS-CoV-2. Lung. 2020; 198:867-877.
3. Huang YF, Bai C, He F, Xie Y, Zhou H. Review on the potential action mechanisms of Chinese medicines in treating Coronavirus Disease 2019 (COVID-19). Pharmacol Res. 2020; 158:104939.
4. Qi F, Tang W. Traditional Chinese medicine for treatment of novel infectious diseases: Current status and dilemma. Biosci Trends. 2021; 15:201-204.
5. Wang J, Qi F. Traditional Chinese medicine to treat COVID-19: The importance of evidence-based research. Drug Discov Ther. 2020; 14:149-150.
6. Chen X, Wu Y, Chen C, Gu Y, Zhu C, Wang S, Chen J, Zhang L, Lv L, Zhang G, Yuan Y, Chai Y, Zhu M, Wu C. Identifying potential anti-COVID-19 pharmacological components of traditional Chinese medicine Lianhuaqingwen capsule based on human exposure and ACE2 biochromatography screening. Acta Pharm Sin B. 2021; 11:222-236.
7. He DD, Zhang XK, Zhu XY, Huang FF, Wang Z, Tu JC. Network pharmacology and RNA-sequencing reveal the molecular mechanism of Xuebijing injection on COVID-19-induced cardiac dysfunction. Comput Biol Med. 2021; 131:104293.
8. Xing Y, Hua YR, Shang J, Ge WH, Liao J. Traditional Chinese medicine network pharmacology study on exploring the mechanism of Xuebijing Injection in the treatment of coronavirus disease 2019. Chin J Nat Med. 2020; 18:941-951.
9. Zhong LLD, Lam WC, Yang W, Chan KW, Sze SCW, Miao J, Yung KKL, Bian Z, Wong VT. Potential targets for treatment of coronavirus disease 2019 (COVID-19):

A review of Qing-fei-pai-du-tang and its major herbs. Am J Chin Med. 2020; 48:1051-1071.
10. Li Y, Wu Y, Li S, Li Y, Zhang X, Shou Z, Gu S, Zhou C, Xu D, Zhao K, Tan S, Qiu J, Pan X, Li L. Identification of phytochemicals in Qingfei Paidu decoction for the treatment of coronavirus disease 2019 by targeting the virus-host interactome. Biomed Pharmacother. 2022; 156:113946.
11. Tao Q, Du J, Li X, Zeng J, Tan B, Xu J, Lin W, Chen XL. Network pharmacology and molecular docking analysis on molecular targets and mechanisms of Huashi Baidu formula in the treatment of COVID-19. Drug Dev Ind Pharm. 2020; 46:1345-1353.
12. Cai Y, Zeng M, Chen YZ. The pharmacological mechanism of Huashi Baidu Formula for the treatment of COVID-19 by combined network pharmacology and molecular docking. Ann Palliat Med. 2021; 10:3864-3895.
13. Simayi J, Nuermaimaiti M, Wumaier A, Khan N, Yusufu M, Nuer M, Maihemuti N, Bayinsang, Adurusul K, Zhou W. Analysis of the active components and mechanism of Shufeng Jiedu capsule against COVID-19 based on network pharmacology and molecular docking. Medicine (Baltimore). 2022; 101:e28286.
14. Zhuang Z, Zhong X, Zhang H, Chen H, Huang B, Lin D, Wen J. Exploring the potential mechanism of Shufeng Jiedu capsule for treating COVID-19 by comprehensive network pharmacological approaches and molecular docking validation. Comb Chem High Throughput Screen. 2021; 24:1377-1394.
15. Li Y, Chu F, Li P, Johnson N, Li T, Wang Y, An R, Wu D, Chen J, Su Z, Gu X, Ding X. Potential effect of Maxing Shigan decoction against coronavirus disease 2019 (COVID-19) revealed by network pharmacology and experimental verification. J Ethnopharmacol. 2021; 271:113854.
16. Lv Y, Wang S, Liang P, Wang Y, Zhang X, Jia Q, Fu J, Han S, He L. Screening and evaluation of anti-SARS-CoV-2 components from *Ephedra sinica* by ACE2/CMC-HPLC-IT-TOF-MS approach. Anal Bioanal Chem. 2021; 413:2995-3004.
17. Mei J, Zhou Y, Yang X, Zhang F, Liu X, Yu B. Active components in *Ephedra sinica* Stapf disrupt the interaction between ACE2 and SARS-CoV-2 RBD: Potent COVID-19 therapeutic agents. J Ethnopharmacol. 2021; 278:114303.
18. Gao K, Song YP, Song A. Exploring active ingredients and function mechanisms of Ephedra-bitter almond for prevention and treatment of Corona virus disease 2019 (COVID-19) based on network pharmacology. BioData Min. 2020; 13:19.
19. Li X, Qiu Q, Li M, Lin H, Cao S, Wang Q, Chen Z, Jiang W, Zhang W, Huang Y, Luo H, Luo L. Chemical composition and pharmacological mechanism of ephedra-glycyrrhiza drug pair against coronavirus disease 2019 (COVID-19). Aging (Albany NY). 2021; 13:4811-4830.
20. Liu J, Meng J, Li R, Jiang H, Fu L, Xu T, Zhu GY, Zhang W, Gao J, Jiang ZH, Yang ZF, Bai LP. Integrated network pharmacology analysis, molecular docking, LC-MS analysis and bioassays revealed the potential active ingredients and underlying mechanism of *Scutellariae radix* for COVID-19. Front Plant Sci. 2022; 13:988655.
21. Lai KH, Chen YL, Lin MF, El-Shazly M, Chang YC, Chen PJ, Su CH, Chiu YC, Illias AM, Chen CC, Chen LY, Hwang TL. Lonicerae Japonicae Flos attenuates neutrophilic inflammation by inhibiting oxidative stress. Antioxidants (Basel). 2022; 11:1781.
22. Liu J, Yuan S, Yao Y, Wang J, Scalabrino G, Jiang S, Sheridan H. Network pharmacology and molecular docking elucidate the underlying pharmacological mechanisms of the herb *Houttuynia cordata* in treating pneumonia caused by SARS-CoV-2. Viruses. 2022; 14:1588.
23. Brevini T, Maes M, Webb GJ, et al. FXR inhibition may protect from SARS-CoV-2 infection by reducing ACE2. Nature. 2022; doi: 10.1038/s41586-022-05594-0.
24. Yu S, Zhu Y, Xu J, Yao G, Zhang P, Wang M, Zhao Y, Lin G, Chen H, Chen L, Zhang J. Glycyrrhizic acid exerts inhibitory activity against the spike protein of SARS-CoV-2. Phytomedicine. 2021; 85:153364.
25. He MF, Liang JH, Shen YN, Zhang JW, Liu Y, Yang KY, Liu LC, Wang J, Xie Q, Hu C, Song X, Wang Y. Glycyrrhizin inhibits SARS-CoV-2 entry into cells by targeting ACE2. Life (Basel). 2022; 12:1706.
26. Hu S, Wang J, Zhang Y, Bai H, Wang C, Wang N, He L. Three salvianolic acids inhibit 2019-nCoV spike pseudovirus viropexis by binding to both its RBD and receptor ACE2. J Med Virol. 2021; 93:3143-3151.
27. Gu YY, Zhang M, Cen H, Wu YF, Lu Z, Lu F, Liu XS, Lan HY. Quercetin as a potential treatment for COVID-19-induced acute kidney injury: Based on network pharmacology and molecular docking study. PLoS One. 2021; 16:e0245209.
28. Xie R, Lin Z, Zhong C, Li S, Chen B, Wu Y, Huang L, Yao H, Shi P, Huang J. Deciphering the potential anti-COVID-19 active ingredients in *Andrographis paniculata* (Burm. F.) Nees by combination of network pharmacology, molecular docking, and molecular dynamics. RSC Adv. 2021; 11:36511-36517.

Received November 30, 2022; Revised December 26, 2022; Accepted December 29, 2022.

*Address correspondence to:
Fanghua Qi, Traditional Chinese Medicine, Shandong Provincial Hospital affiliated to Shandong First Medical University, No. 324 Jingwuweiqi Road, Ji'nan, Shandong, China.
E-mail: qifanghua2006@126.com

Released online in J-STAGE as advance publication January 2, 2023.

Review

DOI: 10.5582/bst.2022.01473

RNA-binding proteins in metabolic-associated fatty liver disease (MAFLD): From mechanism to therapy

Jiawei Xu[1,§], Xingyu Liu[1,§], Shuqin Wu[1], Deju Zhang[2], Xiao Liu[3], Panpan Xia[4], Jitao Ling[4], Kai Zheng[5], Minxuan Xu[4], Yunfeng Shen[4], Jing Zhang[1,6,*], Peng Yu[1,4,*]

[1] The Second Clinical Medical College / The Second Affiliated Hospital of Nanchang University, Nanchang, Jiangxi, China;
[2] Food and Nutritional Sciences, School of Biological Sciences, The University of Hong Kong, Hong Kong, China;
[3] Department of Cardiology, The Second Affiliated Hospital of Sun Yat-Sen University, Guangzhou, Guangdong, China;
[4] Department of Endocrinology and Metabolism, The Second Affiliated Hospital of Nanchang University, Nanchang, Jiangxi, China;
[5] Medical Care Strategic Customer Department, China Merchants Bank Shenzhen Branch, Shenzhen, Guangdong, Guangdong, China;
[6] Department of Anesthesiology, The Second Affiliated Hospital of Nanchang University, Nanchang, China.

SUMMARY Metabolic-associated fatty liver disease (MAFLD) is the most common chronic liver disease globally and seriously increases the public health burden, affecting approximately one quarter of the world population. Recently, RNA binding proteins (RBPs)-related pathogenesis of MAFLD has received increasing attention. RBPs, vividly called the gate keepers of MAFLD, play an important role in the development of MAFLD through transcription regulation, alternative splicing, alternative polyadenylation, stability and subcellular localization. In this review, we describe the mechanisms of different RBPs in the occurrence and development of MAFLD, as well as list some drugs that can improve MAFLD by targeting RBPs. Considering the important role of RBPs in the development of MAFLD, elucidating the RNA regulatory networks involved in RBPs will facilitate the design of new drugs and biomarkers discovery.

Keywords metabolic-associated fatty liver disease (MAFLD), non-alcoholic fatty liver disease (NAFLD), RNA-binding protein (RBP), non-coding RNA, RNA-RBP interaction

1. Introduction

In view of many shortcomings in the term of non-alcoholic fatty liver disease (NAFLD), the international expert panel in 2020 proposed to uniformly rename it as metabolism related fatty liver disease (MAFLD), and further give MAFLD a new and detailed definition (*1*). The diagnostic methods for MAFLD are updated as follows: patients have liver steatosis and metabolic dysfunction at the same time. Patients with metabolic dysfunction meet one of the following three standards, including overweight/obesity, Type 2 diabetes or metabolic disorder (*1,2*). The global prevalence rate of MAFLD is up to 25%, and it is now listed as the most common liver disease and a major threat to human health (*3*). The metabolic defects of MAFLD may also lead to its progression to nonalcoholic steatohepatitis (NASH), liver fibrosis and cirrhosis (*4*). Furthermore, it may eventually evolve into hepatocellular carcinoma (HCC) and liver failure (*5*). In addition, the metabolic syndrome of MAFLD is very similar to obesity, which can lead to multiple complications through different extrahepatic pathways, such as diabetes, cardiovascular disease and hypertension (*6*). The high prevalence, increased risk of death and coexistence of multiple complications all indicate that MAFLD-related liver damage and its complications will pose a significant health and economic burden to patients, their families and society. Therefore, it is necessary to explore effective therapeutic approaches for the treatment of MAFLD.

RNA binding proteins (RBPs) are involved in coordinating (ribonucleic acid) RNA processing and post transcriptional gene regulation (PTGR) as well as the maturation, localization, stabilization and translation of coding and non-coding RNAs (*7*). The loss of RBP function or functional mutation will destroy homeostasis, leading to various diseases, particularly metabolic diseases, which also involves MAFLD (*8,9*). For instance, studies have shown that in cytoplasm rich liver tissues, an RBP called Human antigen R (HuR) interacts with mRNAs that are involved in lipid transport/metabolism, cholesterol metabolism or endoplasmic reticulum (ER) stress response pathway (*10*). HuR dysfunction will cause a series of liver lipid metabolism

disorders, which gradually evolves into MAFLD. A MAFLD mouse model suggests that Quaking I-5 (QKI 5) mediated by Sirtuin 1 (SIRT1) significantly affected the synthesis of triglyceride (TG) in the liver of the MAFLD mouse model. Compared with the control group, the expression level of QKI 5 in MAFLD mice decreased (*11*). Therefore, we think it would be better to clarify the pathogenesis of MAFLD through discussing the roles of RBPs in the development of MAFLD.

Although numerous studies have elaborated the role and mechanism of RBPs in liver diseases, especially in non-alcoholic fatty liver diseases, there is a lack of knowledge summary on this subject at present. Our article reviews the mechanism and complications of different RBPs in MAFLD and some drugs that can improve MAFLD by regulating RBPs, aiming to provide some reference for the pharmacological targeted MAFLD treatment strategies that are based on RBPs regulatory network.

2. RBPs

2.1. Structure and Function

PTGR is essential for the maintenance of cell homeostasis and the coordination of the maturation, transport, stabilization, and degradation of coding and non-coding RNAs (*7*). RBP is a key regulator of PTGR that can interact with multiple RNAs and individual transcripts and has the potential to interfere with a large number of regulatory networks and maintain the integrity of cells (*12*). In RBP, there is an RNA-binding domain (RBD), a functional unit responsible for RNA binding existing in the coding sequence (intron and exon domains), 5' untranslated regions (5'UTR) and 3' untranslated regions (3' UTR) of RNA (*13*). RBPs can be divided into conventional and non-conventional RBPs two groups based on their RBD. Of these, the RBDs of conventional RBPs consist of an RNA recognition motif (RRM), cold-shock domain (CSD), K homology (KH) domain, arginine-glycine-glycine (RGG) motif and zinc-finger domains (*14*), while non-conventional RBPs bind with RNAs through intrinsically disordered regions lacking RBDs (*15*) (Figure 1). Normally multiple RBDs coexist in one RBP and the arrangement of these RBD modules can coordinate and enhance specific binding with RNA (*16*). As many RBDs are small and have few residues as effective parts, they often achieve specific binding with RNA in the form of Hydrogen Bonds, Van der Waals Interactions, Hydrophobic, and p Interactions and Stacking (*17*). The adaptor between RBDs can mediate RNA contacts, by which whether RBDs work independently or cooperatively can be determined (*18*). Some RBDs can also act as the mediator for Protein-Protein Interaction (*19*). RNA Recognition Motif, present in about 1% of all human proteins, is the most extensively seen and studied RBD (*20*). RBD also includes K Homology, Zinc Finger, and Pumilio Homology Domain, which all perform their own duties in RNA metabolism.

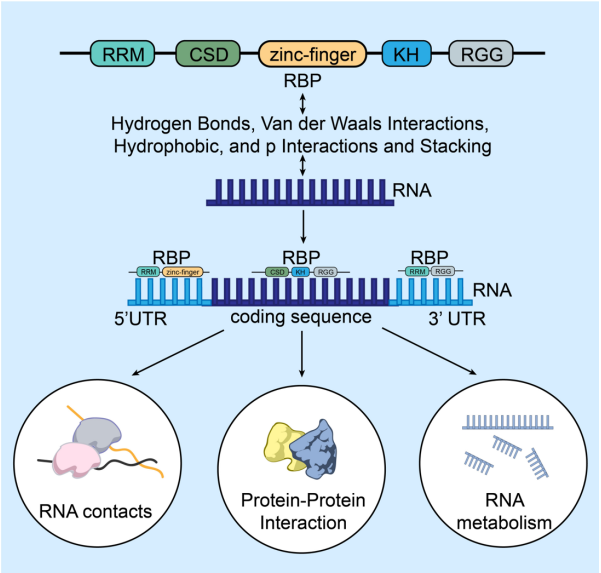

Figure 1. The structure and function of RNA binding proteins. Based on numerous studies, RBP can bind to RNA and the binding of RBP to RNA is via the RBDs in RBP. Depending on the presence or absence of RBD, RBP can be divided into conventional RBPs and non- conventional RBPs. And the RBDs of conventional RBP consist of RRM, CSD, KH, RGG motif and zinc-finger domains, while non-conventional RBP does not have RBDs. RBDs bind with RNA by the forces of Hydrogen Bonds, Van der Waals Interactions, Hydrophobic, and p Interactions and Stacking. With multiple RBDs coexisting of a single RBP, the modules are arranged to coordinate and enhance specific binding to the coding sequence, 5'UTR and 3'UTR of RNA. Eventually, RBP binds to RNA and performs the function of RNA contacts, protein-protein interaction and RNA metabolism.

2.2. The Molecular mechanisms of RBPs in PTGR

The abundance of RBDs allows RBPs to bind to other biomolecules in a variety of ways, which gives RBPs an important role in PTGR. Of them, the molecular mechanisms of RBPs involved in PTGR can be summarized into 3 levels (Figure 2): RBP-RNA, RBP-RBP and RBP-protein-RNA.

2.2.1. RBP-RNA

As a regulator of biological cytology, RBPs are involved in various aspects of RNA regulation, including transcription regulation (*21*), AS (alternative splicing) (*22*), alternative polyadenylation (*23*), stability (*24*), and subcellular localization (*25*). Disturbing levels of RBPs in specific microenvironments or mutations in coding genes can lead to serious diseases. Several serious maladies can be caused when disorder of the RBPs levels in specific microenvironments or mutation of coding genes occur. For example, as an important splicing factor required by AS, serine/arginine splicing factors have a strictly regulated process of phosphorylation, which

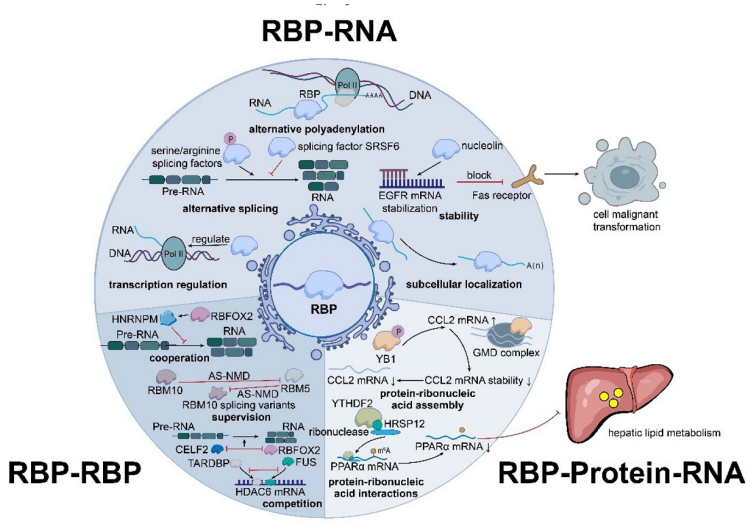

Figure 2. The mechanisms of RNA binding proteins functions. According to many studies, RBPs can bind to various biomolecules to produce different functions. The mechanisms involved in these functions can be summarized as: RBP-RNA, RBP-RBP, and RBP-Protein-RNA. In the RBP-RNA mechanism, RBPs regulate biological cytology and various aspects of RNA through transcription regulation, alternative splicing, alternative polyadenylation, stability and subcellular localization. Meanwhile, RBPs have a cooperation, supervision and competition function with each other at the RBP-RBP level. In the meantime, RBPs also affect hepatic lipid metabolism by regulating and modifying protein-ribonucleic acid assembly and protein-ribonucleic acid interactions. In general, RBP can produce important cellular physiological functions through the three mechanisms described above, and interference with their normal functioning may contribute to the development of disease.

can influence the AS modes of many pre-mRNAs (*26*). Another case in point is that a lower expression of liver splicing factor serine and arginine rich splicing factor 6 in the mice models of MAFLD and NASH can contribute to disorder of RNA splicing, thus worsening MAFLD (*27*). Nucleotin is a multifunctional RBP, relocation on the cell membrane and overexpression of which have been verified to bring about cancers of different tissue origins (*28*). This can be exemplified by a highly expressed nucleolin in actively dividing cancer cells, which can promote the stability of epidermal growth factor receptor mRNA and block Fas receptors that induce apoptosis, contributing to cell malignant transformation (*29*).

2.2.2 RBP-RBP

In addition, the functions of cooperation, supervision, and competition are also represented among RBPs (*30*). Adenosine methylation at the N (6) position (m6A) is a dynamic and abundant epitranscriptomics marker, which can regulate key aspects of the metabolism of eukaryotic RNAs in many biological processes. This modification process involves the collaborative coupling of a series of protein complexes that are defined by researchers as Writer, Eraser, and Reader to correspond to the transmethylation catalase, demethylase, and reading protein of m6A that modifies RNA, respectively (*31*). For example, RNA methyltransferase-like 3 (METTL3) and METTL14 are components of the multi-subunit m6A writer complexes, the enzyme activities of which are significantly higher than those of METTL3/METTL14 alone (*32*). For instance, splicing inhibition mediated by RBP Heterogeneous ribonucleoprotein M is stimulated by RBP FOX-1 homologue 2 (RBFOX2), indicating there is extensive synergy between the two RBPs (*33*). Splicing is one of the methods widely used by RBPs to monitor the expression of other RBPs. RBFOX2 regulates other RBPs by controlling Alternative Splicing Coupled Nonsense-mediated Decay (AS-NMD). While RBP can always regulate itself, RBFOX2 serves as a global controller to dominate self-regulation of RBP (*34*). AS-NMD can also be found in the mutual supervision of RBPs. For example, while AS-NMD is used for the inhibition of RBM10 (RNA binding motif protein 10) to RBM5 (RNA binding motif protein 5), RBM5 also controls the expression of RBM10 splicing variants in turn through AS-NMD to reduce the action of cancer promotion (*35,36*). In RNA processing, there is a competition pattern between RBPs. Genome-wide analysis has revealed the antagonistic effects of splicing regulation between CUGBP (CUG-binding protein 1) Elav-like family member 2 (CELF2) and RBFOX2. These RBPs bind to overlapping sites of several mRNA precursors, with opposite consequences for the processing of exons (*37*). In addition to splicing, other processing steps are also affected by RBPs competition. On the mRNA of recombinant protein histone deacetylase 6, TAR DNA binding protein competes with FUS for overlapping binding sites to regulate its processing and nuclear export (*38*).

2.2.3. RBP-Protein-RNA

RBPs are involved in the formation of spliceosome and other ribonucleoprotein complexes, and in the regulation and modification of the interactions between proteins and ribonucleic acids to maintain accurate RNA translation and splicing (*12*). The Glucocorticoid-GR system acts as a transcriptional activator or inhibitor in the degradation of subsets of mRNAs despite its independence of translations, which is known as GR-mediated mRNA Decay (GMD). At this time, the Glucocorticoid-GR system is deemed as an assembly of RBP (*39*). Y-box binding protein 1 (YB1) is the most common cold shock protein involved in the evolution of many inflammatory diseases. Based on one research finding, the rapid degradation of chemokine (C-C motif) ligand 2 (CCL2) mRNA is mediated by GMD during

the dephosphorylation of YB1. The dephosphorylation of YB1 accelerates the combination of YB1 and GMD complexes. Then, the YB1-GMD complex is guided to CCL2 mRNA through the interaction between YB1 and CCL2 mRNA, thus triggering GMD, which can affect the stability of mRNA and boost the reduction of CCL2 mRNA. Based on this, the evolution of atherosclerosis is influenced by YB1 through inflammation regulation [51]. Gem Nuclear Organelle Associated Protein 5 (GEMIN5), an RBP protein, plays a key role in the formation of Survival Motor Neuron protein complexes and formation of small nuclear ribonucleic proteins (snRNPs). The mutation of GEMIN5 can damage the assembly of the snRNP complexes in neurons of induced pluripotent stem cells of patients, resulting in growth retardation, hypotonia, and cerebellar ataxia (*40*). As an important reading protein for the modification of RNA m6A, YTHN6-Methyladenosine RNA Binding Protein 2 (YTHDF2, YTH Domain Family Protein 2) contains a YTH domain that can specifically recognize the RNA modified by binding m6A and mediate the degradation of RNA. It has been proved that HRSP12 (adapter protein) can be used to connect YTHDF2 with ribonuclease P/MRP, resulting in rapid degradation of YTHDF2 binding RNA (*41*). YTHDF2 can also regulate somatic cell reprogramming by recruiting CCR4-NOT deadenylation complexes (*42*). The circadian clock impairs the hepatic lipid metabolism by cutting down the Peroxisome proliferator-activated receptor α (PPARα) mRNA mediated by YTHDF2, which is why people with irregular schedules are often susceptible to MAFLD (*43*). Similarly, fat mass and obesity-associated (FTO) protein is the first identified RNA demethylase that can erase m6A inside mRNA. A study shows that the down-regulation of FTO can reduce the modification of m6A in PPARα, and then regulate its transcriptional level in an m6A-YTHDF2 dependent manner (*44*).

The level of disorder of RBPs may lead to cellular stress, weaker cell adaption, or cell death as they are involved in a variety of important cellular functions, triggering MAFLD, diabetes, cancer, neurodegenerative diseases, and other kinds of diseases (*45*). Recently, increasingly extensive attention has been paid to the regulation of RBPs to MAFLD and its complications. This review will summarize the mechanisms of different RBPs in MAFLD and its complications, and some drugs that can improve MAFLD by adjusting RBPs, by which the design of new drugs for MAFLD and the disclosing of biomarkers can be advanced.

3. RBPs Implicated in The Occurrence and Development of MAFLD

MAFLD, a reflection of metabolic dysfunction in the liver, is described as a series of liver diseases with a prevalence of 70–80% in obese and diabetic patients, which can manifest initially as insulin resistance and changes in gut flora due to imbalances in energy intake and expenditure (*46,47*). The insulin resistance and changes in gut flora can lead to fatty deposits in the liver. During the accumulation of aberrant fat, there can be more serious hepatic insulin resistance and intracellular damage, which will further exacerbate inflammation, fibrosis, and carcinogenesis (*48*). A small percentage of patients progress from simple steatosis to liver inflammation and fibrosis [nonalcoholic fatty liver disease (NASH)]. During liver damage and repair, dysregulated hepatocytes can promote hepatic stellate cells (HSCs) activation through paracrine signaling, ultimately developing hepatic fibrosis and cirrhosis. Non-coding RNAs particularly play a functional role in MAFLD. Alterations in alternative RNA splicing are associated with inflammation, metabolic disorders and cancer, which are all important markers in the natural course of MAFLD. MicroRNAs (miRNAs), non-coding RNAs, and relevant RBPs are engaged in various core cellular processes (*2,48*). For instance, Zhao *et al*. revealed that the expression of the long noncoding RNA (lncRNA) brown fat-enriched lncRNA 1(Blnc1) in the liver is greatly increased in obesity and MAFLD mice, which is needed for inducing hepatic lipogenic genes. Specific inactivation of Blnc1 can erase insulin resistance and hepatic steatosis that are induced by high-fat diet, thus avoiding occurrence of MAFLD (*49*). And another study reported that hepatic Irs2 mRNA was decreased in MAFLD patients and its downregulation may be associated with insulin resistance (*50*).

Translation-regulated RNA-binding proteins (TTR-RBPs) are important proteins that regulate gene expression patterns. TTR-RBPs can control gene expression by cooperating or competing with specific miRNAs at the post-transcriptional level, affecting pre-mRNA splicing, mRNA transfer to the cytoplasm, turnover, storage, translation and so on (*51,52*). The overwhelming majority of TTR-RBPs can regulate numerous post-transcriptional processes, as HuR and nuclear factor 90 regulate mRNA stability and translation, while only a few TTR-RBPs can regulate a process specifically such as mRNA splicing *via* Tristetraprolin (TTP) and KH-type regulatory protein splicing (*53-55*). Therefore, the present study will introduce some specific RBPs in detail to expound the importance of RBPs in the occurrence and development of MAFLD (Table 1).

3.1. Insulin Resistance and Liver Fat Deposition

Insulin resistance is a systemic disease that affects many organs and insulin regulatory pathways. Fat deposition is negatively associated with insulin resistance. Insulin resistance and Liver Fat Deposition can be early manifestations of MAFLD. By searching relevant articles, we found that the RBPs associated with insulin resistance and hepatic fat deposition included DDX1, QKI 5, TTP, *etc* (*53-55*). We summarized

and demonstrated the first three RBPs with clearer mechanisms in insulin resistance and liver fat deposition (Figure 3).

3.1.1. Tristetraprolin

TTP (also known as zinc finger protein 36) is an mRNA-binding protein that can suppress more than 20 cytokines, including Tumor Necrosis Factor α (TNF-α), interleukin 6 (IL-6), IL-1, and Monocyte Chemoattractant Protein-1 (*56*). Under certain circumstances, inflammation can improve insulin sensitivity. For instance, downregulation of the TNF-α pathway can promote insulin sensitivity (*57,58*). TTP has been reported to control the TNF-α level through binding to the AU-rich element region of TNF-α mRNA (*59*). TTP can also be upregulated by TNF-α treatment (*60*). Therefore, we theorize that TTP and TNF-α reciprocally regulate each other and play a crucial role in inflammation and metabolic disturbance. Recent reports suggest a potentially novel role for TTP in the regulation of metabolism, especially in hepatic glucose and lipid metabolism (*61*). TTP has an antagonistic effect with HuR and their relationship has been extensively studied in the field of metabolic syndrome (*62,63*). In healthy humans, hepatic TTP at a base level can maintain systemic insulin sensitivity. Caracciolo *et al*. demonstrated that in the liver of obese mice, enhancement of TTP expression levels occurred in Kupffer cells but not in hepatocytes, which was associated with increased liver inflammation and protection against insulin resistance (*64*). According to an analysis of secreted hepatic factors by Sawicki *et al*., fibroblast growth factor 21 (FGF21), an important hormone in liver, is posttranscriptionally repressed by TTP and further modulates insulin responsiveness. Loss of TTP also amplifies FGF21 expression (*65*). In summary, lowering hepatic TTP levels, which has significant functional impact on hepatic and systemic insulin sensitivity, may open up a new avenue for treating various metabolic syndromes.

3.1.2 Heterogeneous nuclear ribonucleoprotein A1

Heterogeneous nuclear ribonucleoproteins (hnRNPs) are a big family of over 20 RNA-binding proteins found in mammalian cells (*66*). Human heterogeneous nuclear ribonucleoprotein A1 (HnRNPA1) is a highly enriched hnRNP that is generally used to stabilize mRNA and regulate mRNA gene expression (*67*). Recent evidence suggests that hnRNPA1 plays a key role in regulating lipid and glucose metabolism. HnRNPA1 has been shown to be related to the formation of pyruvate kinase isoform 2 mRNA (*68*). In the adipose tissues of obese patients, hnRNPA1 expression is significantly decreased. Moreover, hnRNPA1 is also associated with insulin receptor alternative splicing in people with weight loss (*69*). According to the experiment conducted by Zhao *et al*., hnRNPA1 knockout mice exhibited decreased glycogen storage, severe insulin resistance and hepatic steatosis (*70*). They further suggested that this was because hnRNPA1 can interact with glycogen synthase 1(gys1) mRNA, thereby promoting glycogen synthesis and maintaining the sensitivity of insulin (*70*). Another study elaborated that lncRNA suppressor of hepatic gluconeogenesis and lipogenesis (lncSHGL) can recruit hnRNPA1, and co-regulate calmodulin (CaM) protein at the post-transcriptional level, which perform an important part in inhibiting hepatic gluconeogenesis and adipogenesis. The lncSHGL/hnRNPA1/CaM pathway also takes part in the regulation of phosphatidyl inositol 3-kinase (PI3K)/Akt pathway activity, which affects the production of hepatic glucose (*71*). Besides, a study by Gui *et al*. also revealed that hnRNPA1 regulates lipid metabolism by interacting with H19 and increasing the translation of fatty acid oxidation-related genes carnitine palmitoyl transferase 1B (CPT1b) and peroxisome proliferators-activated receptor γ coactivator 1 alpha (PGC1α), thereby improving insulin resistance (*72,73*).

3.1.3. Serine rich splicing factor 10

Serine rich splicing factor 10 (SRSF10), which belongs to the SR-like protein family of splicing factors, can regulate RNA processing (*74*). For the past few years, SRSF10 has been demonstrated to be associated with adipocyte differentiation and lipogenesis, and its expression level is decreased in liver and muscle of obese populations (*60*). LPIN1, a key regulator of lipid metabolism, is positively correlated with insulin resistance in adipose tissue and liver (*74,75*). Research shows that SRSF10 can selectively down-regulate the alternative splicing of LPIN1 and produce the LPIN1 β isoform associated with increased expression of adipogenesis genes, thereby stimulating lipogenesis and causing hepatic steatosis (*76*). Besides, insulin can regulate the expression of SRSF10. SRSF10 in liver is increased by the overexpression of constitutively active Forkhead Box 01(Fox01), which is resistant to nuclear exclusion by insulin (*77*). Furthermore, the activation of Cdc2-like kinase family proteins (CLK) by insulin can alter the phosphorylation and activity of SRSF10 (*78*). In addition, several studies also found a class III histone deacetylase in the liver, mainly called SIRT1, which can regulate multiple lipid metabolism pathways such as liver lipogenesis, fatty acid beta-oxidation, lipoprotein uptake and secretion (*11*). The interaction between SRSF10 and SIRT1 has been extensively studied. At both transcriptional and post-transcriptional levels, SRSF10 is upregulated by SIRT1, which is attributed to the increased stability of SRSF10 mRNA. Some studies also speculated that SIRT1 also physically interacted with SRSF10 though altering the acetylation status of SRSF10 and preventing its proteasomal degradation, thereby stabilizing and increasing the expression level of

Table 1. RBPs in the occurrence and development of MAFLD

RBPs	Expression	Target	Expression	Mechanism	*Ref.*
TTP	↑	TNF-α mRNA, Linc-SCRG1	↑	increase liver inflammation and protect against insulin resistance	(*60,127*)
HnRNPA1	↓	gys1 mRNA, CaM, H19	↓	decrease glycogen storage, and induce hepatic gluconeogenesis and adipogenesis	(*70*)
SRSF10	↓	LPIN1	-	stimulate lipogenesis and induce hepatic steatosis	(*79*)
HuR	↓	Insig1 mRNA, C/EBPβ mRNA, APOA4 mRNA,PTEN mRNA, HAMP mRNA	↓	influence liver homeostasis and hepatic iron deposition	(*87,89*)
CPEB1	↓	IL-6, PTEN, STAT3	↑	interfere with glucose metabolism and cause insulin resistance	(*120*)
CPEB4	↑	PFKFB3	↑	regulate UPR	(*97*)
EIF4E	↑	CD36 mRNA	↑	increase liver inflammation	(*100*)
IGF2BP2	↑	IGF1 mRNA	↓	increase hepatic iron deposition and free cholesterol	(*148*)
FTO	↑	TSC1 mRNA	↓	increase ROS release and mitochondrial dysfunction	(*149*)
HnRNPU	↓	TrkB, Blnc1	↑	promote liver inflammation and stress-induced cell death	(*109*)
AEG-1	↑	PPARα NF-κB	↓ ↑	drive hepatic inflammation and fibrosis	(*112*)
LIN28	↑	miR-200c	↓	cause liver fibrosis	(*117*)
CUGBP1	↑	IFN-γ mRNA	↓	promote HSCs activation	(*118*)
RBMS4	↑	Prx1 mRNA	↑	promote HSCs activation	(*121*)

RBPs, RNA binding proteins; MAFLD, metabolic-associated fatty liver disease; TTP, Tristetraprolin; TNF-α, tumor necrosis factor α; HnRNPA1, Human heterogeneous nuclear ribonucleoprotein A1; gys1, glycogen synthase 1; CaM, calmodulin; SRSF10, Serine rich splicing factor 10; HuR, Human antigen R; Insig1, insulin-induced gene 1; C/EBPβ, CCAAT enhancer-binding protein beta; APOA4, Apolipoprotein A-IV; PTEN, phosphatase and tensin homolog; HAMP, Heparin affin regulatory peptide; CPEB1, Cytoplasmic polyadenylation element binding protein 1; PFKFB3, 6-phosphofructo-2-kinase/fructose-2,6-bisphosphatase 3; EIF4E, Eukaryotic initiation factor 4E; CD36, Recombinant Cluster Of Differentiation 36; IGF2BP2, insulin-like growth factor 2 mRNA binding protein; FTO, fat mass and obesity-associated protein; TSC1, tuberous sclerosis 1; hnRNPU, a nuclear matrix protein; TrkB, Tyrosine Kinase receptor B; Blnc1, brown fat-enriched lncRNA 1; AEG-1, astrocyte elevated gene-1; PPARα, Peroxisome proliferator-activated receptor α; NF-κB, nuclear factor kappa-B; CUGBP1, CUG-binding protein 1; IFN-γ, interferon γ; RBMS4, an RNA binding protein; Prx1, Peroxiredoxin 1; ROS, reactive oxygen species; HSCs, hepatic stellate cells.

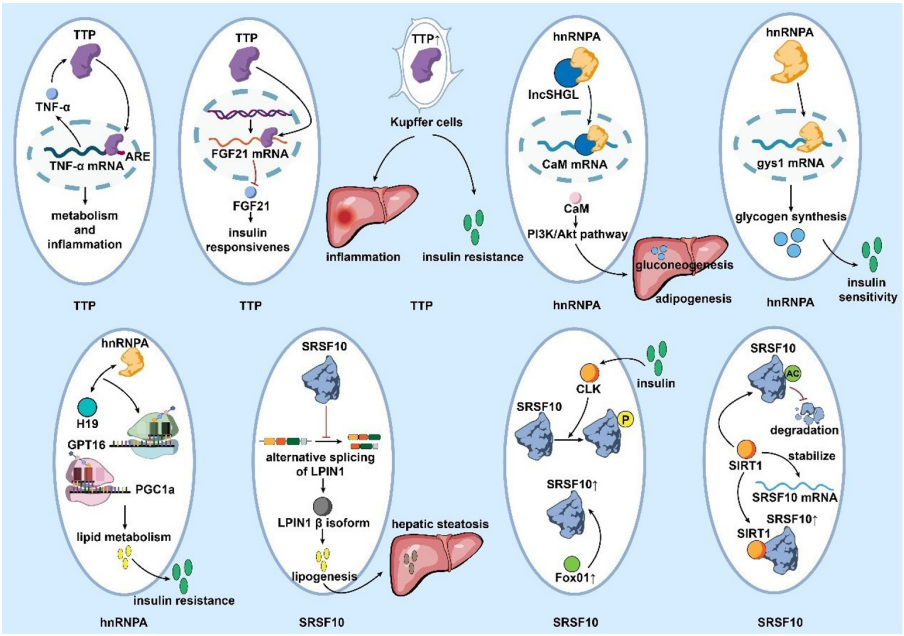

Figure 3. RNA-RBPS interaction in insulin resistance and liver fat deposition. Here, we summarize and show the main mechanisms of RNA-RBPS on insulin resistance and liver fat deposition. TTP can control the TNF-α level by binding to the AU-rich element (ARE) region of TNF-α mRNA and be upregulated by TNF-α treatment therefore playing a role in inflammation and metabolic disturbance. Post-transcriptional repression of FGF21 mRNA by TTP, which in turn regulates insulin responsiveness. Increased levels of TTP expression in Kupffer cells heighten liver inflammation and insulin resistance. lncSHGL regulates CaM levels at the post-transcriptional level and the lncSHGL / hnRNPA1 / CaM pathway is also involved in regulating the activity of the PI3K/Akt pathway to influence hepatic gluconeogenesis and adipogenesis. hnRNPA1 can interact with gys1 mRNA, thereby promoting glycogen synthesis and maintaining the sensitivity of insulin. hnRNPA1 interacts with H19 increasing the translation of fatty acid oxidation-related genes CPT1b and PGC1α, thereby improving insulin resistance. SRSF10 selectively down-regulates alternative splicing of LPIN1 to produce the LPIN1 β isoform, thereby stimulating adipogenesis and leading to hepatic steatosis. Activation of CLK by insulin can alter the phosphorylation and activity of SRSF10, and SRSF10 can be increased in the liver by overexpression of Fox01, which is resistant to nuclear rejection by insulin. SIRT1 upregulates SRSF10 by increasing the mRNA stability of SRSF10. SIRT1 also interacts with SRSF10 and alters the acetylation state of SRSF10 and prevents its proteasomal degradation, thereby increasing the expression level of SRSF10 protein.

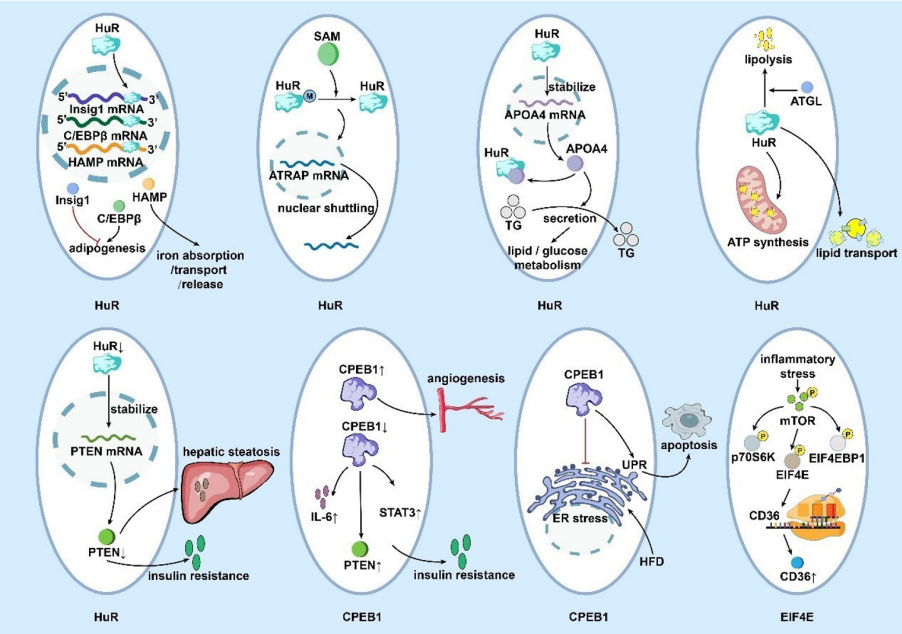

Figure 4. RNA-RBPS interaction in MAFLD. Here, we summarize and show the main mechanisms on RNA-RBPS in MAFLD. HuR can inhibit lipid formation by binding and stabilizing Insig1 mRNAs and C/EBPβ mRNAs and regulate iron absorption, transport and release by binding to the 3'UTR of HAMP mRNA. The low SAM levels induced by MAFLD lead to the demethylation of HuR, resulting in downstream nuclear shuttling of ATRAP mRNA. HuR also interacts directly with APOA4 and stabilizes its mRNA expression, regulating lipid and glucose metabolism by promoting the secretion of TG. ATGL mediates the regulation of lipolysis by HuR, which regulates lipid transport and ATP synthesis to prevent MAFLD. HuR also regulates glucolipid metabolism by increasing the stability of PTEN mRNA. HuR deletion decreases PTEN expression, which exacerbates hepatic steatosis in mice, but also reduces insulin resistance. Elevated levels of CPEB1 induce pathological angiogenesis in chronic liver disease, while decreased levels of CPEB1 lead to upregulation of IL-6, PTEN and STAT3, resulting in insulin resistance. CPEB4 affects the transduction of UPR to pro-apoptotic signaling in hepatocytes, and the translational regulation of CPEB4 contributes to the attenuation of HFD-induced ER stress in the liver. Inflammation enhances phosphorylation of mTOR and its downstream translational regulators such as p70S6K, EIF4E and EIF4EBP1, which then stimulate translation of CD36, leading to increased levels of CD36 protein in the liver.

SRSF10 protein in hepatocytes (*79*). However, to date, the molecular mechanism of how hepatic SRSF10 is regulated remains largely unknown, and further research is necessary.

3.2. MAFLD

MAFLD is the most common chronic liver disease. Despite increasing advances in the understanding of the pathophysiology of MAFLD, the exact mechanisms towards liver damage development remain unclear. And we urgently need to find therapeutic targets for MAFLD. Here, we summarize and show the first three RBPs with more specific mechanisms and more definite pathways in MAFLD (Figure 4).

3.2.1. Human antigen R

HuR is a member of the Hu RNA-binding protein family and is implicated in metabolism of RNAs (*80*). HuR is involved in a variety of important cellular processes, including inflammation, stress responses, carcinogenesis and apoptosis (*81*). HuR is widely considered to be a main regulator of liver homeostasis and the reduced expression of HuR will cause spontaneous steatosis and promote liver fibrosis (*82*). The study by Siang *et al*. has shown that HuR is an important inhibitor of adipogenesis found in both white adipose tissue and brown adipose tissue (*83*). Downregulation of HuR in adipose tissue greatly increases adipose mass, and glucose-intolerance and insulin-resistance appear at the same time. Mechanistically, HuR can inhibit adipogenesis by binding and stabilizing the mRNA of insulin-induced gene 1 (Insig1), which is a passive regulator of adipogenesis. S-adenosylmethionine (SAM) can increase the expression of Ang II type 1 receptor (AT1R)-associated protein (ATRAP) protein, and HuR also plays a vital role in it. Mechanistically, low SAM levels induced by MAFLD lead to demethylation of HuR, thereby resulting in downstream nuclear shuttling of ATRAP mRNA (*84*). Besides, in the early stages of adipogenesis, HuR can directly bind to the 3'UTR of CCAAT enhancer-binding protein beta (C/EBPβ) mRNA, which participates in the initiation of adipogenesis (*85*). HuR can also directly interact with Apolipoprotein A-IV (APOA4) and stabilize its mRNA expression, which is a plasma lipoprotein that regulates lipid and glucose metabolism by promoting the secretion of TG (*86*). In addition, Tian *et al*. also found that HuR could regulate lipid and sugar metabolism though improving the stability of phosphatase and tensin homolog (PTEN) mRNA. Deletion of HuR selectively decreased the

expression of PTEN, thereby aggravating liver steatosis in mice but also alleviating insulin resistance (*87*). Li *et al*. used adipose-specific HuR knockout (HuRAKO) mice as a model and found that HuRAKO mice showed obesity along with insulin resistance and exacerbated hepatic steatosis (*88*). Mechanistically, they suggested that adipose triglyceride lipase (ATGL), the major lipolytic enzyme, mediated the regulation of lipolysis by HuR. Zhang *et al*. also found that HuR can regulate lipid transport and ATP synthesis to prevent MAFLD using an animal model (*89*). SAM, a principle biological methyl donor involved in many metabolic pathways, is enriched in liver and downregulated in MAFLD patients (*90*). The latest studies noted that hepatic iron deposition is significantly associated with advanced MAFLD and liver fibrosis (*91*). Heparin affin regulatory peptide (HAMP) is an important mediator of iron absorption, transport and release, and is mainly expressed in the liver. HuR can bind to the 3'UTR of HAMP mRNA to upregulate its level (*92*). As discussed above, we can conclude that HuR, as a key regulator of lipid and glucose metabolism, may be a useful therapeutic target for MAFLD.

3.2.2. Cytoplasmic polyadenylation element binding protein

The cytoplasmic polyadenylation element binding protein (CPEB) family is a class of RBPs that regulate mRNA translation under hepatic metabolic stress (*93*). The amount of CPEB varies in different species and each member of the CPEB family has its own identity and role. Cytoplasmic polyadenylation element binding protein 1(CPEB1) is the most extensively studied CPEB, which is associated with meiosis, cell senescence, inflammation, glucose metabolism and liver homeostasis (*94*). When CPEB1 levels are reduced, IL-6, PTEN and signal transducer and activator of transcription 3 will be correspondingly up-regulated, thereby interfering with glucose metabolism and causing insulin resistance, which may lead to the occurrence of some liver diseases such as MAFLD (*95*). Moreover, elevated levels of CPEB1 will induce pathological angiogenesis in chronic liver disease (*96*). CPEB4 is identified to be associated with hepatic steatosis under ER stress and can regulate unfolded protein response (UPR), which is of great significance in the pathogenesis of MAFLD (*97*). A study by Maillo *et al*. has shown that the level of CPEB4 mRNA in the liver is mediated in a special circadian way (*97*). There is a connection between biological rhythm and metabolic homeostasis. Alterations in levels of CPEB4 affect the transduction of UPR to pro-apoptotic signals in hepatocytes, while translational regulation of CPEB4 contributes to alleviation of high fat diet (HFD)-induced hepatic ER stress. Thus, CPEB4 deficiency promotes MAFLD.

3.2.3. Eukaryotic Initiation Factor 4E

Eukaryotic initiation factor 4E (EIF4E), an mRNA cap-binding protein, affects mRNA-ribosome interactions and capture-dependent translation through interacting with eukaryotic initiation factor 4G (*98*). Hepatic inflammatory stress is critical for lipid accumulation and is an independent risk factor for the development of MAFLD. The mammalian target of rapamycin(mTOR) is a widely expressed and highly conserved serine/threonine kinase involved in the progression of metabolic syndrome under inflammatory stress (*99*). The mTOR downstream effectors mainly include EIF4E binding proteins and ribosomal protein S6K kinase (*100*). Recombinant Cluster of Differentiation 36(CD36), a transmembrane glycoprotein can promote the intake of long-chain fatty acids to induce hepatic steatosis, thereby leading to MAFLD (*101*). Wang *et al*. demonstrated that inflammatory stress enhanced phosphorylation of mTOR and its downstream translational regulators such as ribosome S6 protein kinase (p70S6K), EIF4E and EIF4E Binding Protein 1(EIF4EBP1), and then stimulated the translation of CD36, ultimately resulting in increased levels of CD36 protein in the liver (*102*). Rapamycin is a specific mTOR inhibitor that has an effect against lipid deposition in MAFLD treatment. Rapamycin can reduce CD36 protein expression through inhibiting mTOR pathway and phosphorylation of downstream effectors (*103*). All of these results show a molecular mechanism underlying the development of MAFLD and provide new evidence for MAFLD treatment. In addition, EIF4E also may play a vital role in progression from MAFLD to HCC (*100*).

3.3. NASH

NASH is a late-stage MAFLD manifestation, and is also one of the most common causes of liver failure globally. NASH is characterized by persistent liver damage, chronic inflammation and different degrees of liver fibrosis (*104*). Here, we list and summarize several RBPs associated with the development of NASH.

M6A is the most abundant form of internal RNA modifications in messenger RNA, microRNA, and non-coding RNA. Methylation of m6A RNA plays a significant part in hepatic lipid metabolism disorder. Both insulin-like growth factor 2 mRNA binding proteins (IGF2BPs) and YTHDF1 can recognize m6A methylation, and then act as signal transducers and facilitators in MAFLD-NASH-HCC progression (*105,106*). The accumulation of free cholesterol in the liver is an important trigger for the occurrence of severe NASH. Simon *et al*. also elaborated that insulin-like growth factor 2 mRNA binding protein (IGF2BP2) can promote NASH by increasing hepatic iron deposition and free cholesterol (*107*). FTO belongs to the AlkB family of enzymes and is also an important class of RBPs that demethylates specifically mRNA m6A. Studies have shown that upregulation of FTO will induce

increased reactive oxygen species (ROS) release and mitochondrial dysfunction, thereby leading to more severe NASH (*108*). Furthermore, hepatocellular specific inactivation of hnRNPU (a nuclear matrix protein) will exacerbate HFD-induced NASH through aberrantly inducing a truncated Tyrosine Kinase receptor B (TrkB) isoform that promotes liver inflammation and stress-induced cell death, including liver injury, inflammation and fibrosis (*109*). Lack of Blnc1 in the liver can improve NASH, while some RBPs can interact with Blnc1, such as endothelial differentiation-related factor 1 (EDF1), YBX1 and hnRNPU (*49*). Jin *et al*. proposed that circRNA_002581 positively regulates CPEB1 *via* sponge miR-122, a pathway with therapeutic potential for NASH (*110*). Hepatic farnesoid X receptor (FXR) is an important regulator of lipid homeostasis that prevents NASH, and its expression correlates with the severity of NASH (*111*). FXR activation can increase HuR, which maintains hepatocyte homeostasis under normal conditions (*82*). In addition, there are also some RBPs that play a vital role in the fibrosis process of NASH. AEG-1 (astrocyte elevated gene-1), an ER membrane-anchored RBP, which regulates fatty acid β-oxidation (FAO) by inhibiting PPARα activation, and promoted translation of mRNAs encoding fatty acid–synthesizing enzymes, thereby promoting de novo lipogenesis (DNL). Moreover, AEG-1 also can activate NF-κB signal pathway to drive hepatic inflammation and fibrosis (*112*). Gerhard *et al*. demonstrated that adipocyte enhancer binding protein 1 (AEBP1) expression parallels the worsening of fibrosis severity in NASH, which can regulate many differentially expressed genes about NASH (*113*). AEBP1 interacted with miR-372-3p and miR-373-3p, which were shown to be significantly downregulated in NASH fibrosis. Furthermore, a mutual effect between AEBP1 and PTEN has been explored and results revealed a vital function of AEBP1 in hepatic fibrosis in NASH patients. These RBPs are increasingly recognized as viable targets for treating NASH and MAFLD-NASH-HCC. Hence, it is essential to get a deep understanding of their functions and mechanisms.

3.4. Liver Cirrhosis

MAFLD and NASH are considered to be the predecessors of liver fibrosis and eventually cirrhosis. The main feature of liver fibrosis is excessive activation of HSCs (*114*). The dysregulated expression of RBPs also has a strong impact on the occurrence of liver cirrhosis (Figure 5), such as HNRNPA1, LIN28, HuR, TTP and so on. HnRNPA1, which usually is located in the nucleus, is overexpressed in mouse HSCs. ER stress in hepatic

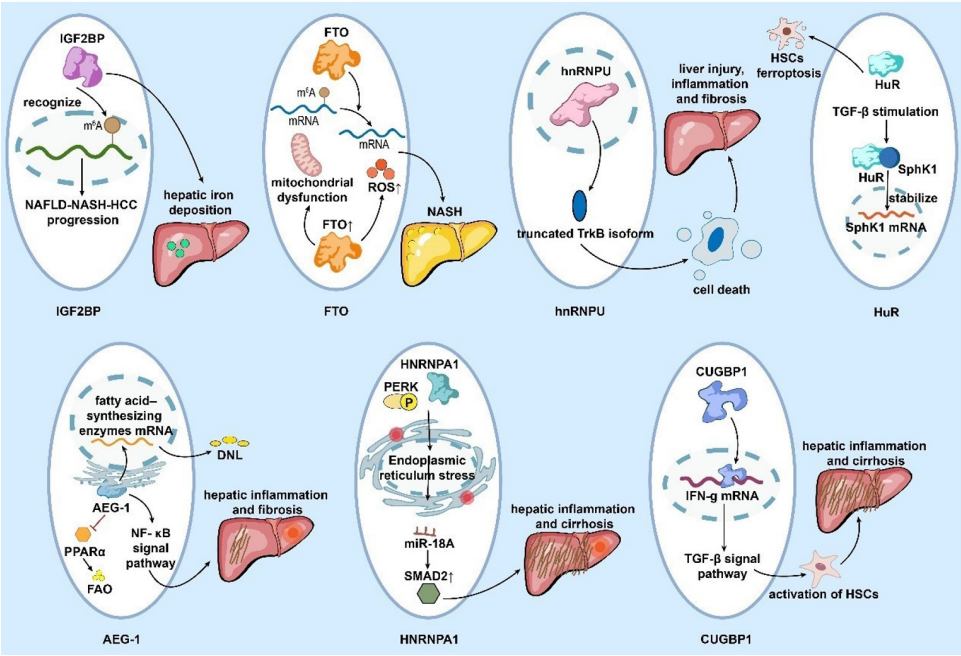

Figure 5. RNA-RBPS interaction in NASH and Liver Cirrhosis. Here, we summarize and show the main mechanisms on RNA-RBPS in NASH and Liver Cirrhosis. IGF2BPs can recognize m6A methylation and facilitate the progression of NAFLD-NASH-HCC. And IGF2BP2 promotes the development of NASH by increasing hepatic iron deposition. FTO specifically demethylates mRNA m6A and upregulation of FTO will initiate increased ROS release and mitochondrial dysfunction, leading to more severe NASH. hnRNPU promotes hepatic inflammation and stress-induced cell death through the induction of truncated TrkB isoforms, leading to liver injury, inflammation and fibrosis. HuR binds to SphK1 and stabilizes its mRNA after TGF-β stimulation. On the other hand, HuR attenuates the effect of HSCs by promoting HSCs ferroptosis. AEG-1 is an ER membrane-anchored RBP that regulates FAO by inhibiting the activation of PPARα and promotes the translation of mRNAs encoding fatty acid synthases, thereby promoting DNL. In addition, AEG-1 activates the NF-κB signaling pathway, driving liver inflammation and fibrosis. Dysregulation of PERK phosphorylation and HNRNPA1 expression mediates endoplasmic reticulum stress in hepatic stellate cells and miR-18A induces SMAD2 overexpression, leading to liver fibrosis and cirrhosis. CUGBP1 binds specifically to IFN-g mRNA and contributes to the TGF-β signaling pathway, thereby promoting the activation of HSCs, ultimately resulting in the development of fibrosis and cirrhosis.

stellate cells is mediated by protein kinase RNA–like endoplasmic reticulum kinase (PERK) phosphorylation and dysregulated expression of HNRNPA1, and then induces recombinant others against decapentaplegic homolog 2(SMAD2) overexpression by miR-18A, thereby causing liver fibrosis and cirrhosis (*115*). LIN28 is a highly conserved RBP involved in many eukaryotic cellular processes and its main function is cell transformation, which is likely to play an important role in liver fibrosis repair (*116*). In the process of MAFLD-NASH-HCC, the expression of LIN28 is abnormally increased. A recent study showed that overexpression of miR-200c bound to LIN28 can promote epithelial-to-mesenchymal transition (EMT) and mesenchymal-to-epithelial transition (MET), and the balance of EMT-MET will decide whether NASH patients recover or develop liver cirrhosis (*117*). Wu *et al*. found that CUG-binding protein 1 (CUGBP1) showed elevated expression in HSCs, which is associated with the severity of liver fibrosis. CUGBP1 specifically binds to interferon (IFN)-γ mRNA and promotes the transforming growth factor (TGF)-β signal pathway, thereby promoting the activation of HSCs, which ultimately leads to the occurrence of fibrosis and liver cirrhosis (*118*). CPEB4, a member of the CPEB family, is highly expressed in the liver and has also been found to prevent HSCs activation and liver fibrosis by silencing (*119*). In the early stage of HSC activation, 6-phosphofructo-2-kinase/fructose-2,6-bisphosphatase 3(PFKFB3) protein is continuously upregulated by CPEB4 and its binding RNA, which has become a potential target for anti-fibrosis and prevention of liver cirrhosis (*120*). An RBP called RBMS3 can specifically bind to the 3'UTR of Peroxiredoxin 1(Prx1) mRNA and increase Prx1 protein expression. Fritz *et al*. found that RBMS3 expression in fibrotic liver was highly expressed, and its expression level increased with increasing HSCs activity(*121*). Moreover, p62 is an RBP class with an RNA-binding motif. Lu *et al*. showed that p62 was sporadically expressed in cirrhotic nodules cells and may be associated with hyperproliferating cells (*122*).

Notably, in recent years, ferroptosis was revealed to be closely associated with liver fibrosis and may become a potential target for liver fibrosis therapy. HuR has long been described as a key player in MAFLD and NASH, and has also been found to contribute to the activation of HSCs and development of liver fibrosis (*113*). In activated HSCs, HuR expression is highly increased (*123*). Upregulation of sphingosine kinase 1 (SphK1) is involved in HSCs activation induced by the TGF-β signaling pathway. On the one hand, HuR can bind to SphK1 and stabilize its mRNA after TGF-β stimulation (*124*). On the other hand, HuR alleviates the effect of HSCs by promoting HSCs ferroptosis (*125*). TTP, which belongs to the same AU-rich element-binding proteins as HuR, has several important roles in different stages of liver fibrosis. TTP has been shown to inhibit HSC ferroptosis by binding to autophagy-related 16-like 1 mRNA (*126*). Finally, gene chip detection identified an lncRNA called linc-SCRG1, which was up-regulated 13.62-fold in human liver cirrhosis (*127*). Linc-SCRG1 can specifically bind to TTP and has the ability to inhibit the phenotypic inactivation of HSCs, thereby delaying the progression of cirrhosis.

4. Non-Coding RNA-RBPs Interaction in MAFLD

MAFLD is closely associated with systemic energy metabolism disorders and can progress from simple steatosis to NASH and eventually to cirrhosis (*2*). Recently, many studies found that the relationship between non-coding RNAs (ncRNAs) and RBP was involved in the occurrence and development of MAFLD. Here, we introduced several key ncRNA-RBP interactions for MAFLD.

HuR mentioned above is an important RBP for MAFLD. Studies have shown that HuR can upregulate multiple lncRNAs, such as lncRNA NEAT1, LINC00336 and lncRNA UFC1, further promoting cell proliferation and invasion and inhibiting cell apoptosis (*85*). Apolipoprotein A-IV (APOA4), a plasma lipoprotein, can regulate glucose and lipid metabolism by promoting the secretion of TG. A study found that both antisense lncRNA APOA4-AS and APOA4 are significantly upregulated in MAFLD, and APOA4-AS can interact with HuR directly. After knockdown of HuR, APOA4-AS levels were significantly reduced, resulting in lower plasma TG and TC levels. CPEB1 has been shown to have an important role in chronic liver disease. MiR-122, the most common miRNA in adult liver, has been identified to be a downstream target of circRNA_002581 and an upstream regulator of CPEB1. Jinet al. confirmed the existence of circRNA_002581-miR-122-CPEB1 axis *in vitro*, which is involved in NASH pathogenesis by inhibiting autophagy related to the PTEN-AMPK-mTOR pathway (*110*). SIRT1 plays an important role in many metabolic diseases, including MAFLD. Among them, SIRT1 in liver can regulate the expression of QKI 5 by the PPARα/FoxO1 signal pathway, which belongs to the STAR family of RNA-binding proteins, and SIRT1 siRNA can induce acetylation of QKI 5 (*11*). A recent study by Chen *et al*. showed that silencing circRNA_0000660 can significantly inhibit miR-693 to upregulate IGFBP1 level, thereby reducing lipid accumulation in liver and alleviating MAFLD (*128*). In addition, several lncRNAs have been demonstrated to be tightly associated with RBPs. Hepatic lncSHGL can participate in MAFLD development by promoting fasting hyperglycemia and lipid deposition in mice. Wang *et al*. also found that lncSHGL can enhance HnRNPA1 to promote CaM mRNA translation (*129*). Moreover, studies found that lncRNA Blnc1 was elevated abnormally in MAFLD mice, which was associated with hepatic steatosis and insulin resistance. Proteomic analysis found that EDF1, YBX1 and hnRNPU all

Table 2. Potential Drugs Targeting RBPs in the development of MAFLD

Drugs	Disease	Target	Function	*Ref.*
SAM	MAFLD	HuR↑	maintain metabolic homeostasis	(*84*)
Betaine	MAFLD	FTO↓	decrease de novo lipogenesis, increase lipolysis	(*137*)
Exenatide	MAFLD	FTO↓	reverse lipid accumulation, promote inflammation regression	(*140*)
eIFsixty-1,4,6	HCC	EIF4E↓	inhibit HCC formation	(*100*)
PHA-781089	HCC	TTP↓	induce apoptosis of HCC	(*145*)

RBPs, RNA binding proteins; MAFLD, metabolic-associated fatty liver disease; NASH, nonalcoholic steatohepatitis; SAM, S-adenosylmethionine; FTO, fat mass and obesity-associated protein; HCC, hepatocellular carcinoma; eIF6, eukaryotic translation initiation factor 6; TTP, Tristetraprolin.

interacted with Blnc1.

Except for RNA-RBP interactions, some RBPs also can directly interact with RBPs or proteins, thereby affecting the development of MAFLD. For instance, Tian *et al*. have showed that HuR can regulate intracellular cholesterol homeostasis by regulating the expression of ATP-binding cassette transporter A1 (ABCA1) (*87*). And Woodhoo *et al*. have found that HuR also reduces profibrotic effects induced by TGF-β through significantly silencing the expression of alpha smooth muscle actin (a-SMA) (*130*). Also, downregulation of CUGBP1 can also suppress a-SMA expression, and can further promote the IFN-γ signaling pathway, which is associated with the progression of liver fibrosis (*118*). Moreover, PINX1 (Pin2/TRF1 interacting protein) has been found to be overexpressed in patients with cirrhosis. A study by Huang *et al*. has demonstrated that inhibition of PinX1 can significantly increase telomere length and telomerase activity, thereby attenuating the progression of MAFLD *in vivo* and *in vitro* (*131*). In addition, DDX1, an RBP that regulates insulin, can increase blood glucose through mediated inhibition of insulin translation. DDX1 can interact with another RBP called eIF4B, which is a well-established factor for translation initiation(*132*). Therefore, it is tempting to speculate about the importance of future studies on the interactions between RBPs and other molecules, and it will help us to elucidate the pathological mechanism of MAFLD.

5. Potential Drugs Targeting RBPs in MAFLD

Nowadays, the development of drugs targeted for RBPs has come to the fore given its significance in the evolution of MAFLD (*7*). This section will discuss the potential therapeutic drugs being studied for MAFLD targeted at RBPs (as shown in Table 2).

Therapeutic targets for improving lipid metabolism of MAFLD can be developed in two ways: 1) to lower the metabolizing substrates in the liver; 2) to accelerate the effective metabolism of lipids in the liver (*133*). For example, SAM is a major biological methyl donor in mammalian cells, which is a defining factor of the subcellular localization of HuR (*134*). ATRAP was shown to potentially prevent abnormal metabolism of tissue, including lipid deposition and hepatic fibrosis (*135*). The low SAM concentration induced by MAFLD will cause HuR demethylation, which directly breaks the dynamic balance of nucleocytoplasmic shuttling of ATRAP mRNA. When SAM supplementation is provided, SAM maintains the nucleocytoplasmic shuttling of ATRAP mRNA by regulating HuR methylation and upregulates the expression of ATRAP, thereby reducing the disorder of lipid metabolism and insulin resistance (*84*). One of the main physiological effects of betaine is to get involved in the methionine cycle in the human liver as a methyl donor (*136*). In addition, experiments in a mouse model have shown that the detected low methylation status of m6A and increased FTO expression could be corrected by betaine supplementation. This suggests that betaine supplementation can significantly reduce the liver function lesions and morphology damage caused by high fat as well as ectopic fat accumulation to prevent MAFLD (*137*). And most remarkably, betaine is a main component of many foods, including wheat, shellfish, spinach, and beets, which enlightens us that perhaps MAFLD can be treated by diet therapy (*138*). Moreover, exenatide is a glucagon like peptide-1 receptor agonist antidiabetic drug that can ameliorate insulin resistance and reduce hepatic steatosis (*139*). Li *et al*. established animal models with MAFLD induced by a HFD and the related cell culture models and studied the protective effect of exenatide on the fatty liver through FTO genes *in vivo* and *in vitro* technologies. Histological analysis indicates that exenatide significantly reverses HF-induced lipid accumulation and inflammatory evolution, accompanied by a dropping expression of FTO mRNA and protein, which may represent an effective treatment strategy for MAFLD (*140*).

The abnormally accumulated fat will advance the development of HCC and the metabolism of fat in the liver is closely related to the regulation of functional proteins (*141*). Translation factors such as EIF4E act continuously on the evolution from MAFLD to HCC (*142*). In this regard, it is identified in a study that three compounds (eIFsixty-1, eIFsixty-4, eIFsixty-6) can inhibit the binding of eIF-6 and 60S and the translation of Lipogenic enzymes, which can delay the formation and growth of HCC nodules without obvious negative side effects (*100*). The RNA-binding protein TTP can regulate about 2500 genes, the functional modification of which represents a promising therapeutic strategy

for HCC (*143*). It has been shown that the consumption of TTP in HCC cell lines prevents HCC cells from apoptosis (*144*). PHA-781089, a MAPKAP2 (MK2) inhibitor, was used as an inhibitor of TTP functions in a study, which showed that mRNA expression of the TTP target can be restored in the presence of MK2 inhibitors and this is a sign that the MK2/TTP pathway plays a role in the proliferation and maintenance of HCC (*145*).

However, we should be careful about the side effects of targeting RBPs in MAFLD therapy. For example, HuR is involved in the production of cellular inflammation. One inflammatory phenotype is largely the driving force behind HuR's implications in heart-related diseases including vascular inflammation and atherosclerosis (*146*). Besides, some pathogenic microorganisms like Hepatitis C virus use HuR biology to promote disease progression (*147*) .

In conclusion, a network of gene expression regulation through multiple approaches involved in RBPs will contribute to the new drug design and biomarker discoveries of MAFLD and other related liver diseases that evolved from MAFLD. The advanced therapies for MAFLD derived from RBP are being tested and will be gradually applied.

6. Conclusion

In recent years, the vital roles of RBPs have been demonstrated in the development of MAFLD. With the development of biological and molecular science, more and more RBPs and target RNAs in MAFLD have been discovered, allowing us to better understand the occurrence of MAFLD. In this review, we conclude that these RBPs are associated with insulin resistance and liver fat deposition, MAFLD, NASH and liver cirrhosis. Therefore, we discuss the ncRBP-RNA interactions in MAFLD and several drugs related to RBPs in MAFLD therapy.

Currently, the research on the specific mechanism of RBP is not well studied, and drug strategies targeting RBPs are still in the start-up stage, just like MAFLD. Notably, the different alternative splicing regulation of RBPs will lead to the complexity of their protein functions. Protein functional structure of targeted RBPs with high selection may be effective in reducing the occurrence of side effects. From what has been discussed above, posttranscriptional modulation by RBPs is becoming an important constructive mechanism in the occurrence and development of MAFLD, which still needs further studies to elucidate the complex regulatory network in MAFLD and other metabolic diseases.

Acknowledgements

We sincerely appreciate the guidance from our tutors and every member in our team. The graphical abstracts were created with BioRender software (BioRender.com).

Funding: This work was supported by the Natural Science Foundation in Jiangxi Province grant [grant numbers No. 20212BAB216051 to J.Z., No. 20212BAB216047 and No. 202004BCJL23049 to P.Y.]; the National Natural Science Foundation of China [grant number No. 82160371 to J.Z., No. 82100869 to P.Y.].

Conflict of Interest: The authors have no conflicts of interest to disclose.

Author contribution statements: JWX, XYL, SQW, JZ and PY designed the review outline. JWX, XYL, SQW and JTL collected the information and data from literature and online, summarized and analyzed the data and drafted the manuscript. JZ, PY, DJZ, XL, PPX, KZ, MXX and YFS advised on the structure and content of the manuscript and revised the manuscript. All authors read and approved the final manuscript.

References

1. Shiha G, Korenjak M, Eskridge W, *et al*. Redefining fatty liver disease: an international patient perspective. Lancet Gastroenterol Hepatol. 2021; 6:73-79.
2. Eslam M, Sanyal AJ, George J, International Consensus P. MAFLD: A Consensus-Driven Proposed Nomenclature for Metabolic Associated Fatty Liver Disease. Gastroenterology. 2020; 158:1999-2014 e1991.
3. Cotter TG, Rinella M. Nonalcoholic Fatty Liver Disease 2020: The State of the Disease. Gastroenterology. 2020; 158:1851-1864.
4. Huby T, Gautier EL. Immune cell-mediated features of non-alcoholic steatohepatitis. Nat Rev Immunol. 2022; 22:429-443.
5. Perakakis N, Stefanakis K, Mantzoros CS. The role of omics in the pathophysiology, diagnosis and treatment of non-alcoholic fatty liver disease. Metabolism. 2020; 111S:154320.
6. Younossi ZM. Non-alcoholic fatty liver disease - A global public health perspective. J Hepatol. 2019; 70:531-544.
7. Gerstberger S, Hafner M, Tuschl T. A census of human RNA-binding proteins. Nat Rev Genet. 2014; 15:829-845.
8. Salem ESB, Vonberg AD, Borra VJ, Gill RK, Nakamura T. RNAs and RNA-Binding Proteins in Immuno-Metabolic Homeostasis and Diseases. Front Cardiovasc Med. 2019; 6:106.
9. Schieweck R, Ninkovic J, Kiebler MA. RNA-binding proteins balance brain function in health and disease. Physiol Rev. 2021; 101:1309-1370.
10. Lachiondo-Ortega S, Delgado TC, Banos-Jaime B, Velazquez-Cruz A, Diaz-Moreno I, Martinez-Chantar ML. Hu Antigen R (HuR) Protein Structure, Function and Regulation in Hepatobiliary Tumors. Cancers (Basel). 2022; 14:2666.
11. Zhang W, Sun Y, Liu W, Dong J, Chen J. SIRT1 mediates the role of RNA-binding protein QKI 5 in the synthesis of triglycerides in non-alcoholic fatty liver disease mice *via* the PPARalpha/FoxO1 signaling pathway. Int J Mol Med. 2019; 43:1271-1280.
12. Seufert L, Benzing T, Ignarski M, Muller RU. RNA-binding proteins and their role in kidney disease. Nat Rev Nephrol. 2022; 18:153-170.

13. Kelaini S, Chan C, Cornelius VA, Margariti A. RNA-Binding Proteins Hold Key Roles in Function, Dysfunction, and Disease. Biology (Basel). 2021; 10:366.
14. Mohibi S, Chen X, Zhang J. Cancer the'RBP'eutics-RNA-binding proteins as therapeutic targets for cancer. Pharmacol Ther. 2019; 203:107390.
15. Neelamraju Y, Hashemikhabir S, Janga SC. The human RBPome: from genes and proteins to human disease. J Proteomics. 2015; 127:61-70.
16. Akira S, Maeda K. Control of RNA Stability in Immunity. Annu Rev Immunol. 2021; 39:481-509.
17. Corley M, Burns MC, Yeo GW. How RNA-Binding Proteins Interact with RNA: Molecules and Mechanisms. Mol Cell. 2020; 78:9-29.
18. Daubner GM, Clery A, Allain FH. RRM-RNA recognition: NMR or crystallography...and new findings. Curr Opin Struct Biol. 2013; 23:100-108.
19. Cienikova Z, Jayne S, Damberger FF, Allain FH, Maris C. Evidence for cooperative tandem binding of hnRNP C RRMs in mRNA processing. RNA. 2015; 21:1931-1942.
20. Shi X, Hanson MR, Bentolila S. Functional diversity of Arabidopsis organelle-localized RNA-recognition motif-containing proteins. Wiley Interdiscip Rev RNA. 2017; 8:doi: 10.1002/wrna.1420.
21. Yamamoto J, Hagiwara Y, Chiba K, Isobe T, Narita T, Handa H, Yamaguchi Y. DSIF and NELF interact with Integrator to specify the correct post-transcriptional fate of snRNA genes. Nat Commun. 2014; 5:4263.
22. Ule J, Blencowe BJ. Alternative Splicing Regulatory Networks: Functions, Mechanisms, and Evolution. Mol Cell. 2019; 76:329-345.
23. Gruber AJ, Zavolan M. Alternative cleavage and polyadenylation in health and disease. Nat Rev Genet. 2019; 20:599-614.
24. Boo SH, Kim YK. The emerging role of RNA modifications in the regulation of mRNA stability. Exp Mol Med. 2020; 52:400-408.
25. Bridges MC, Daulagala AC, Kourtidis A. LNCcation: lncRNA localization and function. J Cell Biol. 2021; 220:e202009045.
26. Zheng X, Peng Q, Wang L, Zhang X, Huang L, Wang J, Qin Z. Serine/arginine-rich splicing factors: the bridge linking alternative splicing and cancer. Int J Biol Sci. 2020; 16:2442-2453.
27. Li Y, Xu J, Lu Y, *et al*. DRAK2 aggravates nonalcoholic fatty liver disease progression through SRSF6-associated RNA alternative splicing. Cell Metab. 2021; 33:2004-2020.e2009.
28. Doron-Mandel E, Koppel I, Abraham O, *et al*. The glycine arginine-rich domain of the RNA-binding protein nucleolin regulates its subcellular localization. EMBO J. 2021; 40:e107158.
29. Carvalho LS, Goncalves N, Fonseca NA, Moreira JN. Cancer Stem Cells and Nucleolin as Drivers of Carcinogenesis. Pharmaceuticals (Basel). 2021; 14:60.
30. Dassi E. Handshakes and Fights: The Regulatory Interplay of RNA-Binding Proteins. Front Mol Biosci. 2017; 4:67.
31. Zaccara S, Ries RJ, Jaffrey SR. Reading, writing and erasing mRNA methylation. Nat Rev Mol Cell Biol. 2019; 20:608-624.
32. Sledz P, Jinek M. Structural insights into the molecular mechanism of the m^6A writer complex. Elife. 2016; 5:e18434.
33. Damianov A, Ying Y, Lin CH, Lee JA, Tran D, Vashisht AA, Bahrami-Samani E, Xing Y, Martin KC, Wohlschlegel JA, Black DL. Rbfox Proteins Regulate Splicing as Part of a Large Multiprotein Complex LASR. Cell. 2016; 165:606-619.
34. Jangi M, Boutz PL, Paul P, Sharp PA. Rbfox2 controls autoregulation in RNA-binding protein networks. Genes Dev. 2014; 28:637-651.
35. Sun Y, Bao Y, Han W, Song F, Shen X, Zhao J, Zuo J, Saffen D, Chen W, Wang Z, You X, Wang Y. Autoregulation of RBM10 and cross-regulation of RBM10/RBM5 *via* alternative splicing-coupled nonsense-mediated decay. Nucleic Acids Res. 2017; 45:8524-8540.
36. Loiselle JJ, Roy JG, Sutherland LC. RBM10 promotes transformation-associated processes in small cell lung cancer and is directly regulated by RBM5. PLoS One. 2017; 12:e0180258.
37. Gazzara MR, Mallory MJ, Roytenberg R, Lindberg JP, Jha A, Lynch KW, Barash Y. Ancient antagonism between CELF and RBFOX families tunes mRNA splicing outcomes. Genome Res. 2017; 27:1360-1370.
38. Kim SH, Shanware NP, Bowler MJ, Tibbetts RS. Amyotrophic lateral sclerosis-associated proteins TDP-43 and FUS/TLS function in a common biochemical complex to co-regulate HDAC6 mRNA. J Biol Chem. 2010; 285:34097-34105.
39. Park OH, Park J, Yu M, An HT, Ko J, Kim YK. Identification and molecular characterization of cellular factors required for glucocorticoid receptor-mediated mRNA decay. Genes Dev. 2016; 30:2093-2105.
40. Kour S, Rajan DS, Fortuna TR, *et al*. Loss of function mutations in GEMIN5 cause a neurodevelopmental disorder. Nat Commun. 2021; 12:2558.
41. Park OH, Ha H, Lee Y, Boo SH, Kwon DH, Song HK, Kim YK. Endoribonucleolytic Cleavage of m(6)A-Containing RNAs by RNase P/MRP Complex. Mol Cell. 2019; 74:494-507 e498.
42. Liu J, Gao M, Xu S, Chen Y, Wu K, Liu H, Wang J, Yang X, Wang J, Liu W, Bao X, Chen J. YTHDF2/3 Are Required for Somatic Reprogramming through Different RNA Deadenylation Pathways. Cell Rep. 2020; 32:108120.
43. Zhong X, Yu J, Frazier K, *et al*. Circadian Clock Regulation of Hepatic Lipid Metabolism by Modulation of m(6)A mRNA Methylation. Cell Rep. 2018; 25:1816-1828 e1814.
44. Yu JT, Hu XW, Chen HY, Yang Q, Li HD, Dong YH, Zhang Y, Wang JN, Jin J, Wu YG, Li J, Ge JF, Meng XM. DNA methylation of FTO promotes renal inflammation by enhancing m(6)A of PPAR-alpha in alcohol-induced kidney injury. Pharmacol Res. 2021; 163:105286.
45. Muller-McNicoll M, Rossbach O, Hui J, Medenbach J. Auto-regulatory feedback by RNA-binding proteins. J Mol Cell Biol. 2019; 11:930-939.
46. Ore A, Akinloye OA. Phytotherapy as Multi-Hit Therapy to Confront the Multiple Pathophysiology in Non-Alcoholic Fatty Liver Disease: A Systematic Review of Experimental Interventions. Medicina (Kaunas). 2021; 57:822.
47. Ciardullo S, Perseghin G. Prevalence of NAFLD, MAFLD and associated advanced fibrosis in the contemporary United States population. Liver Int. 2021; 41:1290-1293.
48. Sakurai Y, Kubota N, Yamauchi T, Kadowaki T. Role of Insulin Resistance in MAFLD. Int J Mol Sci. 2021; 22:4156.
49. Zhao XY, Xiong X, Liu T, Mi L, Peng X, Rui C, Guo L, Li S, Li X, Lin JD. Long noncoding RNA licensing of obesity-linked hepatic lipogenesis and NAFLD

pathogenesis. Nat Commun. 2018; 9:2986.
50. Honma M, Sawada S, Ueno Y, *et al*. Selective insulin resistance with differential expressions of IRS-1 and IRS-2 in human NAFLD livers. Int J Obes (Lond). 2018; 42:1544-1555.
51. Pullmann R, Jr., Kim HH, Abdelmohsen K, Lal A, Martindale JL, Yang X, Gorospe M. Analysis of turnover and translation regulatory RNA-binding protein expression through binding to cognate mRNAs. Mol Cell Biol. 2007; 27:6265-6278.
52. Grifone R, Shao M, Saquet A, Shi DL. RNA-Binding Protein Rbm24 as a Multifaceted Post-Transcriptional Regulator of Embryonic Lineage Differentiation and Cellular Homeostasis. Cells. 2020; 9:1891.
53. Garcia-Maurino SM, Rivero-Rodriguez F, Velazquez-Cruz A, Hernandez-Vellisca M, Diaz-Quintana A, De la Rosa MA, Diaz-Moreno I. RNA Binding Protein Regulation and Cross-Talk in the Control of AU-rich mRNA Fate. Front Mol Biosci. 2017; 4:71.
54. Tiedje C, Diaz-Munoz MD, Trulley P, Ahlfors H, Laass K, Blackshear PJ, Turner M, Gaestel M. The RNA-binding protein TTP is a global post-transcriptional regulator of feedback control in inflammation. Nucleic Acids Res. 2016; 44:7418-7440.
55. Kuwano Y, Kim HH, Abdelmohsen K, Pullmann R, Jr., Martindale JL, Yang X, Gorospe M. MKP-1 mRNA stabilization and translational control by RNA-binding proteins HuR and NF90. Mol Cell Biol. 2008; 28:4562-4575.
56. Sedlyarov V, Fallmann J, Ebner F, Huemer J, Sneezum L, Ivin M, Kreiner K, Tanzer A, Vogl C, Hofacker I, Kovarik P. Tristetraprolin binding site atlas in the macrophage transcriptome reveals a switch for inflammation resolution. Mol Syst Biol. 2016; 12:868.
57. Pamir N, McMillen TS, Kaiyala KJ, Schwartz MW, LeBoeuf RC. Receptors for tumor necrosis factor-alpha play a protective role against obesity and alter adipose tissue macrophage status. Endocrinology. 2009; 150:4124-4134.
58. Awazawa M, Ueki K, Inabe K, *et al*. Adiponectin enhances insulin sensitivity by increasing hepatic IRS-2 expression *via* a macrophage-derived IL-6-dependent pathway. Cell Metab. 2011; 13:401-412.
59. Cao H, Urban JF, Jr., Anderson RA. Insulin increases tristetraprolin and decreases VEGF gene expression in mouse 3T3-L1 adipocytes. Obesity (Silver Spring). 2008; 16:1208-1218.
60. Louis JM, Agarwal A, Aduri R, Talukdar I. Global analysis of RNA-protein interactions in TNF-α induced alternative splicing in metabolic disorders. FEBS letters. 2021; 595:476-490.
61. Bayeva M, Khechaduri A, Puig S, Chang HC, Patial S, Blackshear PJ, Ardehali H. mTOR regulates cellular iron homeostasis through tristetraprolin. Cell Metab. 2012; 16:645-657.
62. Guo J, Lei M, Cheng F, Liu Y, Zhou M, Zheng W, Zhou Y, Gong R, Liu Z. RNA-binding proteins tristetraprolin and human antigen R are novel modulators of podocyte injury in diabetic kidney disease. Cell Death Dis .2020; 11:413.
63. Kratochvill F, Gratz N, Qualls JE, Van De Velde LA, Chi H, Kovarik P, Murray PJ. Tristetraprolin Limits Inflammatory Cytokine Production in Tumor-Associated Macrophages in an mRNA Decay-Independent Manner. Cancer Res. 2015; 75:3054-3064.
64. Caracciolo V, Young J, Gonzales D, Ni Y, Flowers SJ, Summer R, Waldman SA, Kim JK, Jung DY, Noh HL, Kim T, Blackshear PJ, O'Connell D, Bauer RC, Kallen CB. Myeloid-specific deletion of Zfp36 protects against insulin resistance and fatty liver in diet-induced obese mice. Am J Physiol Endocrinol Metab. 2018; 315:E676-E693.
65. Sawicki KT, Chang HC, Shapiro JS, Bayeva M, De Jesus A, Finck BN, Wertheim JA, Blackshear PJ, Ardehali H. Hepatic tristetraprolin promotes insulin resistance through RNA destabilization of FGF21. JCI insight. 2018; 3:e95948.
66. Tauber H, Huttelmaier S, Kohn M. POLIII-derived non-coding RNAs acting as scaffolds and decoys. J Mol Cell Biol. 2019; 11:880-885.
67. Tavanez JP, Madl T, Kooshapur H, Sattler M, Valcarcel J. hnRNP A1 proofreads 3' splice site recognition by U2AF. Mol Cell. 2012; 45:314-329.
68. David CJ, Chen M, Assanah M, Canoll P, Manley JL. HnRNP proteins controlled by c-Myc deregulate pyruvate kinase mRNA splicing in cancer. Nature. 2010; 463:364-368.
69. Kaminska D, Hamalainen M, Cederberg H, Kakela P, Venesmaa S, Miettinen P, Ilves I, Herzig KH, Kolehmainen M, Karhunen L, Kuusisto J, Gylling H, Laakso M, Pihlajamaki J. Adipose tissue INSR splicing in humans associates with fasting insulin level and is regulated by weight loss. Diabetologia. 2014; 57:347-351.
70. Zhao M, Shen L, Ouyang Z, Li M, Deng G, Yang C, Zheng W, Kong L, Wu X, Wu X, Guo W, Yin Y, Xu Q, Sun Y. Loss of hnRNP A1 in murine skeletal muscle exacerbates high-fat diet-induced onset of insulin resistance and hepatic steatosis. J Mol Cell Biol. 2020; 12:277-290.
71. Jo OD, Martin J, Bernath A, Masri J, Lichtenstein A, Gera J. Heterogeneous nuclear ribonucleoprotein A1 regulates cyclin D1 and c-myc internal ribosome entry site function through Akt signaling. J Biol Chem. 2008; 283:23274-23287.
72. Gui W, Zhu WF, Zhu Y, Tang S, Zheng F, Yin X, Lin X, Li H. LncRNAH19 improves insulin resistance in skeletal muscle by regulating heterogeneous nuclear ribonucleoprotein A1. Cell Commun Signal. 2020; 18:173.
73. Schmidt E, Dhaouadi I, Gaziano I, *et al*. LincRNA H19 protects from dietary obesity by constraining expression of monoallelic genes in brown fat. Nat Commun. 2018; 9:3622.
74. Pihlajamaki J, Lerin C, Itkonen P, *et al*. Expression of the splicing factor gene SFRS10 is reduced in human obesity and contributes to enhanced lipogenesis. Cell Metab. 2011; 14:208-218.
75. Croce MA, Eagon JC, LaRiviere LL, Korenblat KM, Klein S, Finck BN. Hepatic lipin 1beta expression is diminished in insulin-resistant obese subjects and is reactivated by marked weight loss. Diabetes. 2007; 56:2395-2399.
76. Yin H, Hu M, Liang X, Ajmo JM, Li X, Bataller R, Odena G, Stevens SM, Jr., You M. Deletion of SIRT1 from hepatocytes in mice disrupts lipin-1 signaling and aggravates alcoholic fatty liver. Gastroenterology. 2014; 146:801-811.
77. Zhang W, Patil S, Chauhan B, *et al*. FoxO1 regulates multiple metabolic pathways in the liver: effects on gluconeogenic, glycolytic, and lipogenic gene expression. J Biol Chem. 2006; 281:10105-10117.
78. Stoilov P, Daoud R, Nayler O, Stamm S. Human

tra2-beta1 autoregulates its protein concentration by influencing alternative splicing of its pre-mRNA. Hum Mol Genet. 2004; 13:509-524.
79. Brosch M, von Schonfels W, Ahrens M, Nothnagel M, Krawczak M, Laudes M, Sipos B, Becker T, Schreiber S, Rocken C, Schafmayer C, Hampe J. SFRS10--a splicing factor gene reduced in human obesity? Cell Metab. 2012; 15:265-266; author reply 267-269.
80. Srikantan S, Tominaga K, Gorospe M. Functional interplay between RNA-binding protein HuR and microRNAs. Curr Protein Pept Sci. 2012; 13:372-379.
81. Abdelmohsen K, Lal A, Kim HH, Gorospe M. Posttranscriptional orchestration of an anti-apoptotic program by HuR. Cell Cycle. 2007; 6:1288-1292.
82. Subramanian P, Gargani S, Palladini A, *et al*. The RNA binding protein human antigen R is a gatekeeper of liver homeostasis. Hepatology. 2022; 75:881-897.
83. Siang DTC, Lim YC, Kyaw AMM, Win KN, Chia SY, Degirmenci U, Hu X, Tan BC, Walet ACE, Sun L, Xu D. The RNA-binding protein HuR is a negative regulator in adipogenesis. Nat Commun. 2020; 11:213.
84. Guo T, Dai Z, You K, Battaglia-Hsu SF, Feng J, Wang F, Li B, Yang J, Li Z. S-adenosylmethionine upregulates the angiotensin receptor-binding protein ATRAP *via* the methylation of HuR in NAFLD. Cell Death Dis. 2021; 12:306.
85. Liu R, Wu K, Li Y, Sun R, Li X. Human antigen R: A potential therapeutic target for liver diseases. Pharmacol Res. 2020; 155:104684.
86. Qin W, Li X, Xie L, Li S, Liu J, Jia L, Dong X, Ren X, Xiao J, Yang C, Zhou Y, Chen Z. A long non-coding RNA, APOA4-AS, regulates APOA4 expression depending on HuR in mice. Nucleic Acids Res. 2016; 44:6423-6433.
87. Tian M, Wang J, Liu S, Li X, Li J, Yang J, Zhang C, Zhang W. Hepatic HuR protects against the pathogenesis of non-alcoholic fatty liver disease by targeting PTEN. Cell Death Dis. 2021; 12:236.
88. Li J, Gong L, Liu S, *et al*. Adipose HuR protects against diet-induced obesity and insulin resistance. Nat Commun. 2019; 10:2375.
89. Zhang Z, Zong C, Jiang M, *et al*. Hepatic HuR modulates lipid homeostasis in response to high-fat diet. Nat Commun. 2020; 11:3067.
90. Guo T, He Y, Ma W, Liu Z, Liu Q. Feasibility and Efficacy of S-Adenosyl-L-methionine in Patients with HBV-Related HCC with Different BCLC Stages. Gastroenterol Res Pract. 2016; 2016:4134053.
91. Parajes S, Gonzalez-Quintela A, Campos J, Quinteiro C, Dominguez F, Loidi L. Genetic study of the hepcidin gene (HAMP) promoter and functional analysis of the c.-582A > G variant. BMC Genet. 2010; 11:110.
92. Lu S, Mott JL, Harrison-Findik DD. Saturated fatty acids induce post-transcriptional regulation of HAMP mRNA *via* AU-rich element-binding protein, human antigen R (HuR). J Biol Chem. 2015; 290:24178-24189.
93. Chen Y, Tsai YH, Tseng SH. Regulation of the Expression of Cytoplasmic Polyadenylation Element Binding Proteins for the Treatment of Cancer. Anticancer Res. 2016; 36:5673-5680.
94. Balvey A, Fernandez M. Translational Control in Liver Disease. Front Physiol. 2021; 12:795298.
95. Alexandrov IM, Ivshina M, Jung DY, Friedline R, Ko HJ, Xu M, O'Sullivan-Murphy B, Bortell R, Huang YT, Urano F, Kim JK, Richter JD. Cytoplasmic polyadenylation element binding protein deficiency stimulates PTEN and Stat3 mRNA translation and induces hepatic insulin resistance. PLoS Genet. 2012; 8:e1002457.
96. Calderone V, Gallego J, Fernandez-Miranda G, Garcia-Pras E, Maillo C, Berzigotti A, Mejias M, Bava FA, Angulo-Urarte A, Graupera M, Navarro P, Bosch J, Fernandez M, Mendez R. Sequential Functions of CPEB1 and CPEB4 Regulate Pathologic Expression of Vascular Endothelial Growth Factor and Angiogenesis in Chronic Liver Disease. Gastroenterology. 2016; 150:982-997 e930.
97. Maillo C, Martín J, Sebastián D, Hernández-Alvarez M, García-Rocha M, Reina O, Zorzano A, Fernandez M, Méndez R. Circadian- and UPR-dependent control of CPEB4 mediates a translational response to counteract hepatic steatosis under ER stress. Nat Cell Biol. 2017; 19:94-105.
98. Hershey JWB, Sonenberg N, Mathews MB. Principles of Translational Control. Cold Spring Harb Perspect Biol. 2019; 11:a032607.
99. Miquilena-Colina ME, Lima-Cabello E, Sanchez-Campos S, Garcia-Mediavilla MV, Fernandez-Bermejo M, Lozano-Rodriguez T, Vargas-Castrillon J, Buque X, Ochoa B, Aspichueta P, Gonzalez-Gallego J, Garcia-Monzon C. Hepatic fatty acid translocase CD36 upregulation is associated with insulin resistance, hyperinsulinaemia and increased steatosis in non-alcoholic steatohepatitis and chronic hepatitis C. Gut. 2011; 60:1394-1402.
100. Scagliola A, Miluzio A, Mori G, Ricciardi S, Oliveto S, Manfrini N, Biffo S. Inhibition of eIF6 Activity Reduces Hepatocellular Carcinoma Growth: An *In Vivo* and *In Vitro* Study. Int J Mol Sci. 2022; 23:7720.
101. Hoosdally SJ, Andress EJ, Wooding C, Martin CA, Linton KJ. The Human Scavenger Receptor CD36: glycosylation status and its role in trafficking and function. J Biol Chem. 2009; 284:16277-16288.
102. Wang C, Hu L, Zhao L, Yang P, Moorhead JF, Varghese Z, Chen Y, Ruan XZ. Inflammatory stress increases hepatic CD36 translational efficiency *via* activation of the mTOR signalling pathway. PLoS One. 2014; 9:e103071.
103. Wang C, Yan Y, Hu L, Zhao L, Yang P, Moorhead JF, Varghese Z, Chen Y, Ruan XZ. Rapamycin-mediated CD36 translational suppression contributes to alleviation of hepatic steatosis. Biochem Biophys Res Commun. 2014; 447:57-63.
104. McCullough AJ. The clinical features, diagnosis and natural history of nonalcoholic fatty liver disease. Clin Liver Dis. 2004; 8:521-533, viii.
105. Zhao Q, Liu J, Deng H, Ma R, Liao JY, Liang H, Hu J, Li J, Guo Z, Cai J, Xu X, Gao Z, Su S. Targeting Mitochondria-Located circRNA SCAR Alleviates NASH *via* Reducing mROS Output. Cell. 2020; 183:76-93.e22.
106. Peng Z, Gong Y, Wang X, He W, Wu L, Zhang L, Xiong L, Huang Y, Su L, Shi P, Cao X, Liu R, Li Y, Xiao H. METTL3-m(6)A-Rubicon axis inhibits autophagy in nonalcoholic fatty liver disease. Mol Ther. 2022; 30:932-946.
107. Simon Y, Kessler SM, Gemperlein K, Bohle RM, Müller R, Haybaeck J, Kiemer AK. Elevated free cholesterol in a p62 overexpression model of non-alcoholic steatohepatitis. World J Gastroenterol. 2014; 20:17839-17850.
108. Lim A, Zhou J, Sinha RA, Singh BK, Ghosh S, Lim KH, Chow PK, Woon ECY, Yen PM. Hepatic FTO expression is increased in NASH and its silencing attenuates palmitic acid-induced lipotoxicity. Biochem Biophys Res Commun. 2016; 479:476-481.
109. Xiong J, Liu T, Mi L, Kuang H, Xiong X, Chen Z, Li S,

Lin JD. hnRNPU/TrkB Defines a Chromatin Accessibility Checkpoint for Liver Injury and Nonalcoholic Steatohepatitis Pathogenesis. Hepatology. 2020; 71:1228-1246.
110. Jin X, Gao J, Zheng R, Yu M, Ren Y, Yan T, Huang Y, Li Y. Antagonizing circRNA_002581-miR-122-CPEB1 axis alleviates NASH through restoring PTEN-AMPK-mTOR pathway regulated autophagy. Cell Death Dis. 2020; 11:123.
111. Musso G, Cassader M, Gambino R. Non-alcoholic steatohepatitis: emerging molecular targets and therapeutic strategies. Nat Rev Drug Discov. 2016; 15:249-274.
112. Rajesh Y, Reghupaty SC, Mendoza RG, Manna D, Banerjee I, Subler MA, Weldon K, Lai Z, Giashuddin S, Fisher PB, Sanyal AJ, Martin RK, Dozmorov MG, Windle JJ, Sarkar D. Dissecting the Balance Between Metabolic and Oncogenic Functions of Astrocyte-Elevated Gene-1/Metadherin. Hepatol Commun. 2022; 6:561-575.
113. Gerhard GS, Hanson A, Wilhelmsen D, Piras IS, Still CD, Chu X, Petrick AT, DiStefano JK. AEBP1 expression increases with severity of fibrosis in NASH and is regulated by glucose, palmitate, and miR-372-3p. PLoS One. 2019; 14:e0219764.
114. Roehlen N, Crouchet E, Baumert TF. Liver Fibrosis: Mechanistic Concepts and Therapeutic Perspectives. Cells. 2020; 9:875.
115. Koo JH, Lee HJ, Kim W, Kim SG. Endoplasmic Reticulum Stress in Hepatic Stellate Cells Promotes Liver Fibrosis *via* PERK-Mediated Degradation of HNRNPA1 and Up-regulation of SMAD2. Gastroenterology. 2016; 150:181-193.e188.
116. Yu J, Vodyanik MA, Smuga-Otto K, Antosiewicz-Bourget J, Frane JL, Tian S, Nie J, Jonsdottir GA, Ruotti V, Stewart R, Slukvin, II, Thomson JA. Induced pluripotent stem cell lines derived from human somatic cells. Science. 2007; 318:1917-1920.
117. McDaniel K, Hall C, Sato K, Lairmore T, Marzioni M, Glaser S, Meng F, Alpini G. Lin28 and let-7: roles and regulation in liver diseases. Am J Physiol Gastrointest Liver Physiol. 2016; 310:G757-765.
118. Wu X, Wu X, Ma Y, Shao F, Tan Y, Tan T, Gu L, Zhou Y, Sun B, Sun Y, Wu X, Xu Q. CUG-binding protein 1 regulates HSC activation and liver fibrogenesis. Nat Commun. 2016; 7:13498.
119. Delgado ME, Cárdenas BI, Farran N, Fernandez M. Metabolic Reprogramming of Liver Fibrosis. Cells. 2021; 10:3604.
120. Mejias M, Gallego J, Naranjo-Suarez S, Ramirez M, Pell N, Manzano A, Suñer C, Bartrons R, Mendez R, Fernandez M. CPEB4 Increases Expression of PFKFB3 to Induce Glycolysis and Activate Mouse and Human Hepatic Stellate Cells, Promoting Liver Fibrosis. Gastroenterology. 2020; 159:273-288.
121. Fritz D, Stefanovic B. RNA-binding protein RBMS3 is expressed in activated hepatic stellate cells and liver fibrosis and increases expression of transcription factor Prx1. J Mol Biol. 2007; 371:585-595.
122. Lu M, Nakamura RM, Dent ED, Zhang JY, Nielsen FC, Christiansen J, Chan EK, Tan EM. Aberrant expression of fetal RNA-binding protein p62 in liver cancer and liver cirrhosis. Am J Pathol. 2001; 159:945-953.
123. Tang H, Wang H, Cheng X, *et al*. HuR regulates telomerase activity through TERC methylation. Nat Commun. 2018; 9:2213.
124. Ge J, Chang N, Zhao Z, Tian L, Duan X, Yang L, Li L. Essential Roles of RNA-binding Protein HuR in Activation of Hepatic Stellate Cells Induced by Transforming Growth Factor-β1. Sci Rep. 2016; 6:22141.
125. Zhang Z, Yao Z, Wang L, Ding H, Shao J, Chen A, Zhang F, Zheng S. Activation of ferritinophagy is required for the RNA-binding protein ELAVL1/HuR to regulate ferroptosis in hepatic stellate cells. Autophagy. 2018; 14:2083-2103.
126. Zhang Z, Guo M, Li Y, Shen M, Kong D, Shao J, Ding H, Tan S, Chen A, Zhang F, Zheng S. RNA-binding protein ZFP36/TTP protects against ferroptosis by regulating autophagy signaling pathway in hepatic stellate cells. Autophagy. 2020; 16:1482-1505.
127. Wu JC, Luo SZ, Liu T, Lu LG, Xu MY. linc-SCRG1 accelerates liver fibrosis by decreasing RNA-binding protein tristetraprolin. FASEB J. 2019; 33:2105-2115.
128. Wu YL, Li HF, Chen HH, Lin H. Emergent Roles of Circular RNAs in Metabolism and Metabolic Disorders. Int J Mol Sci. 2022; 23:1032.
129. Wang J, Yang W, Chen Z, Chen J, Meng Y, Feng B, Sun L, Dou L, Li J, Cui Q, Yang J. Long Noncoding RNA lncSHGL Recruits hnRNPA1 to Suppress Hepatic Gluconeogenesis and Lipogenesis. Diabetes. 2018; 67:581-593.
130. Woodhoo A, Iruarrizaga-Lejarreta M, Beraza N, García-Rodríguez JL, Embade N, Fernández-Ramos D, Martínez-López N, Gutiérrez-De Juan V, Arteta B, Caballeria J, Lu SC, Mato JM, Varela-Rey M, Martínez-Chantar ML. Human antigen R contributes to hepatic stellate cell activation and liver fibrosis. Hepatology. 2012; 56:1870-1882.
131. Huang E, Xu K, Gu X, Zhu Q. PinX1 Depletion Improves Liver Injury in a Mouse Model of Nonalcoholic Fatty Liver Disease *via* Increasing Telomerase Activity and Inhibiting Apoptosis. Cytogenet Genome Res. 2021; 161:449-462.
132. Li Z, Zhou M, Cai Z, Liu H, Zhong W, Hao Q, Cheng D, Hu X, Hou J, Xu P, Xue Y, Zhou Y, Xu T. RNA-binding protein DDX1 is responsible for fatty acid-mediated repression of insulin translation. Nucleic Acids Res. 2018; 46:12052-12066.
133. Friedman SL, Neuschwander-Tetri BA, Rinella M, Sanyal AJ. Mechanisms of NAFLD development and therapeutic strategies. Nat Med. 2018; 24:908-922.
134. Lu SC, Mato JM. S-adenosylmethionine in liver health, injury, and cancer. Physiol Rev. 2012; 92:1515-1542.
135. Li N, Wang HX, Han QY, Li WJ, Zhang YL, Du J, Xia YL, Li HH. Activation of the cardiac proteasome promotes angiotension II-induced hypertrophy by down-regulation of ATRAP. J Mol Cell Cardiol. 2015; 79:303-314.
136. Wang C, Ma C, Gong L, Dai S, Li Y. Preventive and therapeutic role of betaine in liver disease: A review on molecular mechanisms. Eur J Pharmacol. 2021; 912:174604.
137. Chen J, Zhou X, Wu W, Wang X, Wang Y. FTO-dependent function of N6-methyladenosine is involved in the hepatoprotective effects of betaine on adolescent mice. J Physiol Biochem. 2015; 71:405-413.
138. Craig SA. Betaine in human nutrition. Am J Clin Nutr. 2004; 80:539-549.
139. Armstrong MJ, Hull D, Guo K, Barton D, Hazlehurst JM, Gathercole LL, Nasiri M, Yu J, Gough SC, Newsome PN, Tomlinson JW. Glucagon-like peptide 1 decreases lipotoxicity in non-alcoholic steatohepatitis. J Hepatol. 2016; 64:399-408.

140. Li S, Wang X, Zhang J, Li J, Liu X, Ma Y, Han C, Zhang L, Zheng L. Exenatide ameliorates hepatic steatosis and attenuates fat mass and FTO gene expression through PI3K signaling pathway in nonalcoholic fatty liver disease. Braz J Med Biol Res. 2018; 51:e7299.
141. Pope ED, 3rd, Kimbrough EO, Vemireddy LP, Surapaneni PK, Copland JA, 3rd, Mody K. Aberrant lipid metabolism as a therapeutic target in liver cancer. Expert Opin Ther Targets. 2019; 23:473-483.
142. Jiang XM, Yu XN, Huang RZ, Zhu HR, Chen XP, Xiong J, Chen ZY, Huang XX, Shen XZ, Zhu JM. Prognostic significance of eukaryotic initiation factor 4E in hepatocellular carcinoma. J Cancer Res Clin Oncol. 2016; 142:2309-2317.
143. Mukherjee N, Jacobs NC, Hafner M, Kennington EA, Nusbaum JD, Tuschl T, Blackshear PJ, Ohler U. Global target mRNA specification and regulation by the RNA-binding protein ZFP36. Genome Biol. 2014; 15:R12.
144. Huang L, Yu Z, Zhang Z, Ma W, Song S, Huang G. Interaction with Pyruvate Kinase M2 Destabilizes Tristetraprolin by Proteasome Degradation and Regulates Cell Proliferation in Breast Cancer. Sci Rep. 2016; 6:22449.
145. Tran DDH, Koch A, Allister A, Saran S, Ewald F, Koch M, Nashan B, Tamura T. Treatment with MAPKAP2 (MK2) inhibitor and DNA methylation inhibitor, 5-aza dC, synergistically triggers apoptosis in hepatocellular carcinoma (HCC) *via* tristetraprolin (TTP). Cell Signal. 2016; 28:1872-1880.
146. Barton M, Meyer MR. HuR-ry Up: How Hydrogen Sulfide Protects Against Atherosclerosis. Circulation. 2019; 139:115-118.
147. Korf M, Jarczak D, Beger C, Manns MP, Krüger M. Inhibition of hepatitis C virus translation and subgenomic replication by siRNAs directed against highly conserved HCV sequence and cellular HCV cofactors. J Hepatol. 2005; 43:225-234.
148. Stanley TL, Fourman LT, Zheng I, McClure CM, Feldpausch MN, Torriani M, Corey KE, Chung RT, Lee H, Kleiner DE, Hadigan CM, Grinspoon SK. Relationship of IGF-1 and IGF-Binding Proteins to Disease Severity and Glycemia in Nonalcoholic Fatty Liver Disease. J Clin Endocrinol Metab. 2021; 106:e520-e533.
149. Perez-Garcia A, Torrecilla-Parra M, Fernandez-de Frutos M, Martin-Martin Y, Pardo-Marques V, Ramirez CM. Posttranscriptional Regulation of Insulin Resistance: Implications for Metabolic Diseases. Biomolecules. 2022; 12:208.

Received November 11, 2022; Revised January 3, 2023; Accepted January 18, 2023.

[§]These authors contributed equally to this work.

**Address correspondence to:*
Peng Yu, The Second Clinical Medical College / Department of Endocrinology and Metabolism, The Second Affiliated Hospital of Nanchang University, Nanchang, Jiangxi, China.
E-mail: yu8220182@163.com

Jing Zhang, The Second Clinical Medical College / Department of Anesthesiology, The Second Affiliated Hospital of Nanchang University, Nanchang, China.
E-mail: zhangjing666doc@163.com

Released online in J-STAGE as advance publication January 22, 2023.

Original Article

DOI: 10.5582/bst.2023.01012

Simulation of SARS-CoV-2 epidemic trends in Tokyo considering vaccinations, virus mutations, government policies and PCR tests

Jianing Chu, Hikaru Morikawa, Yu Chen*

Department of Human and Engineered Environmental Studies, Graduate School of Frontier Science, The University of Tokyo, Kashiwa, Chiba, Japan.

SUMMARY The eighth wave of COVID-19 infection in the Tokyo area has brought daily confirmed cases to a new higher level. This paper aims to explain the previous seven epidemic waves and forecast the eighth epidemic trend of the area using agent-based modeling and extended SEIR denotation. Four key considerations are investigated in this research, that are: 1. Vaccination, 2. Virus mutations, 3. Government policies and 4. PCR tests. Our study finds that the confirmed cases in the previous seven epidemic waves were only the tip of the iceberg. Using data prior to December 1 2022, the eighth wave is expected to hover high in December 2022 and January 2023. Our research pioneers in the simulation of antibody titer declination on an individual level level. Comparing the simulated results, we find that the arrival of new epidemic waves are related to the decline in the number of antibody possessors, especially during the sixth and the seventh epidemic waves. Our simulation also suggests that faced with low severe and low death rates, PCR tests would not make much difference to reduce overall infections. In this case, maintaining PCR tests to a low level helps to reduce both social cost and public anxiety. However, if faced with the opposite case, PCR tests should be adjusted to a higher level to detect early infections. Such level of PCR tests should be compatible with available medical resources.

Keywords Agent-based modeling, COVID-19, Vaccination, IgG, PCR testing.

1. Introduction

On January 24, 2020, the Tokyo Metropolitan Government detected the first case of COVID-19 infection (*1*). After this detection, Japan promptly took various actions, including distributing masks to households and banning entries from 159 countries and regions. There have already been seven waves of infections since then until October 2022. The epidemic trends in Tokyo have different characteristics compared with those in New York, London and other European countries. Daily confirmed cases of the three cities (Tokyo, New York and London) reached a coincident historical high in January 2022. Daily infections have dropped since then for New York and London, while the reported cases in Tokyo continue to surge to a new high in August 2022. We notice that there is still no timely study on the reason behind such a difference in the past waves, In the meantime, no comprehensive study has been conducted to predict the epidemic trend for the eighth wave based on different scenarios. At the outset of research, we assume that four factors, namely vaccination rollouts, virus mutation, government policies and PCR tests mainly influenced the epidemic trend, under the following considerations: 1) vaccination helps provide antibodies so as to reduce the Coronavirus spread; 2) viruses with mutations may become more infectious by escaping immunity; 3) the government can set up regulations regarding travel restrictions and *etc*. aiming to slow down the spreading of virus; and 4) the capacity of PCR tests has nontrivial impacts on the number of confirmed cases. The reasons for choosing the first three factors are relatively clear, while the reason to include the PCR tests needs a further explanation. In short, there exists a strong correlation between the number of conducted PCR tests and the number of confirmed cases, details of which shall be discussed in Sec. 1.4.

There has been existing research related to our study. Chiba (*2*) discusses the measures to control epidemic spread in Japan from three aspects: mobility control, reducing restaurant hours and working at home. Yamauchi and others (*3*) examine the association beween epidemic dynamics, government measures and the daytime population in Tokyo. Murakami and others (*4*) use agent-based modeling and GPS analysis to simulate infection spread and inhibition in Tokyo, addressing the importance of city lockdown and prevention measures in service facilities. Yasuda and others (*5*) suggest vaccine

distribution strategies based on behavioral differences between residents in Tokyo and Osaka and conclude that high-risk older adults should be given priority when vaccine supplies are sufficient, but if vaccine supplies are scarce, vaccination of specific groups affected by the epidemic should be considered preferentially. It is worth noting that none of the above research took the vaccination, antibody titer declination, traveling policies, virus mutation, agents' heterogeneity and the advocation of PCR testing all into account, while our study is partially motivated by such a research gap.

This research employs SEIR denotation (see Table 1) and agent-based model building. We shall discuss details in the methodology part. Actual data of the aforementioned four factors are provided by the Tokyo Metropolitan Government and shall be fed into our model for validation. We expect that simulations can not only explain the emergence of the past seven waves but also be able to forecast the future trend of coronavirus infections. Specifically, our research aims to reproduce the arrival, the rise and decay, as well as the maximum number of daily infections for each wave. Moreover, the parameters of the model are subject to continuous revision based on online data published by the Tokyo Metropolitan Government, so that we can make timely predictions about future pandemic trends by creating different scenarios. Last but not the least, we hope this research could help to make some recommendations to government policies that may mitigate or even prevent future waves of infection.

We organize the paper as follows: In the Introduction part (Sec. 1), we discuss the four key considerations and their significance to our research. In the Materials and Methods part (Sec. 2), agent-based modeling and extended SEIR modeling approaches are discussed. Also, a detailed explanation on the construction of our model is presented together with a cautious verification and calibration. Then, prudent predictions are put forward in Sec. 3 with six scenarios being considered. Lastly, we summarize our findings and recommendations in the conclusions part (Sec. 4).

We performed a prior investigation on the four postulated factors based on open-source public information and the Tokyo Metropolitan Government website (*1*). All the data and information collected here are used in the model building described in Sec. 2.2.

1.1. Vaccination

It is evident that mass vaccination helps to reduce severe rate and death rate (*6*). Table S1 (*http://www.biosciencetrends.com/action/getSupplementalData.php?ID=134*) summarizes the five rounds of vaccination that have been carried out in Tokyo. At the latest update, Tokyo began the rollout of bivalent shots targeting Omicron variant on September 20, 2022, restricted to those aged 60 and over, and those with preexisting medical conditions as well. Because over 90% of Coronavirus deaths in Japan have been among those aged 60 and older, the rollouts aim to protect the vulnerable and reduce the overall death cases. We notice that Tokyo began the rollout of bivalent shots for all citizens in late October 2022, as the confirmed cases surged to a new high.

Table 1. Summary of eight health status of agents and their meanings

States	Meanings
S1	Susceptible, Healthy, without antibody and vaccination record
E	Within the infection distance to I1 agents, potentially infected
I1	Infected, not unconfirmed and not tested
I2	Infected, confirmed through PCR test
V	Healthy, vaccinated and antibody carried
R	Healthy, cured and antibody carried
S2	Healthy, susceptible, vaccinated but antibody lost
D	Dead

1.2. Virus mutations

Table S2 (*http://www.biosciencetrends.com/action/getSupplementalData.php?ID=134*) summarizes the dates when the notorious mutated viruses were first detected in Japan. Effective reproduction number and severe rate of these viruses are listed in the right columns of the table. As Table S2 (*http://www.biosciencetrends.com/action/getSupplementalData.php?ID=134*) shows, the current trend is that the virus is becoming more infectious periodically judging from the effectiwe reproduction number while less lethal thanks to the combined efforts of continuously advanced policy measures, vaccinations and medical treatments.

1.3. Government policies

When considering government policies, this paper points to the city governance, guidelines for medical treatments, restrictions of border measures and prevention acts towards the Olympics *etc*. The Tokyo Metropolitan Government had imposed a total of seven announcements of emergency states, as shown in Table S3 (*http://www.biosciencetrends.com/action/getSupplementalData.php?ID=134*). Standard regulations were applied in four of these emergency states, and three relaxed regulations were applied in the remaining ones. Tokyo city also adopted the Highly Active Anti-Retroviral Therapy (HAART Therapy, *HAART Therapy comprises the use of two or more monoclonal antibodies, minimizing the risk of drug-resistant virus strains developing.*) for COVID-19 treatment from July 19, 2021, thanks to the proposal of Ms. Yuriko Koike, who was the metropolitan's first female governor. Referring to Table S4 (*http://www.biosciencetrends.com/action/getSupplementalData.php?ID=134*), the adoption of HAART Therapy had greatly decreased the overall death rate. On November 22, 2022, Ministry of Health, Labour and Welfare of Japan granted the emergency use of Shionogi's oral drug

'Xocova' for COVID-19 treatment of those aged over 12 (*7*). The distribution of 'Xocova' started on November 28, 2022, covering about 2,900 medical facilities and supplying 1 million citizens. It is believed that the severe rate and death rate can be further reduced in the near future.

As for the border measures, we summarize timelines of various regulations in Table S5 (*http://www.biosciencetrends.com/action/getSupplementalData.php?ID=134*). Japan had shortly opened its border to foreign residents twice in 2020. After March 1, 2022, the country allowed foreign nationals to enter into the country for non-tourism purposes. On June 10, 2022, Japan reopened its border and began to accept group tours from 98 countries and territories (*8*). The first tour group of tourists landed at Narita Airport on June 22, 2022 (*9*).

Japan held the Tokyo Olympics from July 23, 2021, until August 8, 2021. The country welcomed the first foreign Olympic team on June 1, 2021 (*10*). The International Olympic Committee (*11*) required athletes to depart no later than 48 hours after completing their competition, which implies that the period of leaving starts from July 25, 2021, and lasts until August 10, 2021. Approximately 79,000 people flew to Japan for the Tokyo Olympics (*12*). Details are summarized in Table S6 (*http://www.biosciencetrends.com/action/getSupplementalData.php?ID=134*).

1.4. PCR tests

In Tokyo, PCR tests can be either conducted by the Tokyo Metropolitan Institute of Public Health or at medical institutions, with the latter one undertaking the major inspection work. In general, Tokyo citizens take PCR tests on a voluntary basis, following doctor's advice as well as their judgement of their own health condition, *i.e.*, symptoms of Coronavirus infection such as high fever, cough, headache, fatigue. The shortage of PCR capacity has been constantly criticized. As was reported on February 18, 2022, faced with the sixth wave of infection driven by Omicron Oariant, shortages of antigen and PCR kits are still commonplace (*13*), even two years past the initial outbreak.

The Japanese government has urged to boost PCR testing capacities as well as antigen productivity. According to the Ministry of Health, Labour and Welfare of Japan, PCR tests have been covered by medical insurance since March 6, 2022, which means that medical institutions can directly request tests from private testing institutes and other such bodies. Also, with the insurance coverage approval for antigen detection kit "Lumipulse SARS-CoV-2 Ag", saliva-based tests became available to asymptomatic patients from July 17, 2022 (*14*). In addition, residents can request a free antigen test kit delivered to their residence upon registration on the Tokyo Metropolitan Government website (*15*), if they deem themselves to have symptoms or become close contacts. This act can ease the concentration of tests and consultations at medical institutions. If the antigen test result is positive, the testee can immediately start a 14-day self-quarantine to avoid further spread of the infection.

These measures together encourage the public to take tests as well as help to detect individuals with infectivity, as can be inferred in Figure 1A, where we sum up the number of PCR tests conducted on a daily basis (2020.01.24 ~ 2022.11.30). We also conduct a linear regression test between daily confirmed cases and daily numbers of PCR tests. The results show a multiple R-square value of 0.4843 and a p-value of 2.2×10^{-16}. Accordingly, we consider that there is a relatively strong correlation between the number of PCR tests and the number of confirmed cases. This explains why we consider the PCR testing capacity as a critical issue.

1.5. Other considerations

School vacation is another factor considered in this research. We list the vacation periods in Table S7 (*http://www.biosciencetrends.com/action/getSupplementalData.php?ID=134*). During these vacations, students are apt to travel farther than they do in terms. Summer vacation in 2021 is an exception due to the scheduled 4th announcement of a state of emergency.

2. Materials and Methods

2.1. Methodology

2.1.1. Agent-based modeling

In this study, we use NetLogo (*16*), a beautiful agent-based modeling tool (ABM), for simulation of the epidemic dynamics. The main reason lies in that agent-based modeling can help represent the fine-scale individual heterogeneity faced with complex environments. When describing a large-scale epidemic phenomenon, differences in individual attributes may not be neglected because of the strong social and physical interaction among people. Typically, people have different occupations and versatile behavior patterns, thus their response to the Coronavirus and the vaccination are diverse. At the aggregated level, these differences tend not to be averaged out, implying that modeling of heterogeneity is essentially necessary. In contrast, the major difficulty in applying ABM to the simulation of epidemics is the validation of the model with the real data. Although ABM can mimic the micro-level infection process among individuals, which is basically determined by human-to-human distance, the straightforward feeding of the reported R0 coefficients into the model is not feasible. Nevertheless, ABM can be calibrated by tuning the model parameters so that the calculated R0 of the model may agree with that measured in the real world.

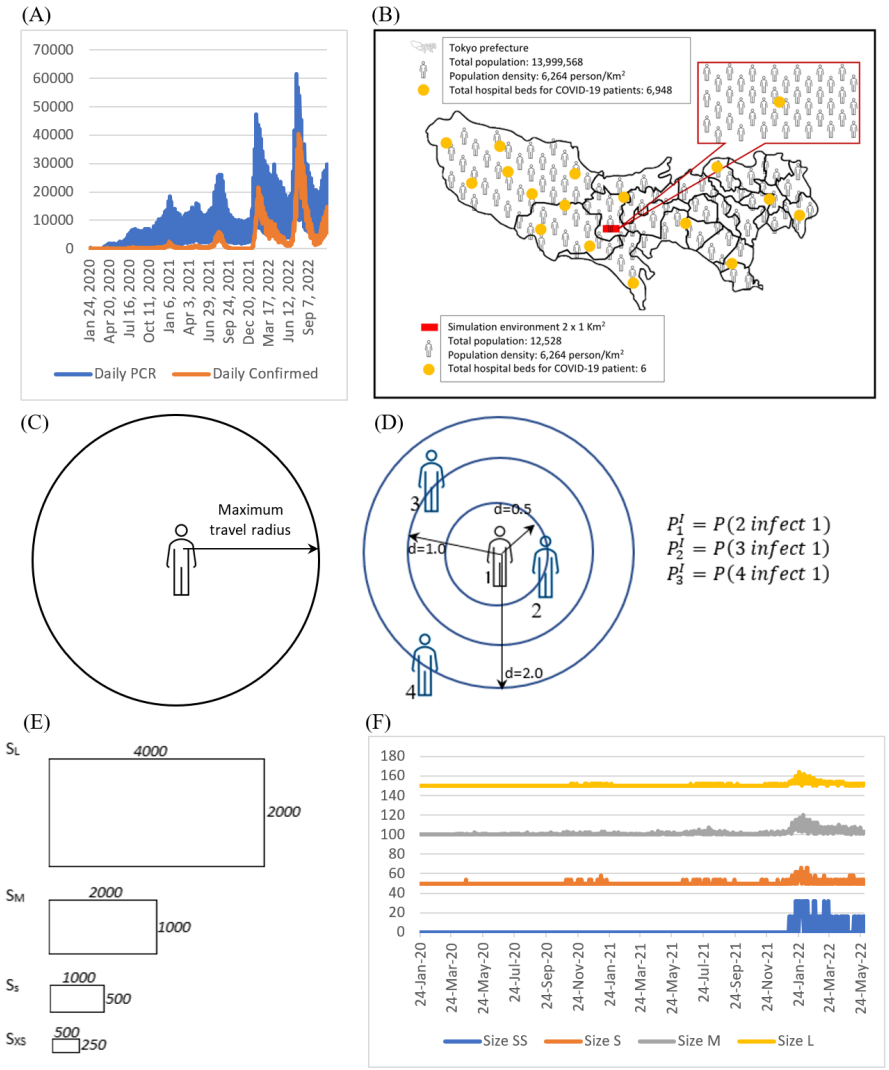

Figure 1. PCR test and confirmed cases; scaled simulation environment, moving patterns and validation of down-scaling. (A), The number of daily conducted PCR tests and daily confirmed cases from 2020.01.24 to 2022.11.30. **(B)**, Illustration of the simulation environment after scaling down. **(C)**, Illustration of agents' moving pattern (see Appendix 3). **(D)**, Illustration of agents' infection pattern (see Appendix 2). **(E)**, Models with different patch sizes. **(F)**, Simulation of models with different sizes.

We are aware that numerous ABM studies on the epidemic dynamics have been done. Here we list some of the latest publications and specify the pros and cons of these models. A data-driven agent-based modeling framework (*17*) is designed to forecast Ebola trends, which comprises three parts: synthetic population, social contact network and disease model. The model not only has a good representation of work or school activities and long-range mobility but also performs well in forecasting. Shamil and others (*18*) use agent-based modeling to explore the impact of contact tracking and find the parameters that lead to termination of the epidemic in a city, though their research does not take vaccination into account. Li and Giabbanelli (*19*) study the effectiveness of vaccine campaigns, the willingness of being vaccinated and the vaccine capacity under different federal plans, with the interactions between nonpharmaceutical interventions and vaccines considered. Although their research covers vaccines, it is noticed that vaccine efficacy decreases as antibody titers in the human body drop, let alone the virus mutates constantly. Kerr and others (*20*) develop the Covasim model to evaluate the effect of different interventions on the epidemic, including physical interventions, diagnostic interventions, and pharmaceutical interventions. Covasim, however, ignores influences from virus mutations, immigration policies and agents' heterogeneity. Comparing these researches, our study tries to take the effect of 4-dose vaccination, antibody titer declination, virus mutation, government policies, and PCR tests together into account.

2.1.2. Extended SEIR modeling

Our model denotes the health status of individuals by borrowing the idea of the SEIR model (Hethcote, 2000). However, we do not simply employ the standard

'Susceptible', 'Exposed', 'Infectious' and 'Recovered' status in the modeling. Because the SEIR model does not have 'vaccinated' or 'dead' status in its concept, it makes it not suitable for COVID-19 infection and vaccination studies. To overcome this deficiency of SEIR, we add the 'Vaccinated' and 'Dead' status and increase the resolution of description of the health status in the meantime, see the details in the model building part (Sec. 2.2).

We should supplement one more reason for the extension of the SEIR model. Although the traditional differential-equation-based SEIR model may conveniently take the measured R0 as an input parameter, the approach suffers from the so-called "time-lag effect," which means that we cannot accurately calculate the R0 coefficient without a large enough number of reported cases, while accumulating such a large sample takes time and resources. Especially when we face the continuous mutations of Coronaviruses, the fast variation of the reported R0 will cause the time-lag effect to be more severe. For example, a research team from Lancaster University came up with an R0 value of 3.8 in the original forecast version, then they updated the number to 2.5, considering many uncertainties, and before long they changed the number to 3.11 (*21*). Yang and others (*22*) also point out the flaws of using the SIR/SEIR model to estimate the basic reproduction number. In view of COVID-19's natural history, severe patients were often hospitalized, hence they should not be treated as transmitters. According to Yang's study (*22*), the R0 value used in SIR/SEIR calculations is usually underestimated.

In the ABM description of the epidemics, however, the infection process at the microscopic (human-to-human) level is much easier to be observed and measured, thus the reported condition for the infection will not change drastically along with the mutation of the virus. For example, a study (*23*) suggests that maintaining a social distance of 2 meters significantly reduces airborne dispersion of tiny droplets, hence the transmission risks from droplet inhalation. It takes approximately 7 seconds for viruses to be projected over a distance of 2 meters. Fundamentally, Coronavirus mutations have not changed such a microscopic mechanism of transmission.

Last, the original SEIR model cannot differentiate individuals by their occupations, work styles, moving patterns, *etc*., hence the influence of heterogeneity at the small scales cannot be investigated easily. With an ABM, diverse attributes of the individuals can be naturally described by associating corresponding state variables and their updating algorithms to the agents.

2.2. Model

2.2.1. Space and population

A total of 13,999,568 people live in Tokyo city, which results in a population density of 6,264 persons per square kilometer (*24*). The total number of hospital beds in the city is approximately 7,291 (*1*). Based on the assumption that all static properties (such as infrastructure) within Tokyo city are uniformly distributed, as well as that all dynamic properties (such as moving population) within the city are identical, our strategy is to build a rectangular block of 2 kilometers, which is geometrically similar to the Tokyo area, and simulate epidemic dynamics within this block using downscaled population and amount of infrastructure. See Figure 1B for more details.

By assuming the uniformity stated above, we linearly scale down the whole Tokyo region, which is composed of 23 municipalities, into a rectangular block with a length of 2km and a width of 1km. The synthetic population in the block is initialized at 12,528 and hospital beds at 6 in the block. We set the size of a patch as one square meter, so that totally 2,000 × 1,000 patches are used to represent such a block. It is important to note that the population density and hospital density in Figure 1B are equal to the actual data. Based on government policies and the outbound and inbound statistics (see Appendix 1), the scaled number of entries and exits into and out of a block varies at each time step. Section 2.3.1 will examine the validity of this linear scaling.

We categorize 62%[#1)] (*25*) of the synthetic population as employees who engage in economic activities and let them have an above average mobility. We also categorize 17%[#2)] (*26*) of the population as students who attend school and have vacations in winter, spring and summer, as mentioned in Sec. 1.5. The other 21% are categorized as unemployed.

Regarding the vaccinated population, the 1st, 2nd and 3rd doses of daily vaccination number are collected from the website of the Tokyo Metropolitan Government (*1*). We assume the pattern of 4th dose daily vaccination to be the same as the 3rd dose. The daily data for the population who received the PCR test and who came, or left Tokyo are collected from the same website. All these daily numbers will be multiplied by the scaling parameter before being fed into the model.

2.2.2. Social contact

We noticed that there are finer ways to model the microscopic behavior of agents and the interactions among them. For example, Venkatramanan and others (*17*) acquire data of daily activity patterns to simulate the flow of population. Specifically, they build the people-location network which allows them to assign agents to locations with durations of visit thus determining their contacts and interactions. As

[#1)] According to the Statistics Bureau of Japan, the work force participation rate in Japan from 2020 to 2022 is around 61% [61.5, 63%].

[#2)] According to the MEXT Japan, the total number of students enrolled in educational institutions in Tokyo is 2,348,260, composing approximately 17% of the total 13,920,000 population.

another example, Kerr and others (*20*) design the contact network with multiple layers in the Covasim model. The Covasim model was constructed with considerations of age structure and household size, using published data from UN Population Division 2019. They presume individuals to move between household, school, workplace and community contact layers during the day, with different probabilities of infection based on unique connections and connection weights. The two studies attempt to simulate the microscopic movements of agents as faithfully as possible. When designing our model, however, we adopted a strategy to largely simplify the social contact process thanks to the restrictions in computation time and workload. Methodologically, our approach can be defended by Kadanoff's theory on Lattice Gas Automata (*27*), which says that while building a microscopic model by minimally extract the essential properties of components, we can still get the desired macroscopic behavior of a system.

In our model, agents are randomly distributed initially, with their position being recorded as their residence. As shown in Figure 1C, we assume that at the beginning of a day, all agents, except for those quarantined ones, can walk outside randomly for 8 hours per day in any direction but within a radius r_{max}, a range which corresponds to their scope of daily activities and depends on their social status (either employee, student or unemployed), see Appendix 1 for detailed numerical values. During the random walk, agents have a chance to meet other walking agents, so as to be infected or to infect others. When a day ends, agents shall move back to their designated residence.

Although the social contact model described in this paper may not fully describe interactions among individuals from a microscopic perspective, we expect its aggregated outcomes will not differ significantly from those observed in macroscopic epidemics. Indeed, our model performed well in mimicking the past waves of infection (see Figure 2A). A similar phenomenon was observed in the microscopic modeling of fluid flows: Although molecules and interacting potentials of different types of fluids differ, large-scale flow dynamics are governed by the same equation. Just as Wolfram stated in his book on complex systems (*28*), (that even though the underlying rules of different systems vary, the overall results are the same.

2.2.3. Detailed model building

The construction and the implementation of our model consists of three parts: the definition of agent states (Sec. 2.2.3.1), the specification of processes for the state transition (Secs. 2.3.3.2-2.2.3.7), and the design of code

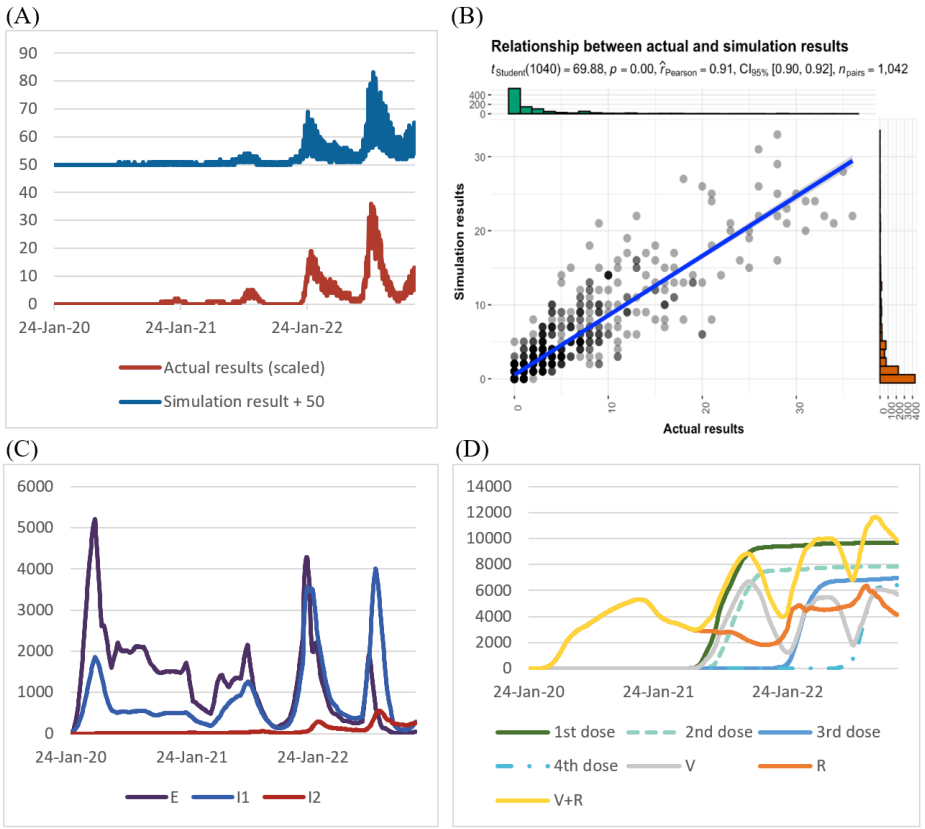

Figure 2. Scaled actual results *vs*. simulation results, Infection. and vaccination. (A), Actual results (scaled) *vs*. Simulation results from 2020.01.24 to 2022.11.30. **(B)**, 'ggstatsplot' of simulation results and actual results. **(C)**, The number of agents in E, I1 and I2 states from 2020.01.24 to 2022.11.30. **(D)**, 1st, 2nd, 3rd and 4th doses of vaccination; the number of agents in V, R, V+R states from 2020.01.24 to 2022.11.30.

structure, which shall be presented in Appendix 2.

2.2.3.1. Health states and population

We extend the SEIR categorization to define totally eight health states for agents. This extension is necessary because it allows us to analyze the effect of vaccination on one side, while fully reflecting the pathological characteristics of COVID-19 on the other side. A summary of the available health states can be found in Table 1. Aside from the conventional S/E/I/R states, we have added the V state to represent the vaccinated individual who carries antibodies against Coronavirus. Furthermore, we separated the susceptible state into S1 and S2 in order to facilitate the modeling of booster doses based on those susceptible agents with antibody records (S2) and those without (S1). Additionally, we divide the infected state into two categories, I1 and I2. Since the confirmed cases (I2) will remain at home and self-quarantine once identified, they will lose their public infectivity in comparison with those infected but unconfirmed agents (I1). Additionally, we added the death state D.

There are a total N^{total} agents in the synthetic population. Among these agents, populations in different states are denoted as N^{S1}, N^{S2}, N^{E}, N^{I1}, N^{I2}, N^{V}, N^{R} , N^{D}, respectively.

2.2.3.2. Susceptible

At $t = 0$, all agents are initialized to be in the Susceptible state (S1), with no one infected with Coronavirus. Home positions are recorded for agents, and they can move from home to places within a radius r_{max} (whose numerical values are listed in Appendix 3). Outing of agents lasts eight hours a day, regardless of direction. Once the space boundary is touched, the agent shall bounce back.

2.2.3.3. Exposure

As the imported cases begin to spread over the Tokyo region since January 24, 2020, we set this date t = 1. Over time, susceptible agents, if exposed to the asymptomatic cases (I1 agents), will have a likelihood to be infected. The odds for a state change from Susceptible to Exposed (S1→E) reads as the following

$$P_{S1\to E} = H(d_{S1,I1} - d_E) \quad (1).$$

where $H(x)$ is the heaviside step function, and $d_{X,Y}$ stands for the shortest distance in the space between agents in state X and agents in state Y. The threshold distance d_E is set to 2 units of patch size, based on the statistics made by the Ministry of Health, Labour and Welfare (MHLW), saying that a physical distance within 2 meters can be deemed as close contact with Coronavirus transmission possibility (*29*).

2.2.3.4. Infection

The probability for an exposed agent (in state E) to be infected by Coronavirus depends specifically on the distance when the agent met an agent in state I1, see Figure 1D.

The probability of infection ($P_{E\to I1}$) is defined differently in three cases,

$$P_{E\to I1} = \begin{cases} P_1^I & 0 \le d_{S1,I1} \le 0.5 \\ P_2^I & 0.5 < d_{S1,I1} \le 1.0 \\ P_3^I & 1.0 < d_{S1,I1} \le 2.0 \end{cases} \quad (2).$$

Here values of P_1^I, P_2^I and P_3^I are specified in Table S8 (*http://www.biosciencetrends.com/action/getSupplementalData.php?ID=134*). Each time the virus mutates, probabilities of infection will be adjusted according to the properties of viruses. If luckily the exposed agents are not infected, their states will change back to S1 (E→S1) by the following probability

$$P_{E\to S1} = 1 - P_{E\to I1} \quad (3).$$

All agents, except those who have been confirmed to be infected (in state I2), will receive PCR tests with a probability ($P^T = \frac{n_T}{N^{total} - N^{I2} - N^D}$) per day, where n_T is the down-scaled daily number of PCR tests published by the Tokyo Metropolitan Government. As soon as the infectivity is confirmed by the PCR tests, the I1 state of infected agents will be re-marked as I2 state, implying that the transition probability can be calculated for an individual as the following,

$$P_{I1\to I2} = \frac{P^T}{N^{total} - N^{I2} - N^D} \quad (4).$$

If currently an agent is in state I2, it will not be allowed to move anywhere until the next state transition either to R (recovery) or to D (death).

2.2.3.5. Recovery or death

Part of the confirmed patients (agents in I2) are transferred into hospital if there are available beds, in this way patients who receive medical treatment will have a lower death rate than those who are in self isolation. In the model, a local hospital is set up in the simulation space to model the treatment of confirmed patients with severe symptoms. The number of acceptable patients for the hospital is determined by referencing to the Tokyo Metropolitan Government website (1), which provides a list of the total capacity of hospital beds for COVID-19 patients. The capacity of the hospital is updated every day if recovered patients (agents in R) are discharged and newly confirmed patients (agents in I2) are admitted.

For agents in hospitals, the recovery (I2→R) rate is assumed to be 100%, whereas the fatality rate P^F

outside of hospitals is determined by the therapies for Coronavirus treatment (See Table S4, *http://www.biosciencetrends.com/action/getSupplementalData.php?ID=134*). Confirmed agents (I2), if not transferred to hospital (self-quarantined), will become either self-cured (I2→R) or dead (I2→D) after fourteen days with the following probabilities,

$$P_{I2\to R} = 1 - P^F, P_{I2\to D} = P^F \quad (5).$$

If the infected agents are not confirmed by PCR tests within fourteen days after infection, they may move freely in the simulated block until self-cure (I1→R) or death occurs (I1→D) with the following probabilities

$$P_{I1\to R} = 1 - P^F, P_{I1\to D} = P^F \quad (6).$$

2.2.3.6. Vaccination

All surviving agents except confirmed ones (I2) are eligible to receive vaccination as long as there are remaining quotas. The health state of the vaccinated changes after a dose of vaccination (S1/E/I1/R/V/S2→V). Between the first and second dose, the duration is 5 to 8 weeks, between the second and third dose is 6 months, and between the third and fourth dose is 5 months.

Although the standards of efficacy testing vary, we can make an approximate estimation of Pfizer's vaccines' efficacy based on published clinical reports. A Pfizer vaccine has a first dose efficacy of 52% and a second dose efficacy of 91% (*30*). Although Tokyo residents can choose between different brands of vaccines, we model vaccine efficacy based on Pfizer's data. In particular, we take into account the decay of antibody titer, which has not been considered in other literature to the best of our knowledge.

For each vaccinated agent in the model, the probability of successfully obtaining the antibody *via* the first dose reads as the following

$$P_{S1/E/I1/R\to V} = \frac{n_V}{N^{S1}+N^E+N^{I1}+N^R} \times 52\% \quad (7).$$

Here the down-scaled daily vaccination quota n_V can be obtained from the record of the Tokyo Metropolitan Government. Similarly, the probability of successfully obtaining the antibody *via* the second, third, or fourth dose vaccination is

$$P_{S1/E/I1/R/V/S2\to V} = \frac{n_V}{N^{S1}+N^E+N^{I1}+N^R+N^V+N^{S2}} \times 91\% \quad (8).$$

Additionally, we consider that there may be an extremely small possibility that agents may die after each vaccination (V→D)

$$P_{V\to D} = 8.1 \times 10^{-6} \quad (9).$$

Numerical value of this death rate is given by the study by Yamaguchi and others (*31*), which indicates that 1,315 cases over 163,059,502 doses of Pfizer vaccination became dead in Japan as of October 15, 2021.

2.2.3.7. Antibody titer declination

Antibodies are acquired through vaccination or self-cure. It is commonly observed that self-recovered people have slower antibody titer decline rates than vaccinated ones (*32*). The immunoglobulin G (IgG) test is a commonly performed method for determining COVID-19 antibody titer levels. Narasimhan *et al*. (*33*) identified anti-SARS-CoV-2 IgG-positive immune responses after vaccination based on a positive threshold of 50 AU/mL. Ebinger and others (*34*) proposed that 4160 AU/mL (corresponding to an ID50 of 1:250) could be used as a surrogate marker of serum neutralizing activity.

In our model, antibody titer levels (IgG levels) for each agent decrease over time as determined by linear regression of data from previous studies. Once agents' antibody titer levels drop below a threshold, which is determined by calibrating the model with actual data in Sec.2.3.2.3, their status will change to S2 (V/R→S2).

According to Ariel Israel and others (*32*), individuals who received Pfizer-BioNTech's mRNA vaccine have differing antibody titer levels when compared with patients who were infected with the SARS-CoV-2 virus. As a result, antibody concentrations acquired from vaccination are higher initially, but decrease exponentially at a much faster rate (*32*). Based on their research, the antibody titer *Y(t)* measured in AU/mL after SARS-CoV-2 infection may be expressed as $Y(t') = 357 \times 0.96^{t'}$, where *t'* is 'month (s)' since the positive PCR tests. Converting into the daily antibody titer change for the self-recovered agents (I1/I2→R), we use the following formula for our model

$$Y(t) = 357 \times 0.998640^{(t-t_i)} \quad (10).$$

where t-t_i represents day(s) since the time of infection (t_i). The change of IgG after the first/second/third/fourth doses have been done in another study (*35*). Data are listed in Table S9 (*http://www.biosciencetrends.com/action/getSupplementalData.php?ID=134*).

Despite the scarcity of data, we may assume the decay of antibody titer acquired from the vaccination follows the power law function found in the decay of antibody titer in the naturally immune case. We simply apply linear regression to the logarithmic coordinates

$$logD = \frac{1}{t_2-t_1}[logY(t_2) - logY(t_1)] \quad (11).$$

where D is decay rate of antibody titer, t_1,t_2 are two separate timing measurements after the vaccination. As a result, we obtained the following formula for the decay of antibody titer acquired from vaccination of different doses

$$Y(t) = Y_0 \times D^{(t-t_0)} \quad (12).$$

where Y_0 is the initial antibody titer after a specific dose of vaccination, D is the decay rate of antibody titer with respect to the elapsed time measured in day(s) since the vaccination, and t_0 the time of vaccination. Numerical values for these parameters in different doses of vaccination are summarized in Table S10 (*http://www.biosciencetrends.com/action/getSupplementalData.php?ID=134*).

In practice, as we understand that as COVID-19 virus keeps mutating, vaccines are becoming less protective, we set a relatively fast declination rate as $D = 0.980916$ in our simulation code for all four doses of vaccination. This simplification is in accordance with the study by Xu *et al*. (*36*), in which authors found that the concentrations of antibodies will increase rapidly after receiving the second dose vaccine and will reach their peak around two weeks (14 days) following the second dose vaccination. Typically, the peak will last for one week and then begin to decrease after three weeks (21 days).

2.3. Verification and Calibration

2.3.1. Verification of linear scaling

In Section 2.2.1, we linearly scale down the entire Tokyo region into a rectangular block with a length of 2km and a width of 1km, containing 12,528 susceptible agents and a hospital that can accommodate 6 infected agents. However, there is still the question of whether, after the simulation has been completed, the results can be scaled back to Tokyo in the real scale. To prove this scaling relationship, we first assume that the confirmed infected population in the real world depends on the area and the total population as the following

$$N^{I2}(S, N^{total}; t) \quad (13).$$

Now if we use a parameter $\lambda < 1$ and perform a simulation in the down-scaled area λS and population λN^{total}, can we obtain the infected population N^{I2} in real space by simply scaling up the simulation results by a factor of $1/\lambda$? The answer is that if the following relation holds true

$$N^{I2}(\lambda S, \lambda N^{total}; t) = \lambda N^{I2}(S, N^{total}; t) \quad (14).$$

results in the original scale can be obtained by linear scaling of the simulation results.

To justify this argument, let us set $\lambda = 1/4$ and perform the simulation on four areas S_L, S_M, S_S and S_{XS}, as shown in Figure 1E. Note that we have S_L:S_M:S_S:S_{XS} = 4:1:(1/4):(1/16), in the meantime, we adjust all quantities including number of agents, hospital, entry and exit, daily vaccination and PCR test rates according to this ratio, but keep the maximum travel distance r_{max} fixed. If linear scaling applies in this extended SEIR modeling, our expectation is that we may have the following relation

$$N_L^{I2}/4 = N_M^{I2} = 4N_S^{I2} = 16N_{XS}^{I2} \quad (15).$$

where N_Y^{I2} is the population of confirmed infection obtained from a simulation in the scaled area Y. In the validation, we set S_M the same size as the model in our study, representing the $2km^2$ block by 2,000 × 1,000 patches, while other scaled areas are set as $S_L = 8km^2$, $S_S = 0.5km^2$), and $S_{XS} = 0.125km^2$. After we obtain the daily infection data from simulations in blocks with different sizes, we show the scaled number of daily infections in Figure 1F, where data are differentiated by shifting with a constant for visualization.

Inspecting results obtained from simulations with different areas may reveal that the scaled dynamics are essentially the same, however time resolution is limited by the size of the simulation block. Moreover, we also find that the shape of the simulation area does not matter, as the scaling relationship merely depends on the area and population. As a result of this validation, we are confident to use the current model to perform the simulation in a small rectangular block to examine, after scaling up the results, the trend of infection in the real Tokyo area, under the assumption that distributions of everything in Tokyo are uniform.

2.3.2. Calibration of the model

In order to calibrate the model, we use data on the confirmed infection cases from January 24, 2020, to October 1, 2022. Parameters such as hospital capacity, initial population, *etc*., are set in the initialization module of the code, while parameters under adjustment are antibody thresholds and infection probabilities in social contact of the agents.

2.3.2.1. Fixed parameters

The parameters that are given at the beginning and fixed during the simulation are summarized in Table S11 (*http://www.biosciencetrends.com/action/getSupplementalData.php?ID=134*). The reasons or backgrounds for such parameter settings are described in Sec. 1 through Sec. 2.2.

2.3.2.2. Parameter adjustments

Recall that we consider four key factors in Sec. 1 that have impacts on the epidemic trends, namely the vaccination, the mutation of virus, the traveling policies and the PCR tests. To reproduce the daily infected cases that correspond with those of the actual data, we select two model parameters, namely the threshold concentration of antibodies and the probability of infection over different contacting distances between agents in state I1 and others, as the parameters to

be adjusted manually. The reason for this choice is explained as follows.

In the calibration of the model, quantities related to traveling policy and PCR tests are not to be adjusted, since there is actual data recording the inbound/outbound populations as well as PCR tests performed in the Tokyo area. We simply take these data as input to the simulation. On the other hand, although the daily numbers of vaccination have also been given, the decay of antibodies of each vaccinated person is not known. This uncertainty in the cutoff concentration of antibodies can be utilized to tune the simulation results. Regarding the mutations of the Coronaviruses, they will result in a different probability of infection. Even though we know the change in the infectivity due to the mutation, we may not be able to measure this probability under various circumstances accurately. This fact provides another space for the adjustment of model parameters.

As a result of trial and error, we found that the cutoff or threshold for antibody effectiveness should be set at 250 AU/mL, below which agents would lose antibodies and be susceptible again. We tested this threshold several times and found this value leads to simulations that are most closely related to Tokyo's case numbers. In fact, the antibody response is heterogeneous (influenced by age, gender, comorbidities, genetics, and other inter-individual variations), for simplicity, we still use 250 AU/mL as a universal cutoff point.

Results of adjusting the probability of infection are shown Table S8 (*http://www.biosciencetrends.com/action/getSupplementalData.php?ID=134*). For variants of the same class, we let P_1^I to remain the same, while increasing P_2^I and P_3^I by 5% or 10% at a time. For instance, Compared With the original Delta variant, Delta N501S is assumed to have the same P_1^I as the original Delta, however, but 5% higher in P_2^I. Similarly, compared with the original Omicron variant, Omicron BA.2 is assumed to have the same P_1^I as other Omicron variants, yet 5% higher in its P_2^I and P_3^I. Nevertheless, the new arriwal of Omicron variants XE and BA.2.75 are considered as exceptions due to their high immunity escaping abilities.

2.3.2.3. Reproducing the seven waves

By adjusting model parameters above, our goal is to reproduce in the simulation, the past seven waves of infection that have been reported in the Tokyo area. Details of these waves of infection are described below..

Table S12 (*http://www.biosciencetrends.com/action/getSupplementalData.php?ID=134*) summarizes the dates and the maximum daily confirmed cases in the past epidemic waves in Tokyo. Immediately following the outbreak of the first wave in late March 2020, Japan implemented PCR testing criteria, closed schools, promoted teleworking, and encouraged people to wear masks. The implementation of the first state of emergency resulted in a 68% reduction in subway passengers, which controlled the infection effectively. After the state of emergency, the second wave began and subsided without further state of emergency measures, a phenomenon that can be explained by the increase in PCR testing capacity (*37*). The second emergency state was declared during the third wave of infection, local governments called for a reduction in business hours and restrictions on activities. With the spread of Delta variant, the advantage of public vaccination became evident in the fourth wave of infection. In contrast to 2,520 cases per day in the third wave, the maximum number of confirmed cases per day was controlled below 1,126. Along with the opening of the Tokyo Olympic Games and the spread of mutated Delta virus, the fifth wave arrived. Despite the declaration of emergency and the first-dose vaccination, the maximum daily confirmed cases reached 5,908. A surge in the confirmed cases in the sixth wave of infection occurred following the outbreak of Omicron variant in late December 2021. The seventh wave of cases started in mid June 2022, dominated by the BA.5 subvariant. Variants Omicron BA.2, Omicron XE, Omicron BA.4 and BA.5 brought the number of newly confirmed cases to a higher level. There were no further emergency measures taken by the Tokyo Metropolitan Government. On the contrary, reopening policies have been implemented to accept groups of tourists from outside Japan. The number of maximum daily infections reached 40,395 on July 28, 2022, almost twice as many as in the sixth wave.

Figure 2A shows the comparison of scaled actual data versus the simulated COVID-19 daily infection cases in Tokyo from 2020.01.24 to 2022.11.30. We obtain the simulation results by averaging the data after 60 times of calculations. Compared with the scaled infection data, we note that our model has successfully reproduced the well-known seven waves of infections in the Tokyo area. Moreover, our model can also correctly predict the maximum daily confirmed infections in each wave, see Table S13 (*http://www.biosciencetrends.com/action/getSupplementalData.php?ID=134*).

Figure 2B shows the scatter plot combined with marginal density plus histogram. These results are obtained by using 'ggscatterstats' in the package 'ggstatsplot' (*38*). The number of data $n_{pairs} = 1042$ corresponds to the period 2020.01.24 ~ 2022.11.30. As can be seen from the graph, we use $p = 0.00 < 0.05$ to reject the null hypothesis. The statistical significance between two groups is supported by $\hat{r}_{Pearson} = 0.91$, which lies in $CI_{95\%}$[0.90,0.92]. Overall, the statistical analysis shows that simulation results agree with the actual data well. We also performed granger causality tests on the two groups of results. The granger causality test is a common practice used to examine if one time series may be used to forecast another. After the calculation, the F test statistic is equal to 64.008 and the p-value that corresponds to the F test statistic is $Pr_{(>F)} = 2.2 \times$

$10^{-16} < 0.05$. Thus, we may reject the null hypothesis and conclude that our simulation results are useful for predicting the actual results.

2.3.3. Findings

2.3.3.1. The unconfirmed infected cases

From Figure 2C, we can see the number of agents in E, I1 and I2 states from January 24, 2020, to November 30, 2022, with their lines marked in purple, blue and red respectively. Figure 2D shows the simulated 1st. 2nd, 3rd and 4th doses of vaccination from January 24, 2020, to November 30. 2022. Figure 2D also shows the number of agents in V, R and V+R states from January 24, 2020, to November 30, 2022. From the observation, we find the following phenomena.

1. As the I1 population increases, the E population surges, which confirms the observation of a positive loop of infection, which implies that the more infected agents, the more exposed agents, and the wider the spread of infections.

2. Since Coronavirus mutations cause an increasing trend of infection probabilities, the difference between populations E and I1 gradually narrows until the late 6th wave. Since the announcement of the reopening policies for non-tourism purposes on June 1, 2022, it is assumed that asymptomatic carriers overseas rush into Japan, causing a rapid increase in I1. Nevertheless, due to the strong protective effect of the 4th dose vaccination starting May 25, 2022 (see Figure 2D), there were fewer E than expected, thus the gap between E and I1 started to broaden.

3. The PCR test numbers were low during the first to fifth epidemic waves, leading to low levels of daily confirmed infections. However, the actual numbers of agents in E and I1 states were high, suggesting that reported cases did not reflect real epidemic trends.

4. Due to the increase in PCR testing capacity, even though the number of E and I1 agents had dropped to historical lows post the 7th wave, the number of reported cases exceeded those during the previous waves.

In light of the strong correlation between PCR tests and daily confirmed cases, it is evident that the number of daily confirmed cases does not fully reflect the actual infection trends in Tokyo. In reality, the confirmed cases detected were only the tip of the iceberg.

2.3.3.2. The reasons behind the seven waves

We hereby summarize the characteristics of the infection trends in Tokyo in Table S14 (*http://www.biosciencetrends.com/action/getSupplementalData.php?ID=134*). Below is a list of the reasons for bringing about these characteristics.

1. First, compared with New York and London, Tokyo started its 1st dose vaccination not until the start of the 4th epidemic wave, which is deemed relatively late and vulnerable to future mutated viruses (Tokyo: April 12, 2021; New York: December 14, 2020; London December 8, 2020).

2. Second, the PCR testing capacity was comparatively low and could not reflect the real infection trends, especially during epidemic waves 1~5. (See Table S14, *http://www.biosciencetrends.com/action/getSupplementalData.php?ID=134*).

3. Third, the PCR testing capacity has improved since the 6th epidemic wave dominated by Omicron Oariant. It is believed by Larrauri and others that previous vaccination as well as self-cure together reduced the overall severe rate and death rate (*6*). However, the outdated antibodies (antibodies not targeting Omicron variant) cannot stop the mass spread of Omicron and its mutated variants. Therefore, the reported confirmed cases during the 6th wave were at an historical high.

4. Fourth, in accordance with the latest research (*39*), BA.2.75 can evade nearly all antibodies, no matter acquired from previous vaccination or self-cure. Even though the vaccination rates were at high levels in the 7th epidemic wave (see Figure 2D), mass spread seems inevitable. In this case, increased PCR testing capacity only leads to a higher level of daily confirmed cases, but limited effectiveness to control overall infection trends in the 7th epidemic wave.

3. Results

3.1. Scenario design

When designing different scenarios to forecast the future epidemic waves, we consider the two most important factors to be the number of daily PCR tests and the number of inbound/outbound travelers, the latter of which is the consequence of travel and border measures of the Japanese government. The other two factors, namely the vaccination rates and virus mutation are set in reference to actual data up to the end of November 2022.

The reason for choosing the number of PCR tests as one of the control parameters is that the number of PCR tests performed is not solely determined by the capacity provided by the government. Voluntary testing, the rate of which is influenced by decision making of each agent based on the published number of confirmed cases, will result in a positive feedback loop between the two dynamics. On the other hand, PCR tests can help to stop the spread of infection by screening out infectious agents by making them self-isolated. For these reasons, the pattern of PCR test number is considered unpredictable, thus needing to be discussed through the designed scenarios.

The numbers of in/outbound travelers are chosen as one of the key considerations because Japan has fully opened its border to oversea visitors since October 11,

2022, together with plans to revive its economy through the weakened Yen and the advertised tourism. Moreover, as winter holidays approach (Christmas, New Year, Spring Festival and *etc.*), it is likely that some citizens might consider going abroad for their holidays, which increases the risk of bringing the virus into Japan. Since the complexity in the real world makes these numbers difficult to be modeled, therefore they should be considered by postulated scenarios.

In contrast, the main reason for us not to choose virus mutations is that, under the premise of an increasing level of antibody obtained either from the infection of the Omicron variant or from the vaccination, probability of infection to the exposed is expected to have reached its limit. If a new variant emerges with stronger ability to escape immunity, we are more inclined to consider it a completely new virus rather than COVID-19. Lastly, by the end of November 2022, the third-dose vaccination rate has reached 65.7% among all Tokyo citizens and the fourth-dose vaccination rate has reached 80.4% among the elderly. Looking into the 1st, 2nd and 3rd doses of public vaccination, we find that the pattern of the vaccination trends does not differ much (*1*). As long as the government maintains its current plan to vaccinate the public, the vaccination trend of the 4th dose is expected to follow the previous ones'.

3.1.1. Parameter settings

We use past vaccination data as reference to generate the vaccination quotas from 2022.10.01 to 2023.02.01. As shown in the upper panel of Table S15 (*http://www.biosciencetrends.com/action/getSupplementalData.php?ID=134*), the 1st, 2nd and 3rd doses of vaccination records during November 13 ~ 19, 2022 are duplicated as the weekly vaccination pattern from December 1, 2022 (Sun) to February 1, 2023 (Wed). Since the daily number of the fourth dose vaccination is not yet available, we use the third dose vaccination records from December 1, 2021 (Wed) to August 10, 2022 (Wed) to surrogate the 4th dose vaccination data from May 25, 2022 (Wed) to February 1, 2023 (Wed), see the lower panel of Table S15 (*http://www.biosciencetrends.com/action/getSupplementalData.php?ID=134*).

At of the end of November 2022, no further mutated virus has been discovered since the discovery of variant XBB on October 28, 2022. The current view is that BA.4 and BA.5 are still dominant variants in Japan. Recently, experts started to worry about variants BQ.1 and BQ1.1, descendants of BA.5, which are deemed to escape immunity and cause severe symptoms. Based on their judgements, variant BQ.1.1 is likely to become the next dominant variant (*40*).

3.1.2. Scenario creation

The statistics of Tokyo PCR testing performed in November 2022 can be obtained from the Tokyo Metropolitan Government Website (*1*). For November 2022, the average number of PCR tests performed on a daily basis is 16,796. Multiplying by the scaling parameter and rounding it to a whole number, we obtain the daily PCR test number as 15 in our model. This number is defined as 'Normal' for estimating the future PCR tests statistics. In addition, we define the 'Active' state of PCR tests as doubling the testing number in the 'Normal' state.

We define 'Super active', 'Active' and 'Normal' scenarios (see Table S16, *http://www.biosciencetrends.com/action/getSupplementalData.php?ID=134*) to be situations where the number of travelers during the winter holiday season (2022.12.10 ~ 2023.01.10) is tripled, doubled and unchanged compared with that in November 2022. We assume that the number of daily PCR tests performed is doubled than that in November 2022, and the situation of daily in/outbound population is 'Super active' for Scenario I, 'Active' for Scenario II and 'Normal' for Scenario III during the winter holiday season (2022.12.10 ~ 2023.01.10). Additionally, we assume that the number of daily PCR tests is the same as that in November, and the daily in/outbound population is 'Super active' for scenario IV, 'Active' for scenario V and 'Normal' for scenario VI during the winter holiday season (2022.12.10 ~ 2023.01.10).

3.2. Results of forecasting

We repeated each simulation of the six scenarios 10 times and obtained the average results in Figure 3A. Overall, the forecast shows that the 8th wave shall peak around mid January and end around early March 2023.

From Figure 3A, we can see that the forecasted results from 2022.12.01 to 2023.03.01 are marked in red, light blue, green, deep blue, pink and brown lines, representing scenarios I, II, III, IV, V and VI respectively. It is clear that the number of daily PCR tests matters to the number of daily confirmed cases, the forecasted results of scenarios I, II and III apparently differentiate from scenarios IV, V and VI. Table S17 (*http://www.biosciencetrends.com/action/getSupplementalData.php?ID=134*) summarizes the key differences among the six scenarios, proving the significance of PCR testing to confirmed cases. While the effect of inbound and outbound tourists is, to some extent, subtle.

Figure 3B-G demonstrates the change in number of agents in E, I1 and I2 states in each of the six scenarios, with the number of E, I1 and I2 agents marked in purple, blue and red lines respectively. Table S18 (*http://www.biosciencetrends.com/action/getSupplementalData.php?ID=134*) summarizes the maximum number of unconfirmed (I1) and confirmed (I1 + I2) cases. The effect of inbound and outbound tourists is thus clear. Fewer the tourists, fewer unconfirmed, fewer total infections and earlier the maximum infection

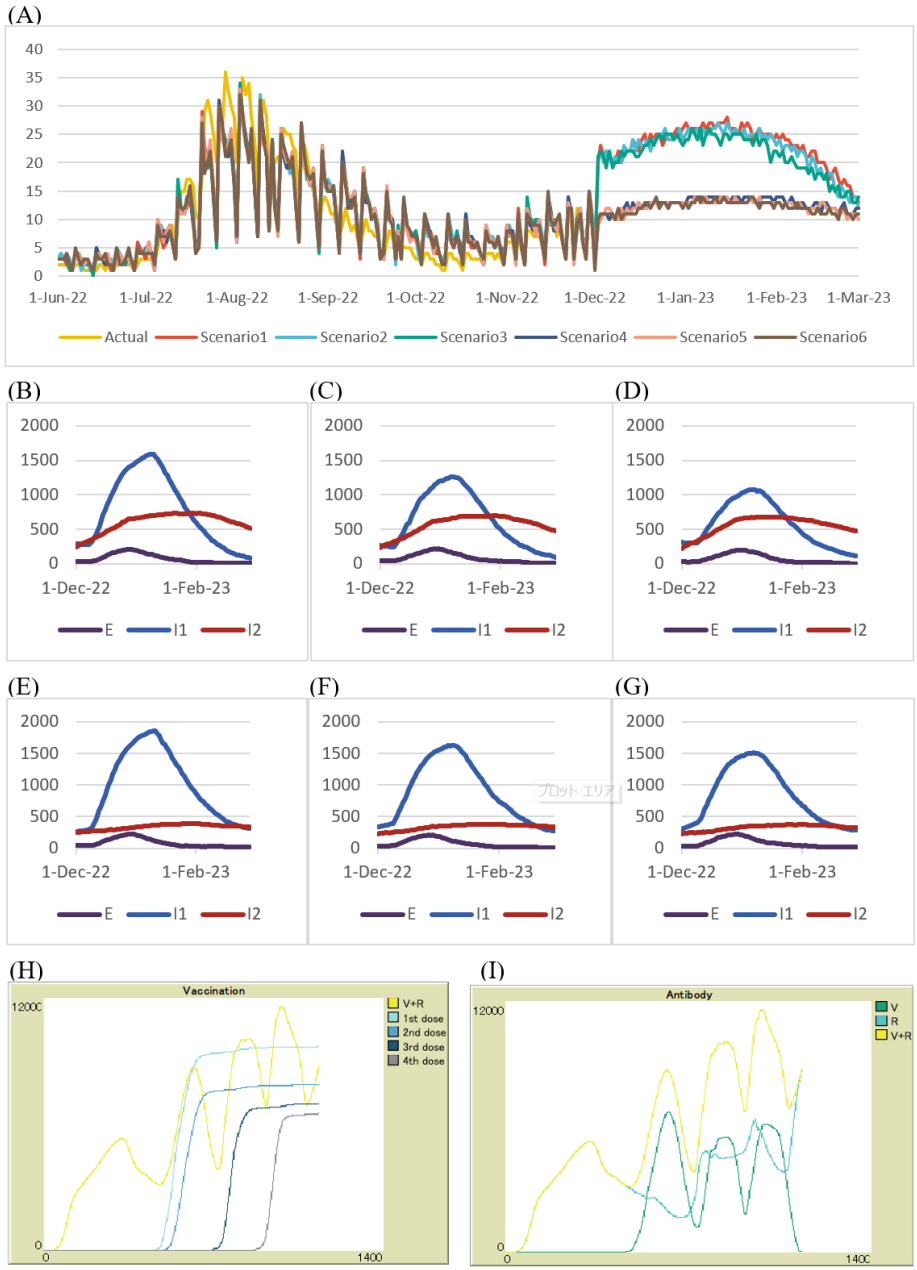

Figure 3. Forecasted results based on 6 scenarios. (A), Actual results post scaling, forecasted results of scenario I ~ VI, from June 1, 2022 to March 1, 2023. **(B)** ~ **(G)**, The number of agents in E, I1 and I2 states for scenario I, II, III, IV, V and VI respectively. **(H)** ~ **(I)**, In scenario IV, 4 doses of vaccination, the number of agents in V, R and V+R states from 2020.01.24 to 2023.03.01.

arrives. Figure 3H-I illustrates the simulation results of vaccination and antibody titer in scenario IV, with the number of V+R, V, R, 1st, 2nd, 3rd and 4th dose marked in yellow, dark green, light green, light blue, blue, dark blue, and gray lines respectively.

3.3. Findings

3.3.1. Infection peak

1. Large scale PCR testing pushes back the peak of the infection, as can be inferred from Table S17 (*http://www.biosciencetrends.com/action/getSupplementalData.php?ID=134*), the infection peak of scenarios I~III is around early to mid January, while that of scenarios IV~VI continues in late January.

2. An explosion in the number of travelers leads to more asymptomatic cases, confirmed cases and therefore postpones the arrival of the infection peak (see Table S17, *http://www.biosciencetrends.com/action/getSupplementalData.php?ID=134*).

3.3.2. Optimal PCR tests

1. Faced with the currently low severe rate and death rate (severe rate = 0.01%, death rate = 0.001%), PCR tests would not make much difference to reduce overall infections, judging from the tiny difference of I1+I2

maximum. Specifically, between '1,930' in Scenario II and '1,989' in Scenario V, as well as '1,756' in Scenario III and '1,863' in Scenario VI (See Table S18, *http://www.biosciencetrends.com/action/getSupplementalData.php?ID=134*). Therefore, maintaining PCR tests to a low level helps to reduce both social cost and public anxiety.

2. As quoted from the Tokyo Metropolitan Government, the total number of hospital beds is 7,291 (*1*) to serve a total of 13,920,000 residents in Tokyo. and the total number of hospital beds targeting severe patients is 383. Based on the above simulation results, the total number of severe patients under infection peak is expected to be $2,292 \div 0.0009 \times 0.01\% = 255 < 383$. Therefore, we can conclude that, currently the medical resources are adequate.

3. However, if faced with a new variant in the future with high severe rate and death rate, PCR tests should be adjusted to a higher level to detect infection and start treatment early. Such a level of PCR tests should be compatible with available medical resources.

4. Discussion

4.1. Summary

This research demonstrates the importance of COVID-19 infection forecast in response to vaccine strategies, virus mutation, government policies and PCR testing. Specifically, this research approaches the problem using agent-based modeling and extended SEIR modeling methods. We justify the simplified social contact model as well as considering antibody titer declination in our research. After conducting simulation forecasts based on synthetic space and population, we conclude that the re-opening policy is subject to continuous monitoring. On one hand, the third-dose public vaccination rate is high; on the other, mutated variants like BQ.1 and BQ.1.1 are likely to become the next dominant variants due to significant evolving and immune escaping abilities (*41*). It is noted that the current trend of mutation is continuing, yet variants become more infective however less fatal. It is also pleasant to see the Tokyo Metropolitan Government has introduced and is encouraging a new round of vaccination against the BA. series. As is observed, the recovery of inbound foreign nations has started since October 11, 2022. It is suggested that continuous monitoring should be carried on with plans being made ahead for various scenarios.

4.2. Recommendations

Since Japan's opening-up policy (see Table S5, *http://www.biosciencetrends.com/action/getSupplementalData.php?ID=134*) cannot be reversed, the country should continue to monitor daily confirmed cases, detecting spreaders and closely monitoring possible mutation and new variants as well as severe rate and fatality rate (see Table S2 and Table S4 (*http://www.biosciencetrends.com/action/getSupplementalData.php?ID=134*)). Although the trend of severe rate and fatality rate has been declining, there is no clear evidence to reject the claim that another troublesome variant with high fatality rate would not arrive in the near future.

In the meantime, the country is expected to improve hospital bed capacity. The current hospital bed occupancy rate has already reached 56.3% in Tokyo. Considering the possible mutated viruses brought by overseas travelers in December 2022 and January 2023, the existing medical resources are far from sufficient.

4.3. Future work

The battle against Coronavirus has lasted for three years. While we wait for the arrival of the final success in the near future, harder work should be carried out preventing possible resurgences and project corresponding reactions.

There are several flaws in the research. First is the moving pattern of agents. While we try to overcome the problem by putting forward the theory of large-scale flow dynamics, it is expected to be improved in the future. Second, natural birth and death rates have not been considered in the research, as well as family combination and separation (i.e marriage and divorce). In pursuit of model perfection, we shall make changes to population structure in the near future. Third, in this research we randomly select agents to conduct PCR tests, whereas in real world agents can freely choose whether to undertake PCR tests or not, based on their judgements to their own health. Lastly, as Dr. Israel once mentioned (*32*), the immune response elicited by vaccination or previous infection is a complex system, which is far frpm being entirely measured by the antibody titers. Although the clinical data of antibody titer can be obtained, we should apply and formulate such data to our studies with caution, in consideration of individual agents' heterogeneity of antibody titer level and decay rate.

Besides from the above, this study shall compare the simulated results with the public data of COVID-19 Infection in Tokyo, improve and try to forecast the March 2023 to June 2023 infection results, update possible new variants and immigration policies. Future study shall identify the influence of changes in vaccination strategies, immigration policies, virus mutation and PCR tests.

Acknowledgements

This paper would not have been possible without the support from a number of important people. I'd like to thank M.D. Ariel Israel for his inspiring paper about IgG titer regression. Also, I'd like to extend my thanks to my friends and all members from the Simulation of Complex Systems (SCS) Laboratory.

Funding: This research received no specific grant from any funding agency in the public, commercial, or not-for-profit sectors.

Conflict of Interest: The authors have no conflicts of interest to disclose.

References

1. Tokyo Metropolitan Government. Tokyo Metropolitan Government COVID-19 Information Website. *https://stopcovid19.metro.tokyo.lg.jp/en* (accessd January 19, 2023).
2. Chiba A. The effectiveness of mobility control, shortening of restaurants' opening hours, and working from home on control of COVID-19 spread in Japan. Health Place. 2021; 70:102622.
3. Yamauchi T, Takeuchi S, Uchida M, Saito M, Kokaze A. The association between the dynamics of COVID-19, related measures, and daytime population in Tokyo. Sci Rep. 2022; 12:1-12.
4. Murakami T, Sakuragi S, Deguchi H, Nakata M. Agent-based model using GPS analysis for infection spread and inhibition mechanism of SARS-CoV-2 in Tokyo. Sci Rep. 2022; 12:20896.
5. Yasuda H, Ito F, Hanaki K-i, Suzuki K. COVID-19 pandemic vaccination strategies of early 2021 based on behavioral differences between residents of Tokyo and Osaka, Japan. Arch Public Health. 2022; 80:1-12.
6. Larrauri B, Malbran A, Larrauri JA. Omicron and vaccines: An analysis on the decline in COVID-19 mortality. medRxiv. 2022. doi: 10.1101/2022.05.20.22275396.
7. Matsuyama K. Shionogi COVID-19 pill Xocova wins emergency approval in Japan | The Japan Times. *https://www.japantimes.co.jp/news/2022/11/22/national/science-health/shionogi-covid-xocova-approval/* (accessd January 19, 2023).
8. Urasaki Y. Japan to reopen to tour groups from 98 nations and regions | Nikkei Asia. *https://asia.nikkei.com/Business/Travel-Leisure/Japan-to-reopen-to-tour-groups-from-98-nations-and-regions* (accessd January 19, 2023).
9. Aoyama Y. First tour group from Hong Kong in 2 years lands at Narita Airport | The Asahi Shimbun. *https://www.asahi.com/ajw/articles/14652069* (accessd January 19, 2023).
10. Zhang Y. Australia's softball players are among the first Olympic athletes to arrive in Japan | The New York Times. *https://www.nytimes.com/2021/06/01/world/asia/australia-olympics-tokyo-japan-softball.html* (accessd January 19, 2023).
11. International Olympic Committee. Tokyo 2020 Olympic Village(s) Period of stay Guidelines for the NOCs. *https://stillmedab.olympic.org/media/Document%20Library/OlympicOrg/News/2020/12/Tokyo-2020-Olympic-Village-Guidelines-for-NOCs-in-relation-to-period-of-stay-eng.pdf* (accessd January 19, 2023).
12. McCurry J. 79,000 people flying in for Tokyo Olympics, Japanese media reports | The Guardian. *http://www.theguardian.com/sport/2021/may/20/organisers-of-tokyo-olympics-press-ahead-despite-covid-fears* (accessd January 19, 2023).
13. Tsukimori O. COVID tests still in short supply in Japan despite peak of sixth wave | The Japan Times. *https://www.japantimes.co.jp/news/2022/02/18/national/covid-tests-shortages/* (accessd January 19, 2023).
14. Ministry of Health, Labour and Welfare. COVID-19 tests. *https://www.mhlw.go.jp/stf/seisakunitsuite/bunya/0000121431_00182.html* (accessd January 19, 2023).
15. Tokyo Metropolitan Government. Test Kit Request Site for Close Contacts. *https://tokyo-testkit.metro.tokyo.lg.jp/closecontacts/form* (accessd January 19, 2023). (in Japanese)
16. Wilensky U. NetLogo. Northwestern University, Evanston, IL: Center for connected learning and computer-based modeling. 1999; *http://ccl.northwestern.edu/netlogo/* (accessd January 19, 2023).
17. Venkatramanan S, Lewis B, Chen J, Higdon D, Vullikanti A, Marathe M. Using data-driven agent-based models for forecasting emerging infectious diseases. Epidemics. 2018; 22:43-49.
18. Shamil M, Farheen F, Ibtehaz N, Khan IM, Rahman MS. An agent-based modeling of COVID-19: validation, analysis, and recommendations. Cognit Comput. 2021;1-12.
19. Li J, Giabbanelli P. Returning to a normal life *via* COVID-19 vaccines in the United States: a large-scale Agent-Based simulation study. JMIR Med Inform. 2021; 9:e27419.
20. Kerr CC, Stuart RM, Mistry D, Abeysuriya RG, Rosenfeld K, Hart GR, Núñez RC, Cohen JA, Selvaraj P, Hagedorn B. Covasim: an agent-based model of COVID-19 dynamics and interventions. PLoS Comput Biol. 2021; 17:e1009149.
21. Read JM, Bridgen JR, Cummings DA, Ho A, Jewell CP. Novel coronavirus 2019-nCoV (COVID-19): early estimation of epidemiological parameters and epidemic size estimates. Philos Trans R Soc Lond B Biol Sci. 2021; 376:20200265.
22. Yang HM, Junior LPL, Yang AC. Are the SIR and SEIR models suitable to estimate the basic reproduction number for the CoViD-19 epidemic? MedRxiv. 2020. doi: 10.1101/2020.10.11.20210831.
23. Li H, Leong FY, Xu G, Kang CW, Lim KH, Tan BH, Loo CM. Airborne dispersion of droplets during coughing: a physical model of viral transmission. Sci Rep. 2021; 11:1-10.
24. Live Japan. 6 Crazy Facts About Tokyo's Population (2021) - Inside the World's Top Megacity | LIVE JAPAN travel guide. *https://livejapan.com/en/in-tokyo/in-pref-tokyo/in-tokyo_suburbs/article-a0002533/* (accessd January 19, 2023).
25. Ministry of Internal Affairs & Communications. Japan Labor Force Participation Rate - December 2022 Data - 1953-2021 Historical | Trading Economics. *https://tradingeconomics.com/japan/labor-force-participation-rate* (accessd January 19, 2023).
26. MEXT (Japan). Japan: number of students at schools by prefecture 2021 | Statista. *https://www.statista.com/statistics/1192991/japan-number-students-schools-by-prefecture/* (accessd January 19, 2023).
27. Kadanoff LP, McNamara GR, Zanetti G. A Poiseuille viscometer for lattice gas automata. In: Lattice Gas Methods for Partial Differential Equations. Complex Syst. 1987; 1:791-803
28. Wolfram S, Gad-el-Hak M. A new kind of science. Appl Mech Rev. 2003; 56:B18-B19.
29. Ministry of Health, Labour and Welfare. COVID-19 Q&A. *https://www.mhlw.go.jp/stf/covid-19/qa.html* (accessd January 19, 2023).

30. Polack FP, Thomas SJ, Kitchin N, Absalon J, Gurtman A, Lockhart S, Perez JL, Marc GP, Moreira ED, Zerbini C. Safety and efficacy of the BNT162b2 mRNA Covid-19 vaccine. N Engl J Med. 2020; 383:2603-2615.
31. Yamaguchi T, Iwagami M, Ishiguro C, Fujii D, Yamamoto N, Narisawa M, Tsuboi T, Umeda H, Kinoshita N, Iguchi T. Safety monitoring of COVID-19 vaccines in Japan. Lancet Reg Health West Pac. 2022; 23:100442.
32. Israel A, Shenhar Y, Green I, Merzon E, Golan-Cohen A, Schäffer AA, Ruppin E, Vinker S, Magen E. Large-scale study of antibody titer decay following BNT162b2 mRNA vaccine or SARS-CoV-2 infection. Vaccines. 2022; 10:64.
33. Narasimhan M, Mahimainathan L, Araj E, Clark AE, Markantonis J, Green A, Xu J, SoRelle JA, Alexis C, Fankhauser K. Clinical evaluation of the Abbott Alinity SARS-CoV-2 spike-specific quantitative IgG and IgM assays among infected, recovered, and vaccinated groups. J Clin Microbiol. 2021; 59:e00388-00321.
34. Ebinger JE, Fert-Bober J, Printsev I, Wu M, Sun N, Prostko JC, Frias EC, Stewart JL, Van Eyk JE, Braun JG. Antibody responses to the BNT162b2 mRNA vaccine in individuals previously infected with SARS-CoV-2. Nat Med. 2021; 27:981-984.
35. Regev-Yochay G, Gonen T, Gilboa M, Mandelboim M, Indenbaum V, Amit S, Meltzer L, Asraf K, Cohen C, Fluss R. Efficacy of a fourth dose of COVID-19 mRNA vaccine against omicron. N Engl J Med. 2022; 386:1377-1380.
36. Xu Q-Y, Xue J-H, Xiao Y, Jia Z-J, Wu M-J, Liu Y-Y, Li W-L, Liang X-M, Yang T-C. Response and duration of serum anti-SARS-CoV-2 antibodies after inactivated vaccination within 160 days. Front Immunol. 2021; 12.
37. Karako K, Song P, Chen Y, Tang W, Kokudo N. Overview of the characteristics of and responses to the three waves of COVID-19 in Japan during 2020-2021. Biosci Trends. 2021; 15:1-8.
38. Patil I. Visualizations with statistical details: The'ggstatsplot'approach. J. Open Source Softw. 2021; 6:3167.
39. Sheward DJ, Kim C, Fischbach J, Sato K, Muschiol S, Ehling RA, Björkström NK, Hedestam GBK, Reddy ST, Albert J. Omicron sublineage BA. 2.75. 2 exhibits extensive escape from neutralising antibodies. Lancet Infect Dis. 2022; 22:1538-1540.
40. Edamatsu Y. Experts warn BQ.1 becoming dominant virus strain in Japan | The Asahi Shimbun. *https://www.asahi.com/ajw/articles/14787896* (accessd January 19, 2023).
41. Ito J, Suzuki R, Uriu K, Itakura Y, Zahradnik J, Deguchi S, Wang L, Lytras S, Tamura T, Kida I. Convergent evolution of the SARS-CoV-2 Omicron subvariants leading to the emergence of BQ. 1.1 variant. bioRxiv. 2022. doi: 10.1101/2022.12.05.519085.
42. Novel Coronavirus Domestic infection Situation | Toyo keizai Online. *https://toyokeizai.net/sp/visual/tko/covid19/* (accessd January 19, 2023). (in Japanese)
43. Higashide M. Ratio of severely ill patients (to number of patients receiving medical treatment). *https://uub.jp/cvd/* (accessd January 19, 2023). (in Japanese)
44. Fujii D, Nakata T. COVID-19 and economic activity in Japan. *https://covid19outputjapan.github.io/JP/* (accessd January 19, 2023). (in Japanese)

Received January 15, 2023; Revised February 8, 2023; Accepted February 9, 2023.

Address correspondence to:
Yu Chen, SCS Laboratory, Room 216, Environment Building, The University of Tokyo Kashiwa Campus, Kashiwanoha 5-1-5, Kashiwa, Chiba 277-8563, Japan.
E-mail: chen@edu.k.u-tokyo.ac.jp

Released online in J-STAGE as advance publication February 11, 2023.

Original Article

DOI: 10.5582/bst.2022.01522

Delayed gastric emptying after aggressive surgery for retroperitoneal sarcoma – Incidence, characteristics, and risk factors

Ang Lv[§], Rongze Sun[§], Hui Qiu, Jianhui Wu, Xiuyun Tian, Chunyi Hao[*]

Key Laboratory of Carcinogenesis and Translational Research (Ministry of Education, Beijing), Department of Hepato-Pancreato-Biliary Surgery/ Sarcoma Center, Peking University Cancer Hospital & Institute, Beijing, China.

SUMMARY Delayed gastric emptying (DGE) after aggressive resection of retroperitoneal sarcoma (RPS) has rarely been described. This study aimed to determine the incidence and characteristics of DGE after surgery for RPS and explore its potential risk factors. Patients with RPS who had undergone surgery between January 2010 and February 2021 were retrospectively analyzed. DGE was defined and graded according to the International Study Group of Pancreatic Surgery classification and classified as primary or secondary to other complications. Patients with clinically relevant DGE (crDGE, grade B+C) were compared to those with no or mild DGE (grade A). Multivariate logistic regression analysis of clinicopathological and surgical parameters was performed to identify risk factors for crDGE. Of the 239 patients studied, 69 (28.9%) had experienced DGE and 54 (22.6%) had experienced crDGE. Patients with primary and secondary DGE accounted approximately half and half. The most common concurrent complications included abdominal infection, postoperative pancreatic fistula, and abdominal bleeding. Patients with crDGE were more likely to have multifocal tumors and the liposarcoma subtype, with a larger tumor size, longer operating time, more resected organs, and a history of combined resection of the stomach, pancreas, small intestine, and/or colon. In multivariate analysis, the tumor size, operating time, and combined pancreatic resection were independent risk factors for crDGE. In conclusion, the current results indicated that approximately one-fourth of patients experienced DGE after aggressive surgery for RPS and that DGE was primary or secondary to other underlying conditions. A large tumor involving long, difficult surgery and combined pancreatic resection highly predicted the incidence of crDGE. The prevention and management of DGE remain challenging.

Keywords delayed gastric emptying, retroperitoneal sarcoma, multivisceral resection, major complication, risk factor

1. Introduction

Retroperitoneal sarcomas (RPS) constitute a heterogeneous group of rare malignant tumors that often grow to a large size and involve adjacent organs before detection. Considering the overall limited effect of pharmacotherapy for most subtypes, surgery is the cornerstone of RPS management (*1,2*). Compared with simple tumor resection, aggressive multivisceral resection (MVR) en bloc with involved or adjacent organs is associated with a significantly decreased local recurrence rate and improved survival (*3-6*). However, aggressive surgery may inevitably lead to an increased risk of complications. Surgery for RPS has been found to have a major complication rate as high as approximately 15-31% and a mortality rate as high as approximately 3-7%, even in high-volume centers (*3,6-10*).

Delayed gastric emptying (DGE) is one of the predominant complications of major abdominal surgery, especially pancreatic and upper gastrointestinal surgery. DGE is diagnosed based on characteristic symptoms, the absence of gastric outlet obstruction, and evidence of an objective delay in gastric emptying (*11*). DGE delays oral intake, prolongs hospitalization, decreases quality of life, and increases the total cost of hospitalization (*12-15*). The exact etiology and pathogenesis of postoperative DGE remains unclear. The proposed risk factors and mechanisms are related to pre-existing conditions (such as diabetes mellitus and malnutrition), surgical procedures (such as

pyloric or antral ischemia, pylorospasm secondary to the disruption of the perigastric vagal nerves, and aggressive lymphadenectomy), and postoperative intra-abdominal complications (such as gastric dysrhythmias due to a postoperative pancreatic fistula [POPF], hemorrhage, or infection) (*14,16-20*).

The incidence of DGE reportedly ranges from 17.3% to 51.8% after pancreaticoduodenectomy (PD) (*21-24*), 5% to 24% after distal pancreatectomy (DP) (*25,26*), and 4.3% to 15.5% after distal gastrectomy (*27,28*). Considering the extensiveness, complexity, and high rate of intra-abdominal complications of aggressive surgery for RPS, DGE may be common after resection of RPS. However, the incidence and characteristics of and risk factors for DGE after surgery for RPS remain unclear. To the extent known, only one study has explicitly reported the incidence and severity of DGE after MVR for RPS (*29*); in that study, all 100 patients had primary RPS. As one of the largest specialized sarcoma centers in China, we established a treatment algorithm and performed aggressive surgery in patients with primary and recurrent RPS. This study aimed to investigate the incidence and characteristics of DGE after aggressive surgery for RPS using a larger sample of patients with either primary or recurrent disease and to analyze its potential risk factors.

2. Materials and Methods

2.1. Patients and data collection

We retrospectively analyzed a cohort of consecutive patients who had undergone surgery for RPS at the Peking University Cancer Hospital Sarcoma Center between January 2010 and February 2021. Patients with benign retroperitoneal tumors, desmoid-type fibromatosis, gastrointestinal stromal tumors, or subtypes other than RPS were excluded. Data on sex, age, body mass index (BMI), medical history, presentation status, pathological subtype, tumor grading, tumor size, tumor focality, surgical information (operating time, estimated blood loss, completeness of surgery, and the number and type of resected organs), and postoperative course (removal and re-insertion of a nasogastric tube, intensive care unit [ICU] admission, postoperative hospitalization, postoperative complications, and reoperation) were retrieved from electronic medical records.

This study's primary outcomes were the incidence and grade of DGE. To evaluate the clinical impact of DGE, patients experiencing clinically relevant DGE (grades B and C) were analyzed and compared to those with no or mild DGE (grade A). Patients who died of complications within 1 week of surgery were excluded because their DGE status could not be assessed.

This study was reported according to the STROBE guidelines. The study was approved by the Ethics Committee of Peking University Cancer Hospital and conducted in accordance with the 1975 Declaration of Helsinki, as revised in 2013. All patients provided written informed consent before surgery for the use of their anonymized data.

2.2. Perioperative management

All patients underwent surgery by the same surgical team led by Hao. The treatment algorithm and surgical procedures have been described previously (*3*). According to the general principles of surgical and supportive care, standard postoperative treatments were administered, including fluid balance, adequate electrolyte replacement, prophylactic anti-infection, and total parenteral nutrition.

A nasogastric tube was inserted during surgery when suturing repair, tangential resection, or anastomosis of the upper gastrointestinal tract was performed. If the amount of gastric juice was < 300 mL per day, the nasogastric tube was removed after flatus was expelled. When gastric retention, anastomotic leakage, or bowel obstruction was confirmed on abdominal radiography or upper gastroenterography, the nasogastric tube was re-inserted. Patients not undergoing resection or anastomosis of the gastrointestinal tract were permitted a liquid diet after flatus expulsion and subsequently transitioned to a semi-liquid and general diet. Patients undergoing resection or anastomosis of the stomach or duodenum were not permitted liquid diet intake until an upper gastroenterography had been performed on day 5-6 postoperatively to prevent anastomotic leakage, stricture, or DGE.

Upon diagnosis of DGE, efforts were made to mobilize the patient, use prokinetic agents, and aggressively treat any other complications, such as POPF and abdominal infection.

2.3. Definitions

DGE was defined and graded according to the standards published by the International Study Group of Pancreatic Surgery (ISGPS) (*14*). As alluded to above, grade B or C DGE was considered clinically relevant. DGE was classified as primary (unrelated to other complications) or secondary to other surgical complications. Other causes of aphagosis, such as anastomotic leakage and bowel obstruction, were carefully reviewed and ruled out. Complications other than DGE were graded using the Clavien–Dindo classification and considered "major" if graded III or higher (*30*). Pathological subtypes were classified according to the 2020 World Health Organization (Geneva) criteria for soft tissue tumors (*31*). Tumor grading was determined using the three-tiered grading system of the Fédération Nationale des Centres de Lutte Contre le Cancer (FNCLCC) criteria (*32*). Tumor size was defined as the sum of the largest

tumor diameters. Surgical resections were classified as macroscopically complete (R0/R1) or incomplete (R2) in accordance with most previous studies, because the large surface area and anatomical location of the RPS casts doubt on the use of a reliable microscopic margin assessment (*33*).

2.4. Statistical Analysis

Clinicopathological, surgical, and postoperative parameters are expressed as frequencies and percentages for categorical variables and medians and ranges for continuous variables. The chi-square test and *t*-test were used to compare categorical and continuous variables, respectively. Multivariate binary logistic regression with a forward LR strategy was used to analyze clinicopathological and surgical variables and explore the independent risk factors for clinically relevant DGE. Variables with *P*-values <0.1 from univariate analysis or clinical significance were incorporated into the multivariate model. Results were considered statistically significant if a two-sided *P*-value < 0.05 was obtained. Statistical analyses were performed using SPSS (version 26.0; SPSS Inc., Chicago, IL).

3. Results

Among 242 consecutive patients who underwent surgery for RPS, three patients were excluded because of death within 7 days postoperatively, and the remaining 239 patients were enrolled in this study. A flowchart illustrates the selection and subgrouping process (Figure 1).

Of the 239 enrolled patients, 69 (28.9%) experienced DGE and 54 (22.6%) experienced clinically relevant DGE. DGE was classified as grade A (15/69, 21.7%), B (21/69, 30.4%), or C (33/69, 47.8%) based on the ISGPS definition. DGE was primary in 34 (49.3%) patients (grade A in 10, grade B in 6, and grade C in 18) and secondary to other postoperative complications in 35 (50.7%) (grade A in 5, grade B in 15, and grade C in 15) (Figure 2A). Abdominal infection (n = 16),

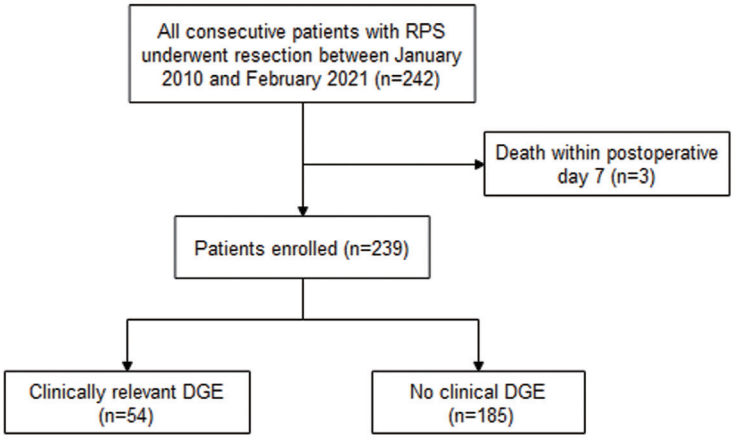

Figure 1. Flowchart for the selection and subgrouping process. DGE, delayed gastric emptying; RPS, retroperitoneal sarcoma.

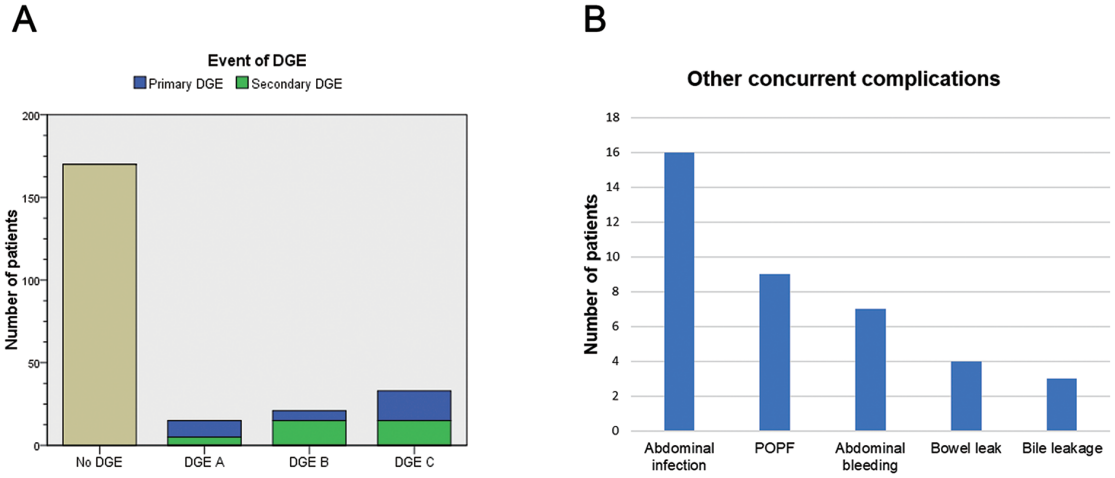

Figure 2. Grade and category of DGE (**A**) and its most common concurrent complications (**B**). DGE, delayed gastric emptying; POPF, postoperative pancreatic fistula.

POPF (n = 9), abdominal bleeding (n = 7), bowel leak (n = 4), and bile leakage (n = 3) were the predominant concurrent complications associated with clinically relevant DGE (Figure 2B).

Patient clinicopathological characteristics are shown in Table 1. Sex, age, BMI, previous diabetes, presentation status, and FNLCC grade were not associated with clinical DGE. Compared to patients not experiencing clinical DGE, those who experienced clinically relevant DGE had a larger tumor size (median 26.5 cm *vs*. 17.0 cm, $P < 0.001$) and higher proportion of multifocal tumors (25/54, 46.3% *vs*. 58/185, 31.3%, $P = 0.042$) and dedifferentiated liposarcoma subtypes (57.4% *vs*. 34.6%, $P = 0.021$). In terms of pathological subtypes, the incidence rate of clinical DGE was highest in liposarcomas (40/128, 31.3%) and lowest in leiomyosarcomas (3/40, 7.5%).

The surgical characteristics of patients are shown in Table 2. A significantly longer operating time (median: 551 min *vs*. 406 min, $P < 0.001$), greater estimated blood loss (median: 2000 mL *vs*. 800 mL, $P = 0.002$), and a greater number of organs removed during surgery (median: 7 *vs*. 5, $P < 0.001$) were noted in patients who experienced clinically relevant DGE. Moreover, combined gastric resection (23/54, 42.6% *vs*. 31/185, 16.8%; $P < 0.001$), pancreatic resection (33/54, 61.1% *vs*. 54/185, 29.2%; $P < 0.001$), major colon resection (49/54, 90.7% *vs*. 117/185, 63.2%; $P < 0.001$), and small intestine resection (23/54, 42.6% *vs*. 33/185, 17.8%; $P < 0.001$) were significantly more common in patients with clinical DGE. Patients who had undergone PD were more likely to experience clinical DGE than those who had undergone DP ($P = 0.016$). The completeness of resection and resection of the kidney

Table 1. Clinicopathological characteristics of patients

Parameter	Total (n = 239)	No clinical DGE (n = 185)	Clinical DGE (n = 54)	P
Sex ratio, n (male:female)	124:115	92:93	32:22	0.218
Age (years)*	55 (16-86)	55 (16-83)	58 (20-86)	0.208
BMI (kg/m^2)*	23.4 (15.6-39.0)	23.4 (15.6-39.0)	23.3 (16.9-32.2)	0.594
Diabetes, n (%)	24 (10.0%)	17 (9.2%)	7 (13.0%)	0.125
Presentation status, n (primary:recurrent)	144:95	117:68	27:27	0.080
Pathological subtypes, n (%)				0.021
DDLPS	95 (39.7%)	64 (34.6%)	31 (57.4%)	
WDLPS	33 (13.8%)	24 (13.0%)	9 (16.7%)	
LMS	40 (16.7%)	37 (20.0%)	3 (5.6%)	
UPS	17 (7.1%)	14 (7.6%)	3 (5.6%)	
SFT	16 (6.7%)	14 (7.6%)	2 (3.7%)	
Other	38 (15.9%)	32 (17.2%)	6 (11.0%)	
FNCLCC grade, n (%)				0.243
1	43 (18.0%)	36 (19.5%)	7 (13.0%)	
2	99 (41.4%)	79 (42.7%)	20 (37.0%)	
3	97 (40.6%)	70 (37.8%)	27 (50.0%)	
Tumor size (cm)*	19.0 (1.6-69.0)	17.0 (3.5-69.0)	26.5 (1.6-69.0)	< 0.001
Tumor focality, n (single:multifocal)	156:83	127:58	29:25	0.042

*Median with range. DGE, delayed gastric emptying; BMI, body mass index; P-POSSUM, physiological and operative severity score for the enumeration of mortality and morbidity; DDLPS, dedifferentiated liposarcoma; WDLPS, well-differentiated liposarcoma; LMS, leiomyosarcoma; UPS, undifferentiated pleomorphic sarcoma; SFT, solitary fibrous tumor; FNCLCC, Fédération Nationale des Centres de Lutte Contre le Cancer.

Table 2. Operative data on patients

Parameter	Total (n = 239)	No clinical DGE (n = 185)	Clinical DGE (n = 54)	P
Operating time (min)*	432 (71-1030)	406 (71-1030)	551 (300-995)	< 0.001
Estimated blood loss (mL)*	1000 (10-16000)	800 (10-16000)	2000 (100-15600)	0.002
No. of resected organs*	5 (0-14)	5 (0-14)	7 (1-13)	< 0.001
Complete resection (R0/R1), n (%)	215 (90.0%)	170 (91.9%)	45 (83.3%)	0.066
Partial gastric resection, n (%)	54 (22.6%)	31 (16.8%)	23 (42.6%)	< 0.001
Pancreatic resection, n (%)	87 (36.4%)	54 (29.2%)	33 (61.1%)	< 0.001
Type of pancreatic resection, n (%)				0.016
Pancreaticoduodenectomy	31 (35.6%)	14 (25.9%)	17 (51.5%)	
Distal pancreatectomy	56 (64.4%)	40 (74.1%)	16 (48.5%)	
Colon resection, n (%)	166 (69.5%)	117 (63.2%)	49 (90.7%)	< 0.001
Small intestine resection, n (%)	56 (23.4%)	33 (17.8%)	23 (42.6%)	< 0.001
Kidney resection, n (%)	130 (54.4%)	96 (51.9%)	34 (63.0%)	0.151
Major vessel resection, n (%)	61 (25.5%)	45 (24.3%)	16 (29.6%)	0.431

*Median with range. DGE: delayed gastric emptying.

or major vessels were not associated with clinical DGE.

Multivariate analysis, which included the aforementioned clinicopathological and surgical variables, indicated that the tumor size (odds ratio [OR]: 1.034; 95% confidence interval [CI]: 1.006-1.062; $P = 0.016$), operating time (OR: 1.003; 95% CI: 1.001-1.005; $P = 0.003$), and combined pancreatic resection (OR: 2.521; 95% CI: 1.243-5.113; $P = 0.010$) were independent risk factors for clinical DGE (Table 3). To further explore the independent risk factors for primary clinically relevant DGE, univariate and multivariate analyses of clinicopathological and surgical variables were also performed. The tumor size ($P = 0.016$), operating time ($P = 0.033$), and the number of resected organs ($P = 0.048$) were found to be associated with primary clinically relevant DGE in univariate analysis, and the tumor size (OR: 1.035; 95% CI: 1.006-1.066; $P = 0.019$) was identified as the unique independent risk factor in multivariate analysis.

The patients' postoperative courses are shown in Table 4. The rates of nasogastric tube insertion during surgery (43/54, 79.6% *vs*. 64/185, 34.6%, $P < 0.001$), delayed nasogastric tube removal (median: 9 *vs*. 5 days, $P < 0.001$), and nasogastric tube re-insertion (25/54, 46.3% *vs*. 11/185, 5.9%, $P < 0.001$) were significantly higher in patients experiencing clinical DGE. In addition, rates of ICU admission (37/54, 68.5% *vs*. 52/185, 28.1%, $P < 0.001$), major complications (26/54, 48.1% *vs*. 27/185, 14.6%, $P < 0.001$), reoperation (16/54, 29.6% *vs*. 9/185, 4.9%, $P < 0.001$), and 90-day postoperative mortality (5/54, 9.3% *vs*. 5/185, 2.7%, $P = 0.034$) were significantly higher in patients with clinical DGE. Accordingly, the total duration of hospitalization was longer in patients with clinical DGE (median: 34 *vs*. 16 days; $P < 0.001$).

4. Discussion

Postoperative DGE was first described by Warshaw *et al*. (*34*). Considering the rarity and complexity of surgery for RPS, only one study has specifically reported DGE after MVR for RPS in the English literature to date (*29*). The current study, which included 239 patients, is potentially the largest single-center case series thus far. In addition, to the extent known, this study is the first to compare patients experiencing clinically relevant DGE to those experiencing no or mild DGE in patients both with primary and recurrent RPS.

Rather than those potential life-threatening risks, the key threats to patients with DGE are delayed oral intake, prolonged hospitalization, and an increased

Table 3. Multivariate regression analysis of the clinicopathological and surgical factors influencing clinically relevant DGE

Clinicopathological parameters	Clinical DGE		Surgical parameters	Clinical DGE	
	OR (95% CI)	*P*		OR (95% CI)	*P*
Presentation status (primary*: recurrent)			Operating time	1.003 (1.001-1.005)	0.003
Pathology			Estimated blood loss		
DDLPS:Other*			No. of resected organs		
WDLPS:Other*			Complete resection (yes:no*)		
LMS:Other*			Partial gastric resection (yes:no*)		
Tumor size	1.034 (1.006-1.062)	0.016	Pancreatic resection (yes:no*)	2.521 (1.243-5.113)	0.010
Tumor focality (multifocal:single*)			Small intestine resection (yes:no*)		
			Colon resection (yes:no*)		

*is for reference. CI, confidence interval; OR, odds ratio; DGE, delayed gastric emptying; DDLPS, dedifferentiated liposarcoma; WDLPS, well-differentiated liposarcoma; LMS, leiomyosarcoma; P-POSSUM, physiological and operative severity score for enumeration of mortality and morbidity.

Table 4. Postoperative course of patients

Parameter	Total ($n = 239$)	No clinical DGE ($n = 185$)	Clinical DGE ($n = 54$)	*P*
Nasogastric tube placement intraoperatively, *n* (%)	107 (44.8%)	64 (34.6%)	43 (79.6%)	< 0.001
Removal of a nasogastric tube (POD)*	6 (2-57)	5 (2-18)	9 (2-57)	< 0.001
Re-insertion of a nasogastric tube, *n* (%)	36 (15.1%)	11 (5.9%)	25 (46.3%)	< 0.001
ICU admission, *n* (%)	89 (37.2%)	52 (28.1%)	37 (68.5%)	< 0.001
ICU days*	4 (1-35)	3 (1-35)	5 (2-21)	0.274
Postoperative hospitalization (day)*	19 (6-149)	16 (6-105)	34 (15-149)	< 0.001
Major complications other than DGE, *n* (%)	53 (22.2%)	27 (14.6%)	26 (48.1%)	< 0.001
Re-operation, *n* (%)	25 (10.5%)	9 (4.9%)	16 (29.6%)	< 0.001
90-day postoperative mortality, *n* (%)	10 (4.2%)	5 (2.7%)	5 (9.3%)	0.034

*Median with range. DGE, delayed gastric emptying; POD, days postoperatively; ICU, intensive care unit.

total cost of hospitalization. Therefore, when reporting major complications of surgery for RPS, DGE is often overlooked, even in high-volume centers, such as the Transatlantic Australasian RPS Working Group (*35,36*), resulting in a lack of data on the incidence and severity of DGE after surgery for RPS. Based on the widely accepted definition and grading standards proposed by the ISGPS, the incidence of DGE was 28.9% (69/239) and that of clinically relevant DGE was 22.6% (54/239); the rates were slightly lower than those reported by Baia *et al*. (42% and 28%, respectively) (*29*). In this case series, patients with primary and secondary DGE accounted approximately half and half, while DGE secondary to other complications was more often observed in patients with clinical DGE (30/54, 55.6%) than in those with mild DGE (5/15, 33.3%). A similar trend was also observed in other studies, in which the proportion of patients with secondary clinical DGE reached 64.3% (18/28) after surgery for RPS (*29*) and 84.1% (37/44) after pancreatic surgery (*23*). Accordingly, abdominal infection, POPF, and abdominal bleeding (*23,24,29*) were the most common concurrent complications associated with clinically relevant DGE in the current study.

The influence of intra-abdominal complications on the incidence of postoperative DGE was first reported by Henegouwen *et al*. (*37*) in 1997. In that prospective study, the incidence of DGE after standard PD (n = 100) was compared to that after pylorus-preserving PD (n = 100). With a postoperative DGE prevalence of 65%, the study demonstrated that the presence of postoperative intra-abdominal complications was the predominant risk factor for DGE ($P < 0.0001$). Subsequently, several studies, including meta-analyses, yielded similar results (*16,23,29,38*). Therefore, some researchers have suggested that, without any obvious etiology, DGE could be regarded as a sentinel event of severe complications in pancreatic and RPS surgery (*23,39*). Moreover, Baia *et al*. reported that satisfactory outcomes (a resumption of oral feeding) were potentially achievable after the treatment of complications causing secondary DGE (*29*). In addition to major complications, the current results indicated that the rates of ICU admission (68.5% *vs*. 28.1%), reoperation (29.6% *vs*. 4.9%), and 90-day mortality (9.3% *vs*. 2.7%) were also significantly higher in patients with clinically relevant DGE. The possible reasons for the link between the presence of major complications or other adverse postoperative courses and the incidence of DGE remain unclear. This indicates that clinical DGE may be considered the result of local inflammation and a manifestation of the patient's poor condition overall.

While analyzing the relationship between postoperative course and DGE, we looked for independent risk factors among clinicopathological and surgical variables. In multivariate analysis, the tumor size, operating time, and combined pancreatic resection were independent factors associated with clinical DGE. Pancreatic resection itself, regardless of PD or DP, is a relatively high-risk operation, and DGE is one of its most common complications (*21-26*). During resection of RPS, removal of the pancreas is sometimes necessary for oncological or technical reasons. However, compared to combined resection of other organs (such as the colon and kidney), combined resection of the pancreas for RPS is more controversial due to the potentially high risk of morbidity and mortality (*40-43*). In the current study, the prominent complications after combined pancreatic resection included POPF, abdominal infection, and abdominal bleeding, which were also found to be the most common complications leading to DGE. This potentially explains why a combined pancreatic resection increases the risk of clinical DGE.

The tumor size and operating time were other independent risk factors for postoperative DGE. Considering that all patients underwent surgery by the same experienced surgical team led by Hao, operating time could be regarded as an indicator of the surgery's complexity. Owing to its biological characteristics and anatomic location, RPS often grows to a vast size and involves adjacent organs before being detected. When a large tumor is located in the upper quadrant, compression of the stomach, duodenum, or small intestine is common. The changes caused by long-term compression and relief of the upper gastrointestinal tract after tumor removal may also be a possible reason for postoperative DGE (*29*). Moreover, the incidence of DGE varies among subtypes. The highest incidence was noted with liposarcoma, in approximately 1/3 of patients (40/128), and the lowest with leiomyosarcoma, at a rate of 7.5% (3/40). This may be because leiomyosarcoma typically arises from retroperitoneal vessels, such as the inferior vena cava or renal/gonadal/iliac vein; therefore, it is usually smaller in size and seldom requires gastrointestinal or pancreatic resection. In contrast, liposarcomas are generally larger in size, with a more indistinct border and a greater tendency to involve other organs (*44*), and they present as intra-abdominal multifocal recurrence rather than distant metastasis. Patients with larger and multifocal tumors involving adjacent organs usually undergo longer surgeries, more complex surgical procedures, and the resection of more organs, possibly explaining why these patients are at a higher risk of developing clinically relevant DGE.

The prevention and management of DGE remain challenging because the results of the current analysis indicated that the incidence of clinical DGE may depend more on the characteristics of the tumor rather than the surgical procedure. Considering the overall high recurrence tendency of RPS, from the perspective of local control, long hours of extensive MVR are

usually necessary for a large invasive tumor. Given that no specific agent can provide a faster recovery, the potential measures could include: effective preoperative systemic therapy to shrink the tumor and make it easier to remove, selection of an appropriate surgical approach and skilled surgical techniques to reduce the operating time as much as possible, a personalized histology-specific surgical strategy to determine the possibility of pancreatic-preserving resection, and timely appropriate treatment to control underlying complications. All of these measures above are predicated on an experienced multidisciplinary team, and this is a significant reason why patient management in a high-volume specialized sarcoma center is strongly recommended (*45,46*).

The main limitations of this study include its retrospective nature and the inclusion of patients from a single institution over a long period of time exceeding 10 years. Nonetheless, this study has analyzed the largest case series to date and it provides meaningful insights into the characteristics of, risk factors for, and management of DGE after aggressive surgery for RPS. The current findings could help to understand this issue and improve clinical decision-making.

In conclusion, the current study found that approximately one-fourth of patients have DGE after aggressive surgery for RPS and that DGE was primary or secondary to other underlying conditions. A large tumor involving long, difficult surgery and combined pancreatic resection highly predicted the incidence of clinically relevant DGE. The prevention and management of DGE remain challenging.

Funding: This work was supported by the Capital Health Research and Development of Special Funds (approval no. 2020-1-1021), Beijing Excellent Talent Training Project (approval no. 2018000021469G269), Beijing Municipal Administration of Hospital's Ascent Plan (approval no. DFL20181104), and Beijing Municipal Administration of Hospitals' Youth Program (approval no. QML20181104).

Conflict of Interest: The authors have no conflicts of interest to disclose.

Author contributions: Lv A and Hao CY contributed to the conception and design of the study. Lv A, Sun RZ, Qiu H, Wu JH, and Tian XY collected, analyzed, and interpreted patient data. Lv A and Sun RZ wrote the first draft of this manuscript. Qiu H, Wu JH, and Tian XY wrote the manuscript. All authors contributed to manuscript revision and read and approved the submitted version.

References

1. Swallow CJ, Strauss DC, Bonvalot S, *et al*. Management of primary retroperitoneal sarcoma (RPS) in the adult: An updated consensus approach from the Transatlantic Australasian RPS Working Group. Ann Surg Oncol. 2021; 28:7873-7888.
2. Trans-Atlantic RPS Working Group. Management of recurrent retroperitoneal sarcoma (RPS) in the adult: A consensus approach from the Trans-Atlantic RPS Working Group. Ann Surg Oncol. 2016; 23:3531-3540.
3. Lv A, Li Y, Li ZW, Mao LL, Tian XY, Hao CY. Treatment algorithm and surgical outcome for primary and recurrent retroperitoneal sarcomas: A long-term single-center experience of 242 cases. J Surg Oncol. 2022; 126:1288-1298.
4. Fairweather M, Gonzalez RJ, Strauss D, Raut CP. Current principles of surgery for retroperitoneal sarcomas. J Surg Oncol. 2018; 117:33-41.
5. Gronchi A, Miceli R, Allard MA, *et al*. Personalizing the approach to retroperitoneal soft tissue sarcoma: histology-specific patterns of failure and postrelapse outcome after primary extended resection. Ann Surg Oncol. 2015; 22:1447-1454.
6. Bonvalot S, Miceli R, Berselli M, Causeret S, Colombo C, Mariani L, Bouzaiene H, Le Péchoux C, Casali PG, Le Cesne A, Fiore M, Gronchi A. Aggressive surgery in retroperitoneal soft tissue sarcoma carried out at high-volume centers is safe and is associated with improved local control. Ann Surg Oncol. 2010; 17:1507-1514.
7. Gronchi A, Strauss DC, Miceli R, *et al*. Variability in patterns of recurrence after resection of primary retroperitoneal sarcoma (RPS): A report on 1007 patients from the multi-institutional collaborative RPS working group. Ann Surg. 2016; 263:1002-1009.
8. Smith HG, Panchalingam D, Hannay JA, Smith MJ, Thomas JM, Hayes AJ, Strauss DC. Outcome following resection of retroperitoneal sarcoma. Br J Surg. 2015; 102:1698-1709.
9. Lehnert T, Cardona S, Hinz U, Willeke F, Mechtersheimer G, Treiber M, Herfarth C, Buechler MW, Schwarzbach MH. Primary and locally recurrent retroperitoneal soft-tissue sarcoma: local control and survival. Eur J Surg Oncol. 2009; 35:986-993.
10. Hamilton TD, Cannell AJ, Kim M, Catton CN, Blackstein ME, Dickson BC, Gladdy RA, Swallow CJ. Results of resection for recurrent or residual retroperitoneal sarcoma after failed primary treatment. Ann Surg Oncol. 2017; 24:211-218.
11. Navas CM, Wadas ED, Zbib NH, Crowell MD, Lacy BE. Gastroparesis and severity of delayed gastric emptying: comparison of patient characteristics, treatments and medication adverse events. Dig Dis Sci. 2021; 66:526-534.
12. Akizuki E, Kimura Y, Nobuoka T, Imamura M, Nagayama M, Sonoda T, Hirata K. Reconsideration of postoperative oral intake tolerance after pancreaticoduodenectomy: Prospective consecutive analysis of delayed gastric emptying according to the ISGPS definition and the amount of dietary intake. Ann Surg. 2009; 249:986-994.
13. Kawai M, Tani M, Hirono S, Okada K, Miyazawa M, Yamaue H. Pylorus-resecting pancreaticoduodenectomy offers long-term outcomes similar to those of pylorus-preserving pancreaticoduodenectomy: Results of a prospective study. World J Surg. 2014; 38:1476-1483.
14. Wente MN, Bassi C, Dervenis C, Fingerhut A, Gouma DJ, Izbicki JR, Neoptolemos JP, Padbury RT, Sarr MG, Traverso LW, Yeo CJ, Büchler MW. Delayed gastric emptying (DGE) after pancreatic surgery: A suggested

definition by the International Study Group of Pancreatic Surgery (ISGPS). Surgery. 2007; 142:761-768.
15. Welsch T, Borm M, Degrate L, Hinz U, Büchler MW, Wente MN. Evaluation of the International Study Group of Pancreatic Surgery definition of delayed gastric emptying after pancreatoduodenectomy in a high-volume center. Br J Surg. 2010; 97:1043-1050.
16. Qu H, Sun GR, Zhou SQ, He QS. Clinical risk factors of delayed gastric emptying in patients after pancreaticoduodenectomy: a systematic review and meta-analysis. Eur J Surg Oncol. 2013; 39:213-223.
17. Park YC, Kim SW, Jang JY, Ahn YJ, Park YH. Factors influencing delayed gastric emptying after pylorus-preserving pancreatoduodenectomy. J Am Coll Surg. 2003; 196:859-865.
18. Kim DK, Hindenburg AA, Sharma SK, Suk CH, Gress FG, Staszewski H, Grendell JH, Reed WP. Is pylorospasm a cause of delayed gastric emptying after pylorus-preserving pancreaticoduodenectomy? Ann Surg Oncol. 2005; 12:222-227.
19. Futagawa Y, Kanehira M, Furukawa K, Kitamura H, Yoshida S, Usuba T, Misawa T, Okamoto T, Yanaga K. Impact of delayed gastric emptying after pancreaticoduodenectomy on survival. J Hepatobiliary Pancreat Sci. 2017; 24:466-474.
20. Khan AS, Williams G, Woolsey C, Liu J, Fields RC, Doyle MMB, Hawkins WG, Strasberg SM. Flange gastroenterostomy results in reduction in delayed gastric emptying after standard pancreaticoduodenectomy: a prospective cohort study. J Am Coll Surg. 2017; 225:498-507.
21. Mirrielees JA, Weber SM, Abbott DE, Greenberg CC, Minter RM, Scarborough JE. Pancreatic fistula and delayed gastric emptying are the highest-impact complications after Whipple. J Surg Res. 2020; 250:80-87.
22. Eshuis WJ, van Eijck CH, Gerhards MF, Coene PP, de Hingh IH, Karsten TM, Bonsing BA, Gerritsen JJ, Bosscha K, Spillenaar Bilgen EJ, Haverkamp JA, Busch OR, van Gulik TM, Reitsma JB, Gouma DJ. Antecolic versus retrocolic route of the gastroenteric anastomosis after pancreatoduodenectomy: A randomized controlled trial. Ann Surg. 2014; 259:45-51.
23. Vandermeeren C, Loi P, Closset J. Does pancreaticogastrostomy decrease the occurrence of delayed gastric emptying after pancreatoduodenectomy? Pancreas. 2017; 46:1064-1068.
24. Hayama S, Senmaru N, Hirano S. Delayed gastric emptying after pancreatoduodenectomy: comparison between invaginated pancreatogastrostomy and pancreatojejunostomy. BMC Surg. 2020; 20:60.
25. Glowka TR, von Websky M, Pantelis D, Manekeller S, Standop J, Kalff JC, Schäfer N. Risk factors for delayed gastric emptying following distal pancreatectomy. Langenbeck's Arch Surg. 2016; 401:161-167.
26. Degisors S, Caiazzo R, Dokmak S, Truant S, Aussilhou B, Eveno C, Pattou F, El Amrani M, Piessen G, Sauvanet A. Delayed gastric emptying following distal pancreatectomy: incidence and predisposing factors. HPB (Oxford). 2022; 24:772-781.
27. Matsumoto S, Wakatsuki K, Migita K, Ito M, Nakade H, Kunishige T, Kitano M, Nakatani M, Sho M. Predictive factors for delayed gastric emptying after distal gastrectomy with Roux-en-Y reconstruction. Am Surg. 2018; 84:1086-1090.
28. Hirao M, Fujitani K, Tsujinaka T. Delayed gastric emptying after distal gastrectomy for gastric cancer. Hepatogastroenterology. 2005; 52:305-309.
29. Baia M, Conti L, Pasquali S, Sarre-Lazcano C, Abatini C, Cioffi SPB, Della Valle S, Greco G, Vigorito R, Casirati A, Proto P, Gavazzi C, Gronchi A, Fiore M. Delayed gastric emptying after multivisceral resection for retroperitoneal sarcoma. Ann Surg Oncol. 2022; 29:3264-3270.
30. Dindo D, Demartines N, Clavien P-A. Classification of surgical complications: A new proposal with evaluation in a cohort of 6336 patients and results of a survey. Ann Surg. 2004; 240:205-213.
31. WHO Classification of Tumours Editorial Board. Soft Tissue and Bone Tumours. International Agency for Research on Cancer, Lyon, France, 2020.
32. Trojani M, Contesso G, Coindre JM, Rouesse J, Bui NB, de Mascarel A, Goussot JF, David M, Bonichon F, Lagarde C. Soft-tissue sarcomas of adults; study of pathological prognostic variables and definition of a histopathological grading system. Int J Cancer. 1984; 33:37-42.
33. Anaya DA, Lev DC, Pollock RE. The role of surgical margin status in retroperitoneal sarcoma. J Surg Oncol. 2008; 98:607-610.
34. Warshaw AL, Torchiana DL. Delayed gastric emptying after pylorus-preserving pancreaticoduodenectomy. Surg Gynecol Obstet. 1985; 160:1-4.
35. MacNeill AJ, Gronchi A, Miceli R, *et al*. Postoperative morbidity after radical resection of primary retroperitoneal sarcoma: a report from the Transatlantic RPS Working Group. Ann Surg. 2018; 267:959-964.
36. Nessim C, Raut CP, Callegaro D, *et al*. Postoperative morbidity after resection of recurrent retroperitoneal sarcoma: a report from the Transatlantic Australasian RPS Working Group (TARPSWG). Ann Surg Oncol. 2021; 28:2705-2714.
37. van Berge Henegouwen MI, van Gulik TM, DeWit LT, Allema JH, Rauws EA, Obertop H, Gouma DJ. Delayed gastric emptying after standard pancreaticoduodenectomy versus pylorus-preserving pancreaticoduodenectomy: An analysis of 200 consecutive patients. J Am Coll Surg. 1997; 185:373-379.
38. Riediger H, Makowiec F, Schareck WD, Hopt UT, Adam U. Delayed gastric emptying after pylorus-preserving pancreatoduodenectomy is strongly related to other postoperative complications. J Gastrointest Surg. 2003; 7:758-765.
39. Baia M, Pasquali S, Fiore M. ASO Author Reflection: Delayed gastric emptying as a sentinel event of severe complications in retroperitoneal sarcoma surgery. Ann Surg Oncol. 2022; 29:3271-3272.
40. Lv A, Liu DN, Wang Z, Li CP, Liu BN, Liu Q, Tian XY, Hao CY. Short- and long-term surgical outcomes of pancreatic resection for retroperitoneal sarcoma: a long-term single-center experience of 90 cases. J Surg Oncol. 2022; 1-12.
41. Tseng WW, Tsao-Wei DD, Callegaro D, *et al*. Pancreaticoduodenectomy in the surgical management of primary retroperitoneal sarcoma. Eur J Surg Oncol. 2018; 44:810-815.
42. Flacs M, Faron M, Mir O, Mihoubi F, Sourouille I, Haddag-Miliani L, Dumont S, Terrier P, Levy A, Dousset B, Boudou-Rouquette P, Le Cesne A, Gaujoux S, Honoré C. Postoperative outcome of surgery with pancreatic resection for retroperitoneal soft tissue sarcoma: Results

of a retrospective bicentric analysis on 50 consecutive patients. J Gastrointest Surg. 2021; 25:2299-2306.
43. Bagaria SP, Swallow C, Suraweera H, *et al*. Morbidity and outcomes after distal pancreatectomy for primary retroperitoneal sarcoma: an analysis by the Trans-Atlantic Australasian Retroperitoneal Sarcoma Working Group. Ann Surg Oncol. 2021; 28:6882-6889.
44. Wang Z, Wu J, Lv A, Li C, Li Z, Zhao M, Hao C. Infiltration characteristics and influencing factors of retroperitoneal liposarcoma: Novel evidence for extended surgery and a tumor grading system. Biosci Trends. 2018; 12:185-192.
45. Bagaria SP, Neville M, Gray RJ, Gabriel E, Ashman JB, Attia S, Wasif N. The volume-outcome relationship in retroperitoneal soft tissue sarcoma: Evidence of improved short- and long-term outcomes at high-volume institutions. Sarcoma. 2018; 2018:3056562.
46. Keung EZ, Chiang YJ, Cormier JN, Torres KE, Hunt KK, Feig BW, Roland CL. Treatment at low-volume hospitals is associated with reduced short-term and long-term outcomes for patients with retroperitoneal sarcoma. Cancer. 2018; 124:4495-4503.

Received December 15, 2022; Revised January 27, 2023; Accepted February 5, 2023.

[§]These authors contributed equally to this work.

**Address correspondence to:*
Chunyi Hao, Department of Hepato-Pancreato-Biliary Surgery/Sarcoma Center, Peking University Cancer Hospital & Institute, No. 52, Fucheng Road, Haidian District, Beijing 100142, China.
E-mail: haochunyi@bjmu.edu.cn

Released online in J-STAGE as advance publication February 10, 2023.

Correspondence

DOI: 10.5582/bst.2023.01005

For COVID-19, what are the priorities of normalized prevention and control strategies?

Mingyu Luo[1,§], Fuzhe Gong[2,§], Jimin Sun[1,§], Zhenyu Gong[1,*]

[1] Department of Communicable Disease Control and Prevention, Zhejiang Provincial Center for Disease Control and Prevention, Hangzhou, Zhejiang, China;
[2] Zhejiang University School of Medicine, Hangzhou, Zhejiang, China.

SUMMARY The COVID-19 pandemic has ravaged the world for three years. Most countries have adjusted policies and strategies in response to the burden of COVID-19. The severity of COVID-19 seems to be diminishing as the case fatality rate has declined and the number of vaccinated people has increased markedly. Given the large population worldwide, we need to pay attention to the continuing COVID-19 burden. Globally, the number of cases remains at a certain level, and the number of cases is still increasing in China. We also need to deal with shortages of medical resources, antipyretics, and home nursing facilities. SARS-CoV-2 will coexist with humans for a long time, and predicting viral mutations and pandemic trends will be difficult. The reform of the whole public health system is imperative. A comprehensive surveillance system should be created to determine the proportion of various pathogens and to guard against mixed infections of respiratory infectious diseases. A comprehensive response mechanism, including preventive measures and medical treatments, should be created as soon as possible to monitor the status of the epidemic and to deal with the long-term health burden of SARS-CoV-2.

Keywords COVID-19 (SARS-CoV-2 infection), SARS-CoV-2, health burden, surveillance, global health

Three years have passed since the pandemic due to coronavirus disease 2019 (COVID-19) began to ravage the world (*1*). As of January 5, 2023, over 657 million confirmed cases and over 6.6 million deaths have been reported globally (data from the World Health Organization, WHO) (Figure 1 A,B) (*2*). Severe acute respiratory syndrome coronavirus 2 (SARS-CoV-2) continues to mutate and the global pandemic persists; most countries have adjusted policies and strategies in response to the burden of COVID-19. Current efforts to prevent and control COVID-19 have been normalized worldwide.

China has also adjusted its prevention and control policies in accordance with the status of the COVID-19 epidemic. On November 11, 2022, the Joint Prevention and Control Mechanism of the State Council issued 20 new rules that emphasize simplifying categories of COVID-19 risk areas, halting the identification of secondary contacts, ending mass nucleic acid testing in most areas, and a series of strategies. On December 7, 2022, China issued the "10 new measures" to ease COVID-19 related restrictions and to optimize response strategies. This optimization emphasized that patients with asymptomatic or mild cases can choose to be isolated at home, and negative results of nucleic acid testing are no longer required to enter public places. On December 26, 2022, the National Health Commission announced two significant adjustments. First, pneumonia caused by the novel coronavirus SARS-CoV-2 was renamed SARS-CoV-2 infection (COVID-19). Second, COVID-19 will be managed as a Class B infectious disease as of January 8, 2023 (Figure 2). Quarantine measures will not be imposed on patients infected with the virus, close contacts will not be identified, COVID-risk areas will not be designated, and COVID-19-related quarantines will not be imposed on persons or goods entering the country.

The severity of COVID-19 seems to be diminishing (*3*). The case fatality rate (CFR) has declined, and the number of vaccinated people has increased markedly. In Singapore, the CFR has fallen from 0.363% during the outbreak of the Delta variant (from June 7, 2021 to January 5, 2022) to 0.045% during the outbreak of the Omicron variant (from January 6, 2022 to November 16, 2022) (data from Singapore's Ministry of Health) (*4*). As of December 23, 2022, more than 13 billion doses of the vaccine have been administered and more than 5 billion persons have been fully vaccinated (data from

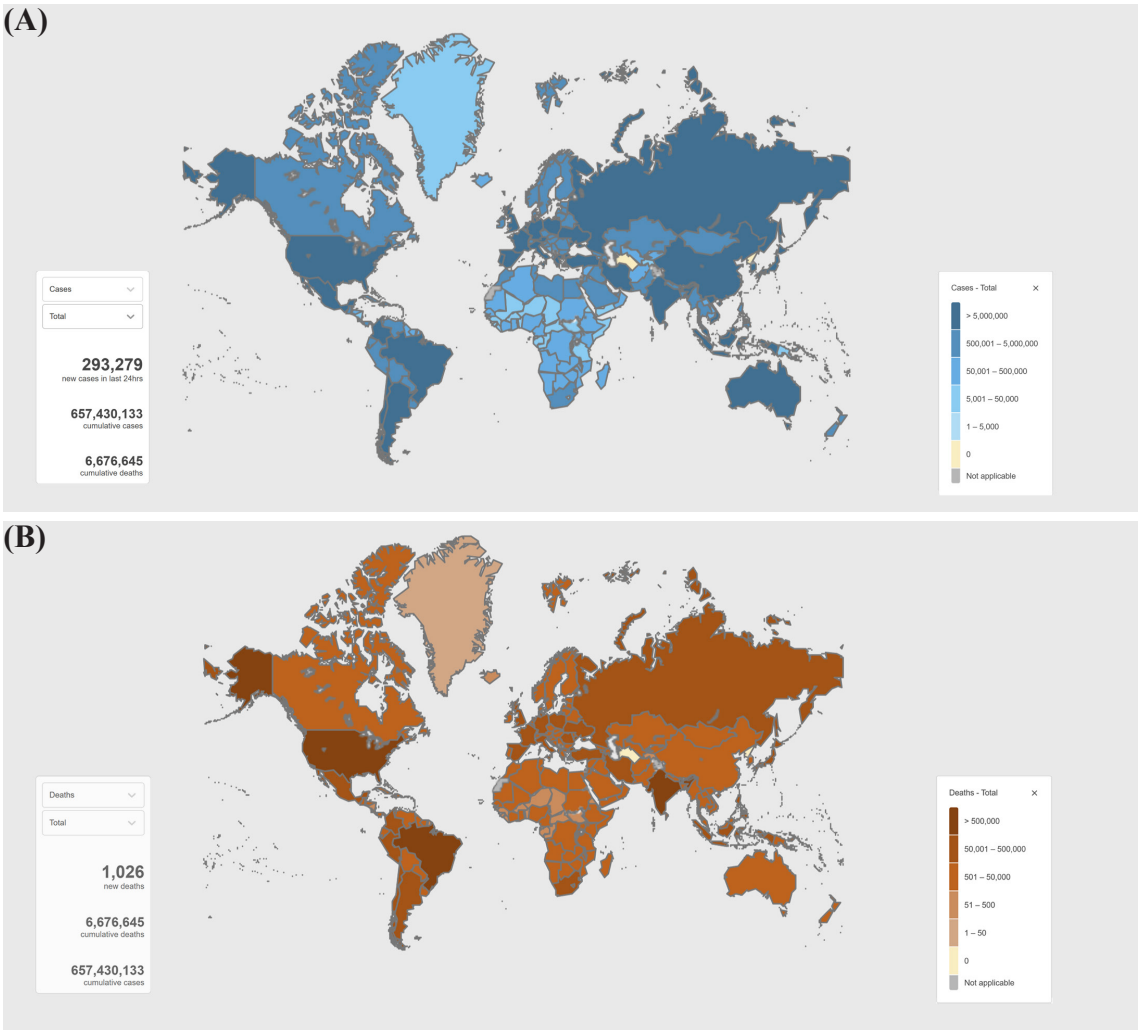

Figure 1. (A) Global confirmed cases of COVID-19 reported to the WHO as January 5, 2023; (B) Global deaths due to COVID-19 reported to the WHO as January 5, 2023. As of 4:33 PM CET on January 5, 2023, there have been 657,430,133 confirmed cases of COVID-19 globally, including 6,676,645 deaths, reported to the WHO.

the WHO) (*5*).

Given the large population worldwide, we need to pay attention to the continuing COVID-19 burden. Over 13.7 million cases and over 40,000 new fatalities were reported globally in four weeks before December 18, 2022, and the number of cases has remained at a certain level (data from the WHO) (*6*). The number of cases is still increasing in China. According to an online survey (the second such survey) in Sichuan Province on December 24, 2022, 100,679 of 158,506 respondents reported testing positive according to a nucleic acid or antigen test (*7*). The rate of infection (63.52%) had risen 16.53% since the first survey (46.93%) on December 19, 2022. As of December 30, 2022, the estimated rate of infection in Hainan Province reached 50% (*8*). As of December 31, 2022, 66,298 confirmed cases were reported on the Chinese mainland, 2,718 (4.10%) of which were severe cases (*9*). The proportion of severe cases remains at low. In big cities like Beijing and Shanghai, the infection has peaked as the number of visits to fever clinics and emergency calls for ambulances have decreased. The proportion of severe cases may peak in the near future. Infection may soon peak in rural areas. Responses should be devised in advance.

Regardless of the trends in the rate of infection or the proportion of severe cases, the sheer number of patients, and especially these with severe cases, will strain medical resources like intensive care units (ICU) or converted ICU beds. A peak in infection will also strain the supply of antipyretics and medical equipment at home nursing facilities (like thermometers and oximeters) all over the world (*10*). Moreover, the strain on medical resources and the shortage of drugs and related home care equipment will pose psychological challenges to the public without proper guidance.

The transmissibility of COVID-19 continues to increase as SARS-CoV-2 mutates. This is another hidden danger. The effective reproduction number (Re) of BA.4 and BA.5 are respectively 1.19 and 1.21 times that of BA.2 (*11*). The global spread of respiratory infectious diseases like COVID-19 has already become the norm, and a global response framework needs to be seriously considered.

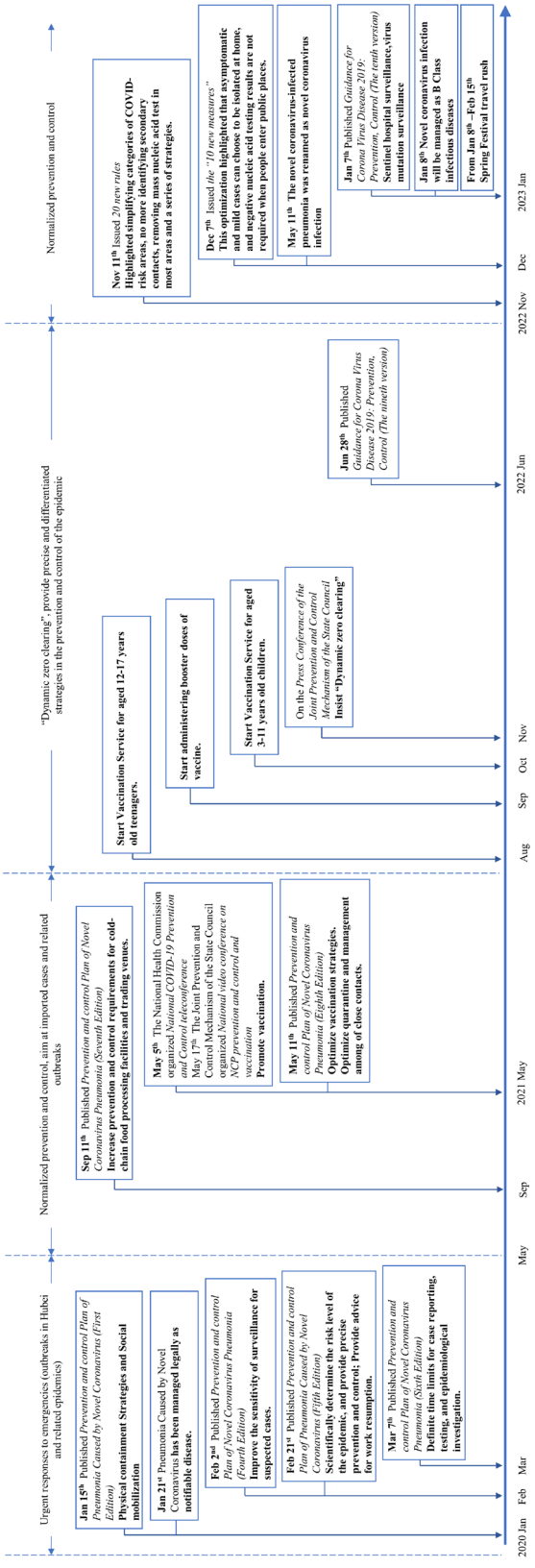

Figure 2. Prevention and control processes and strategies to combat COVID-19 in China since 2020.

To deal with the large number people who are about to be infected, the government should continue to create a hierarchical medical system as soon as possible. Many rural and community health service centers (CHS) require training and guidance to enhance primary care. Medical facilities at all levels need to stock a certain amount of antivirals, and pharmaceutical companies should plan to enhance their production capacity of drugs. The scale of departments of critical care medicine and respiratory medicine at medical facilities should be increased appropriately to accommodate more patients. The government should also pay attention to the tide of public opinion on medical treatment. Timely and transparent explanations from the authorities can provide credible guidance and psychological relief for the public.

Due to the mutation of SARS-CoV-2, existing vaccines barely prevent infection. However, medical professionals all agree that people who have been fully vaccinated have a lower risk of severe illness, hospitalization, and death from COVID-19 than those who are unvaccinated or not fully vaccinated. Vaccination should still be encouraged for the elderly population. Having been fully vaccinated and having received boosters, individuals who are over 80 years old with underlying conditions should receive the fifth heterologous dose as soon as possible. The mRNA vaccine is also recommended for the public to better guard against the pandemic. When the vaccine is less effective at protecting against infection and it only protects against severe illness, attention should also be paid to how to encourage the public's willingness (and especially the elderly) to receive a booster (*12,13*).

Non-pharmaceutical interventions (NPIs) should still be emphasized, and especially in key places with vulnerable population (such as nursing homes for the elderly and schools) and at important times when public travel increases (such as New Year's Day and Spring Festival). As the Spring Festival approaches and people return to their hometowns, gatherings of people in rural areas should be restricted to delay the peak of infection and severe illness. Classic preventive measures, such as wearing a mask, social distancing, and hand hygiene, have always been considered effective at preventing and controlling various infectious diseases, and especially in the early stage of an outbreak or pandemic in the absence of vaccines or other effective medicines (*14,15*).

As prevention and control becomes normalized, a national or even an international surveillance system for COVID-19 should be created. Simply depending on the influenza surveillance system is insufficient because SARS-CoV-2 is more contagious and causes more serious symptoms, so medical and prevention efforts should be integrated. First, sentinel hospital surveillance can be conducted based on the national influenza surveillance system. Nucleic acid or antigen testing can be implemented among outpatient or emergency cases

of influenza-like illness (ILI) and inpatients with severe acute respiratory infection (SARI) at sentinel hospitals. Second, symptoms should be monitored in nursing facilities for the elderly, social welfare institutions, schools, and other key places. In addition, entities and institutions should promptly report clusters of cases, and centers for disease control and prevention (CDC) should promptly conduct field investigations and implement an epidemic response.

On the one hand, etiological surveillance should ascertain the spectrum of respiratory pathogens, including SARS-CoV-2 and the influenza virus, to determine the proportion of various pathogens and to guard against mixed infections of respiratory infectious diseases such as influenza and COVID-19. On the other hand, we should pay attention to the current status of strains around the world. The XBB variant has been detected among people entering China. We need to pay attention as to whether it will become a prevalent strain (*16*).

We should see if preventive interventions by the CDC system have promoted public health at the front line of clinical treatment. The reform of the whole CDC system is imperative. The CDC system should focus on two types of emerging infectious diseases (EIDs) (one is respiratory infectious diseases like COVID-19 and the other is vector-borne and zoonotic diseases like monkeypox), and it should mainly work on monitoring, providing an early warning, and facilitating emergency control of emergent acute infectious diseases. The government should foster personnel and provide material and financial support to the CDC system.

To avoid disasters like COVID-19, China's experience in containing the pandemic warrants further recognition (*1*). It proved that we need to pay adequate attention to infectious diseases in their early stages. Relying solely on conventional public health measures and utilizing new technologies such as nucleic acid testing and mobile communications, we are fully capable of eliminating an infectious disease early and locally and eliminating its risk of becoming a worldwide pandemic despite the absence of vaccines and specific drugs.

Funding: None.

Conflict of Interest: The authors have no conflicts of interest to disclose.

Author Contribution: M.Y.L, F.Z.G, and J.M.S analyzed the results and wrote the manuscript. G.Z.Y conducted the study, revised the manuscript, and approved the manuscript.

References

1. Luo M, Liu Q, Wang J, Gong Z. From SARS to the Omicron variant of COVID-19: China's policy adjustments and changes to prevent and control infectious diseases. Biosci Trends. 2022; 15:418-423.
2. WHO. WHO Coronavirus (COVID-19) Dashboard. Website World Heal. Organ. 2023. *https://covid19.who.int/* (accessed January 5, 2023).
3. Karako K, Song P, Chen Y, Karako T. Trends in managing COVID-19 from an emerging infectious disease to a common respiratory infectious disease: What are the subsequent impacts on and new challenges for healthcare systems? BioSci Trends. 2022; 16: 381-385.
4. Xu Z. Singapore's latest rate of severe disease and case fatality rate released! Morbidity and mortality rates for XBB are 21 to 62% of influenza. Singapore Eye Official WeChat Account. *https://mp.weixin.qq.com/s?search_click_id=15670140554785809472-1672478460447-6401020312&__biz=MzU4NTU0MDgzOA==&mid=2247922727&idx=3&sn=81400ec692ed010bcd82c3df9f966081&chksm=fd80c1aecaf748b8fbe65acc06b41b93385d0bd4a9018e6f604c40e23fd33e779076f2674a1b&sce* (accessed November 17, 2022). (in Chinese)
5. WHO Coronavirus (COVID-19) Dashboard with Vaccination Data. WHO. 2022. *https://covid19.who.int/* (accessed December 23, 2022).
6. WHO. COVID-19 weekly epidemiological update. 2022 *https://www.who.int/publications/m/item/covid-19-weekly-epidemiological-update*. (accessed January 5, 2023).
7. Sichuan Provincial Center for Disease Control and Prevention. Results of a survey on the prevalence of COVID-19 in Sichuan Province (Second survey). *https://www.sccdc.cn/view.aspx?id=31245* (accessed January 3, 2023). (in Chinese)
8. Hainan Epidemic Prevention and Control. Hainan Province: Infection has peaked in Sanya and Haikou, and the rate of infection in the whole province is expected to reach 50%. Official WeChat Account. *https://mp.weixin.qq.com/s/Va_qh6tSpllUlYoQ6jvThQ* (accessed December 30, 2022). (in Chinese)
9. Chinese Center for Disease Control and Prevention. Update on the COVID-19 pandemic as of 24:00 on December 31. *https://www.chinacdc.cn/jkzt/crb/zl/szkb_11803/jszl_11809/202301/t20230101_263164.html* (accessed January 1, 2023). (in Chinese)
10. Beijing News. The shortage of antipyretics is unexpectedly spreading all over the world. Tencent Online. *https://new.qq.com/rain/a/20221219A05QSU00* (accessed December 19, 2022). (in Chinese)
11. Kimura I, Yamasoba D, Tamura T, *et al*. Virological characteristics of the novel SARS-CoV-2 Omicron variants 2 including BA.2.12.1, BA.4 and BA.5. bioRxiv 2022. DOI:10.1101/2022.05.26.493539.
12. Caycho-Rodríguez T, Tomás JM, Carbajal-León C, Vilca LW, Reyes-Bossio M, Intimayta-Escalante C, Vivanco-Vidal A, Saroli-Araníbar D, Esteban RFC, White M. Sociodemographic and psychological predictors of intention to receive a COVID-19 vaccine in elderly Peruvians. Trends Psychol 2022; 30:206-223.
13. Gallant AJ, Nicholls LAB, Rasmussen S, Cogan N, Young D, Williams L. Changes in attitudes to vaccination as a result of the COVID-19 pandemic: A longitudinal study of older adults in the UK. PLoS One. 2021; 16:e0261844.
14. Lai S, Ruktanonchai NW, Zhou L, Prosper O, Luo W, Floyd JR, Wesolowski A, Santillana M, Zhang C, Du X, Yu H, Tatem AJ. Effect of non-pharmaceutical interventions to contain COVID-19 in China. Nature.

2020; 585:410-413.
15. Luo M, Sun J, Gong Z, Wang Z. What is always necessary throughout efforts to prevent and control COVID-19 and other infectious diseases? A physical containment strategy and public mobilization and management. Biosci Trends 2021; 15:188-191.
16. Stein R. RSV recedes and flu peaks as a new COVID variant shoots 'up like a rocket'. NPR Podcasts & Shows. *https://www.npr.org/sections/health-shots/2023/01/06/1147372029/new-covid-omicron-subvariant-spreading-fast-data* (accessed January 7, 2023).

Received January 7, 2023; Revised January 13, 2023; Accepted January 15, 2023.

[§]These authors contributed equally to this work.
**Address correspondence to:*
Zhenyu Gong, Department of Communicable Disease Control and Prevention, Zhejiang Provincial Center for Disease Control and Prevention, Hangzhou 310051, Zhejiang, China. E-mail: zhygong@cdc.zj.cn

Released online in J-STAGE as advance publication January 16, 2023.

Correspondence

DOI: 10.5582/bst.2022.01438

Updated information regarding acute severe hepatitis of unknown origin in children: Viewpoints of and insights from pediatricians

Liping Pan[1,§], Lulu Sun[1,§], Tetsuya Asakawa[2,§,*], Xiaoming Ben[1,*], Hongzhou Lu[3,*]

[1] Department of Pediatrics, Third People's Hospital of Shenzhen, Shenzhen, Guangdong, China;
[2] Institute of Neurology, Third People's Hospital of Shenzhen, Shenzhen, Guangdong, China;
[3] Department of Infectious Diseases, National Clinical Research Center for Infectious Diseases, Third People's Hospital of Shenzhen, Shenzhen, Guangdong, China.

SUMMARY Recently, the morbidity of acute severe hepatitis of unknown origin in children (SHIC) has tended to decrease, but this condition should not be ignored because of its uncertain but severe nature. The current study briefly summarizes updated information regarding the epidemiological, clinical, and etiological aspects of SHIC based on the newest information available. Opinions from pediatricians are also presented. In light of the *status quo* of SHIC and COVID-19 globally, several suggestions are proposed to improve future studies, which could help to further explore the underlying mechanisms of SHIC in the context of COVID-19.

Keywords acute severe hepatitis of unknown origin in children, COVID-19, adenovirus, SARS-CoV-2, immune reaction

Acute severe hepatitis of unknown origin in children (SHIC) was first reported on March 31, 2022 in Scotland (*1*). The World Health Organization (WHO) subsequently reported ten cases of analogous severe hepatitis in children on April 15, 2022, mainly occurring in the United Kingdom (UK) (*2*). Later, a total of 746 cases of SHIC were reported in 36 countries and regions other than the UK (*3*). There were no subsequent reports indicative of a SHIC pandemic, and only 44 new cases were reported in 10 countries according to data as of August 26, 2022 (Figure 1) (*4*). Nonetheless, this condition has garnered considerable attention because of its "uncertain but severe" nature as well as the fact that it "only" affects children. A number of studies have attempted to elucidate the pathophysiology of this hepatitis in terms of its epidemiology (*5*), immunology (*3*), and clinical manifestations (*6*). A viral infection seems to be the leading hypothesis among many researchers (*5,7-9*), but there is limited evidence to identify a definitive pathology. Previous studies by the current authors presented primary information regarding SHIC in June (*10*) and August (*11*) of 2022. The current study offers comments and insights on SHIC from the perspective of pediatricians based on updated information. These opinions might help to explore the etiology and improve the diagnosis and treatment of this hepatitis.

1. A summary of what is known

The status quo of SHIC globally

From April 5, 2022 to September 30, 2022, a total of 555 cases of SHIC were reported in 22 countries (*4*), but only 44 new cases were reported from July 29, 2022 to August 26, 2022 (Figure 1). Hence, SHIC does not represent a global pandemic, and its incidence is decreasing.

Hypotheses regarding its etiology

According to a report from the WHO, 231 (53.1%) of 435 patients tested positive for adenovirus, and whole blood specimens exhibited the highest positivity. Approximately 11% tested positive for SARS-CoV-2 according to a PCR assay, while 62.2% tested positive according to serology (*4*). These findings strongly imply a close association between viral infection and SHIC, a contention that is supported by most researchers (*5,7-9*). Abnormal susceptibility or an aberrant host response due to an infection (particularly a viral one), toxin, drug, or environmental exposure might play a role in the pathophysiology of SHIC. Thus far, conventional hepatitis A-E virus and COVID-19 vaccines have been eliminated from its etiology (*12*). Conversely, several potential pathogens were considered: 1) Adenovirus:

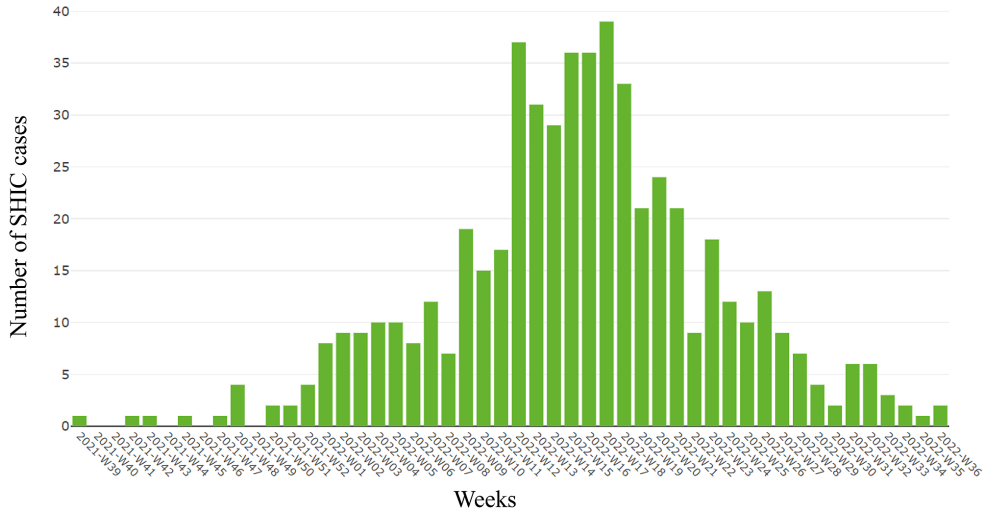

Figure 1. Number of SHIC cases per week (Updated on September 29, 2022). All data (Figure) are publicly available information from the Joint ECDC-WHO Regional Office. *https://www.ecdc.europa.eu/en/hepatitis/joint-hepatitis-unknown-origin-children-surveillance-bulletin*

Early in 2008, Ozbay *et al*. found that an adenovirus infection might cause acute liver failure in healthy children (*13*). Adenovirus, and particularly the 41F strain, is regarded as the most likely pathogen causing SHIC (*2*) since 53.1% cases were reported to test positive according to whole blood specimens (*4*). A report from the UK Health Security Agency speculated that infection with the adenovirus may alter immunity in healthy children, thus leading to SHIC (*14*). Vidal *et al*. found that positivity for adenovirus was closely associated with indicators of disease severity, such as ICU admission and liver transplantation (*5*). Kelly *et al*. also discussed whether a mutation of the adenovirus triggers an abnormal immune response and potentially causes SHIC (*15*). Thus far, however, there is insufficient conclusive or direct evidence regarding the role of adenovirus. Perez-Gracia *et al*. found that approximately half of patients tested positive for adenovirus according to while blood specimens. However, none tested positive according to liver and plasma samples (*7*). These findings lessen adenovirus as a potential etiology of SHIC. 2) SARS-CoV-2: SARS-CoV-2 is the second pathogen that is considered relevant to SHIC. Sacco *et al*. contended that SARS-CoV-2 living in the gastrointestinal tract can act as a superantigen, receiving continuous and repeated activating stimuli from the adenovirus (or co-infection) and eventually causing SHIC (*16*). This hypothesis regards SHIC as part of a multi-system inflammatory syndrome.

Clinical characteristics of reported cases

All of the reported cases of SHIC involve children under 16 years of age; most involved children ages 0-5, a few involved those ages 6-10, and very few involved those ages 11-15 (in the study by Vidal *et al*., the respective proportions were 77.3%, 14.8%, and 8.0%) (*5*). In the report by the WHO, children ages 0-5 accounted for 75.9% of cases (*4*). All of the children presented with manifestations of acute hepatitis, i.e., significantly elevated (over 500 U/L) serum levels of aspartate transaminase (AST) and/or alanine transaminase (ALT) (*6*). The symptoms were nonspecific and included jaundice, vomiting, pale stools, fever, and gastrointestinal symptoms. Hepatomegaly and hepatic encephalopathy were also reported (*17*). Of 344 children, 252 (73.3%) recovered, but 89 (25.8%) required intensive care, and 22 (6.4%) of the latter required liver transplantation (*4*). Vidal *et al*. found that patients of a young age and with an adenovirus infection were more likely to develop severe hepatitis and thus need to be admitted to the ICU or undergo a liver transplantation (*5*).

Diagnosis and treatment

The etiology of SHIC remains unclear, so all the available diagnostic protocols seem to be oriented toward an "exclusionary" or "exploratory" diagnosis (*6*). A diagnosis of exclusion means two steps: 1) Confirmation of hepatitis: usually using indices like ALT and/or AST and 2) Exclusion of hepatitis with known causes, such as an infection with hepatitis virus A, B, C, D, or E; medication/vaccine or toxin-related hepatitis; autoimmune-related hepatitis; and secondary hepatitis related to a disease in some other system. An exploratory diagnosis means a spectrum of laboratory tests/examinations and imaging studies including 1) hepatitis-related indices to confirm hepatitis and assess its severity; 2) virus-related indices to eliminate known viruses and to identify potential pathogens; and 3) imaging studies to confirm hepatitis and its complications (such as hepatic encephalopathy). Samples including whole blood, plasma, nasopharyngeal swabs, stool, and urine should be collected. If possible, a liver biopsy is also suggested.

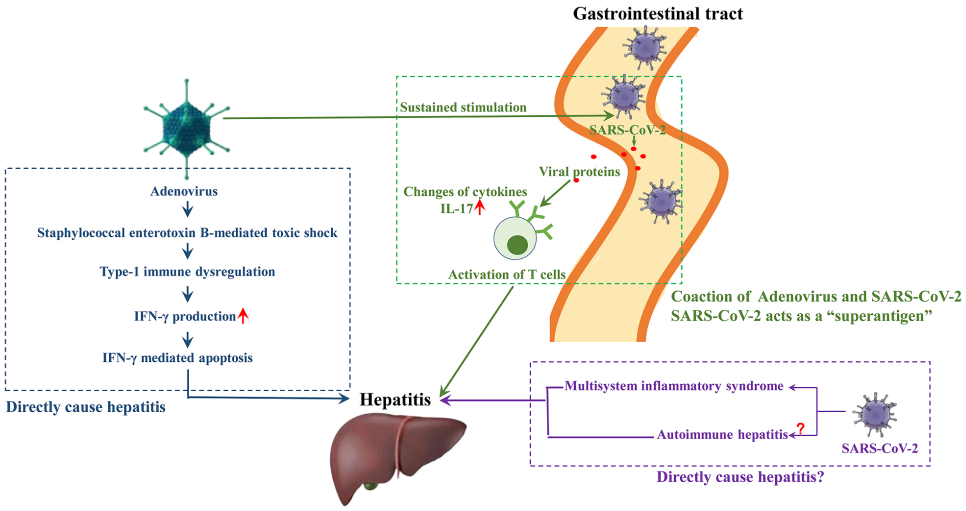

Figure 2 Potential mechanisms of SHIC on the basis of the interactions among adenovirus, SARS-CoV-2, and immune reactions. Three potential pathways of SHIC: Adenovirus-related (blue), SARS-CoV-2-related (purple), and interaction-related (green).

Thus far, there is no specific treatment for SHIC. Reported therapeutic strategies including 1) supportive therapy, 2) symptomatic therapy, and 3) antiviral therapy is only recommended for patients who are positive for a viral infection, such as administration of ribavirin to treat an adenovirus infection (*18*). Strategies also include 4) treatment of complications and 5) liver transplantation as the option of last resort for patients with severe hepatic damage. These strategies are not specific in comparison to those used to treat severe hepatitis with a known etiology.

2. Opinions regarding SHIC

Is SHIC an emerging infectious disease (EID)?

Evidence of a source of infection, a route of transmission, and susceptible hosts is essential to identifying an EID. Thus far, however, there is insufficient evidence regarding the source of infection. The available reports have noted a close association among adenovirus, SARS-CoV-2, and SHIC, but there is no evidence that these viruses cause SHIC. In addition, no novel hepatitis viruses have been found. Hence, the source of infection is unknown. All of the cases seem to be sporadic, though they did resemble an "outbreak" in the middle of 2022. None of the reports have documented evidence of human-to-human transmission. An important finding is the lack of any specific antibody related to this "outbreak." Hence, there are insufficient grounds to classify SHIC as an EID based on currently available information.

Are children susceptible hosts?

In an era of COVID-19, measures to prevent COVID-19 (wearing a mask, social distancing, *etc*.) might limit children's exposure to pathogens (including adenovirus), and particularly childhood viruses. This might cause an abnormal immune response, particularly among children with insufficient acquired immunity. This is considered an "immune gap" (*19*) and might be a potential explanation for why most of the cases involved young children.

Another potential problem is "reporting bias." An "outbreak among children in a short period of time" is an eye-catching description. However, whether acute severe hepatitis of unknown etiology also develops in adults is unknown, and this fact cannot be ignored.

The potential pathophysiological interpretation of SHIC

On the basis of the available information, the potential pathophysiological interpretation of the pathogenesis of SHIC might lie in the interactions/crosstalk among adenovirus, SARS-CoV-2, and the immune system. Common pathogens like adenovirus can cause hepatitis in children (*13*) and adults (*20*) with compromised immunity. Moreover, the role of SARS-CoV-2 cannot be ignored. Several studies have reported that SARS-CoV-2 acts as a "superantigen" in the gastrointestinal tract (*3,16,21*), and this may play a role in the pathogenesis of SHIC. In addition, acquired immunity in children might be insufficient in the context of COVID-19. The complex interactions among the adenovirus, gastrointestinal SARS-CoV-2, and abnormal immune reactions might explain the incidence of SHIC during the COVID-19 pandemic (Figure 2). This hypothesis warrants further investigation. However, some researchers have also pointed out that SHIC developed during the COVID-19 pandemic, hence the presence of COVID-19 in SHIC might be a coincidence (*3*) that may be related to vaccination or the virus itself.

3. Concluding remarks: Challenges and prospects for the future

At this moment, the morbidity of SHIC is tending to decrease, but SHIC should not be ignored. As a disease with an etiology and pathogenesis that remain unclear, no one knows when and where an "outbreak" of SHIC will occur again in the future. The following suggestions have been offered from the viewpoint of pediatricians:

Epidemiology: Creating and enhancing a global surveillance/reporting system for hepatitis of unknown origin is an urgent task. This system should include not only the cases in children but also in adults. This would help to collect detailed information and provide a comprehensive understanding regarding this indeterminate form of hepatitis.

Pathology: A liver biopsy is the gold standard for identification of pathological changes as well as pathogens and immune reactions in local lesions. A liver biopsy should be performed in all patients with this indeterminate form of hepatitis.

Mechanisms: Interactions/crosstalk among adenovirus, SARS-CoV-2, and immune reactions should be further investigated. Additional mainstream technologies like high-throughput sequencing and -omic analyses should be used to help with these investigations.

Prevention: Common preventive measures, such as prevention of fecal-oral transmission, should be enhanced particularly in young children. Likewise, preventive measures by family members, medical personnel, and caregivers should also be emphasized due to the uncertain nature of this disease.

Thus far, there is limited available information with which to obtain a comprehensive understanding of and insights into SHIC. More efforts should be made to investigate this hepatitis of unknown etiology by pediatricians and also by all researchers working in the field of infectious diseases.

Funding: This work is supported by the Shenzhen Science and Technological Foundation (no. JSGG20220301090005007) and the Third People's Hospital of Shenzhen Foundation (nos. G2021027 and G2022062).

Conflict of Interest: The authors have no conflicts of interest to disclose.

References

1. Marsh K, Tayler R, Pollock L, Roy K, Lakha F, Ho A, Henderson D, Divala T, Currie S, Yirrell D, Lockhart M, Rossi MK, Phin N. Investigation into cases of hepatitis of unknown aetiology among young children, Scotland, 1 January 2022 to 12 April 2022. Euro Surveill. 2022; 27:2200318.
2. Verma A, Vimalesvaran S, Lampejo T, Deep A, Dhawan A. Use of cidofovir in recent outbreak of adenovirus-associated acute liver failure in children. Lancet Gastroenterol Hepatol. 2022; 7:700-702.
3. Gao SH, Gong MC, Song HM. Acute severe hepatitis of unknown origin in children: Considerations from the perspective of immunology. World J Pediatr. 2022; 18:529-532.
4. ECDC. Joint ECDC-WHO Regional Office for Europe Hepatitis of Unknown Origin in Children Surveillance Bulletin. *https://cdn.ecdc.europa.eu/novhep-surveillance/* (accessed October 3, 2022).
5. Vidal AR, Vaughan A, Innocenti F, *et al*. Hepatitis of unknown aetiology in children - Epidemiological overview of cases reported in Europe, 1 January to 16 June 2022. Euro Surveill. 2022; 27:2200483.
6. Chen YH, Lou JG, Yang ZH, Chen QJ, Hua CZ, Ye S, Zhang CM, Chen J, Huang ZW, Yu JD, Gao ZG, Shu Q. Diagnosis, treatment, and prevention of severe acute hepatitis of unknown etiology in children. World J Pediatr. 2022; 18:538-544.
7. Perez-Gracia MT, Tarin-Pello A, Suay-Garcia B. Severe acute hepatitis of unknown origin in children: What do we know today? J Clin Transl Hepatol. 2022; 10:711-717.
8. Li J, Hu W, Zhang JY, Wang FS. Pediatric Acute severe hepatitis of unknown origin: What is new? J Clin Transl Hepatol. 2022; 10:509-514.
9. Zhang LY, Huang LS, Yue YH, Fawaz R, Lim JK, Fan JG. Acute hepatitis of unknown origin in children: Early observations from the 2022 outbreak. J Clin Transl Hepatol. 2022; 10:522-530.
10. Zhou X, Lu H. Advances in acute severe hepatitis of unknown etiology in children. Zoonoses. 2022; DOI: 10.15212/ZOONOSES-2022-0023
11. Chen G, Lu H. Attention should be paid to acute hepatitis of unknown etiology in children. Intractable Rare Dis Res. 2022; 11:153-157.
12. Uwishema O, Mahmoud A, Wellington J, Mohammed SM, Yadav T, Derbieh M, Arab S, Kolawole B. A review on acute, severe hepatitis of unknown origin in children: A call for concern. Ann Med Surg (Lond). 2022; 81:104457.
13. Ozbay Hosnut F, Canan O, Ozcay F, Bilezikci B. Adenovirus infection as possible cause of acute liver failure in a healthy child: A case report. Turk J Gastroenterol. 2008; 19:281-283.
14. Agency UHS. Acute hepatitis: Technical briefing. *https://www.gov.uk/government/publications/acute-hepatitis-technical-briefing* (accessed October 3, 2022).
15. Kelly DA, Stamataki Z. Sudden onset hepatitis in children. Nat Rev Gastroenterol Hepatol. 2022; 19:553-554.
16. Sacco K, Castagnoli R, Vakkilainen S, *et al*. Immunopathological signatures in multisystem inflammatory syndrome in children and pediatric COVID-19. Nat Med. 2022; 28:1050-1062.
17. Baker JM, Buchfellner M, Britt W, *et al*. Acute hepatitis and adenovirus infection among children-Alabama, October 2021-February 2022. Am J Transplant. 2022; 22:1919-1921.
18. Park UJ, Hyun SK, Kim HT, Cho WH, Han SY. Successful treatment of disseminated adenovirus infection with ribavirin and intravenous immunoglobulin in an adult renal transplant recipient: A case report. Transplant Proc. 2015; 47:791-793.
19. Samarasekera U. Mystery outbreak of severe acute hepatitis in children. The Lancet Gastroenterol Hepatol. 2022; https://doi.org/10.1016/S2468-1253(22)00159-5
20. Khalifa A, Andreias L, Velpari S. Adenovirus hepatitis in immunocompetent adults. J Investig Med High Impact

Case Rep. 2022; 10:23247096221079192.
21. Brodin P, Arditi M. Severe acute hepatitis in children: Investigate SARS-CoV-2 superantigens. Lancet Gastroenterol Hepatol. 2022; 7:594-595.

Received October 5, 2022; Revised October 17, 2022; Accepted October 19, 2022.

[§]These authors contributed equally to this work.
**Address correspondence to:*
Hongzhou Lu, Department of Infectious Diseases, National Clinical Research Center for Infectious Diseases, the Third People's Hospital of Shenzhen, 29 Buji Bulan Road, Shenzhen, Guangdong Province 518112, China.
E-mail: luhongzhou@fudan.edu.cn

Xiaoming Ben, Department of Pediatrics, The Third People's Hospital of Shenzhen, 29 Buji Bulan Road, Shenzhen, Guangdong Province 518112, China.
E-mail: benxm@163.com

Tetsuya Asakawa, Institute of Neurology, The Third People's Hospital of Shenzhen, 29 Buji Bulan Road, Shenzhen, Guangdong Province 518112, China.
E-mail: asakawat1971@gmail.com

Released online in J-STAGE as advance publication October 21, 2022.

Correspondence

DOI: 10.5582/bst.2022.01476

Detecting latent tuberculosis infection with a breath test using mass spectrometer: A pilot cross-sectional study

Liang Fu[1,§], Yong Feng[2,§], Tantan Ren[1,§], Min Yang[1], Qianting Yang[3], Yi Lin[1], Hui Zeng[4], Jiaohong Zhang[5], Lei Liu[1], Qingyun Li[2], Mengqi He[2], Peize Zhang[1,*], Haibin Chen[2,*], Guofang Deng[1,*]

[1] Division Two of Pulmonary Diseases Department, The Third People's Hospital of Shenzhen, National clinical research center for infectious disease, Southern University of Science and Technology, Shenzhen, Guangdong, China;
[2] Breax Laboratory, PCAB Research Center of Breath and Metabolism, Beijing, China;
[3] Guangdong Key Lab for Diagnosis & Treatment of Emerging Infectious Disease, The Third People's Hospital of Shenzhen, National clinical research center for infectious disease, Southern University of Science and Technology, Shenzhen, Guangdong, China;
[4] Medical Examination Department, The Third People's Hospital of Shenzhen, National clinical research center for infectious disease, Southern University of Science and Technology, Shenzhen, Guangdong, China;
[5] Pulmonary Diseases Out-patient Department, The Third People's Hospital of Shenzhen, National clinical research center for infectious disease, Southern University of Science and Technology, Shenzhen, Guangdong, China.

SUMMARY *Mycobacterium tuberculosis* (M.tb) infects a quarter of the world's population and may progress to active tuberculosis (ATB). There is no gold standard for diagnosing latent tuberculosis infection (LTBI). Some immunodiagnostic tests are recommended to detect LTBI but can not distinguish ATB from LTBI. The breath test is useful for diagnosing ATB compared to healthy subjects but was never studied for LTBI. This proof-of-concept study (Chinese Clinical Trials Registry number: ChiCTR2200058346) was the first to explore a novel, rapid, and simple LTBI detection method *via* breath test on high-pressure photon ionization time-of-flight mass spectrometry (HPPI-TOFMS). The case group of LTBI subjects (n = 185) and the control group (n = 250), which included ATB subgroup (n = 121) and healthy control (HC) subgroup (n = 129), were enrolled. The LTBI detection model indicated that a breath test *via* HPPI-TOFMS could distinguish LTBI from the control with a sensitivity of 80.0% (95% CI: 67.6%, 92.4%) and a specificity of 80.8% (95% CI: 71.8%, 89.9%). Nevertheless, further intensive studies with a larger sample size are required for clinical application.

Keywords latent tuberculosis infection, tuberculosis, diagnosis, volatile organic compounds, breath

It is estimated that *Mycobacterium tuberculosis* (M.tb) infected a quarter of the world's population (*1*). Latent tuberculosis infection (LTBI) constitutes a broad spectrum of infection states that differ by the degree of pathogen replication, host immune response, and inflammation (*2*). Approximately 5-10% of those with LTBI will progress to active tuberculosis (ATB) (*3*). WHO recommends immunodiagnostic tests for LTBI detection, either a tuberculin skin test (TST) or interferon-gamma (IFN-γ) release assays (IGRAs) (*4*). However, these tests are not precise enough. In certain situations, TB exposure can be used as a surrogate for LTBI (*5*). Furthermore, TST and IGRAs can not differentiate LTBI from ATB (*6*). Thus, a more precise tool is urgently needed for the consecutive management of uninfected status, LTBI, and ATB.

Recent studies indicate that breathomics may be a useful rule-in or rule-out tool for diagnosing ATB (*7*), which uncovers the host-pathogen interaction *via* comprehensive exhaled breath analysis. Breathomics may hold promise to distinguish healthy subjects, LTBI and ATB (*8*) if a breath test can find the trace and tell the difference of M.tb in consecutive states in the host (*9*). High-pressure photon ionization time-of-flight mass spectrometry (HPPI-TOFMS) is designed and developed by our team, which can directly detect volatile organic compounds (VOCs) in exhaled breath (*10*). In our previous studies, this breath detection platform has been verified in lung cancer (*11,12*), esophagus cancer (*13*), and Corona Virus Disease 2019 (COVID-19) (*14*). In this study, we explored the use of this novel, rapid, simple, and inexpensive breath test to detect LTBI.

We conducted a cross-sectional study (Chinese Clinical Trials Registry number: ChiCTR2200058346) in which a breath sample was collected from 435 participants with informed consent signed at the Third

People's Hospital of Shenzhen in Shenzhen, China, between March 2020 and November 2022. This study (No.2022017) was approved by the Ethics Committee of the Third People's Hospital of Shenzhen. The study population consisted of three main groups. The LTBI group included the participants who were contacts of ATB patients and had a positive IGRA result, with normal chest imaging and no evidence of ATB (n = 185). The control group consisted of two main subcategories: 1) ATB group (n = 121): ATB subjects in whom M.tb culture or GeneXpert TB-DNA was positive, and chest imaging was suggestive of ATB; 2) healthy control (HC) group (n = 129): healthy subjects who came for physical examination and had no known contacts with ATB patients, with a negative IGRA result and a normal chest imaging. All participants were enrolled in the queue. Because of the selection offset, the enrolled HC is younger than other groups. The age is significantly ($p < 0.001$) different between the case and control groups, whose median ages are 41 and 28, respectively. There is no significant difference ($p = 0.397$) in gender between the case and control groups.

Breath samples were collected using a predefined protocol and tested in our developed HPPI-TOFMS within twenty-four hours (*10*). The sampling apparatus comprised a disposable gas nipple and a sampling bag made of polyether-ether-ketone (PEEK). In this study, we set standard sampling demands and protocols to minimize the influence of the daily diet. Firstly, we conducted sampling at a second visit if he/she was an inpatient and informed the participants to prepare for sampling in advance: no smoking, alcohol, or diets within an hour before sampling. Secondly, participants were required to rinse their mouths with purified water instantly before sampling. Thirdly, all samples must be collected in the same environment, which could minimize the effects of environmental facts. With a deep nasal inhalation, participants completely exhaled the air into the sampling bag with over 1.2 L volume.

All the enrolled participants were randomly split into three groups: 50% of them for model construction, 20% for internal validation, and the remaining 30% for model-blinded testing. Thus, 92 LTBI patients and 123 controls were randomly selected as the discovery data set for Random Forest (RF) (*15*) based LTBI detection model training, which was evaluated on an internal validation dataset (37 LTBI patients and 51 controls) and blinded test dataset (56 LTBI patients and 76 controls).

To transfer the mass spectrum data produced by HPPI-TOFMS, noise-reducing, and baseline correction were applied *via* anti-symmetric wavelet transformation after mass calibration. Then, the area of the strongest peak in the range of (x – 0.1, x + 0.1) was calculated as the feature of VOC with *m/z* close to x. In this way, a mass spectrum would be transferred into 1500 ion features in the *m/z* range of (20, 320). To avoid over-fitting in model training, the features without significant difference ($p > 0.05$) and features with high correlation coefficient but low peak area were excluded. Then, the model-based feature selection was executed based on training and validation datasets, and the top ten VOC ions were selected according to the ranked feature importance.

In this study, the receiver operating characteristic (ROC) curve analysis was implemented. The sensitivity (SEN), specificity (SPE), positive prediction value (PPV), negative prediction value (NPV), accuracy (ACC), area under the ROC curve (AUC), and their relative 95% confidence interval (CI) were calculated to evaluate the performance of LTBI detection model.

As shown in Table 1 and Figures 1a and 1b, with the cut-off value of 0.5 (over 0.5 is considered LTBI), the LTBI detection model achieved good discrimination performance with an SEN and an SPE of 78.4 (95% CI: 63.4%, 94.3%) and 84.3% (95% CI: 74.3%, 94.3%) in the internal validation dataset. In the test dataset, the model performance slightly dropped, with the AUC decreasing from 0.913 (95% CI: 0.854, 0.972) to 0.867 (95% CI: 0.809, 0.925). The SEN and SPE achieved in the test dataset were 80.4% (95% CI: 68.7%, 92.0%) and 80.3% (95% CI: 71.3%, 89.2%). Since there are two subgroups in the controls, we also evaluated the performances in discriminating LTBI with ATB and HC, respectively. The LTBI model performed better in discriminating LTBI and HC with an AUC of 0.952 (95% CI: 0.909, 0.995) than in discriminating LTBI and ATB with an AUC of 0.777 (95% CI: 0.692, 0.861).

To evaluate the selected VOC ions in LTBI detection, we trained the LTBI detection model on each single VOC ion and evaluated it in the test dataset. The ROC curve in Figure 1c demonstrates that the discrimination of a single VOC ion is also good but limited ($0.64 < AUC < 0.80$), which is much inferior to the performance (AUC = 0.867) of the combination of all ten VOCs. It implies that the panel of VOC ions is the basis for breathomics-based LTBI detection. Figure 1d illustrates the patterns of these ten VOC ions that are visually different in ATB, LTBI, and HC groups. Figure 1e illustrated there are significant differences ($p < 0.001$) among LTBI, HC, and ATB groups for almost all ten VOC ions, except for the VOC with *m/z* of 129 between LTBI and ATB ($p = 0.589$). Since the TOF mass spectrometer can only confirm the *m/z* of detected VOCs, we need to infer the possible chemicals of these LTBI related VOC ions based on their *m/z* (121, 145, 129, 135, 105, 130, 117, 93, 77, 109), peak area distribution, other published potential biomarkers, and the human breathomics database (*16*). The VOC ions with *m/z* of 145, 135, 130, and 109 should be 1,4-dimethyl-indol, benzothiazole, 2-ethyl-1-hexanol, and 4-aminophenol, respectively. The VOC ions with *m/z* of 145, 135, 121, 129, 117, and 77 would be the protonated ion of octanoic acid, 1-methyl-4-(1-methyl ethyl)-, 4-ethyltoluene, naphthalene, 2-methyl propyl acetate, and carbon-disulfide, respectively. The VOC

Table 1. Qualitative evaluation of RF-based LTBI detection model in validation and test sets

Data set (*n*)	SEN (%)	SPE (%)	PPV (%)	NPV (%)	ACC (%)	AUC
Validation (88)						
LTBI (37) *vs*. Control (51)	78.4 (63.4, 93.4)	84.3 (74.3, 94.3)	78.4 (67.1, 89.7)	84.3 (72.6, 96.0)	81.8 (73.8, 89.9)	0.913 (0.854, 0.972)
LTBI (37) *vs*.. HC (26)	78.4 (63.4, 93.4)	100 (100, 100)	100 (100, 100)	76.5 (61.0, 91.9)	87.3 (79.1, 95.5)	0.975 (0.937, 1.000)
LTBI (37) *vs*. ATB (25)	78.4 (63.4, 93.4)	68.0 (49.7, 86.3)	78.4 (62.2, 94.5)	68.0 (53.0, 83.0)	74.2 (63.3, 85.1)	0.848 (0.758, 0.937)
Test (132)						
LTBI (56) *vs*. Control (76)	80.4 (68.7, 92.0)	80.3 (71.3, 89.2)	75.0 (65.0, 85.0)	84.7 (75.6, 93.8)	80.3 (73.5, 87.1)	0.867 (0.809, 0.925)
LTBI (56) *vs*. HC (39)	80.4 (68.7, 92.0)	97.4 (92.5, 100)	97.8 (93.7, 100)	77.6 (65.5, 89.6)	87.4 (80.7, 94.0)	0.952 (0.909, 0.995)
LTBI (6) *vs*. ATB (37)	80.4 (68.7, 92.0)	62.2 (46.5, 77.8)	76.3 (62.0, 90.6)	67.6 (55.7, 79.6)	73.1 (64.1, 82.1)	0.777 (0.692, 0.861)

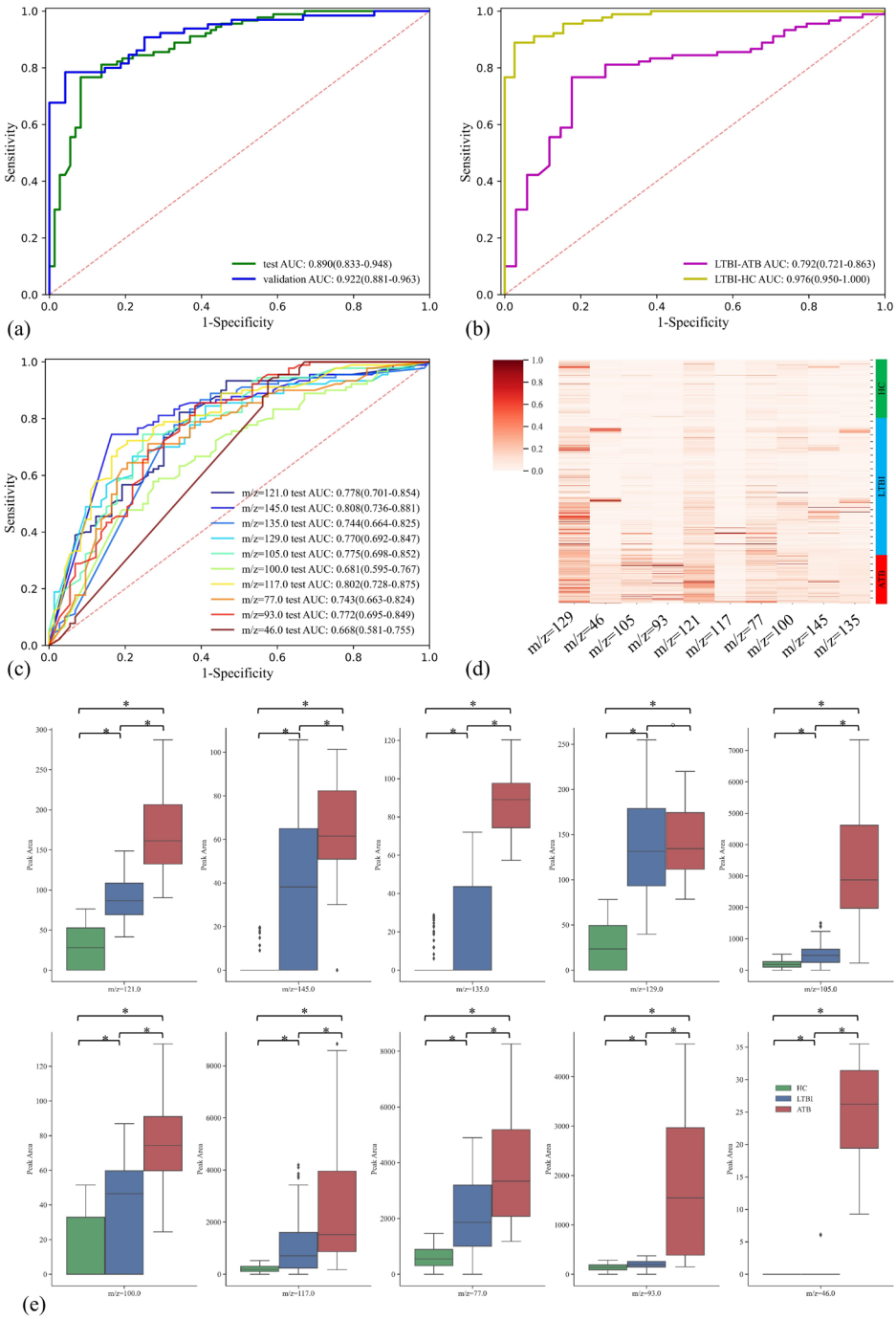

Figure 1. The ROC comparisons and the top ten VOC ions of the developed LTBI detection model. ROC comparison in validation and test datasets **(a)** and test set **(b)**. The LTBI detection power of the top ten selected VOC ions in the test dataset **(c)**. The heatmap of peak area distribution in all HC, LTBI, and ATB samples **(d)**. The box plot of peak area in all HC, LTBI, and ATB samples. * and ° represent significant or insignificant differences between the two groups **(e)**.

ions with *m/z* of 105 should be the combination ion of H_3O^+ and butanal, 3-methyl-. The VOC ion with *m/z* of 93 would be pyridine, 3-methyl- or the protonated ion of toluene. Among these related chemicals, octanoic acid (*m/z* = 144), 2-ethyl-1-hexanol (*m/z* = 130), and toluene (*m/z* = 92) were proven related to pulmonary tuberculosis (PTB) (*17*). 1,4-Dimethyl-indol (*m/z* = 145), naphthalene (*m/z* = 128), and 1-methyl-4-(1-methyl ethyl)- (*m/z* = 134) were reported as the VOC biomarkers of PTB *via* gas chromatography-mass spectrometer (GC-MS) detection in Machel Phillips's study (*18*). Their chemical would be closely related to the metabolites of M.tb or the metabolic changes accused by M.tb. However, these chemicals are not completely confirmed, and their metabolic mechanism is poorly understood.

Our study had several strengths. All breath samples of ATB subjects were taken before anti-tuberculosis treatment so that drugs did not influence our results. For ATB, we used GeneXpert as a complementary diagnostic test to verify a true-negative result in subjects found to be negative with a sputum test (*19*). Healthy subjects were sampled in the same site as LTBI and ATB subjects, which raised no concerns regarding possible geographical bias affecting the results. Since there is no gold standard for LTBI, choosing IGRA as the diagnostic test may miss LTBI people with undetectable IFN-γ response (*6*). Thus, we confirmed the LTBI and HC groups based on the IGRA results and TB exposure. For instance, we excluded close contacts with a negative IGRA from the LTBI group. On the other hand, the stronger standard for LTBI and ATB also limited the applicability and extensibility of the developed LTBI detection model. Other limitations include: 1) these VOC ions were not completed qualitatively identified, although we have extrapolated the possible chemicals based on their formula weight and published biomarkers; 2) there may be selection bias in selecting HC; 3) Participants with other respiratory diseases were not enrolled in this study, which is meaningful for the method evaluation in related application scenarios, but is unfavorable for discovering the potential biomarkers for tuberculosis infection. We expect to optimize our research and conduct more profound studies in LTBI-related VOCs in the future.

In summary, this study provided a potential noninvasive, simple, and fast method for LTBI diagnosis. The preliminary proof-of-concept results indicate that a breath test *via* HPPI-TOFMS may be a valuable tool to distinguish LTBI from HC and ATB, which achieved an accuracy of 80.3% (95% CI: 73.5%, 87.1%) and an AUC of 0.867 (95% CI: 0.809, 0.925). Before the clinical application of breath test-based LTBI diagnosis technologies, more extensive cohort studies are required.

Acknowledgements

We thank all the physicians and assistants that participated in this study and enrolled patients. We thank Jun Cheng for assistance in study design from National Center for Tuberculosis Control and Prevention of the Chinese Center for Disease Control and Prevention.

Funding: This work was supported by the National Natural Science Foundation of China (No. 82070016), the National Key Research and Development Plan (No. 2020YFA0907200, 2019YFC0840602), the Guangdong Foundation for Basic and Applied Basic Research (No. 2019B1515120041), the Guangdong Provincial Clinical Research Center for Tuberculosis Project (No. 2020B1111170014), the Shenzhen Scientific and Technological Foundation (No. KCXFZ202002011007083, JCYJ20180228162112889), Summit Plan for Foshan High-level Hospital Construction (No. FSSYKF-2020001) and Project funded by Shenzhen Third People's Hospital (No. G2022051).

Conflict of Interest: The authors have no conflicts of interest to disclose.

References

1. Houben RM, Dodd PJ. The global burden of latent tuberculosis infection: A re-estimation using mathematical modelling. Plos Med. 2016; 13:e1002152.
2. Esmail H, Barry CE, Young DB, Wilkinson RJ. The ongoing challenge of latent tuberculosis. Philos Trans R Soc Lond B Biol Sci. 2014; 369:20130437.
3. Behr MA, Edelstein PH, Ramakrishnan L. Revisiting the timetable of tuberculosis. BMJ. 2018; 362:k2738.
4. WHO. Latent tuberculosis infection: updated and consolidated guidelines for programmatic management. Geneva: World Health Organization. 2018.
5. Stout JE, Wu Y, Ho CS, Pettit AC, Feng PJ, Katz DJ, Ghosh S, Venkatappa T, Luo R. Evaluating latent tuberculosis infection diagnostics using latent class analysis. Thorax. 2018; 73:1062-1070.
6. Heyckendorf J, Georghiou SB, Frahm N, Heinrich N, Kontsevaya I, Reimann M, Holtzman D, Imperial M, Cirillo DM, Gillespie SH, Ruhwald M. Tuberculosis treatment monitoring and outcome measures: New interest and new strategies. Clin Microbiol Rev. 2022; 35:e22721.
7. Nakhleh MK, Jeries R, Gharra A, Binder A, Broza YY, Pascoe M, Dheda K, Haick H. Detecting active pulmonary tuberculosis with a breath test using nanomaterial-based sensors. Eur Respir J. 2014; 43:1522-1525.
8. Ibrahim W, Carr L, Cordell R, Wilde MJ, Salman D, Monks PS, Thomas P, Brightling CE, Siddiqui S, Greening NJ. Breathomics for the clinician: The use of volatile organic compounds in respiratory diseases. Thorax. 2021; 76:514-521.
9. Bruderer T, Gaisl T, Gaugg MT, Nowak N, Streckenbach B, Müller S, Moeller A, Kohler M, Zenobi R. On-line analysis of exhaled breath. Chem Rev. 2019; 119:10803-10828.
10. Wang Y, Jiang J, Hua L, Hou K, Xie Y, Chen P, Liu W, Li Q, Wang S, Li H. High-pressure photon ionization

source for TOFMS and its application for online breath analysis. Anal Chem. 2016; 88:9047-9055.
11. Meng S, Li Q, Zhou. Z, Fu L. Assessment of an exhaled breath test using high-pressure photon ionization time-of-flight mass spectrometry to detect lung cancer. JAMA Netw Open. 2021; 4:e213486.
12. Wang P, Huang Q, Meng S, Mu T, Liu Z, He M, Li Q, Zhao S, Wang S, Qiu M. Identification of lung cancer breath biomarkers based on perioperative breathomics testing: A prospective observational study. EClinicalMedicine. 2022; 47:101384.
13. Huang Q, Wang S, Li Q, Wang P, Li J, Meng S, Li H, Wu H, Qi Y, Li X, Yang Y, Zhao S, Qiu M. Assessment of breathomics testing using high-pressure photon ionization time-of-flight mass spectrometry to detect esophageal cancer. JAMA Netw Open. 2021; 4:e2127042.
14. Zhang P, Ren T, Chen H, Li Q, He M, Feng Y, Wang L, Huang T, Yuan J, Deng G, Lu H. A feasibility study of Covid-19 detection using breath analysis by high-pressure photon ionization time-of-flight mass spectrometry. J Breath Res. 2022; 16. doi: 10.1088/1752-7163/ac8ea1.
15. Breiman L. Random forests. Mach Learn. 2001; 45:5-32.
16. Kuo TC, Tan CE, Wang SY, Lin OA, Su BH, Hsu MT, Lin J, Cheng YY, Chen CS, Yang YC, Chen KH, Lin SW, Ho CC, Kuo CH, Tseng YJ. Human breathomics database. Database (Oxford). 2020; 2020:baz139.
17. Vishinkin R, Busool R, Mansour E, Fish F, Esmail A, Kumar P, Gharaa A, Cancilla JC, Torrecilla JS, Skenders G, Leja M, Dheda K, Singh S, Haick H. Profiles of volatile biomarkers detect tuberculosis from skin. Adv Sci. 2021; 8:e2100235.
18. Phillips M, Cataneo RN, Condos R, Ring EG, Greenberg J, La Bombardi V, Munawar MI, Tietje O. Volatile biomarkers of pulmonary tuberculosis in the breath. Tuberculosis (Edinb). 2007; 87:44-52.
19. Theron G, Peter J, Meldau R, Khalfey H, Gina P, Matinyena B, Lenders L, Calligaro G, Allwood B, Symons G, Govender U, Setshedi M, Dheda K. Accuracy and impact of Xpert MTB/RIF for the diagnosis of smear-negative or sputum-scarce tuberculosis using bronchoalveolar lavage fluid. Thorax. 2013; 68:1043-1051.

Received November 14, 2022; Revised December 6, 2022; Accepted December 25, 2022.

[§]These authors contributed equally to this work.
*Address correspondence to:
Peize Zhang and Guofang Deng, Division Two of Pulmonary Diseases Department, The Third People's Hospital of Shenzhen, National clinical research center for infectious disease, Southern University of Science and Technology, Shenzhen 518112, Guangdong, China.
E-mail: 82880246@qq.com (PZ); jxxk1035@yeah.net (GD)

Haibin Chen, Breax Laboratory, PCAB Research Center of Breath and Metabolism Beijing, 100074, China.
E-mail: haibinc@hotmail.com (HC)

Released online in J-STAGE as advance publication January 2, 2023.

Comment

DOI: 10.5582/bst.2023.01009

Different clinical guidelines, common goal: To reduce COVID-19 mortality

Liqin Sun[1], Jiaye Liu[2], Fang Zhao[1], Jun Chen[3], Hongzhou Lu[1,*]

[1] National Clinical Research Center for Infectious Diseases, The Third People's Hospital of Shenzhen and the Second Hospital Affiliated with the Southern University of Science and Technology, Shenzhen, Guangdong, China;
[2] School of Public Health, Shenzhen University Health Science Center, Shenzhen, People's Republic of China, Shenzhen, Guangdong, China;
[3] Department of Infectious diseases and Immunology, Shanghai Public Health Clinical Center, Fudan University, Shanghai, China.

SUMMARY The tendency of the Omicron variant to rapidly became the dominant SARS-CoV-2 strain and its weaker virulence than other strains worldwide has prompted many countries to adjust their public health strategies. This work summarizes all appropriate clinical interventions to reduce the public health burden caused by COVID-19 according to guidelines from the World Health Organization and 10 countries, *i.e.*, the United States of America (USA), India, France, Germany, Brazil, South Korea, Japan, Italy, the United Kingdom (UK), and China. Five stages of COVID-19 were identified: asymptomatic infection and mild, moderate, severe, and critical illness. Most guidelines recommend antivirals starting with mild cases for those from Germany and India. Since more drugs are being developed and are becoming available to COVID-19 patients, guidelines are increasingly being updated with new pharmacological intervention strategies. Thus, a global view needs to be adopted to provide helpful options and precise treatment strategies during the lasting fight against the COVID-19 pandemic.

Keywords Covid-19, SARS-COV-2, guidelines, emerging infectious disease, public health

The coronavirus disease 2019 (Covid-19) pandemic was a global public health emergency and it remains a public health and economic burden. Over the past three years, many countries have adopted various strategies to respond to the global pandemic. Most countries have shifted their public health strategies from a strict infection prevention and control strategy (IPC) to a loose IPC strategy. From the perspective of clinical management, physicians treated the viral infection as a common respiratory infectious disease thanks to widespread vaccination, the Omicron strain being less virulent, and the accumulation of more clinical experience with treatment. The case fatality rate (CFR) has dropped to less than 0.1% since June 2022 among the countries with the highest number of new confirmed cases over the past year (*e.g.*, the United States of America (US), India, France, Germany, Brazil, South Korea, Japan, Italy and the United Kingdom (UK)). (*1*). The vaccine's efficiency and effectiveness, especially in terms of preventing severe disease, was widely confirmed. As of December 2022, the vaccination rates (two or more doses of vaccine per 100 people) for the aforementioned countries had reached 67.09-86.27% (*1*). All of these countries formulated COVID-19 treatment guidelines and updated them according to the latest evidence (*2-9*). Summarized here are differences in these updated treatment guidelines from the World Health Organization (WHO) and 6 countries, including the USA, India, Germany, Japan, the UK, and China, in detail. However, treatment guidelines from France, Brazil, South Korea, and Italy were not included because their latest version was updated before the outbreak of omicron.

Patients with COVID-19 can experience a range of clinical manifestations, from no symptoms to critical illness. COVID-19 staging provides valuable frameworks and benchmarks for clinical decision-making in patient management, improved prognostication, and evidence-based treatment selection. Most countries have classified clinical stages of COVID-19 with clear criteria for each stage (Table 1, Table S1, *http://www.biosciencetrends.com/action/getSupplementalData.php?ID=132*). Guidelines from these countries (*e.g.*, the USA (*5*)) have detailed clinical staging for COVID-19 that includes asymptomatic infection and mild, moderate, severe, and critical illness. In specific terms, the staging criteria are mostly based on whether the patients have symptoms, or evidence of hypoxemia (shortness of breath, high respiratory rate, or low SpO2), or whether they need

Table 1. Classification for COVID-19 from several countries and organizations

Country	Clinical characters	
	Type	Criterion
Japan	Mild	• SpQ2 ≥ 96%, no respiratory symptoms
	Moderate 1	• 93% < SpQ2 < 96%, shortness of breath, symptoms of pneumonia
	Moderate 2	• SpQ2 ≤ 93%, need for oxygen
	Severe	• Need for mechanical ventilation
India	Mild	• No shortness of breath or hypoxia
	Moderate	• Any of the following: 1. Respiratory rate ≥ 24/min, breathlessness; 2.SpO2: 90% to ≤ 93% on room air
	Severe	• Any of the following: 1.Respiratory rate > 30/min, breathlessness; 2.SpO2 < 90% on room air
WHO	Non-severe	• Absence of signs or severe or critical disease
	Severe	• SpO2 < 90% on room air, signs of pneumonia, signs of severe respiratory distress
	Critical	• Requires life-sustaining treatment, acute respiratory distress syndrome, sepsis, septic shock
USA	Asymptomatic or presymptomatic infection	• No symptoms that are consistent with COVID-19
	Mild illness	• Symptomatic but do not have shortness of breath, dyspnea, or abnormal chest imaging
	Moderate illness	• Having evidence of lower respiratory disease and SpO2 ≥ 94% on room air at sea level
	Severe illness	• Individuals who have SpO2 < 94% on room air at sea level, PaO2/FiO2 < 300 mm Hg, a respiratory rate > 30 breaths/min, or lung infiltrates > 50%
	Critical illness	• Respiratory failure, septic shock, and/or multiple organ dysfunction
UK	Non-severe	• Absence of signs or severe or critical disease
	Severe	• SpO2 < 90% on room air, signs of pneumonia, signs of severe respiratory distress
	Critical	• Defined by the criteria for acute respiratory distress syndrome (ARDS), sepsis, septic shock, or other conditions that would normally require the provision of life-sustaining therapies such as mechanical ventilation (invasive or non-invasive) or vasopressor therapy
Germany	Mild	• COVID-19-positive patients who did not require oxygen during hospitalization (WHO stages 1-3)
	Severe/Critical	• SpO2 < 90%, respiratory rate > 30/min, ARDS, sepsis, ventilation, vasopressor administration
	Early stage	• < 72 hours after the first positive PCR result and/or < 7 days after the onset of symptoms
China	Mild illness	• Symptomatic but without shortness of breath, dyspnea, or abnormal chest imaging
	Moderate illness	• Persistent high fever > 3 days or/and cough, shortness of breath, but respiratory rate (RR) < 30 times/min and at rest, oxygen saturation obtained from the finger was > 93% on room air at sea level, and imaging showed characteristic manifestations of novel coronavirus pneumonia
	Severe illness	• Individuals who have SpO2 ≤ 93% on room air at sea level, PaO2/FiO2 ≤ 300 mmHg, a respiratory rate ≥ 30 breaths/min, the clinical symptoms worsened progressively, and lung imaging showed that the lesion progressed significantly > 50% within 24-48 hours
	Critical illness	• Respiratory failure requiring mechanical ventilation, septic shock, and/or multiple organ dysfunction requires ICU care

organ support. The stage of COVID-19 also determines whether the patients should be isolated at home, hospitalized, or even admitted to the ICU.

The first stage of COVID-19 is the rapid period of viral replication, in which tissue and organ damage and abnormal immune activation are not obvious and do not need to be dealt with first. Early use of antivirals to inhibit viral replication as soon as possible should significantly reduce the damage to cells and tissues caused by viral replication, which is a key point of treatment. Small molecule drugs and monoclonal neutralizing antibodies are two types of drugs with antiviral action. Antiviral therapy is recommended for patients with COVID-19 according to the guidelines in most countries, but the recommended drugs and clinical stages vary by countries. Notably, only guidelines from the WHO (*8*), Japan (*4*), the UK (*3*), and the USA (*5*) recommended nirmatrelvir/ritonavir, remdesivir, and molnupiravir for mild cases. Several neutralizing monoclonal antibodies were recommended in the early guidelines from the USA (*5*) and Japan (*4*). However, the effectiveness of these antibodies decreased as new variants emerged, so these monoclonal antibodies were not recommended by most guidelines. Similarly, convalescent plasma is no longer mentioned or recommended in these guidelines.

For patients with hypoxemia, all of the guidelines recommend oxygen therapy, which also includes HFNC, noninvasive ventilation, machine ventilation, and ECMO. Prone position ventilation, including awake prone position ventilation, is now incorporated in several guidelines. Anticoagulants are also highly recommended by several guidelines as mounting evidence has indicated that they reduce the need for organ support and the progression to intubation and death.

During the later stage of COVID-19, the secondary immune damage becomes a major factor even though viral replication is almost undetectable. Therefore, immunomodulators, including glucocorticoids, IL-6R inhibitors, and JAK inhibitors, are supposed to prevent an excessive inflammatory response. All of these drugs are recommended to treat severe or critical ill patients while glucocorticoids and baricitinib can also be used to treat moderate COVID-19.

In summary, the guidelines in various countries have small differences in their classification of COVID-19 severity. However, the treatment principles of COVID-19 are basically the same, while the medicines vary according to the availability of drugs in each country. As more drugs become available and research results are published, the latest guidelines may include more drugs as options or they may feature more precise treatment than previous versions.

Although the CFR is declining, the impact of COVID-19 on the healthcare system cannot be ignored. With the emergence of new sub-lineages of omicron, clinicians need to pay more attention to potential disease manifestations and whether there are new high-risk groups. An important aspect of treatment is closely monitoring the antiviral action of existing and upcoming antivirals and neutralizing antibodies against new sub-lineages. Patients who may benefit from immunomodulators need to be identified and the duration of treatment needs to be determined more accurately. At the same time, clinicians need more information and guidance on managing the long-term effects of COVID-19.

Funding: This work was supported by the National Natural Science Foundation of China (no. 92169119) and the Shenzhen Municipal Science and Technology Innovation Committee (no. JCYJ20220531102202005).

Conflict of Interest: The authors have no conflicts of interest to disclose.

References

1. WHO Coronavirus (COVID-19) *Dashboard. https://covid19.who.int/* (Accessed January 13, 2023).
2. AIIMS/ ICMR-COVID-19 National Task Force/Joint Monitoring Group (Dte.GHS). Ministry of Health & Family Welfare, Government of India. Clinical Guidance for Management of Adult COVID-19 Patients. *https://cdnbbsr.s3waas.gov.in/s3850af92f8d9903e7a4e0559a98ecc857/uploads/2022/01/2022011845.pdf* (Accessed January 13, 2023).
3. National Institute for Health and Care Excellence. COVID-19 rapid guideline: Managing COVID-19. *https://www.nice.org.uk/guidance/NG191* (Accessed January 13, 2023).
4. Health Care Tokushima. Covid-19 treatment guide, ver. 8.1. *https://anshin.pref.tokushima.jp/med/experts/docs/2022101300122/* (Accessed January 13, 2023). (in Japanese)
5. National Institutes of Health. Coronavirus Disease 2019 (COVID-19) Treatment Guidelines. *https://www.covid19treatmentguidelines.nih.gov/* (Accessed January 13, 2023).
6. Kim SB, Ryoo S, Huh K, *et al*. Revised Korean Society of Infectious Diseases/National Evidence-based Healthcarea Collaborating Agency Guidelines on the Treatment of Patients with COVID-19. Infect Chemother. 2021; 53:166-219.
7. Malin JJ, Spinner CD, Janssens U, *et al*. Key summary of German national treatment guidance for hospitalized COVID-19 patients: Key pharmacologic recommendations from a national German living guideline using an Evidence to Decision Framework (last updated 17.05.2021). Infection. 2022; :93-106.
8. World Health Organization. Therapeutics and COVID-19: Living guideline. *https://www.who.int/publications/i/item/WHO-2019-nCoV-therapeutics-2022.5* (Accessed January 13, 2023).
9. National Health Commission of the People's Republic of China. Guidelines for the diagnosis and treatment of Coronavirus Disease 2019 from the National Health Commission (10th Draft Version). *http://www.nhc.gov.cn/xcs/zhengcwj/202301/32de5b2ff9bf4eaa88e75bdf7223a65a.shtml* (Accessed January 15, 2023). (in Chinese)

Received January 6, 2023; Revised January 17, 2023; Accepted January 20, 2023.

*Address correspondence to:
Hongzhou Lu, Department of Infectious Diseases, National Clinical Research Center for Infectious Diseases, Shenzhen Third People's Hospital, Shenzhen 518112, Guangdong, China.
E-mail: luhongzhou@fudan.edu.cn

Released online in J-STAGE as advance publication January 22, 2023.

Letter to the Editor

DOI: 10.5582/bst.2022.01530

Pre-enriched saline gargle samples for detection of SARS-CoV-2

Peng Xu[1,2], Jing Chen[2], Chengchen Qian[2], Wenqiang Yu[1,*]

[1] Laboratory of RNA Epigenetics, Institutes of Biomedical Sciences & Shanghai Public Health Clinical Center, Shanghai Medical College, Fudan University, Shanghai, China;
[2] Research and Development Department, Shanghai Epiprobe Biotechnology Co., Ltd, Shanghai, China;

SUMMARY A self-collected gargle sample, which avoids discomfort and largely reduces the dependency on medical resources, is emerging for detection of SARS-CoV-2. However, the incomplete usage of starting materials for both routine oropharyngeal swabs (OPS)/nasopharyngeal swabs (NPS) and saline gargle (SG) samples implies sensitivity can be further improved. Presented here is a bead-based strategy for pre-enrichment of SG samples, and results revealed that it acquired about 20 times the starting materials obtained from OPS samples for downstream detection of SARS-CoV-2. The sensitivity and specificity of this pre-enrichment strategy were validated in 100 paired pre-enriched saline gargle (PenSG) and OPS samples and 89 PenSG samples from healthy volunteers. In addition to detection of SARS-CoV-2, this pre-enrichment strategy may also be implemented in more clinical settings to optimize detection of other diseases.

Keywords detection of SARS-CoV-2, saline gargle, pre-enrichment strategy, COVID-19

To the Editor,

Over the past three years, severe acute respiratory syndrome coronavirus 2 (SARS-CoV-2), the cause of coronavirus disease 2019 (COVID-19), has infected more than 650 million, around 1/12 of the planet's population, and its variants are still evolving. Although the emerging variants, such as Omicron, have been found to cause less severe disease, they are much more infectious than the previous variants (*1*) and they continue to cause uncertainty worldwide. The shifting of public health policies in countries such as China and the newly acquired characteristics of SARS-CoV-2 variants require more timely, sensitive, and less clinically intensive testing strategies. Self-sampling and self-testing are two promising solutions. Antibody-based self-testing is easy to use, but it has relatively low sensitivity, especially for the dominant asymptomatic individual (*2*). Theoretically, sensitivity could be enhanced with SARS-CoV-2 nucleic acid self-testing, but large-scale population-based studies are needed to indicate its robustness. Moreover, such tests are not readily available in many countries and are relatively more expensive than other tests. Self-sampling coupled with a quantitative reverse transcription PCR (RT-qPCR) test represents a feasible and easily implemented approach at the current point in time.

A suitable method of self-sampling should comply with the following five criteria: 1) easily accessible/acquired by the public; 2) low dependency on medical resources; 3) user-friendly for most populations; 4) easy to standardize, thus ensuring the consistency of test results; and 5) compatible with downstream testing (Table 1). Saliva and gargle samples are emerging for detection of SARS-CoV-2 (*3*-*5*). Compared to conventional oropharyngeal swabs (OPS) and nasopharyngeal swabs (NPS), both saliva and gargle samples, which can be self-collected, avoid discomfort and largely reduce the dependency on medical resources. However, Landry *et al*. reported that pure saliva had a relatively low sensitivity (85.7%) in detecting SARS-CoV-2 (*5*), suggesting its unsuitability for high-volume testing and the need to optimize saliva collection and processing. Moreover, a study involving 108 patients with COVID-19 found that 46.3% experienced dry mouth (*6*), which in turn affects saliva production. Ease of standardization and sample accessibility are marked advantages of gargling samples over saliva. Recently, Qiao *et al* indicated that the saline gargle (SG) sample is also capable of detecting the currently dominant Omicron variants in both asymptomatic and symptomatic groups (*4*).

Currently, OPS and NPS are stored in 2-6 mL of virus preservation solution, and only 200 μL of sample is used for RNA extraction. In the aforementioned study, Qiao *et al*. also used 200 μL of saline gargle as the starting material for RNA purification and downstream detection of SARS-CoV-2 (*4*). All of these methods discard most of the materials. The incomplete usage of a

Table 1. The five basic principles of sampling to detect SARS-CoV-2

Strategy	Self-sampling		Non-self-sampling	
Type of sample	Gargle	Saliva	Oropharyngeal swab	Nasopharyngeal swab
Accessibility	Very easy	Limited in some situations, such as a dry mouth (*6*)	Difficult for individuals who are sensitive to sampling	
Dependency	No	Low	High	High
User-friendly	Yes	Yes	Causes slight discomfort	Cause moderate discomfort
Standardized	Easy	Hard	Depends on the skills and experience of medical personnel	
Compatibility	Yes	Yes	Yes	Yes

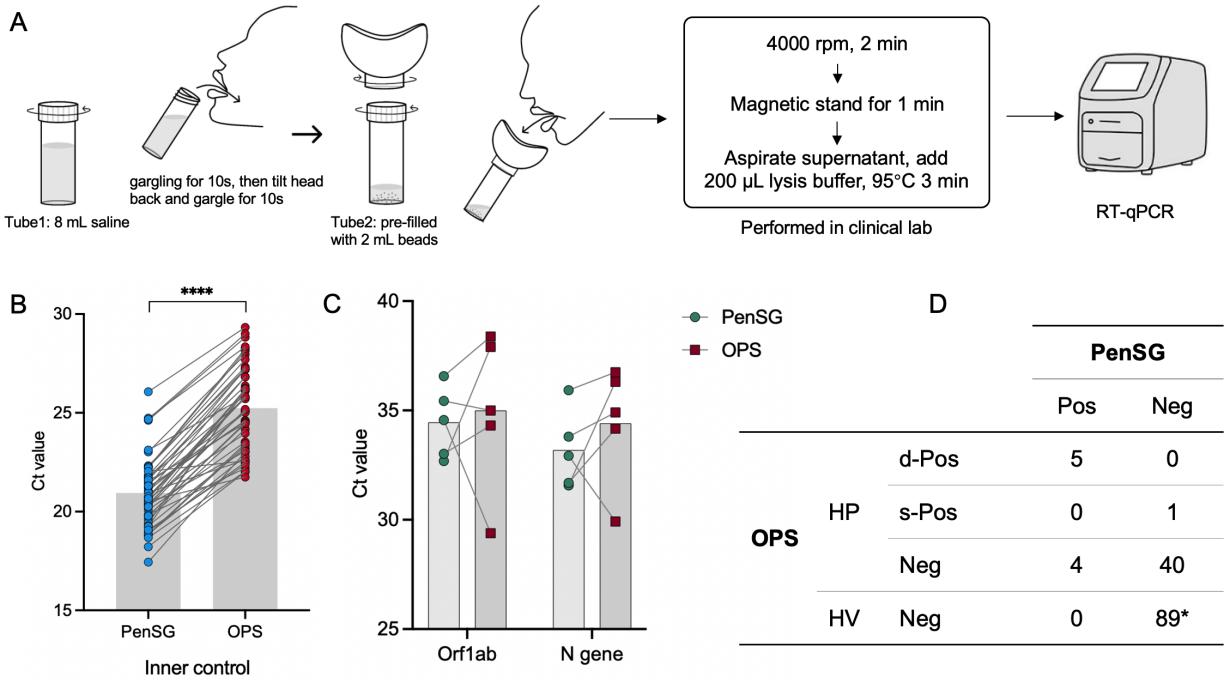

Figure 1. Using a pre-enriched saline gargle (PenSG) to detect SARS-CoV-2. (A) The steps in PenSG-based detection of SARS-CoV-2. **(B)** Ct values for the internal control in paired PenSG and OPS samples; **(C)** Ct values for the Orf1ab and N genes in paired PenSG and OPS samples in the group positive for both genes; **(D)** The overall performance of PenSG and OPS. 89* means the healthy volunteers tested negative but not at the same time with PenSG. HP, hospitalized patients; HV, healthy volunteers; d-pos, double-gene-positive; s-pos, single-gene-positive. In **(B)**, a paired *t*-test was conducted with GraphPad Prism 9; ****, *p*-value < 0.0001.

sample implies that the sensitivity of current methods can be further improved. To fully utilize all of a sample and to improve the sensitivity to the utmost extent, we pre-enriched SG samples with specialized beads that were conjugated to Concanavalin A (ConA) and able to bind to cells. Then, we use a magnetic stand to concentrate the beads and aspirate the supernatant of the saline gargle. Finally, a lysis buffer was directly added to the bead-bound system and the mixture was then subjected to routine RT-qPCR (Figure 1A).

To test the performance of this bead-based pre-enriched saline gargle (PenSG) in clinical settings, 100 paired PenSG and OPS samples were collected from 50 hospitalized patients with COVID-19 who were infected with the currently predominant SARS-CoV-2 Omicron variant (in different courses) in the Third People's Hospital of Shenzhen (June to July 2022). An additional 89 PenSG samples were collected from 89 healthy volunteers. This study strictly conforms to the provisions of the Declaration of Helsinki of the World Medical Association (2000) and was approved by the ethics committee of the Third People's Hospital of Shenzhen (no.2022-116-03). Detailed procedures and the clinical design can be found in the Supplementary Materials. All paired testing results are available in Table S1 (*http://www.biosciencetrends.com/action/getSupplementalData.php?ID=131*).

First, the internal control (IC) for each paired sample was compared. It revealed that the cycle threshold (Ct) values for each PenSG were significantly lower than those for the OPS, with a mean differential Ct of 4.3 (20.95 *vs.* 25.24, Figure 1B), suggesting that PenSG could acquire about 20 (2^4.3) times the starting materials for downstream testing. Importantly, PenSG-based testing was able to detect all 5 patients who tested positive for both genes by the current routine strategy (OPS coupled with RT-qPCR). Most PenSG samples (3/5) had lower Ct values than OPS (Figure 1C), further

corroborating PenSG's superior sensitivity over OPS. Interestingly, PenSG detected 40 negatives among 44 cases detected negative for both genes by using OPS; the other 2 samples tested positive for a single gene and 2 samples tested positive for both genes. Since these samples came from hospitalized patients with COVID-19, special attention should be paid to these "false positives" and PenSG may help to improve the sensitivity of OPS to avoid potential "false negatives", thus establishing more strict decontamination criteria. Eighty-nine PenSG samples from healthy volunteers were used to further examine the specificity of PenSG, and all of the them were tested negative, further corroborating the specificity of PenSG. Taken together, these results validated the ability of PenSG to detect SARS-CoV-2 (Figure 1D).

SARS-CoV-2 enters the human body through the upper respiratory tract (URT); its viral load is associated with the risk of transmission, duration of infectiousness, disease severity, and mortality (*7*). PenSG, which is virus characteristic-based sampling, has all of the advantages of saline gargling but it also greatly enhances sensitivity by utilizing the whole sample, making it a robust alternative for detection of SARS-CoV-2. A limitation of the current study is mainly the relatively small sample size, precluding accurate assessment of the sensitivity and specificity of PenSG. However, this novel strategy revealed a long-neglected aspect of detecting SARS-CoV-2.

The biggest difference between the PenSG strategy and that used in the study by Qiao *et al*. is that PenSG utilized all 8 mL of the collected saline gargle to yield 200 uL of a nucleic acid solution without RNA purification, while the method used by Qiao *et al*. only used 200 uL from 8 mL of the collected saline gargle for RNA purification to yield 50 uL of nucleic acid eluate (according to the product manual) (*4*). The study by Qiao *et al*. revealed the advantage of SG over OPS as evinced by lower Ct values in the asymptomatic subgroup. However, PenSG can acquire about 20 times the materials as an OPS sample from all patients (regardless of symptoms and courses), suggesting that the unique PenSG strategy itself could further enhance sensitivity in addition to its advantage in terms of the type of sample. What makes PenSG stands out over previous approaches using a saline gargle and conventional OPS are that 1) PenSG can obtain more materials for downstream detection, thus further enhancing sensitivity; and 2) it avoids the RNA purification step, making this strategy especially suitable for in vitro diagnostics (IVDs).

A point worth noting is that the successful implementation of PenSG is based on these essential details: 1) the saline gargle can be standardized; 2) the efficiency of customized beads; 3) the lysis buffer, which is directly added to the beads without additional nucleic acid extraction steps, must be compatible with routine RT-qPCR kits. Fortunately, both the beads and lysis buffer are commercially available. In the near future, we are expanding the usage of PenSG to the detection of other viruses that infect the URT, such as the influenza virus and adenoviruses (*8*), and we will deploy this strategy of pre-enrichment in more settings, particularly for the detection of various diseases based on bodily fluids such as blood, urine, and even bronchoalveolar lavage fluid and vaginal secretions, in order to benefit a wider population.

Acknowledgements

The authors wish to thank the members of the Clinical Laboratory at the Third People's Hospital of Shenzhen for their assistance in sample collection. The authors also wish to thank Yuxin Wang and Chengyang Wang of Shanghai Epiprobe Biotech for their assistance with the experiments.

Funding: This work was supported by the Fudan University Medical Engineering Project (no. IDH2310063).

Conflict of Interest: Peng Xu and Wenqiang Yu are listed as inventors on pending patents related to this work; Jing Chen and Chengchen Qian are employees of Shanghai Epiprobe Biotech. Peng Xu used to be an employee of Shanghai Epiprobe Biotech. Wenqiang Yu serves on the Scientific Advisory Board of Shanghai Epiprobe Biotech.

Author Contribution Statements: Wenqiang Yu and Peng Xu conceived the project. Peng Xu developed the method under the supervision of Wenqiang Yu. Jing Chen and Chengchen Qian performed some of the experiments. Peng Xu drafted the manuscript. All authors read and approved the final version of the manuscript.

References

1. Shrestha LB, Foster C, Rawlinson W, Tedla N, Bull RA. Evolution of the SARS-CoV-2 omicron variants BA.1 to BA.5: Implications for immune escape and transmission. Rev Med Virol. 2022; 32:e2381.
2. Mungomklang A, Trichaisri N, Jirachewee J, Sukprasert J, Tulalamba W, Viprakasit V. Limited sensitivity of a rapid SARS-CoV-2 antigen detection assay for surveillance of asymptomatic individuals in Thailand. Am J Trop Med Hyg. 2021; 105:1505-1509.
3. Saito M, Adachi E, Yamayoshi S, Koga M, Iwatsuki-Horimoto K, Kawaoka Y, Yotsuyanagi H. Gargle Lavage as a Safe and Sensitive Alternative to Swab Samples to Diagnose COVID-19: A Case Report in Japan. Clin Infect Dis. 2020; 71:893-894.
4. Qiao K, Tao X, Liu H, Zheng M, Asakawa T, Lu H. Verification of the efficiency of saline gargle sampling for detection of the Omicron variant of SARS-CoV-2, a pilot study. Biosci Trends. 2022; 16:451-454.

5. Landry ML, Criscuolo J, Peaper DR. Challenges in use of saliva for detection of SARS CoV-2 RNA in symptomatic outpatients. J Clin Virol. 2020; 130:104567.
6. Chen L, Zhao J, Peng J, Li X, Deng X, Geng Z, Shen Z, Guo F, Zhang Q, Jin Y, Wang L, Wang S. Detection of SARS-CoV-2 in saliva and characterization of oral symptoms in COVID-19 patients. Cell Prolif. 2020; 53:e12923.
7. Chen PZ, Bobrovitz N, Premji ZA, Koopmans M, Fisman DN, Gu FX. SARS-CoV-2 shedding dynamics across the respiratory tract, sex, and disease severity for adult and pediatric COVID-19. Elife. 2021; 10:e70458.
8. Subbarao K, Mahanty S. Respiratory virus infections: Understanding COVID-19. Immunity. 2020; 52:905-909.

Received December 23, 2022; Revised January 4, 2023; Accepted January 15, 2023.

*Address correspondence to:
Wenqiang Yu, Laboratory of RNA Epigenetics, Institutes of Biomedical Sciences, Shanghai Medical College, Fudan University, Shanghai 200032, China.
E-mail: wenqiangyu@fudan.edu.cn

Released online in J-STAGE as advance publication January 17, 2023.

BST
BioScience Trends

Guide for Authors

1. Scope of Articles

BioScience Trends (Print ISSN 1881-7815, Online ISSN 1881-7823) is an international peer-reviewed journal. *BioScience Trends* devotes to publishing the latest and most exciting advances in scientific research. Articles cover fields of life science such as biochemistry, molecular biology, clinical research, public health, medical care system, and social science in order to encourage cooperation and exchange among scientists and clinical researchers.

2. Submission Types

Original Articles should be well-documented, novel, and significant to the field as a whole. An Original Article should be arranged into the following sections: Title page, Abstract, Introduction, Materials and Methods, Results, Discussion, Acknowledgments, and References. Original articles should not exceed 5,000 words in length (excluding references) and should be limited to a maximum of 50 references. Articles may contain a maximum of 10 figures and/or tables. Supplementary Data are permitted but should be limited to information that is not essential to the general understanding of the research presented in the main text, such as unaltered blots and source data as well as other file types.

Brief Reports definitively documenting either experimental results or informative clinical observations will be considered for publication in this category. Brief Reports are not intended for publication of incomplete or preliminary findings. Brief Reports should not exceed 3,000 words in length (excluding references) and should be limited to a maximum of 4 figures and/or tables and 30 references. A Brief Report contains the same sections as an Original Article, but the Results and Discussion sections should be combined.

Reviews should present a full and up-to-date account of recent developments within an area of research. Normally, reviews should not exceed 8,000 words in length (excluding references) and should be limited to a maximum of 10 figures and/or tables and 100 references. Mini reviews are also accepted, which should not exceed 4,000 words in length (excluding references) and should be limited to a maximum of 5 figures and/or tables and 50 references.

Policy Forum articles discuss research and policy issues in areas related to life science such as public health, the medical care system, and social science and may address governmental issues at district, national, and international levels of discourse. Policy Forum articles should not exceed 3,000 words in length (excluding references) and should be limited to a maximum of 5 figures and/or tables and 30 references.

Communications are short, timely pieces that spotlight new research findings or policy issues of interest to the field of global health and medical practice that are of immediate importance. Depending on their content, Communications will be published as "Comments" or "Correspondence". Communications should not exceed 1,500 words in length (excluding references) and should be limited to a maximum of 2 figures and/or tables and 20 references.

Editorials are short, invited opinion pieces that discuss an issue of immediate importance to the fields of global health, medical practice, and basic science oriented for clinical application. Editorials should not exceed 1,000 words in length (excluding references) and should be limited to a maximum of 10 references. Editorials may contain one figure or table.

News articles should report the latest events in health sciences and medical research from around the world. News should not exceed 500 words in length.

Letters should present considered opinions in response to articles published in *BioScience Trends* in the last 6 months or issues of general interest. Letters should not exceed 800 words in length and may contain a maximum of 10 references. Letters may contain one figure or table.

3. Editorial Policies

For publishing and ethical standards, *BioScience Trends* follows the Recommendations for the Conduct, Reporting, Editing, and Publication of Scholarly Work in Medical Journals issued by the International Committee of Medical Journal Editors (ICMJE, *https://icmje.org/recommendations*), and the Principles of Transparency and Best Practice in Scholarly Publishing jointly issued by the Committee on Publication Ethics (COPE, *https://publicationethics.org/resources/guidelines-new/principles-transparency-and-best-practice-scholarly-publishing*), the Directory of Open Access Journals (DOAJ, *https://doaj.org/apply/transparency*), the Open Access Scholarly Publishers Association (OASPA, *https://oaspa.org/principles-of-transparency-and-best-practice-in-scholarly-publishing-4*), and the World Association of Medical Editors (WAME, *https://wame.org/principles-of-transparency-and-best-practice-in-scholarly-publishing*).

BioScience Trends will perform an especially prompt review to encourage innovative work. All original research will be subjected to a rigorous standard of peer review and will be edited by experienced copy editors to the highest standards.

Ethical Approval of Studies and Informed Consent: For all manuscripts reporting data from studies involving human participants or animals, formal review and approval, or formal review and waiver, by an appropriate institutional review board or ethics committee is required and should be described in the Methods section. When your manuscript contains any case details, personal information and/or images of patients or other individuals, authors must obtain appropriate written consent, permission and release in order to comply with all applicable laws and regulations concerning privacy and/or security of personal information. The consent form needs to comply with the relevant legal requirements of your particular jurisdiction, and please do not send signed consent form to *BioScience Trends* to respect your patient's and any other individual's privacy. Please instead describe the information clearly in the Methods (patient consent) section of your manuscript while retaining copies of the signed forms in the event they should be needed. Authors should also state that the study conformed to the provisions of the Declaration of Helsinki (as revised in 2013, *https://wma.net/what-we-do/medical-ethics/declaration-of-helsinki*). When reporting experiments on animals, authors should indicate whether the institutional and national guide for the care and use of laboratory animals was followed.

Reporting Clinical Trials: The ICMJE (*https:// icmje.org/recommendations/browse/publishing-and-editorial-issues/clinical-trial-registration.html*) defines a clinical trial as any research project that prospectively assigns people or a group of people to an intervention, with or without concurrent comparison or control groups, to study the relationship between a health-related intervention and a health outcome. Registration of clinical trials in a public trial registry at or before the time of first patient enrollment is a condition of consideration for publication in *BioScience Trends*, and the trial registration number will be published at the end of the Abstract. The registry must be independent of for-profit interest and publicly accessible. Reports of trials must conform to CONSORT 2010 guidelines (*https://consort-statement.org/consort-2010*). Articles reporting the results of randomized trials must include the CONSORT flow diagram showing the progress of patients throughout the trial.

Conflict of Interest: All authors are required to disclose any actual or potential conflict of interest including financial interests or relationships with other people or organizations that might raise questions of bias

in the work reported. If no conflict of interest exists for each author, please state "There is no conflict of interest to disclose".

Submission Declaration: When a manuscript is considered for submission to *BioScience Trends*, the authors should confirm that 1) no part of this manuscript is currently under consideration for publication elsewhere; 2) this manuscript does not contain the same information in whole or in part as manuscripts that have been published, accepted, or are under review elsewhere, except in the form of an abstract, a letter to the editor, or part of a published lecture or academic thesis; 3) authorization for publication has been obtained from the authors' employer or institution; and 4) all contributing authors have agreed to submit this manuscript.

Initial Editorial Check: Immediately after submission, the journal's managing editor will perform an initial check of the manuscript. A suitable academic editor will be notified of the submission and invited to check the manuscript and recommend reviewers. Academic editors will check for plagiarism and duplicate publication at this stage. The journal has a formal recusal process in place to help manage potential conflicts of interest of editors. In the event that an editor has a conflict of interest with a submitted manuscript or with the authors, the manuscript, review, and editorial decisions are managed by another designated editor without a conflict of interest related to the manuscript.

Peer Review: *BioScience Trends* operates a single-anonymized review process, which means that reviewers know the names of the authors, but the authors do not know who reviewed their manuscript. All articles are evaluated objectively based on academic content. External peer review of research articles is performed by at least two reviewers, and sometimes the opinions of more reviewers are sought. Peer reviewers are selected based on their expertise and ability to provide quality, constructive, and fair reviews. For research manuscripts, the editors may, in addition, seek the opinion of a statistical reviewer. Every reviewer is expected to evaluate the manuscript in a timely, transparent, and ethical manner, following the COPE guidelines (*https://publicationethics.org/files/cope-ethical-guidelines-peer-reviewers-v2_0.pdf*). We ask authors for sufficient revisions (with a second round of peer review, when necessary) before a final decision is made. Consideration for publication is based on the article's originality, novelty, and scientific soundness, and the appropriateness of its analysis.

Suggested Reviewers: A list of up to 3 reviewers who are qualified to assess the scientific merit of the study is welcomed. Reviewer information including names, affiliations, addresses, and e-mail should be provided at the same time the manuscript is submitted online. Please do not suggest reviewers with known conflicts of interest, including participants or anyone with a stake in the proposed research; anyone from the same institution; former students, advisors, or research collaborators (within the last three years); or close personal contacts. Please note that the Editor-in-Chief may accept one or more of the proposed reviewers or may request a review by other qualified persons.

Language Editing: Manuscripts prepared by authors whose native language is not English should have their work proofread by a native English speaker before submission. If not, this might delay the publication of your manuscript in *BioScience Trends*.

The Editing Support Organization can provide English proofreading, Japanese-English translation, and Chinese-English translation services to authors who want to publish in *BioScience Trends* and need assistance before submitting a manuscript. Authors can visit this organization directly at *https://www.iacmhr.com/iac-eso/support.php?lang=en*. IAC-ESO was established to facilitate manuscript preparation by researchers whose native language is not English and to help edit works intended for international academic journals.

Copyright and Reuse: Before a manuscript is accepted for publication in *BioScience Trends*, authors will be asked to sign a transfer of copyright agreement, which recognizes the common interest that both the journal and author(s) have in the protection of copyright. We accept that some authors (*e.g.*, government employees in some countries) are unable to transfer copyright. A JOURNAL PUBLISHING AGREEMENT (JPA) form will be e-mailed to the authors by the Editorial Office and must be returned by the authors by mail, fax, or as a scan. Only forms with a hand-written signature from the corresponding author are accepted. This copyright will ensure the widest possible dissemination of information. Please note that the manuscript will not proceed to the next step in publication until the JPA Form is received. In addition, if excerpts from other copyrighted works are included, the author(s) must obtain written permission from the copyright owners and credit the source(s) in the article.

4. Cover Letter

The manuscript must be accompanied by a cover letter prepared by the corresponding author on behalf of all authors. The letter should indicate the basic findings of the work and their significance. The letter should also include a statement affirming that all authors concur with the submission and that the material submitted for publication has not been published previously or is not under consideration for publication elsewhere. The cover letter should be submitted in PDF format. For an example of Cover Letter, please visit: *https://www.biosciencetrends.com/downcentre* (Download Centre).

5. Submission Checklist

The Submission Checklist should be submitted when submitting a manuscript through the Online Submission System. Please visit Download Centre (*https://www.biosciencetrends.com/downcentre*) and download the Submission Checklist file. We recommend that authors use this checklist when preparing your manuscript to check that all the necessary information is included in your article (if applicable), especially with regard to Ethics Statements.

6. Manuscript Preparation

Manuscripts are suggested to be prepared in accordance with the "Recommendations for the Conduct, Reporting, Editing, and Publication of Scholarly Work in Medical Journals", as presented at *https://www.ICMJE.org*.

Manuscripts should be written in clear, grammatically correct English and submitted as a Microsoft Word file in a single-column format. Manuscripts must be paginated and typed in 12-point Times New Roman font with 24-point line spacing. Please do not embed figures in the text. Abbreviations should be used as little as possible and should be explained at first mention unless the term is a well-known abbreviation (*e.g.* DNA). Single words should not be abbreviated.

Title page: The title page must include 1) the title of the paper (Please note the title should be short, informative, and contain the major key words); 2) full name(s) and affiliation(s) of the author(s), 3) abbreviated names of the author(s), 4) full name, mailing address, telephone/fax numbers, and e-mail address of the corresponding author; 5) author contribution statements to specify the individual contributions of all authors to this manuscript, and 6) conflicts of interest (if you have an actual or potential conflict of interest to disclose, it must be included as a footnote on the title page of the manuscript; if no conflict of interest exists for each author, please state "There is no conflict of interest to disclose").

Abstract: The abstract should briefly state the purpose of the study, methods, main findings, and conclusions. For articles that are Original Articles, Brief Reports, Reviews, or Policy Forum articles, a one-paragraph abstract consisting of no more than 250 words must be included in the manuscript. For Communications, Editorials, News, or Letters, a brief summary of main content in 150 words or fewer should be included in the manuscript. For articles reporting clinical trials, the trial registration number should be stated at the end of the Abstract. Abbreviations must be kept to a minimum and non-standard

abbreviations explained in brackets at first mention. References should be avoided in the abstract. Three to six key words or phrases that do not occur in the title should be included in the Abstract page.

Introduction: The introduction should provide sufficient background information to make the article intelligible to readers in other disciplines and sufficient context clarifying the significance of the experimental findings

Materials/Patients and Methods: The description should be brief but with sufficient detail to enable others to reproduce the experiments. Procedures that have been published previously should not be described in detail but appropriate references should simply be cited. Only new and significant modifications of previously published procedures require complete description. Names of products and manufacturers with their locations (city and state/country) should be given and sources of animals and cell lines should always be indicated. All clinical investigations must have been conducted in accordance Materials/ Patients and Methods.

Results: The description of the experimental results should be succinct but in sufficient detail to allow the experiments to be analyzed and interpreted by an independent reader. If necessary, subheadings may be used for an orderly presentation. All Figures and Tables should be referred to in the text in order, including those in the Supplementary Data.

Discussion: The data should be interpreted concisely without repeating material already presented in the Results section. Speculation is permissible, but it must be well-founded, and discussion of the wider implications of the findings is encouraged. Conclusions derived from the study should be included in this section.

Acknowledgments: All funding sources (including grant identification) should be credited in the Acknowledgments section. Authors should also describe the role of the study sponsor(s), if any, in study design; in the collection, analysis, and interpretation of data; in the writing of the report; and in the decision to submit the paper for publication. If the funding source had no such involvement, the authors should so state.

In addition, people who contributed to the work but who do not meet the criteria for authors should be listed along with their contributions.

References: References should be numbered in the order in which they appear in the text. Citing of unpublished results, personal communications, conference abstracts, and theses in the reference list is not recommended but these sources may be mentioned in the text. In the reference list, cite the names of all authors when there are fifteen or fewer authors; if there are sixteen or more authors, list the first three followed by *et al*. Names of journals should be abbreviated in the style used in PubMed. Authors are responsible for the accuracy of the references. The EndNote Style of *BioScience Trends* could be downloaded at **EndNote** (*https://ircabssagroup.com/examples/ BioScience_Trends.ens*).

Examples are given below:

Example 1 (Sample journal reference):

Inagaki Y, Tang W, Zhang L, Du GH, Xu WF, Kokudo N. Novel aminopeptidase N (APN/CD13) inhibitor 24F can suppress invasion of hepatocellular carcinoma cells as well as angiogenesis. Biosci Trends. 2010; 4:56-60.

Example 2 (Sample journal reference with more than 15 authors):

Darby S, Hill D, Auvinen A, *et al*. Radon in homes and risk of lung cancer: Collaborative analysis of individual data from 13 European case-control studies. BMJ. 2005; 330:223.

Example 3 (Sample book reference):

Shalev AY. Post-traumatic stress disorder: Diagnosis, history and life course. In: Post-traumatic Stress Disorder, Diagnosis, Management and Treatment (Nutt DJ, Davidson JR, Zohar J, eds.). Martin Dunitz, London, UK, 2000; pp. 1-15.

Example 4 (Sample web page reference):

World Health Organization. The World Health Report 2008 – primary health care: Now more than ever. *http://www.who.int/whr/2008/whr08_ en.pdf* (accessed September 23, 2022).

Tables: All tables should be prepared in Microsoft Word or Excel and should be arranged at the end of the manuscript after the References section. Please note that tables should not in image format. All tables should have a concise title and should be numbered consecutively with Arabic numerals. If necessary, additional information should be given below the table.

Figure Legend: The figure legend should be typed on a separate page of the main manuscript and should include a short title and explanation. The legend should be concise but comprehensive and should be understood without referring to the text. Symbols used in figures must be explained. Any individually labeled figure parts or panels (A, B, *etc*.) should be specifically described by part name within the legend.

Figure Preparation: All figures should be clear and cited in numerical order in the text. Figures must fit a one- or two-column format on the journal page: 8.3 cm (3.3 in.) wide for a single column, 17.3 cm (6.8 in.) wide for a double column; maximum height: 24.0 cm (9.5 in.). Please make sure that the symbols and numbers appeared in the figures should be clear. Please make sure that artwork files are in an acceptable format (TIFF or JPEG) at minimum resolution (600 dpi for illustrations, graphs, and annotated artwork, and 300 dpi for micrographs and photographs). Please provide all figures as separate files. Please note that low-resolution images are one of the leading causes of article resubmission and schedule delays.

Units and Symbols: Units and symbols conforming to the International System of Units (SI) should be used for physicochemical quantities. Solidus notation (*e.g.* mg/kg, mg/mL, mol/mm^2/min) should be used. Please refer to the SI Guide *www.bipm.org/en/si/* for standard units.

Supplemental data: Supplemental data might be useful for supporting and enhancing your scientific research and *BioScience Trends* accepts the submission of these materials which will be only published online alongside the electronic version of your article. Supplemental files (figures, tables, and other text materials) should be prepared according to the above guidelines, numbered in Arabic numerals (*e.g.*, Figure S1, Figure S2, and Table S1, Table S2) and referred to in the text. All figures and tables should have titles and legends. All figure legends, tables and supplemental text materials should be placed at the end of the paper. Please note all of these supplemental data should be provided at the time of initial submission and note that the editors reserve the right to limit the size and length of Supplemental Data.

5. Submission Checklist

The Submission Checklist will be useful during the final checking of a manuscript prior to sending it to *BioScience Trends* for review. Please visit Download Centre and download the Submission Checklist file.

6. Online Submission

Manuscripts should be submitted to *BioScience Trends* online at *https://www.biosciencetrends.com/login*. Receipt of your manuscripts submitted online will be acknowledged by an e-mail from Editorial Office containing a reference number, which should be used in all future communications. If for any reason you are unable to submit a file online, please contact the Editorial Office by e-mail at *office@ biosciencetrends.com*

8. Accepted Manuscripts

Page Charge: Page charges will be levied on all manuscripts accepted for publication in *BioScience Trends* (Original Articles / Brief Reports / Reviews / Policy Forum / Communications: $140 per page for black white pages, $340 per page for color pages; News / Letters: a total cost of $600). Under exceptional circumstances, the author(s) may apply to the editorial office for a waiver of the publication charges by stating the reason in the Cover Letter when the manuscript online.

Misconduct: *BioScience Trends* takes seriously all allegations of potential misconduct and adhere to the ICMJE Guideline (*https://icmje.org/recommendations*) and COPE Guideline (*https://publicationethics.org/files/Code_of_conduct_for_journal_editors.pdf*). In cases of suspected research or publication misconduct, it may be necessary for the Editor or Publisher to contact and share submission details with third parties including authors' institutions and ethics committees. The corrections, retractions, or editorial expressions of concern will be performed in line with above guidelines.

(As of December 2022)

BioScience Trends
Editorial and Head Office
Pearl City Koishikawa 603,
2-4-5 Kasuga, Bunkyo-ku,
Tokyo 112-0003, Japan.
E-mail: office@biosciencetrends.com